AD-A070 526 DEFENSE NUCLEAR AGENCY WASHINGTON DC F/G 19/1
MISERS BLUFF. PRELIMINARY RESULTS REPORT. VOLUME I. PHASE I.(U)
JAN 79 R G DERAAD
UNCLASSIFIED DNA-POR-6980-VOL-1 DOE-WT-6980-VOL-1 NL

1 OF 2
AD
A070526

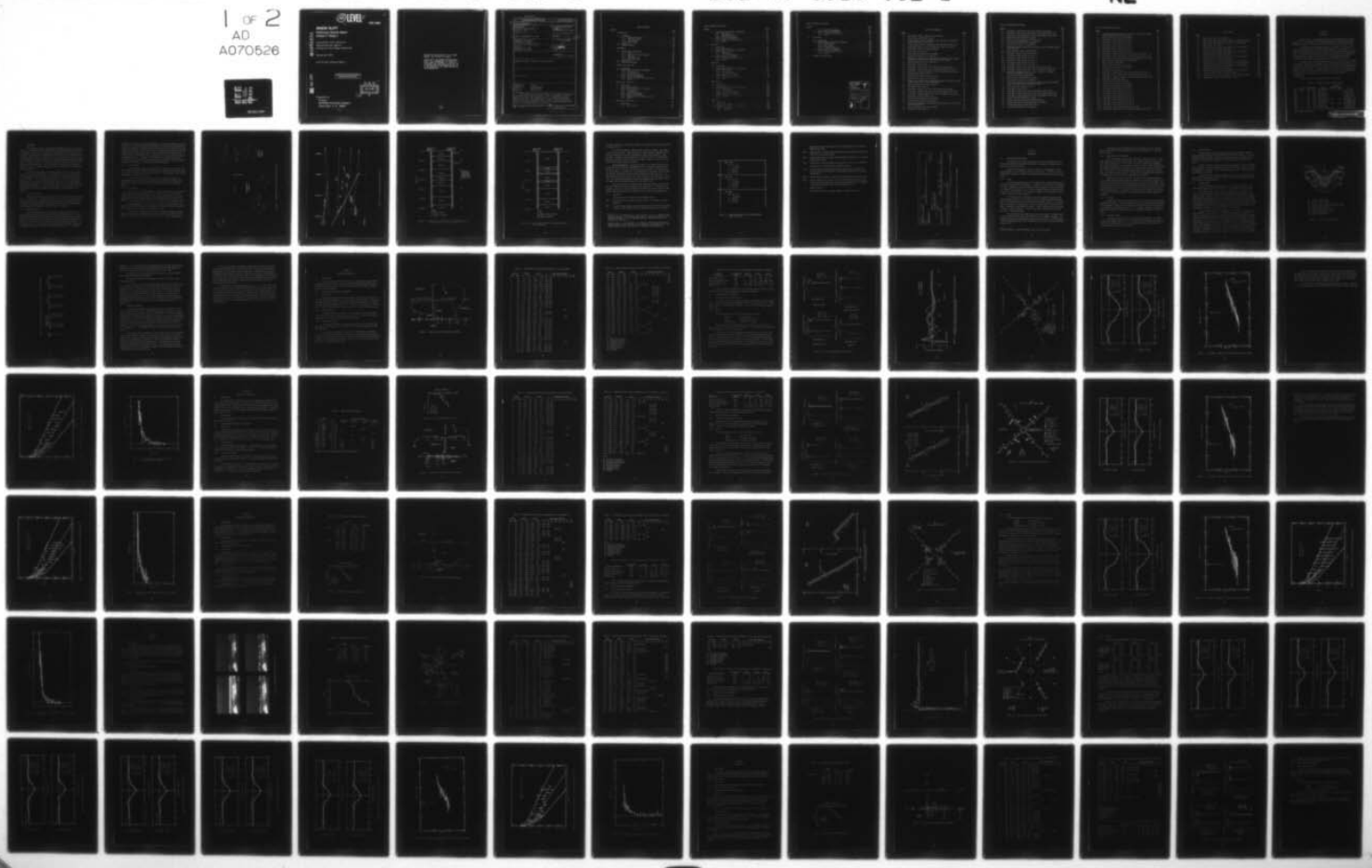

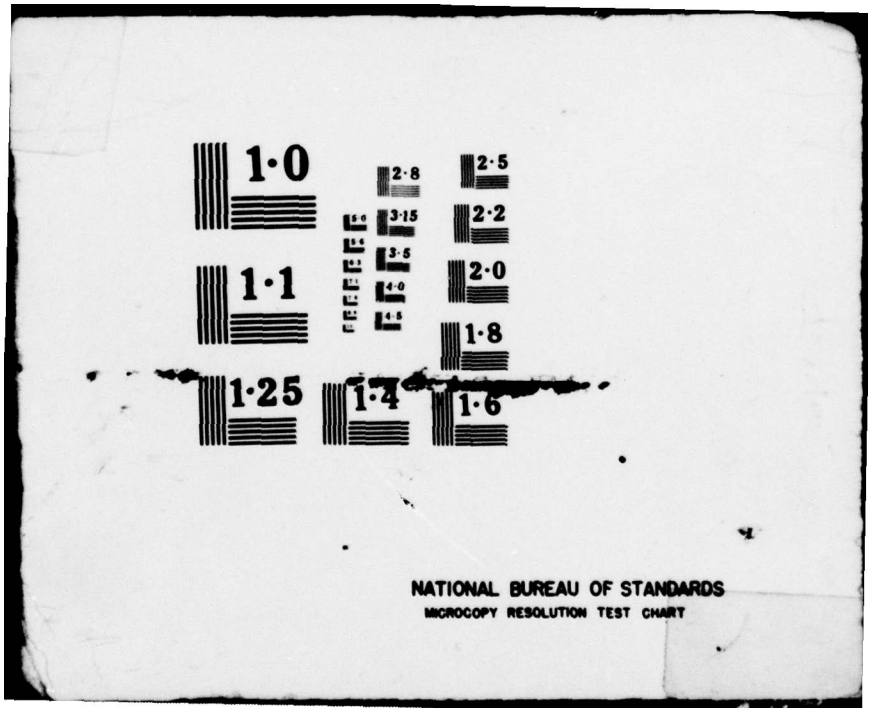
1·0
1·1
1·25
1·4
1·6
2·8
3·15
3·5
4·0
4·5
2·5
2·2
2·0
1·8
NATIONAL BUREAU OF STANDARDS
MICROCOPY RESOLUTION TEST CHART

(12) LEVEL II

POR 6980

MISERS BLUFF

Preliminary Results Report
Volume I—Phase I

Commander, Field Command
Defense Nuclear Agency
Kirtland Air Force Base, NM 87115

22 January 1979

Final Project Officers Report

Prepared for
Director
DEFENSE NUCLEAR AGENCY
Washington, D. C. 20305

Destroy this report when it is no longer needed. Do not return to sender.

PLEASE NOTIFY THE DEFENSE NUCLEAR AGENCY, ATTN: TISI, WASHINGTON, D.C. 20305, IF YOUR ADDRESS IS INCORRECT, IF YOU WISH TO BE DELETED FROM THE DISTRIBUTION LIST, OR IF THE ADDRESSEE IS NO LONGER EMPLOYED BY YOUR ORGANIZATION.

UNCLASSIFIED

SECURITY CLASSIFICATION OF THIS PAGE (When Data Entered)

REPORT DOCUMENTATION PAGE		READ INSTRUCTIONS BEFORE COMPLETING FORM
1. REPORT NUMBER DNA POR-6980 (WT 6980) VOL-1 (NT)	2. GOVT ACCESSION NO.	3. RECIPIENT'S CATALOG NUMBER
4. TITLE (and Subtitle) MISERS BLUFF Preliminary Results Report. Volume I, Phase I.		5. TYPE OF REPORT & PERIOD COVERED Final Project Officers Report 6. PERFORMING ORG. REPORT NUMBER
7. AUTHOR(s) Robert G. DeRaad / Captain, USAF		8. CONTRACT OR GRANT NUMBER(s) DOE WT-6980-VOL-1
9. PERFORMING ORGANIZATION NAME AND ADDRESS Commander, Field Command Defense Nuclear Agency Kirtland Air Force Base, NM 87115		10. PROGRAM ELEMENT, PROJECT, TASK AREA & WORK UNIT NUMBERS 164 p.
11. CONTROLLING OFFICE NAME AND ADDRESS Director Defense Nuclear Agency Washington, D.C. 20305		12. REPORT DATE 22 January 1979 13. NUMBER OF PAGES 164
14. MONITORING AGENCY NAME & ADDRESS(if different from Controlling Office)		15. SECURITY CLASS. (of this report) UNCLASSIFIED 15a. DECLASSIFICATION DOWNGRADING SCHEDULE

16. DISTRIBUTION STATEMENT (of this Report)

Approved for public release; distribution unlimited

17. DISTRIBUTION STATEMENT (of the abstract entered in Block 20, if different from Report)

18. SUPPLEMENTARY NOTES

19. KEY WORDS (Continue on reverse side if necessary and identify by block number)

MISERS BLUFF	Ejecta
Ground Motion	Cloud Formation
Airblast	High Explosives
Cratering	Multiple Burst

20. ABSTRACT (Continue on reverse side if necessary and identify by block number)

This report describes the preliminary results obtained from Phase I of the MISERS BLUFF Field Test Program. Phase I consisted of a series of eight high explosive tests conducted on the White Sands Missile Range, New Mexico in 1977. The primary purpose of these events was to develop a multiple burst ground motion data base. Included in this report are a description of the experimental plan for each test and typical ground motion, airblast and cratering results for each test.

DD FORM 1 JAN 73 1473 EDITION OF 1 NOV 65 IS OBSOLETE

UNCLASSIFIED

SECURITY CLASSIFICATION OF THIS PAGE (When Data Entered)

406 762

TABLE OF CONTENTS

TABLE OF CONTENTS (Continued)

TABLE OF CONTENTS (Continued)

LIST OF ILLUSTRATIONS

LIST OF ILLUSTRATIONS (Continued)

LIST OF ILLUSTRATIONS (Continued)

LIST OF TABLES

SECTION 1

INTRODUCTION

MISERS BLUFF was a Defense Nuclear Agency (DNA) sponsored series of high explosive (HE) tests designed to investigate multiple burst induced ground motion phenomena in support of Missile-X (M-X) Weapon System basing mode option studies.

The MISERS BLUFF test program consisted of two phases. Phase I was conducted at the White Sands Missile Range (WSMR), New Mexico and consisted of a series of eight high explosive (TNT) events with both single and multiburst charges. Phase II was conducted at Planet Ranch, Arizona and consisted of one single burst and one multiburst ammonium nitrate and fuel oil (ANFO) high explosive event. Each charge of the Phase II tests contained 120 tons (109,000 kg) of ANFO.

The MISERS BLUFF Program was developed specifically to address the problems of multiburst weapon effects phenomena which are critical to the M-X concept. In particular, a multiburst ground shock data base was required to validate and update predictive model techniques. With this objective in mind, Phase I was designed to develop a relatively large initial data input from a series of small charge tests [generally 454 kg (1000 pounds)] in a variety of single and multiburst configurations.

Table 1.1 shows the MISERS BLUFF Phase I test program.

Table 1.1. MISERS BLUFF Phase I test program.

Event	No. of Charges	Charge Weight (kg)	(lb)	Charge Configuration	Spacing Between Charges (m)	(ft)	Date
MBI-1	1	454	1000	Half-Buried			2 August 1977
MBI-2	1	454	1000	Surface Tangent			15 August 1977
MBI-3	1	454	1000	Half-Buried			23 August 1977
MBI-4	6	454	1000	Surface Tangent	21.3	70	7 September 1977
MBI-5	1	454	1000	Tangent Below			22 September 1977
MBI-6	6	454	1000	Half-Buried	36.6	120	13 October 1977
MBI-7	1	116	256	Half-Buried			26 October 1977
MBI-8	24	454	1000	Surface Tangent	21.3	70	7 December 1977

MBI = MISERS BLUFF Phase I

1.1 BACKGROUND

The M-X weapon system, currently under development by the U.S. Air Force, derives its survivability from a combination of system hardening and proliferation as conceived in the multiple aim point (MAP) basing concept. The MAP concept involves the generation of many hardened missile launch sites only a portion of which actually contain missiles. The missiles will be covertly moved from site to site in a random manner, therefore, each site is an equally appropriate target for enemy attack. System survivability is attained by deploying more launch points than the enemy could attack one-on-one. The launch points are assumed to be grouped as closely as possible in order to minimize the real estate necessary for the deployment of the system.

Survivability and design of the enemy's reentry vehicles place certain constraints on the incoming attack. It is reasonable to consider the possibility of a large number of near simultaneous bursts on launch points adjacent to unattacked facilities. A key facility design question is, "May the launch facilities be designed to survive the airblast and ground shock effects of a single weapon attack and does the nature of a multiple burst attack lead to a substantially more severe design environment?" This question has given rise to the need to investigate multiple burst effects phenomena and consequently the MISERS BLUFF test program.

1.1.1 Single Burst Events

The single burst events of MISERS BLUFF Phase I provided the baseline data for use in evaluation of a superposition principle in predicting the ground shock effects of the multiburst experiments. Additionally, they provided an opportunity to evaluate the current empirical procedures for predicting the ground shock and crater/ejecta effects generated by high explosive (HE) charges.

1.1.2 Multiburst Events

The MAP basing concept for the proposed M-X weapon system derives its survivability by creating more targets than can be attacked one-on-one. An estimate of the deployment pattern for the M-X system places neighboring aim points at, nominally, one mile from a "baseline" threat. For many geologic conditions, this range is in the "transition" or "plateau" region for ground-motion phenomena. In this region there is little attenuation of ground motion with range, so that peak amplitudes of motion are insensitive to distance from the source. Preliminary

estimates of the effect of multiburst phenomenon, assuming the superposition principle to be valid, indicate that unattacked elements of the system are subjected to a greater ground motion environment than that which results for a single burst at the designed miss distance. An evaluation of the superposition assumption, by the Data Analysis Working Group (DAWG) using the limited available data, indicates that superposition of ground motions from a single burst is not a satisfactory estimate of multiburst effects. In general, in the interior of the charge array and to considerable depths, superposition underestimated the period of oscillatory ground motion and either under- or overestimated the peak amplitudes.

1.1.3 Site Location

The test bed for Phase I of MISERS BLUFF was located at the Queen 15 site on the White Sands Missile Range (WSMR), New Mexico, approximately 1220 meters east of the Pre-DICE THROW (PDT) II test bed (Figure 1.1). The locations of the various ground zeroes are shown in Figure 1.2.

The Queen 15 site was chosen for the Phase I experiments because the geology was well characterized and documented during the Pre-DICE THROW work and because the site was readily available in response to an early test execution schedule.

1.1.4 Site Geology

The test site is characterized by 2.1 meters of brown silty clay overlying a soft, gray clay that extends to a depth of 5 to 6 meters. Below this lies a fine-to-coarse silty sand, with gravel, that extends to the 11 to 12 meter depth. Alternating layers of clay, sand, and silt lie below the sand to a depth of 131 meters. The groundwater table is about 2.1 to 2.4 meters below the ground surface.

Seismic Properties. Due to the close proximity of the MISERS BLUFF site to the PDT site no seismic survey was conducted. Therefore, the seismic properties were considered to be the same as those at the PDT site.

Seismic tests performed for the PDT events included cross hole, up hole, and surface refraction. P-wave and S-wave velocity profiles interpreted from the results of these tests are shown in Figures 1.3 and 1.4. Detailed information is

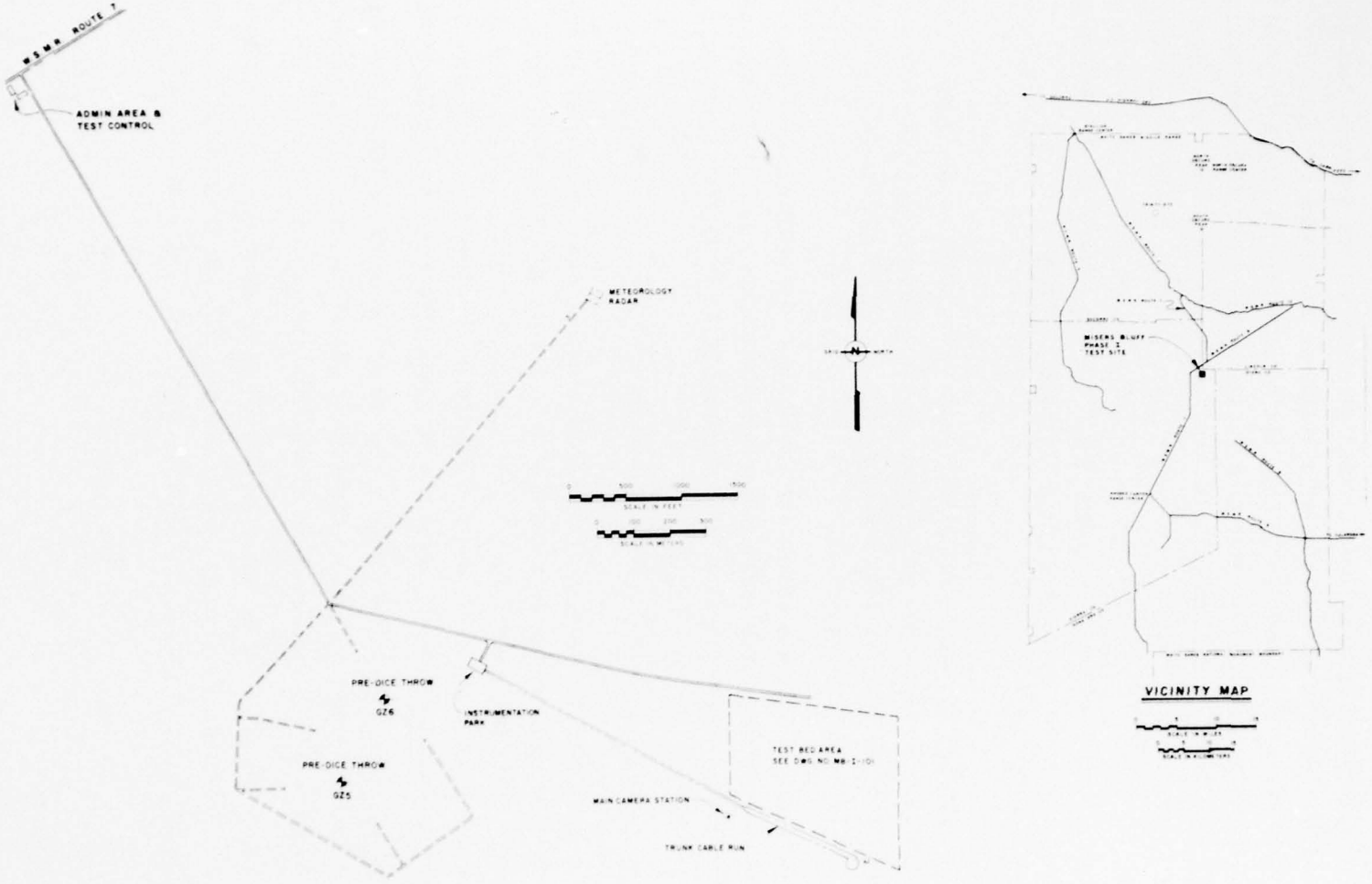

Figure 1.1. MISERS BLUFF, Phase I (MBI) test bed location.

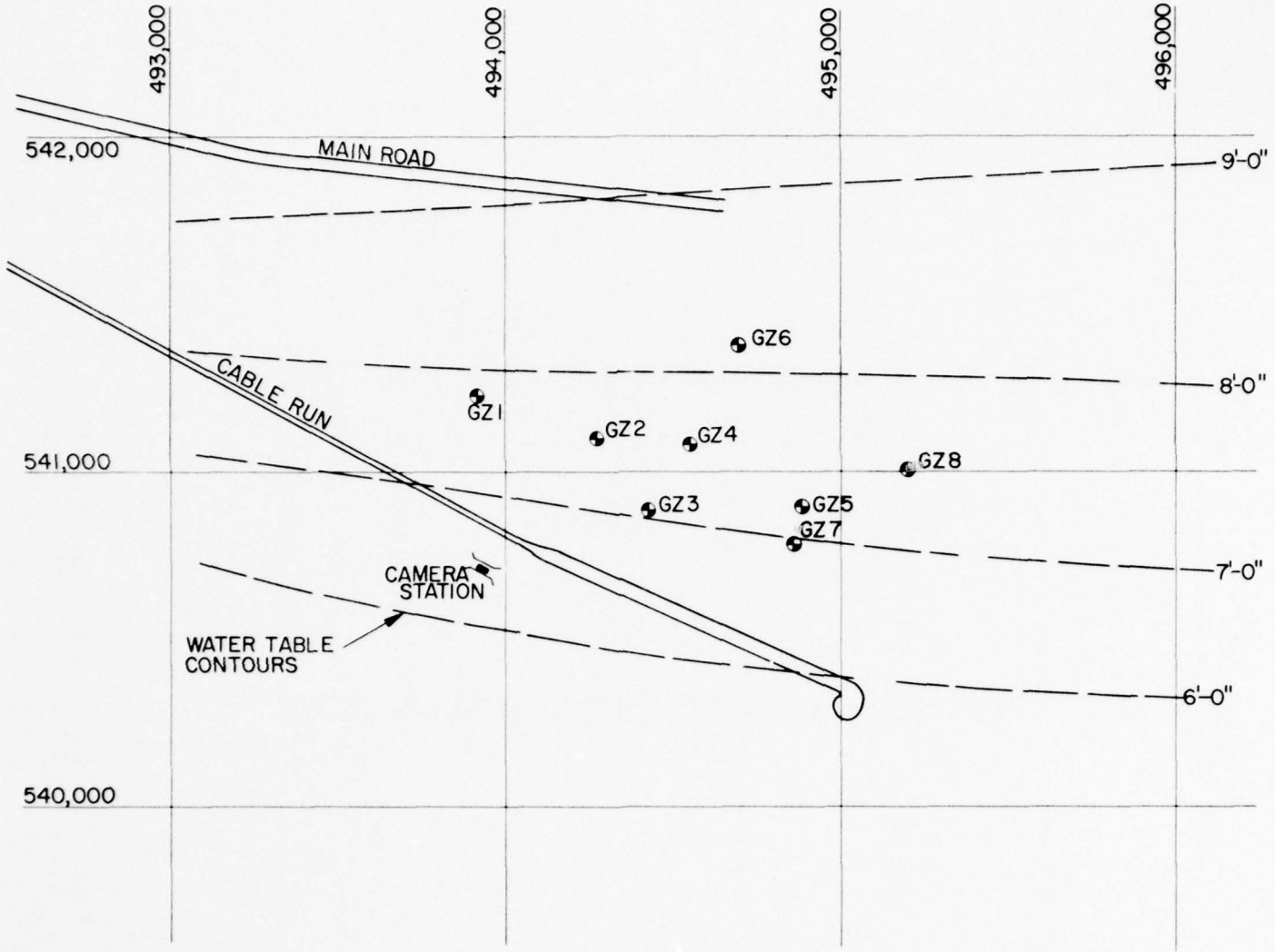

Figure 1.2. Test bed plan, MISERS BLUFF Phase I.

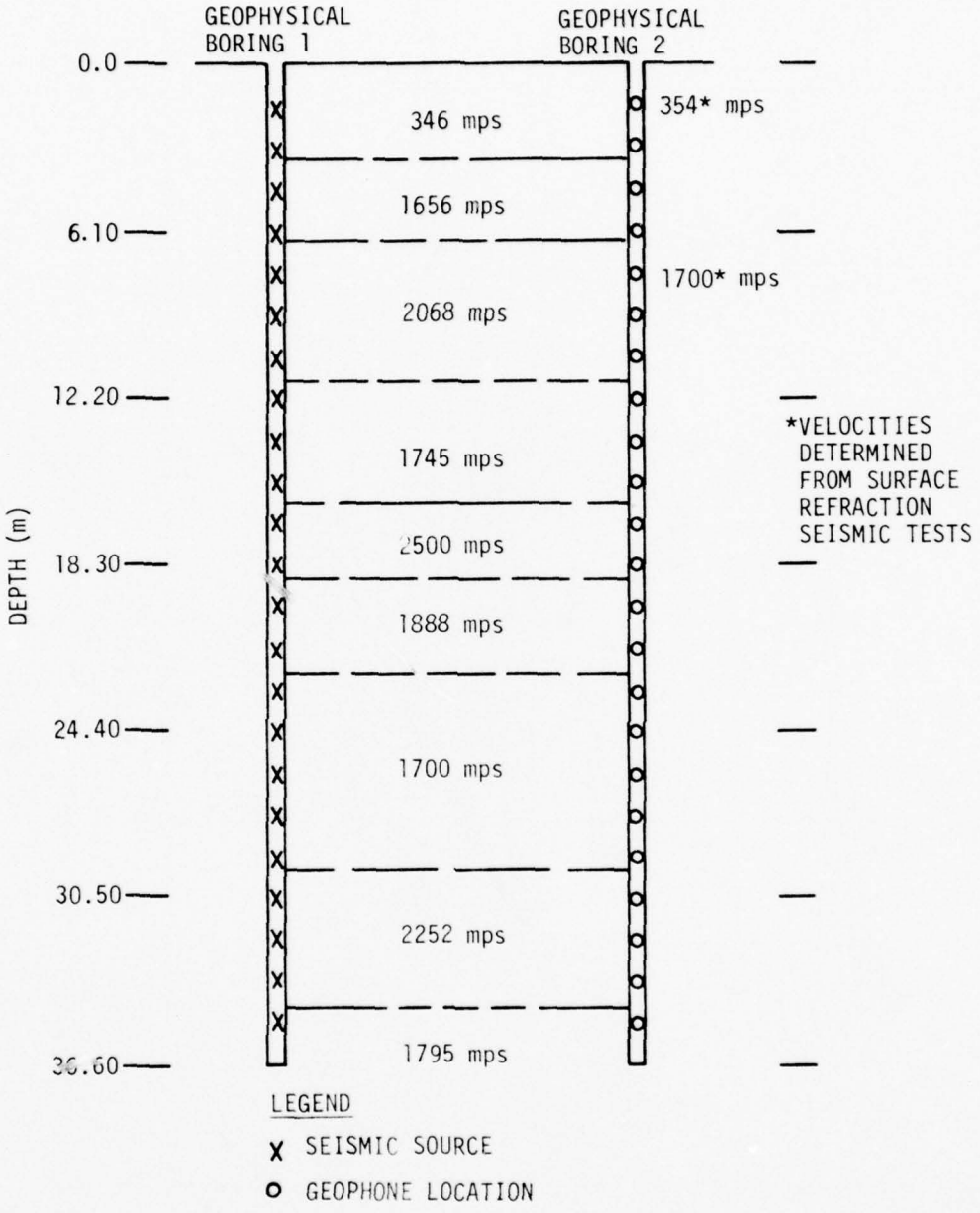

Figure 1.3. P-wave velocity profile interpreted from cross hole, up hole and surface refraction seismic data.

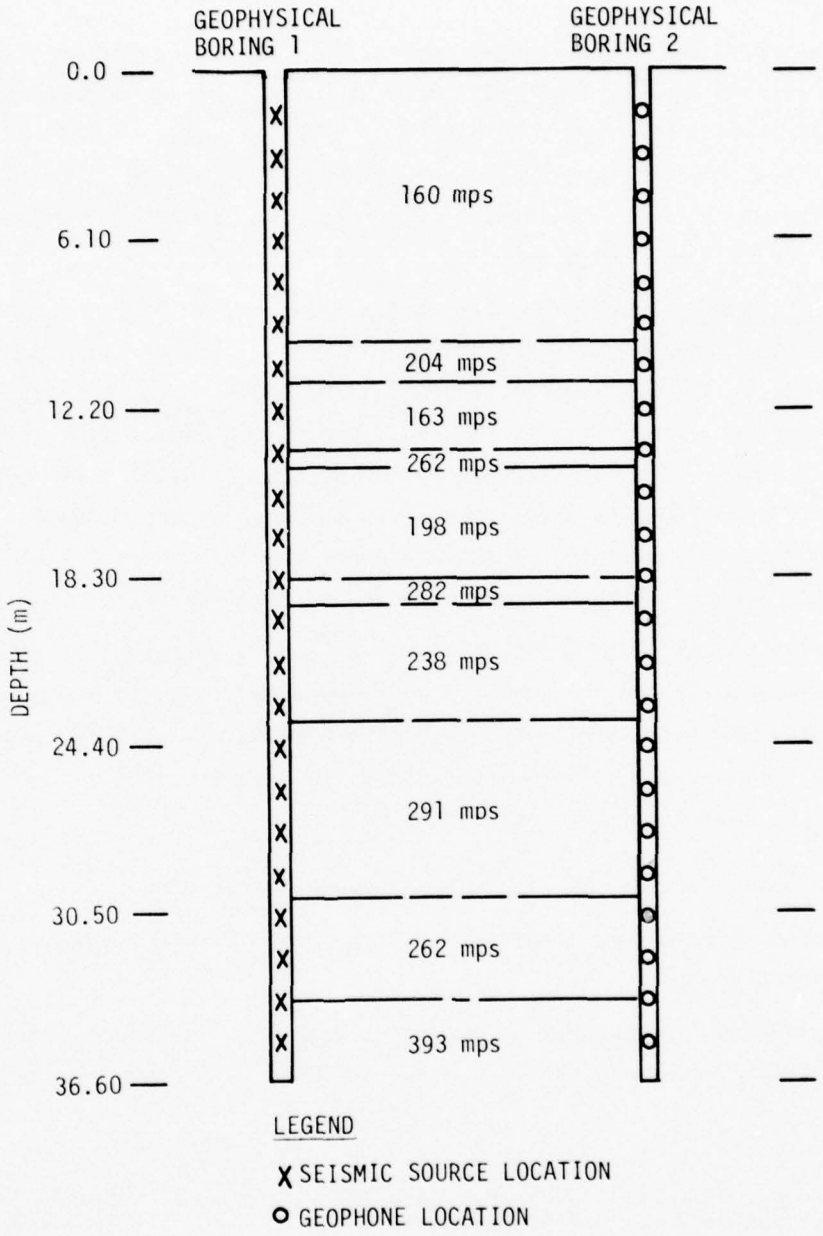

Figure 1.4. S-wave velocity profile interpreted from cross hole seismic data.

available, however, for the Pre-DICE THROW test area nearby, and has been published by Jackson, et al., [1,2].

These profiles indicate numerous seismic reversals; however, the changes in velocity are not large. These high velocity layers probably represent zones of increased cementation of greater percentages of gravel (and, therefore, higher densities). Neither of these conditions are typically uniform in the horizontal direction, therefore, the simplified profile shown in Figure 1.5 was used for prediction and preliminary analysis purposes.

Material Properties. The material properties for MISERS BLUFF were also assumed to be the same as those determined for PDT. The material property tests run for PDT were: (1) routine classification and index tests, (2) water content, (3) specific gravity, (4) density, (5) undrained static and dynamic uniaxial strain and isotropic compression, and (6) static and dynamic triaxial shear tests. In addition, two Cylindrical In-Situ Tests (CIST 15 and 16) were conducted at the PDT site. These data are presented in the Air Force Weapons Laboratory (AFWL) Technical Report (TR) 76-209 dated February 1977 and AFWL-TR-78-251.

During the MISERS BLUFF Program water content measurements were made for the near surface soils and are included in the description. This was done since seasonal variations in rainfall and weather conditions may lead to changes in near surface conditions which could be important to near surface ground motion data.

1.2 OBJECTIVES

The objectives of the single burst experiments were to:

MBI-1 Provide half-buried single burst data baseline for multiburst waveform synthesis.

MBI-2 Provide surface tangent single burst data baseline for multiburst waveform synthesis; identify depth-of-burst phenomena differences in oscillatory

---

[1] Jackson, A. E., Jr., Ballard, R. F., Jr., and Curro, J. R., Jr.; "Material Property Investigation for the Pre-DICE THROW I and II: Results from the Subsurface Exploration Programs," U.S. Army Engineer Waterways Experiment Station, CE, Vicksburg, MS, June 1976.

[2] Jackson, A. E., Jr., and Peterson, R. W.; "Material Property Investigation for Pre-DICE THROW I and II: Results from the Laboratory Test Programs," U.S. Army Engineer Waterways Experiment Station, CE, Vicksburg, MS, November 1976.

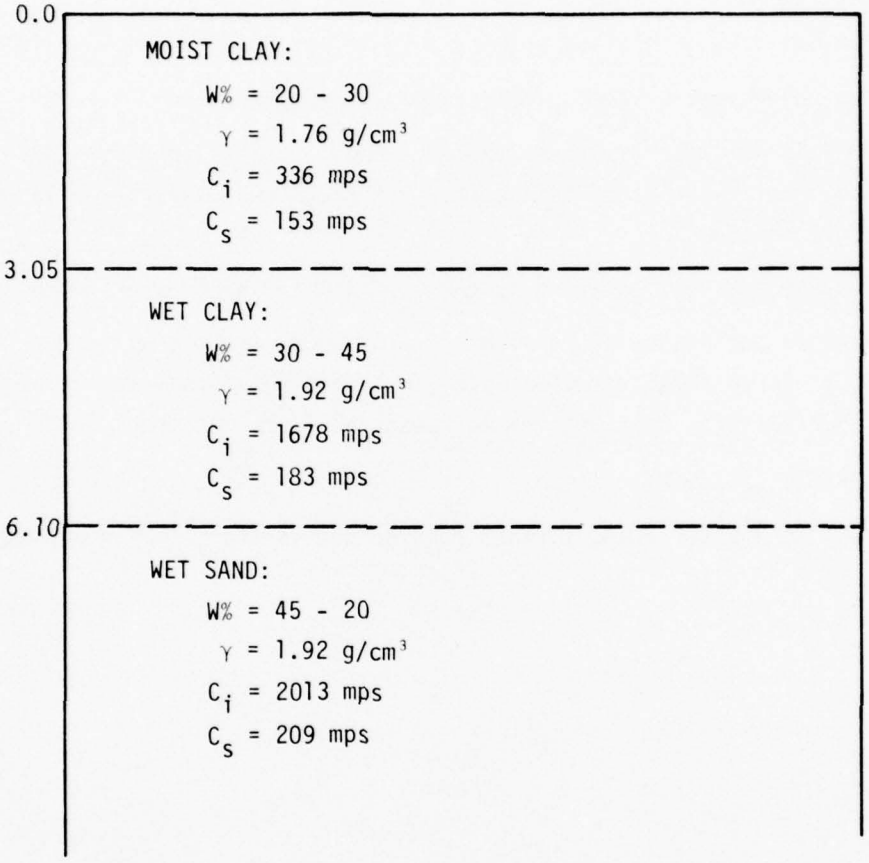

Figure 1.5. Simplified seismic profile of MISERS BLUFF Phase I test bed.

ground motion region; provide data for scaling comparisons with Pre-DICE THROW 100 ton event.

MBI-3 Repeat of MBI-1 to obtain data on reproducibility and emphasize definitions of motions in the plateau region.

MBI-5 Identify depth-of-burst (fully buried) phenomena differences in oscillatory ground motion region.

MBI-7 Provide data on scaling between 2.09 GJ and 53.5 GJ (1 ton = 4.184E+09[20]J).

The objectives of the multiburst experiments were to:

MBI-4 Provide data for waveform synthesis model, comparisons with MBI-2 data, and identification of height-of-burst phenomena differences in multiburst configurations.

MBI-6 Provide data for waveform synthesis model and comparisons with MBI-1 data.

MBI-8 Resolve importance of an outer ring of charges and their effect on a central charge array; provide data for assessing reproducibility and symmetry (configuration contained seven identical 6-charge arrays).

1.3 PLANNING SCHEDULE

The MISERS BLUFF Phase I Planning Schedule is shown in Figure 1.6.

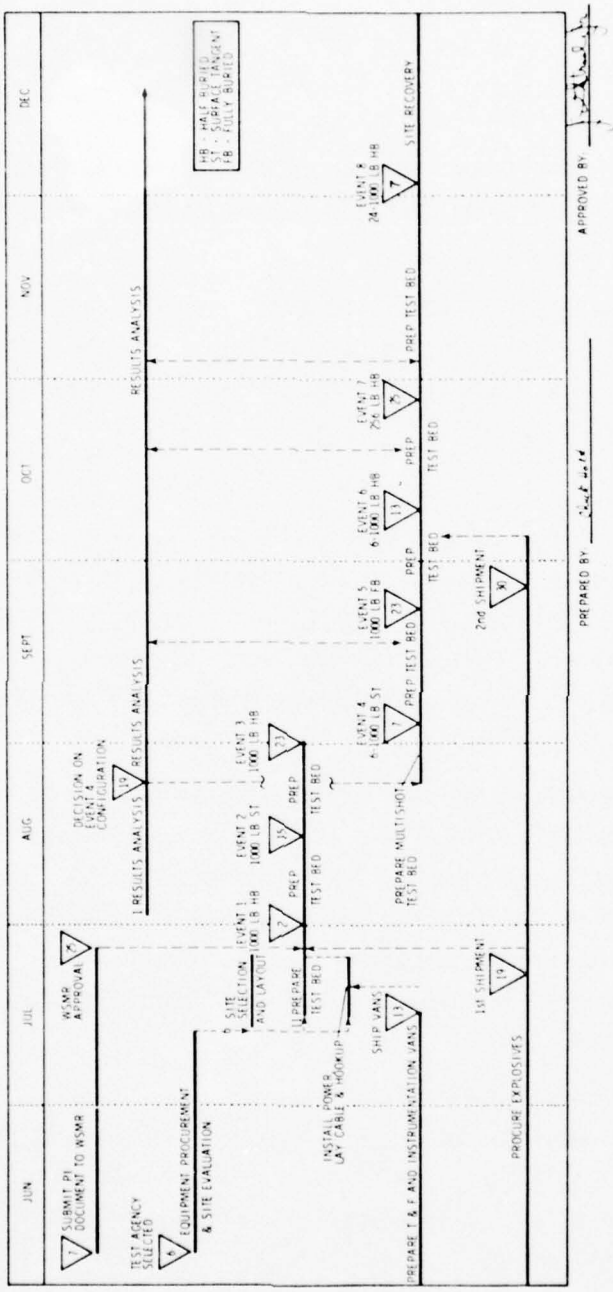

Figure 1.6. MISERS BLUFF, Phase I, planning schedule.

SECTION 2

EXPERIMENTS

2.1 GROUND MOTION AND AIRBLAST

The experiments for ground motion and airblast were conducted by the U.S. Army Engineer Waterways Experiment Station (WES), Vicksburg, Mississippi and are described in detail by Murrell.[3]

Ground shock transducers consisted primarily of accelerometers, with a limited number of particle velocity and soil stress gages. In addition, airblast measurements were made in support of the ground motion program on each of the eight events.

2.1.1 Gages

The principal motion sensors used on MISERS BLUFF were the Endevco Corporation Models 2262 and 2264 accelerometers, in ranges of 25 to 20,000 g. These gages are small, lightweight, sensitive and have natural frequencies of 2,500 to 100,000 Hz, depending on gage range. Their effective frequency responses range from 750 Hz for the 25 g unit to 20,000 Hz for the 20,000 g models; all accelerometers respond to static acceleration (zero frequency).

The primary velocity gage used was the latest commercial version of the Sandia Corporation Model DX. This gage consists of a highly overdamped pendulum and a variable reluctance pickup which senses the pendulum position. The displacement of the pendulum is proportional to the gage velocity over a relatively broad band of frequencies which depends on damping. Typical bandwidths were on the order of one Hz to several hundred Hz. The Bell and Howell integrating velocity gage was used in limited application.

WES developed the diaphragm gages used as stress gages. The gage consists of two stainless steel housings, each containing a stiff integral diaphragm. Two matched semiconductor strain gages are bonded to each diaphragm. The half-bridges from each diaphragm are electrically completed to form a full (four-arm) Wheatstone bridge circuit.

---

[3]Murrell, Donald W., "WES Miscellaneous Paper," W-78-4, June 1978.

WES used semiconductor airblast gages, Kulite Model HKS-375 for pressure above 2.1 MPa (300 psi) and Kulite Model XTS-1-190 for pressures of 2.1 MPa (300 psi) and below.

2.1.2 Gage Canisters and Placement

Most free field motion gages were installed in aluminum canisters. Three basic types were used, the "micro," "mini," and "regular" canisters, so named for their relative physical size. The "micro" and "mini" canisters were designed to make biaxial measurements of acceleration, and were too small to hold velocity gages. The "regular" canister held a biaxial array of both velocity gages and accelerometers. At depths of 10 feet and deeper where gages were not recovered, accelerometers were placed in epoxy canisters. In these, the accelerometers were mounted on an aluminum stud, with the entire assembly encased in an epoxy.

Both motion and stress gages were inserted in 8-inch diameter boreholes using 1-1/4-inch square aluminum tubing for insertion. An integral threaded fitting on the motion gage canisters allowed attachment and release of the placement tubing. Except for Event 8, a gripping tool with the same threaded fitting was used to place stress gage plugs (in which stress gages had been cast with the same grout used to backfill the gage holes). For Event 8, the stress gages were pressed into position in the in-situ soil at the bottom of the borehole using the "paddle" emplacement technique.

2.1.3 Grouting

Motion gage canisters were fixed in place with a hard, quick-setting grout designated "Quick-set". As soon as the grout had set, the placement rod was removed and the borehole filled with a different grout, designed to more closely match the soil properties and designated "mix E-2 (E)". All holes containing a shallow (0.5 meter depth) canister, were topped out with hand-tamped local topsoil in lieu of grout.

2.1.4 Recording System

Data were recorded on 32-track FM magnetic tape recorders. The models used were the Sangamo Sabre IV and 4700. These provided 30 data channels each with a single track allotted each to zero time (detonation pulse) and to Interrange Instrumentation Group (IRIG) timing signals.

2.1.5 Data Processing

All data were reduced to digital format on the WES high-speed analog-to-digital converter and then processed through the WES digital computer. Processing included baseline correction, filtering, integration routines, and generation of a plot tape. Typical data are presented in the appropriate event section of this report.

Digital filtering routines were applied as necessary to reduce background noise on the data. Filters were generally of the low-pass type. These are listed, for example, as "F2 low-pass 1900 Hz" which indicates an upper frequency response down 5 percent at 1900 Hz.

In order to produce adequate integrations over the relatively long processing times of one second (two seconds for Event 5), baseline corrections were generally applied to the measurements.

2.2 CRATER/EJECTA

These experiments were conducted by the University of New Mexico Civil Engineering Research Facility (CERF) for the Air Force Weapons Laboratory (AFWL).

CERF measured the craters and debris parameters for all events. Four radial lines were surveyed for each crater to determine the parameters for each apparent crater. Figure 2.1 shows a cross section of a typical crater. Permanent displacements were measured by means of displacement pins and sand columns; ejecta areal densities were measured on flat plates; debris enhancement data was collected by using pits, pails and simulated verticle structures in the debris flow field and the wind velocity and direction was recorded at the time of each detonation. The experimental layouts for each event are given in later sections.

Apparent crater volumes range between 6.98 m^3 to 99.42 m^3 on this experimental program. The crater data and the pretest predictions are summarized in Table 2.1. Predicted crater volumes varied from about 31 percent below the actual measured data for the tangent below experiment to about 44 percent above the measured values for the 53.5 TJ half-buried experiment. Both the half-buried 2.09 GJ experiments were predicted to be about 14 percent less than the actual measured values. The probability that this variation is rather typical of the error expected, when current state-of-the-art crater volume prediction procedures are applied, is excellent. Examination of the predicted and measured radii and depths, however, indicates that there is a systematic trend in the errors of the current prediction

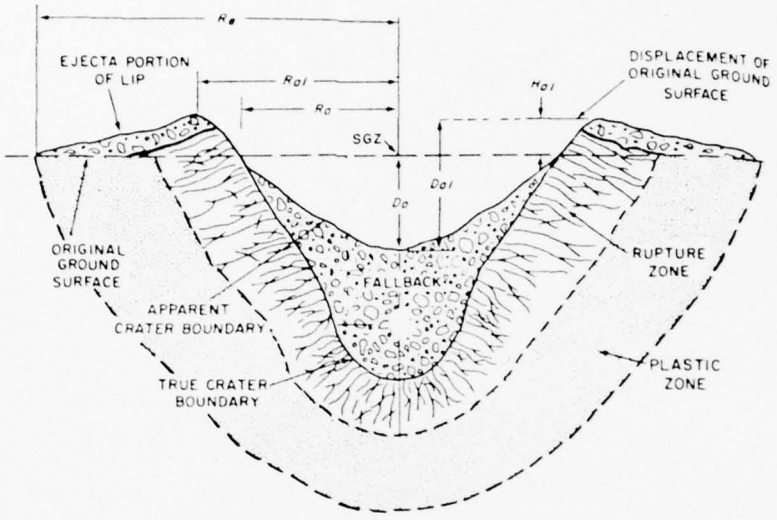

D_a Apparent crater depth

D_{al} Height of the lip crest

H_{al} Height of the lip above the ground surface

R_a Apparent crater radius

R_{al} Radius to the crater lip crest

R_e Radius of continuous ejecta

SGZ Surface ground zero

Figure 2.1. Cross section of a crater.

Table 2.1. Crater predictions versus data for Phase I single burst events.

Event MBI-	Apparent Crater Volume (m^3)		R_a(m)		D_a(m)	
	Predicted	Actual	Predicted	Actual	Predicted	Actual
1	34.05	39.84	3.89	3.72	1.62	2.29
2	11.35	9.36	2.70	2.59	1.12	1.43
3	34.05	39.10	3.89	3.48	1.62	2.47
5	68.09	99.42	4.90	4.58	2.04	3.32
7	10.07	6.98	2.59	2.14	1.08	1.37

procedure. In all cases the radius was overpredicted and the depth underpredicted. These errors in crater volume will be propagated directly into the comparison of the crater related motion and the prediction based on crater volumes.

For the half-buried and tangent-below configurations, the displacements were significantly greater than predicted.

For the surface-tangent configuration the actual and predicted crater volumes were close.

Due to the nature of the soil and moisture content at this test site, the material tended to lump together and to be deposited in rather large masses over the ejecta field. In some cases one or more of these lumps landed on a debris collector, thus, significantly increasing that collector's areal density, while conversely such lumps were deposited just inches away from a collector and its areal density was relatively low. This effect contributed to the wide range of enhancement (higher than average) values. With the limited number of measurements the effectiveness of these structures and pits as enhancement indicators is obfuscated.

2.3 TECHNICAL PHOTOGRAPHY

The technical photography instrumentation was the responsibility of the Denver Research Institute (DRI). WSMR provided equipment and manpower to support technical photography requirements under direction of DRI. Ground level technical photography was supplied by the DRI/WSMR team whereas, aerial technical photographic coverage for the three multiburst events was provided by subcontract from DRI to the Williamson Aircraft Company. The photographic and photoelectric instrumentation consisted of high-speed cameras which ranged in framing rates from 6 to 26,000 frames per second (fr/s) and eight photometric devices with rise times on the order of 1 microsecond (μs). The photometric devices' sensing elements were silicone solar cells.

The technical motion photography effort was designed to provide a detailed record of the detonation sequence to include the fireball growth and interaction (multiple burst events), the shock wave developments, separations and interactions, and the cloud development and interaction. Each of these phenomenon required specialized camera and framing rate applications. The photometric devices were included in this effort in an attempt to monitor first light breakout from the charge surfaces such that a quantitative measure of charge detonation simultaneity could be made for all multiburst events.

Most of the cameras for the single- and multiburst events were located in the main camera bunker south of the test bed area at distances which ranged from approximately 153 to 427 meters (500 to 1,400 feet). Two remote camera stations [located 1829 to 2438 meters (6,000 to 8,000 feet) from SGZ and at approximately a 1.57 radians (90°) angle from each other] were used to photograph the cloud development for each event. The multiple events were also photographically and photometrically covered from three auxiliary stations for Events 4 and 6 and from five auxiliary locations for Event 8.

The photoelectric instrumentation consisted of: (1) six unit light radiation (ULR) devices, (2) one ULR device previously used by DRI on other events, and (3) one total light radiation (TLR) device also used by DRI on other events. The TLR unit was not focused on a single point, rather the unit sensed the presented light radiation from all the charges in the multiple arrays. The eight photometric signals from these devices were recorded on four dual-beam oscilloscopes located in a manned bunker which was situated approximately 213 to 396 meters (700 to 1,300 feet) from SGZ.

SECTION 3

MISERS BLUFF EVENT MBI-1

3.1 DESCRIPTION

The first event of MISERS BLUFF Phase I was conducted on 2 August 1977 at the White Sands Missile Range. This event used a 454-kg (1,000-pound) cast TNT, half-buried sphere to provide single-burst baseline data for multiburst waveform synthesis model development.

3.2 GROUND MOTION AND AIRBLAST EXPERIMENTS

3.2.1 Gage Layout

Ground shock instrumentation covered ranges of 4.57 to 73.2 meters (15 to 240 feet) from SGZ and depths of 0.24 to 12.2 meters (0.67 to 40 feet). Gages were installed principally along a single radian [designated the 0 radian (0°) radial] with supplementary measurements made at 1.57, 3.14 and 4.71 radians (90°, 180°, and 270°). Figure 3.1 presents both a plan view and cross section of the gage array.

3.2.2 Instrumentation

One hundred gages were installed; 74 accelerometers, 18 velocity gages, 5 soil stress gages, and 3 airblast gages. Table 3.1 is a listing of each gage, designated by an arbitrarily assigned measurement number.

3.2.3 Typical Data Results

Calibration and recorder start signals from the timing and firing (T&F) unit were properly received and translated, and all equipment operated as planned for Event MBI-1.

Data recovery was excellent. One vertical accelerometer, measurement No. 1105, yielded no useful data; measurement No. 1103 had considerable background noise and is of questionable usefulness. Several others had small signals relative to the claibration factor, or had signals truncated in time as cables failed, however, all of these produced useful data.

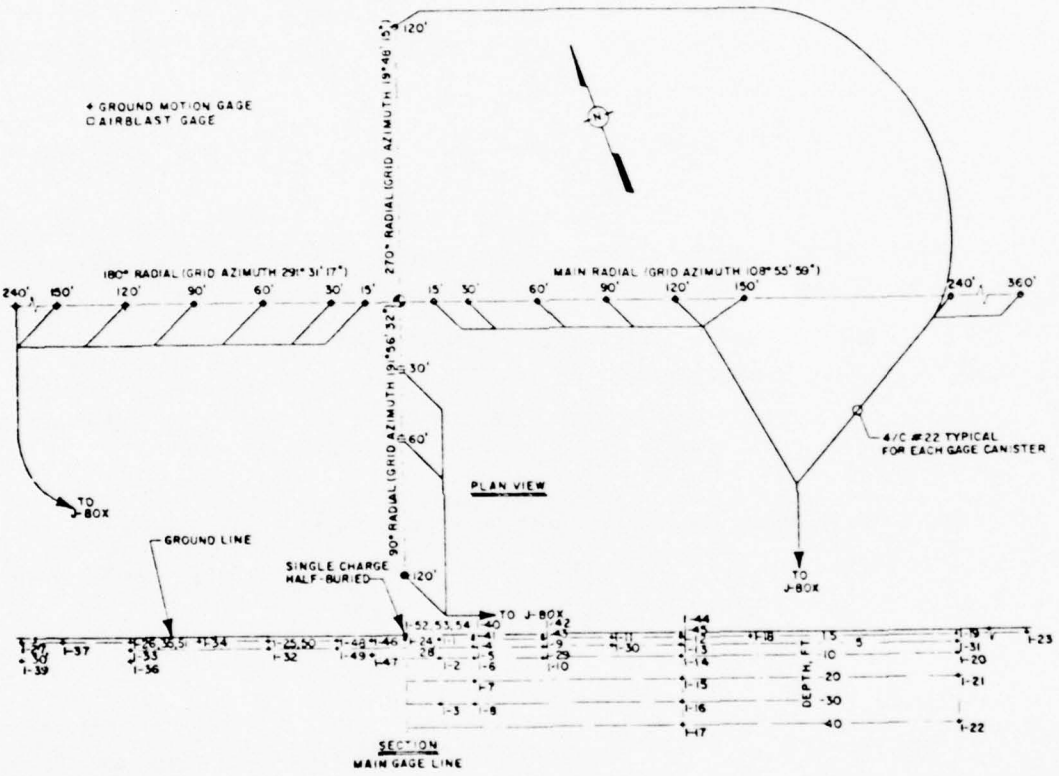

Figure 3.1. Gage layout for MISERS BLUFF Event MBI-1.

Table 3.1. Ground motion and airblast measurement list for Event MBI-1.

Radial		Range		Depth		Measurement Numbers							
Rad	(Deg)	m	(ft)	m	(ft)	AV	AH	AT	UV	UH	SV	SH	AB
0	(0)	4.57	(15)	0.457	(1.5)	1101	1102						
0	(0)	4.57	(15)	0.305	(1.0)	1103	1104						
0	(0)	4.57	(15)	9.14	(30)	1105	1106						
0	(0)	9.14	(30)	0.204	(0.67)	1163	1164						
0	(0)	9.14	(30)	0.305	(1.0)	1165	1166						
0	(0)	9.14	(30)	0.457	(1.5)	1107	1108						
0	(0)	9.14	(30)	1.52	(5)	1109	1110						
0	(0)	9.14	(30)	3.05	(10)	1111	1112						
0	(0)	9.14	(30)	6.10	(20)	1113	1114						
0	(0)	9.14	(30)	9.14	(30)	1115	1116						
0	(0)	18.3	(60)	0.204	(0.67)	1167	1168						
0	(0)	18.3	(60)	0.305	(1.0)	1169	1170						
0	(0)	18.3	(60)	0.457	(1.5)	1117	1118						
0	(0)	18.3	(60)	1.52	(5)						1201		
0	(0)	18.3	(60)	3.05	(10)	1119	1120						
0	(0)	27.4	(90)	0.457	(1.5)	1121	1122						
0	(0)	27.4	(90)	1.52	(5)						1202		
0	(0)	36.6	(120)	0.204	(0.67)	1171	1172						
0	(0)	36.6	(120)	0.305	(1.0)	1173	1174						
0	(0)	36.6	(120)	0.457	(1.5)	1123	1124						
0	(0)	36.6	(120)	1.52	(5)	1125	1126						
0	(0)	36.6	(120)	3.05	(10)	1127	1128						
0	(0)	36.6	(120)	6.10	(20)	1129	1130						
0	(0)	36.6	(120)	9.14	(30)	1131	1132						
0	(0)	36.6	(120)	12.2	(40)	1133	1134						
0	(0)	45.7	(150)	0.457	(1.5)	1135	1136						
0	(0)	73.2	(240)	0.457	(1.5)	1137	1138						
0	(0)	73.2	(240)	1.52	(5)						1203		
0	(0)	73.2	(240)	3.05	(10)	1139	1140						
0	(0)	73.2	(240)	6.10	(20)	1141	1142						
0	(0)	73.2	(240)	12.2	(40)	1143	1144						
0	(0)	109.7	(360)	0.457	(1.5)	1145	1146						

Table 3.1. Ground motion and airblast measurement list for Event MBI-1 (Continued).

Radial		Range		Depth		Measurement Numbers							
Rad	(Deg)	m	(ft)	m	(ft)	AV	AH	AT	UV	UH	SV	SH	AB
1.57	(90)	9.14	(30)	0	(0)								1301
1.57	(90)	18.3	(60)	0	(0)								1302
1.57	(90)	36.6	(120)	0	(0)								1303
1.57	(90)	36.6	(120)	0.457	(1.5)	1147	1148						
3.14	(180)	4.57	(15)	0.457	(1.5)				1707	1709			
3.14	(180)	4.57	(15)	0.457	(1.5)				1708	1710			
3.14	(180)	4.57	(15)	2.44	(8)				1719	1720			
3.14	(180)	9.14	(30)	0.457	(1.5)				1701	1702			
3.14	(180)	9.14	(30)	1.52	(5)				1721	1722			
3.14	(180)	18.3	(60)	0.457	(1.5)	1149	1150						
3.14	(180)	18.3	(60)	0.457	(1.5)				1711	1713			
3.14	(180)	18.3	(60)	0.457	(1.5)				1712	1714			
3.14	(180)	18.3	(60)	1.52	(5)							1204	
3.14	(180)	27.4	(90)	0.457	(1.5)			1157					
3.14	(180)	36.6	(120)	0.457	(1.5)	1151	1152						
3.14	(180)	36.6	(120)	0.457	(1.5)			1158					
3.14	(180)	36.6	(120)	0.457	(1.5)				1715	1717			
3.14	(180)	36.6	(120)	0.457	(1.5)				1716	1718			
3.14	(180)	36.6	(120)	1.52	(5)							1205	
3.14	(180)	36.6	(120)	3.05	(10)			1159					
3.14	(180)	36.6	(120)	0.457	(1.5)			1160					
3.14	(180)	73.2	(240)	0.457	(1.5)	1153	1154						
3.14	(180)	73.2	(240)	0.457	(1.5)			1161					
3.14	(180)	73.2	(240)	3.05	(10)			1162					
4.71	(270)	36.6	(120)	0.457	(1.5)	1155	1156						

NOTES:

AV Vertical Acceleration
AH Horizontal Acceleration
AT Transverse Acceleration
UV Vertical Velocity
UH Horizontal Velocity
SV Vertical Stress
SH Horizontal Stress
AB Airblast

Typical time histories for the following gages are presented in Figure 3.2:

Type of Measurement	Instrumentation Number	Radial Rad	(Deg)	Range m	(ft)	Depth m	(ft)
Vertical Stress (SV)	1201	0	(0)	18.3	(60)	1.52	(5)
Vertical Acceleration (AV)	1117	0	(0)	18.3	(60)	0.457	(1.5)
Vertical Velocity (UV)	1715	3.14	(180)	36.6	(120)	0.457	(1.5)
Airblast (AB)	1301	1.57	(90)	9.14	(30)	0	(0)

Figure 3.3 shows the comparison of measured and predicted vertical velocity waveforms at the 18.3 meter range and at a depth of 0.457 meter.

3.3 CRATER AND EJECTA EXPERIMENTS

3.3.1 Crater and Ejecta Collector Layout

Four radial lines were surveyed to determine the parameters for the apparent crater. Free field areal density measurements were made along four radials. Several types of debris collection devices were used. Figure 3.4 shows the debris sampling array layout.

3.3.2 Results

The average apparent values for the Event MBI-1 crater are:

Volume: 39.8 m^3 (1404 ft^3)
Radius: 3.72 meters (12.2 feet)
Depth below SGZ: 2.26 meters (7.4 feet)

The maximum depth recorded along the survey lines was 2.29 meters (7.5 feet). Figure 3.5 is a plot of the crater profiles. Local meterological conditions were not measured at the time of this event.

Free field areal density measurements were made along four radials. Average values of the areal densities for these radials with the maximum and minimum values for each range are shown in Figure 3.6. The line through the average value points represents the power curve fit to a linear regression model. The relatively wide spread between the minimum-maximum values is attributed to effects of the wind, the lump nature of the ejecta field and the usual nonuniformity of debris distribution (rays).

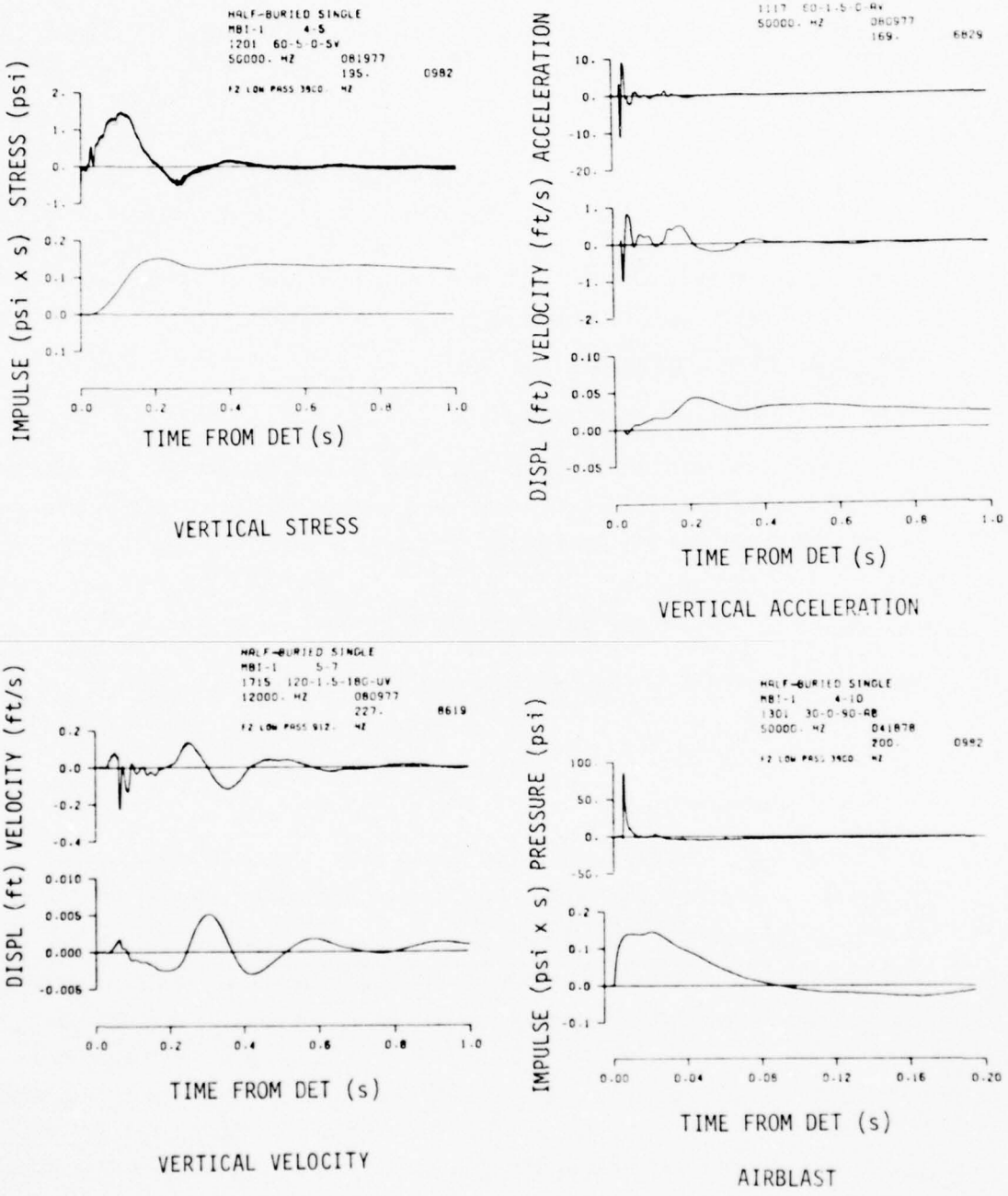

Figure 3.2. Typical time histories for Event MBI-1.

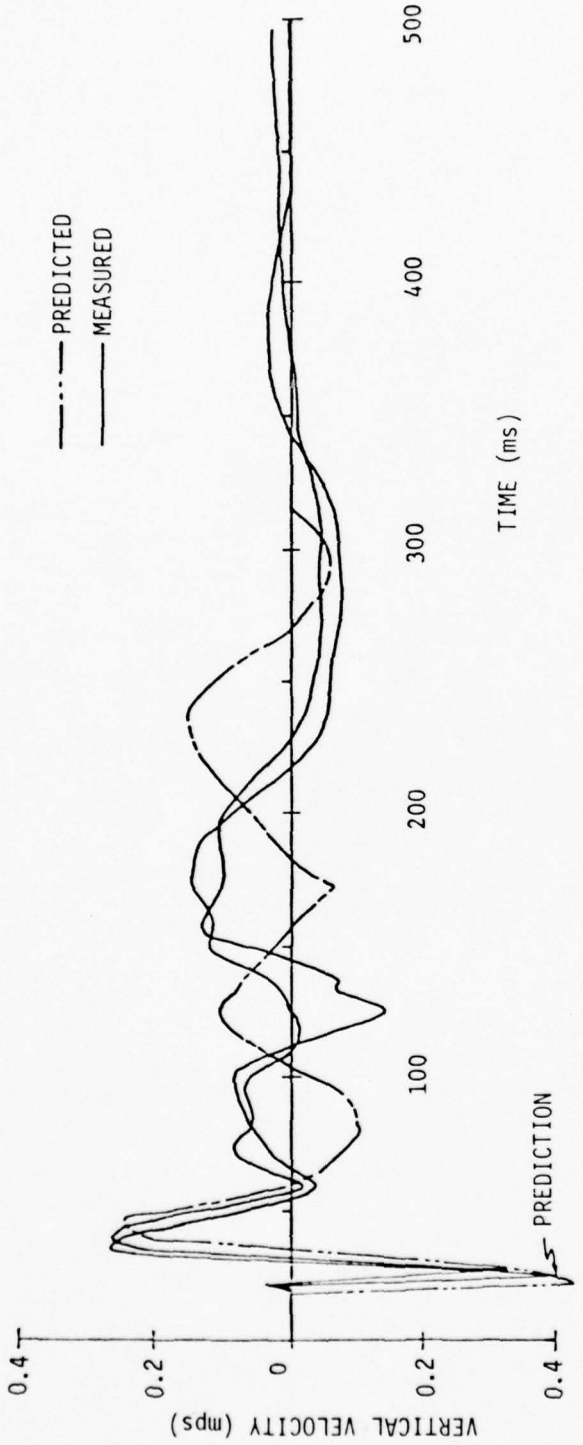

Figure 3.3. Event MBI-1, comparison of measured and predicted vertical velocity waveforms at the 18.3 meter range and 0.457 meter depth.

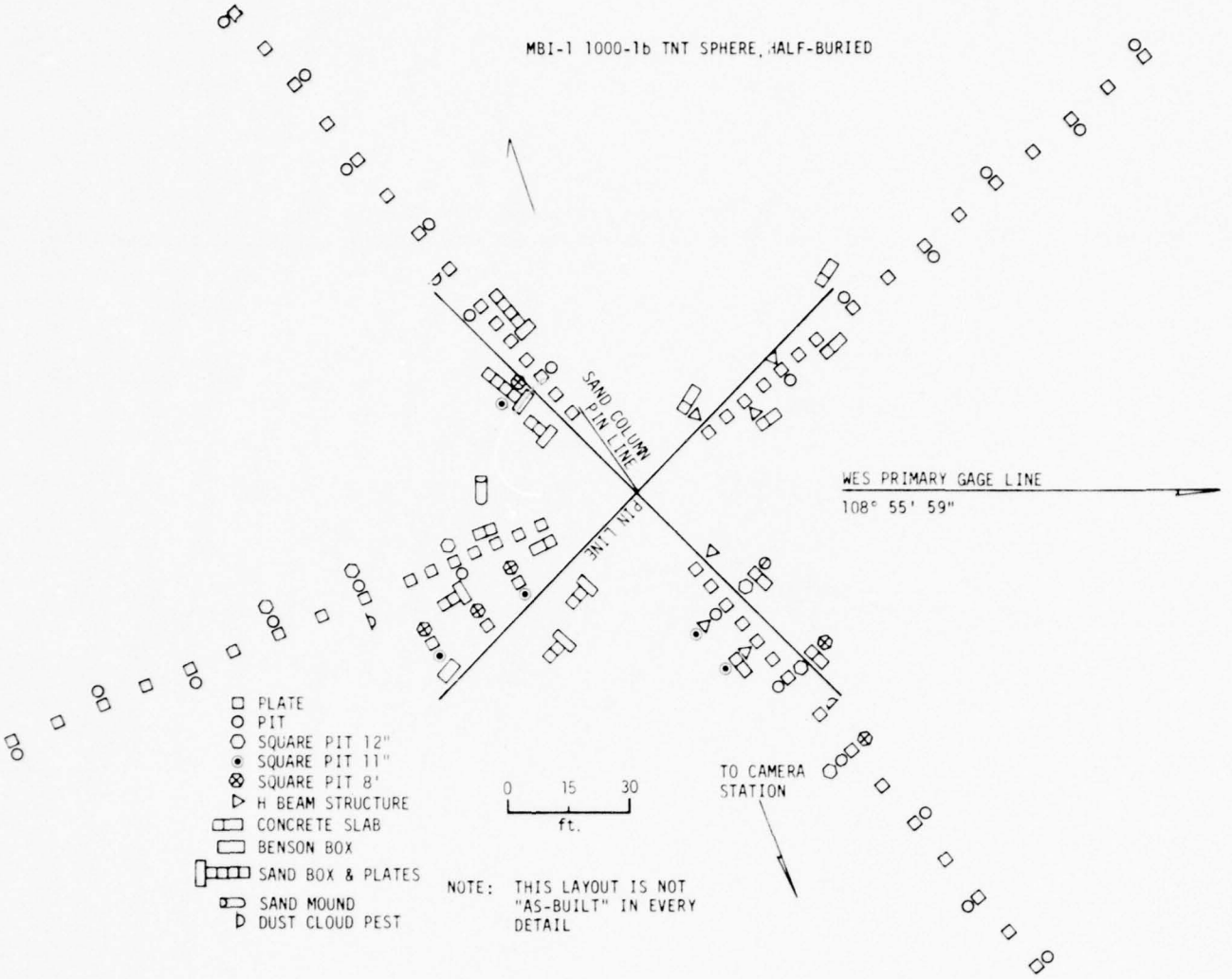

Figure 3.4. Debris collector layout for Event MBI-1.

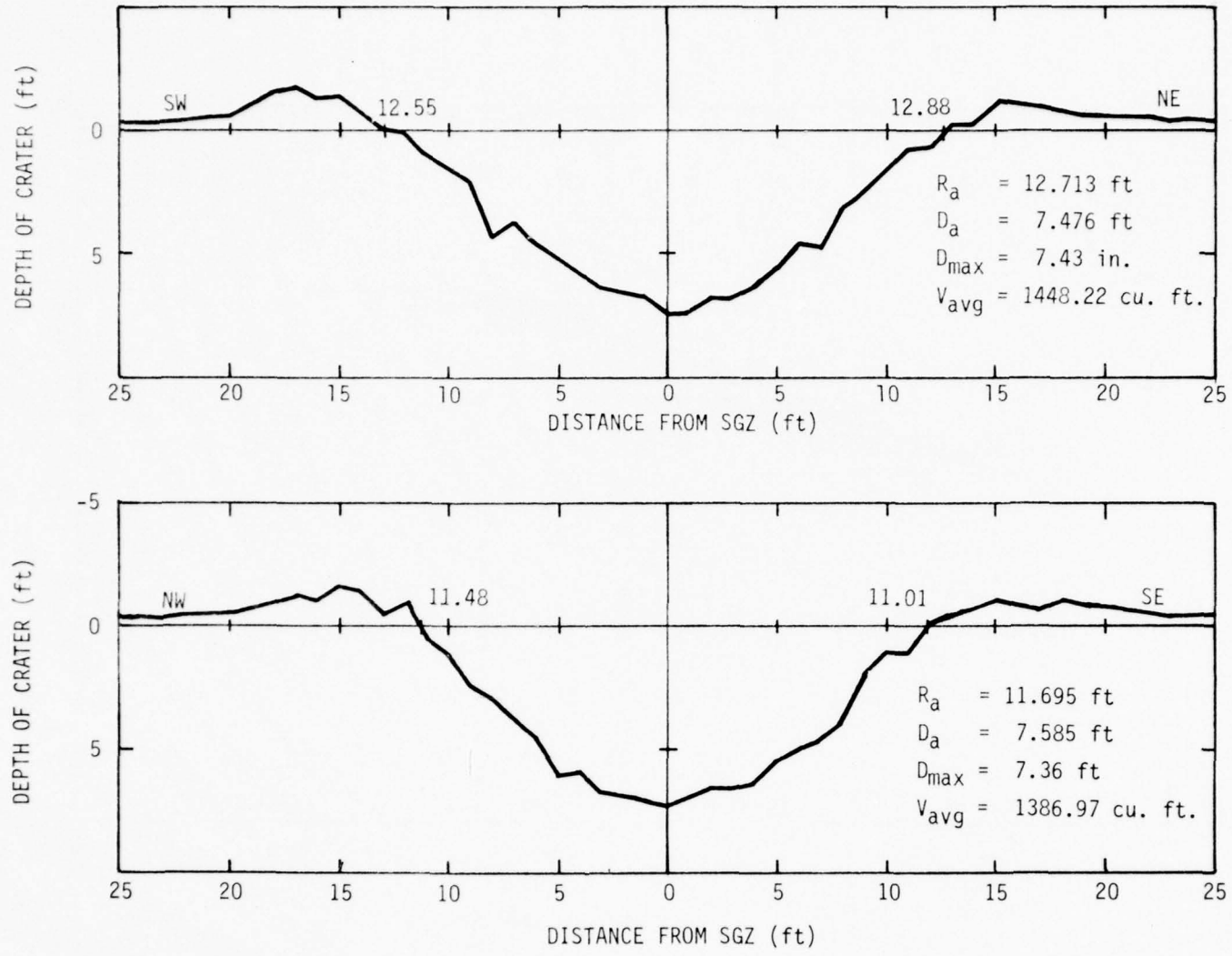

Figure 3.5. Event MBI-1 crater profiles.

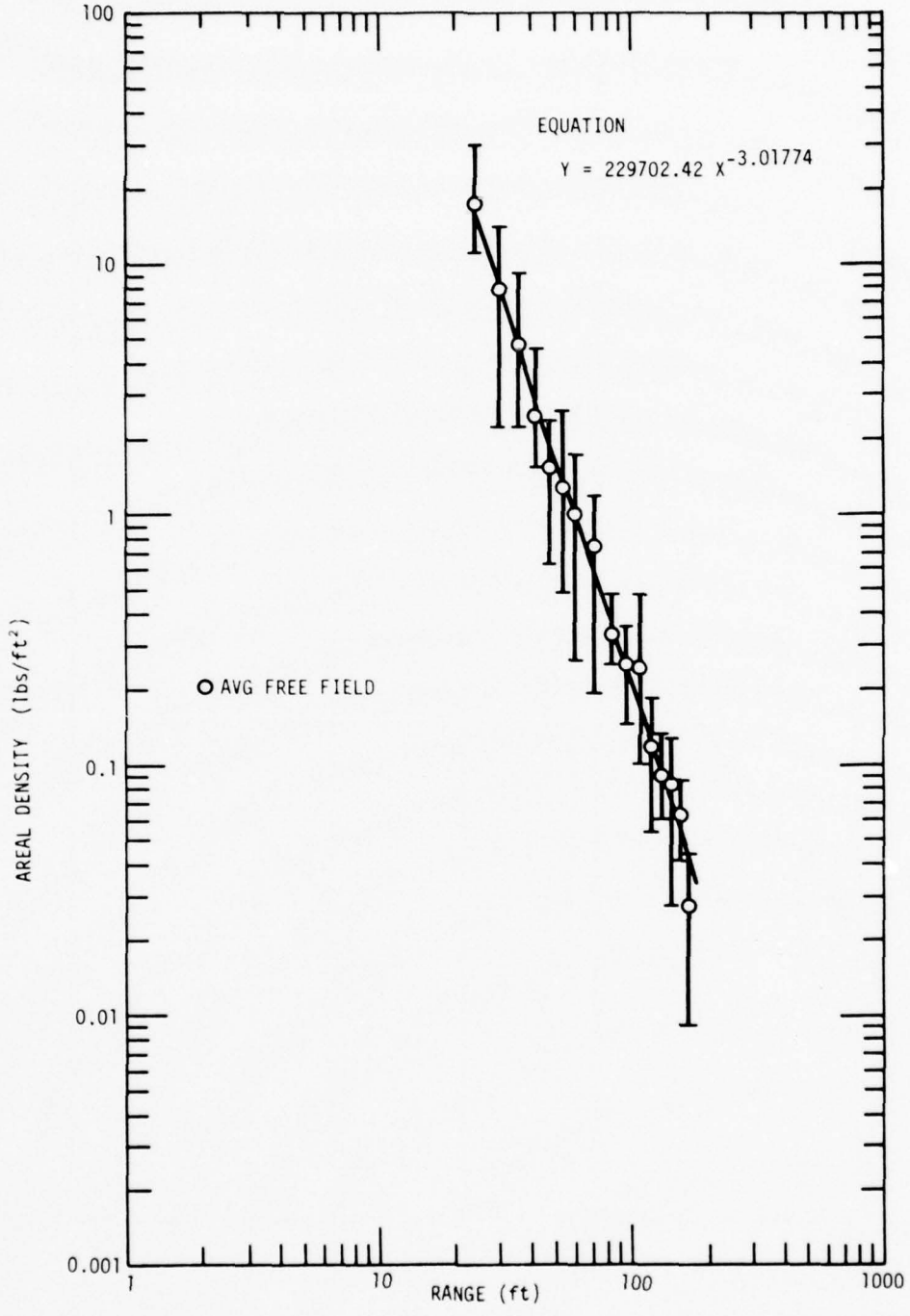

Figure 3.6. Event MBI-1, average free field areal density versus range.

Figure 3.7 shows the average debris depth on the free field plates and in the round pits with the scatter for each versus range, both debris depth and range are normalized by the cube root of the apparent crater volume. The curves plotted on this graph are the predictions for maximum, median (dashed-line), and minimum debris depth, given the actual MBI-1 apparent crater volume.

The four radials of permanent displacement data were averaged. Figure 3.8 is a plot of the average vertical displacement with the scatter at each range shown.

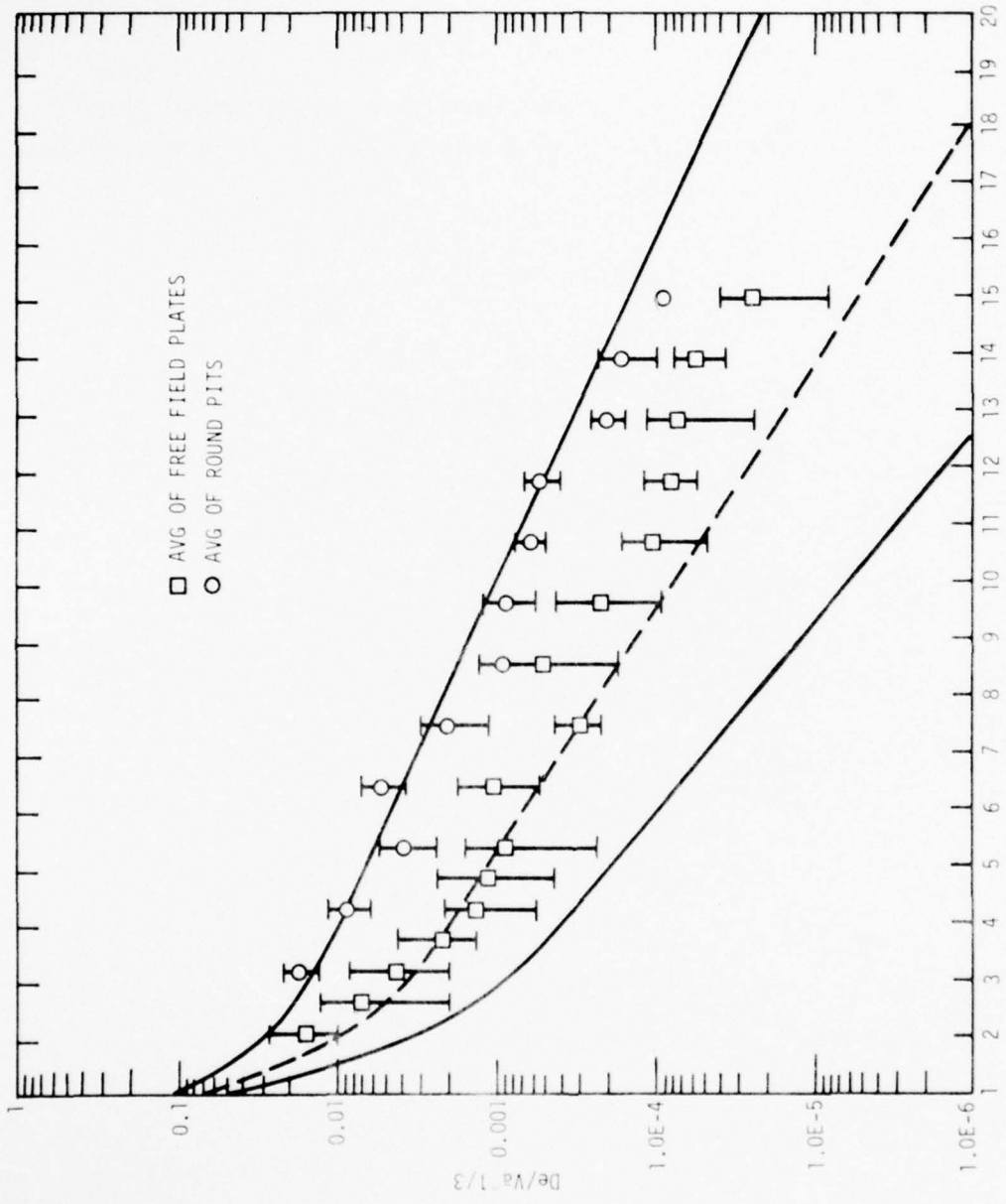

Figure 3.7. Event MBI-1, debris depth versus range both normalized by $V_a^{1/3}$.

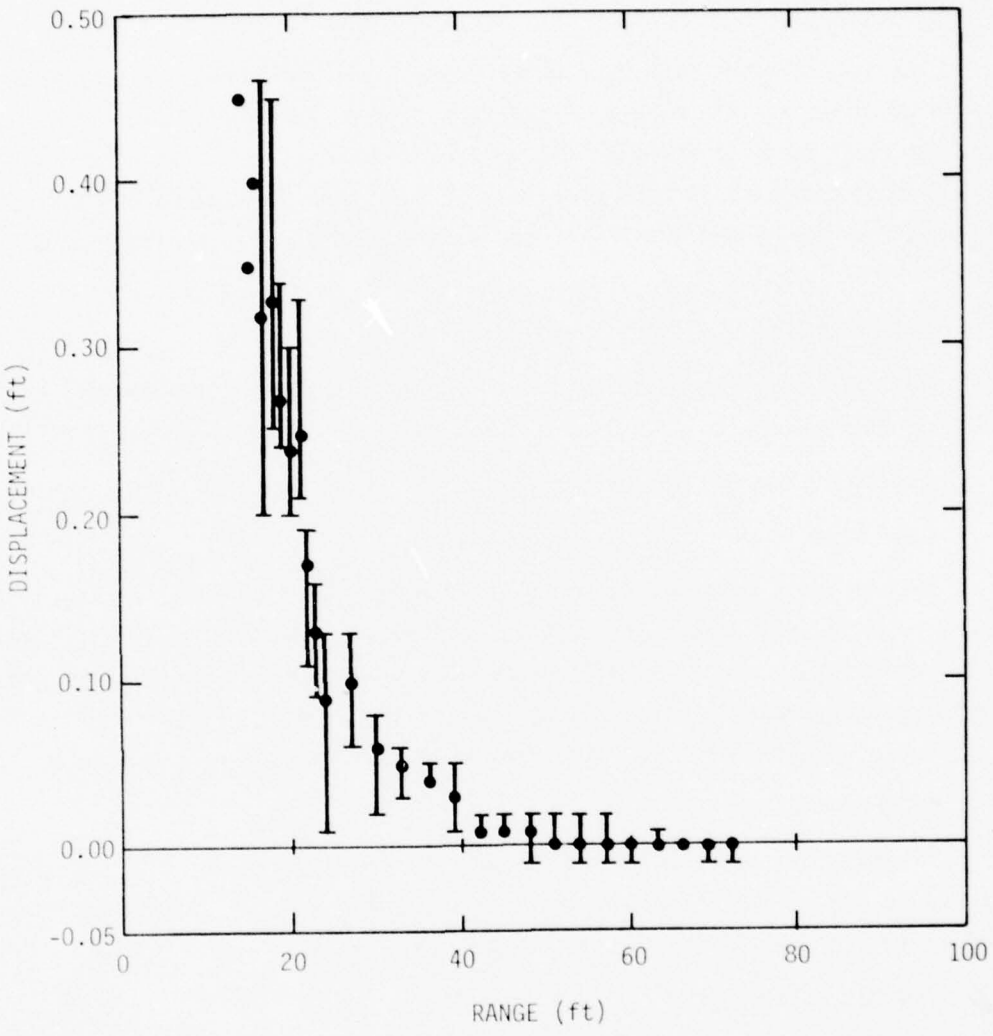

Figure 3.8. Event MBI-1, average permanent vertical displacement versus range.

SECTION 4

MISERS BLUFF EVENT MBI-2

4.1 DESCRIPTION

The second event of MISERS BLUFF Phase I was conducted on 15 August 1977 at the White Sands Missile Range. This event used a 454-kg (1,000-pound) cast TNT, surface-tangent sphere to identify the half-buried versus the tangent sphere phenomenological differences in ground shock at the outrunning ground ranges. (Outrunning ranges are those where the crater-induced ground motions precede those induced by overpressure "airslap".)

4.1.1 Water Content

Soil moisture data were obtained for Event MBI-2 and are shown in Table 4.1 and plotted in Figure 4.1.

4.2 GROUND MOTION AND AIRBLAST EXPERIMENTS

4.2.1 Gage Layout

Ground shock instrumentation covered ranges of 3.96 to 42.7 meters (13 to 140 feet) from SGZ and depths of 0.204 to 12.2 meters (0.67 to 40 feet). Gages were installed principally along a single radial [designated the 0 radian (0°) radial] with supplementary measurements made at 1.57, 3.14 and 4.71 radians (90°, 180° and 270°). Figure 4.2 presents both plan view and cross section of the gage array.

4.2.2 Instrumentation

Ninety-eight gages were installed: 72 accelerometers, 18 velocity gages, 5 soil stress gages, and 3 airblast gages. Table 4.2 is a listing of each gage, denoted by an arbitrarily assigned measurement number.

4.2.3 Typical Data Records

Calibration and recorder start signals from the timing and firing (T&F) unit were properly received and translated. All equipment operated as planned for Event MBI-2.

Data recovery was excellent. Two accelerometers produced data of questionable quality. Measurement No. 2105 showed a peculiar response at shock arrival, and measurement No. 2116 was beset with 60 Hz background noise which could not be filtered out. The remainder of the gages produced good data.

Table 4.1. Water content test record.

Depth		% Moisture Content			
m	ft	10 Aug 77	12 Aug 77	13 Aug 77	15 Aug 77
0 - 0.0305	0 - 0.1				10.5
0 - 0.0366	0 - 0.12		19.0[1]		
0 - 0.0488	0 - 0.16			14.9	
0 - 0.152	0 - 0.5	11.1			
0.305 - 0.152	0.1 - 0.5				8.4
0.0366 - 0.152	0.12 - 0.5		6.7		
0.0488 - 0.152	0.16 - 0.5			7.9	
0.305 - 0.457	1 - 1.5	15.2	13.2	13.2	14.3
0.610 - 0.762	2 - 2.5	15.4			14.8
0.914 - 1.067	3 - 3.5	19.9			18.5
1.22 - 1.37	4 - 4.5	21.0			20.6

[1] 36.6 cm (0.12 ft) upper layer wet due to morning rain.

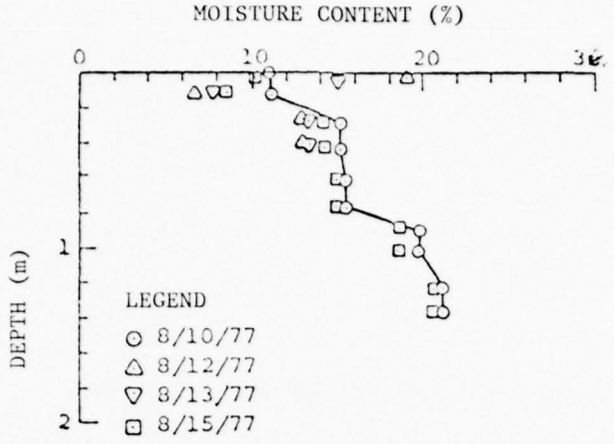

Figure 4.1. Moisture content data for MBI-2.

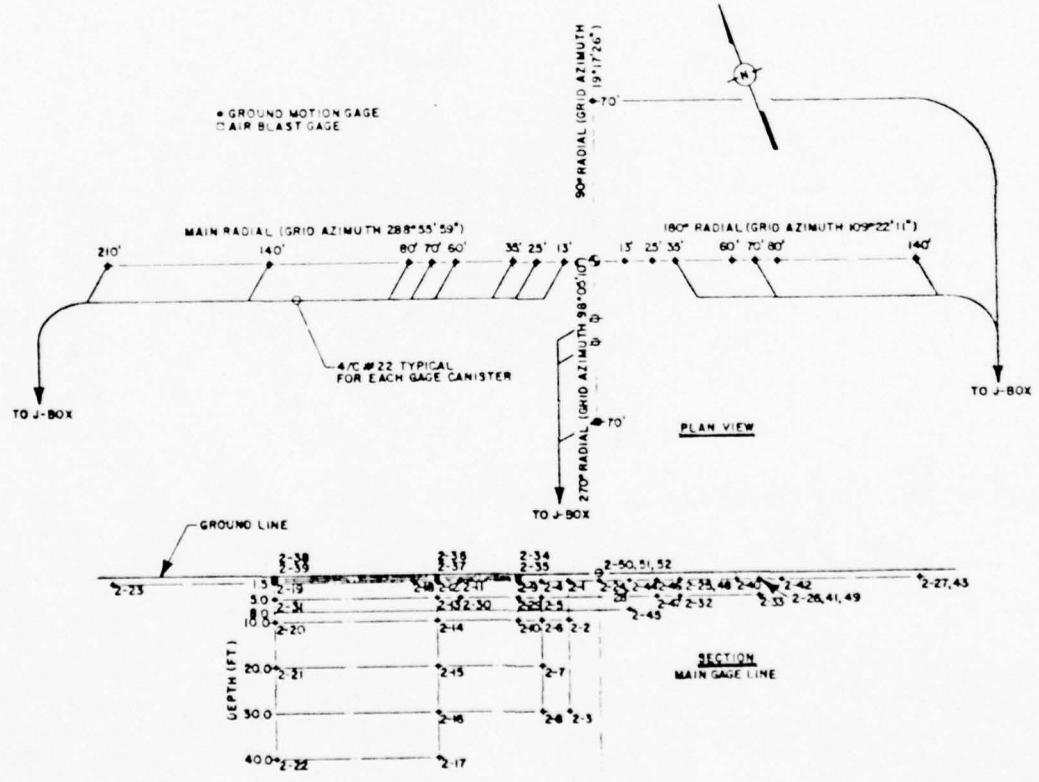

Figure 4.2. Gage layout for MISERS BLUFF Event MBI-2.

Table 4.2. Ground motion and airblast measurement list for Event MBI-2.

Radial		Range		Depth		Measurement Numbers							
Rad	(Deg)	m	(ft)	m	(ft)	AV	AH	AT	UV	UH	SV	SH	AB
0	(0)	3.96	(13)	0.457	(1.5)	2101	2102						
0	(0)	3.96	(13)	3.05	(10)	2103	2104						
0	(0)	3.96	(13)	9.14	(30)	2105	2106						
0	(0)	7.62	(25)	0.457	(1.5)	2107	2108						
0	(0)	7.62	(25)	1.52	(5)	2109	2110						
0	(0)	7.62	(25)	3.05	(10)	2111	2112						
0	(0)	7.62	(25)	6.10	(20)	2113	2114						
0	(0)	7.62	(25)	9.14	(30)	2115	2116						
0	(0)	10.7	(35)	0.204	(0.67)	2163	2164						
0	(0)	10.7	(35)	0.305	(1.0)	2165	2166						
0	(0)	10.7	(35)	0.457	(1.5)	2117	2118						
0	(0)	10.7	(35)	1.52	(5)						2201		
0	(0)	10.7	(35)	3.05	(10)	2119	2120						
0	(0)	18.3	(60)	0.457	(1.5)	2121	2122						
0	(0)	18.3	(60)	1.52	(5)						2202		
0	(0)	21.3	(70)	0.204	(0.67)	2167	2168						
0	(0)	21.3	(70)	0.305	(1.0)	2169	2170						
0	(0)	21.3	(70)	0.457	(1.5)	2123	2124						
0	(0)	21.3	(70)	1.52	(5)	2125	2126						
0	(0)	21.3	(70)	3.05	(10)	2127	2128						
0	(0)	21.3	(70)	6.10	(20)	2129	2130						
0	(0)	21.3	(70)	9.14	(30)	2131	2132						
0	(0)	21.3	(70)	12.2	(40)	2133	2134						
0	(0)	24.4	(80)	0.457	(1.5)	2135	2136						
0	(0)	42.7	(140)	0.204	(0.67)	2171	2172						
0	(0)	42.7	(140)	0.305	(1.0)	2173	2174						
0	(0)	42.7	(140)	0.457	(1.5)	2137	2138						
0	(0)	42.7	(140)	1.52	(5)						2203		
0	(0)	42.7	(140)	3.05	(10)	2139	2140						
0	(0)	42.7	(140)	6.1	(20)	2141	2142						
0	(0)	42.7	(140)	12.2	(40)	2143	2144						
0	(0)	64.0	(210)	0.457	(1.5)	2145	2146						

Table 4.2. Ground motion and airblast measurement list for Event MBI-2 (Continued).

Radial		Range		Depth		Measurement Numbers							
Rad	(Deg)	m	(ft)	m	(ft)	AV	AH	AT	UV	UH	SV	SH	AB
1.57	(90)	21.3	(70)	0.457	(1.5)	2147	2148						
3.14	(180)	3.96	(13)	0.457	(1.5)				2707	2709			
3.14	(180)	3.96	(13)	0.457	(1.5)				2708	2710			
3.14	(180)	3.96	(13)	2.44	(8)				2719	2720			
3.14	(180)	7.62	(25)	0.457	(1.5)				2701	2702			
3.14	(180)	7.62	(25)	1.52	(5)				2721	2722			
3.14	(180)	10.7	(35)	0.457	(1.5)	2149	2150						
3.14	(180)	10.7	(35)	0.457	(1.5)				2711	2713			
3.14	(180)	10.7	(35)	0.457	(1.5)				2712	2714			
3.14	(180)	10.7	(35)	1.52	(5)							2204	
3.14	(180)	18.3	(60)	0.457	(1.5)			2157					
3.14	(180)	21.3	(70)	0.457	(1.5)	2151	2152						
3.14	(180)	21.3	(70)	0.457	(1.5)			2158					
3.14	(180)	21.3	(70)	0.457	(1.5)				2715	2717			
3.14	(180)	21.3	(70)	0.457	(1.5)				2716	2718			
3.14	(180)	21.3	(70)	1.52	(5)							2205	
3.14	(180)	24.4	(80)	0.457	(1.5)			2160					
3.14	(180)	42.7	(140)	0.457	(1.5)	2153	2154						
3.14	(180)	42.7	(140)	0.457	(1.5)			2161					
4.71	(270)	7.62	(25)	0	(0)								2301
4.71	(270)	10.7	(35)	0	(0)								2302
4.71	(270)	21.3	(70)	0	(0)								2303
4.71	(270)	21.3	(70)	0.457	(1.5)	2155	2156						

NOTES:

AV Vertical Acceleration
AH Horizontal Acceleration
AT Transverse Acceleration
UV Vertical Velocity
UH Horizontal Velocity
SV Vertical Stress
SH Horizontal Stress
AB Airblast

Typical time histories of the following gages are in Figure 4.3.

Type of Measurement	Instrumentation Number	Radial		Range		Depth	
		Rad	(deg)	m	(ft)	m	(ft)
Vertical Stress (SV)	2202	0	(0)	18.3	(60)	1.52	(5)
Vertical Acceleration (AV)	2121	0	(0)	18.3	(60)	0.45	(1.5)
Vertical Velocity (UV)	2715	3.14	(180)	21.3	(70)	0.45	(1.5)
Airblast (AB)	2301	4.71	(270)	7.62	(25)	0	(0)

Figure 4.4 shows the comparison of measured and predicted peak values of airblast induced velocity for several measurement depths.

4.3 CRATER AND EJECTA EXPERIMENTS

4.3.1 Crater and Ejecta Collector Layout

Four radial lines were surveyed to determine the parameters for the apparent crater. Free field areal density measurements were made along four radials. Figure 4.5 shows the debris sampling array layout.

4.3.2 Results

The average apparent values for the Event MBI-2 crater are:

Volume:	9.34 m^3 (330 ft^3)
Radius:	2.59 meters (8.5 feet)
Depth below SGZ:	1.40 meters (4.6 feet)

Maximum depth recorded along the survey lines was 1.42 meters (4.7 feet). Figure 4.6 is a plot of the individual crater profiles. The wind speed at the time of the test was 16.1 km/h (10 mph) from about 4.80 radians (275°) as indicated on Figure 4.5.

Free field areal density measurements were made along four radials. Average values of the areal density for these radials with the maximum and minimum values for each range are shown in Figure 4.7. The line through the average value points represents the power curve fit to a linear regression model. The relatively wide spread between the minimum-maximum values is attributed to effects of the wind, the lumpy nature of the ejecta field, and the usual rays of nonuniformity in the debris distribution.

Several types of collection devices were used to obtain debris enhancement information. The primary enhancement collector devices were 5-gallon paint

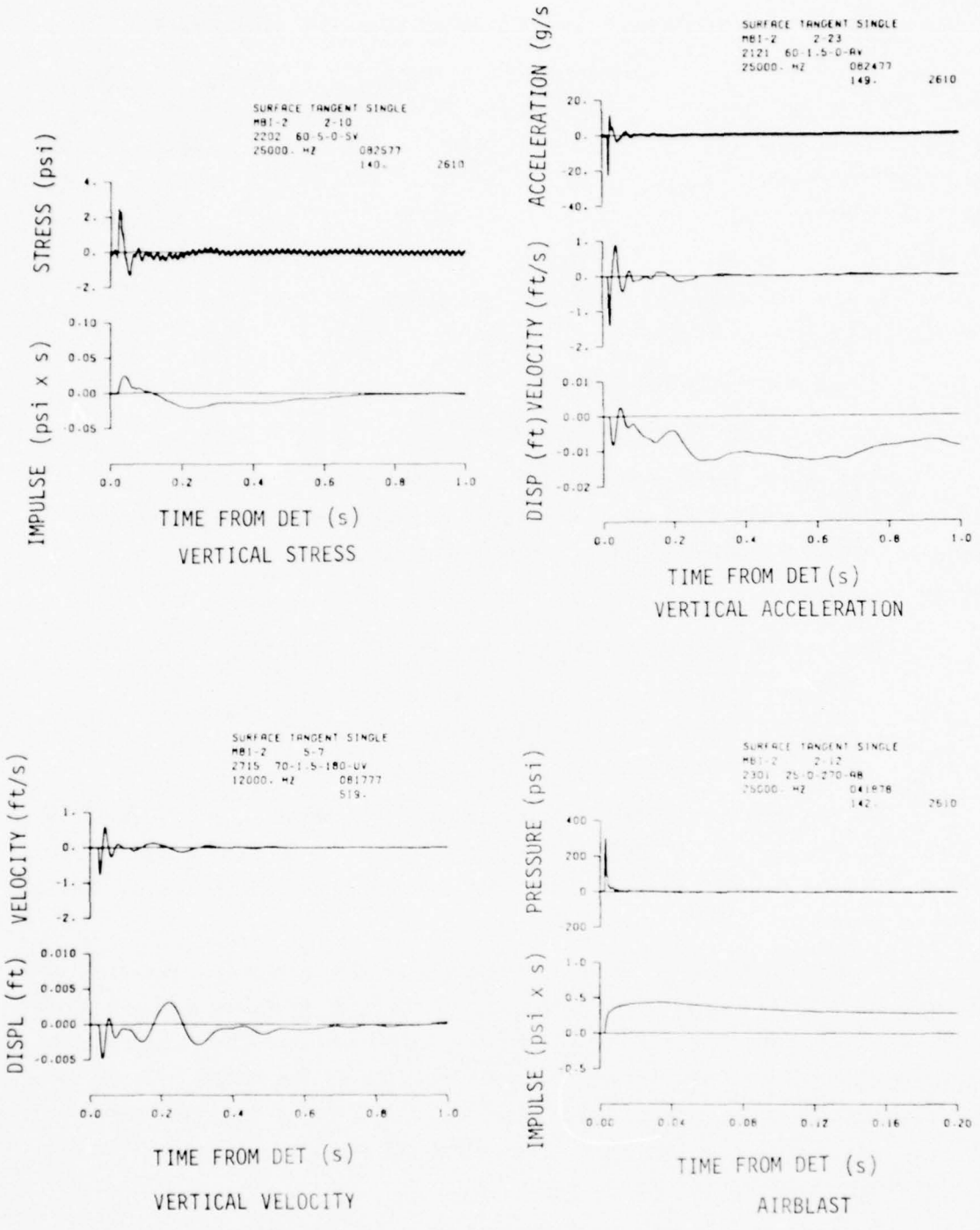

Figure 4.3. Typical time histories for Event MBI-2.

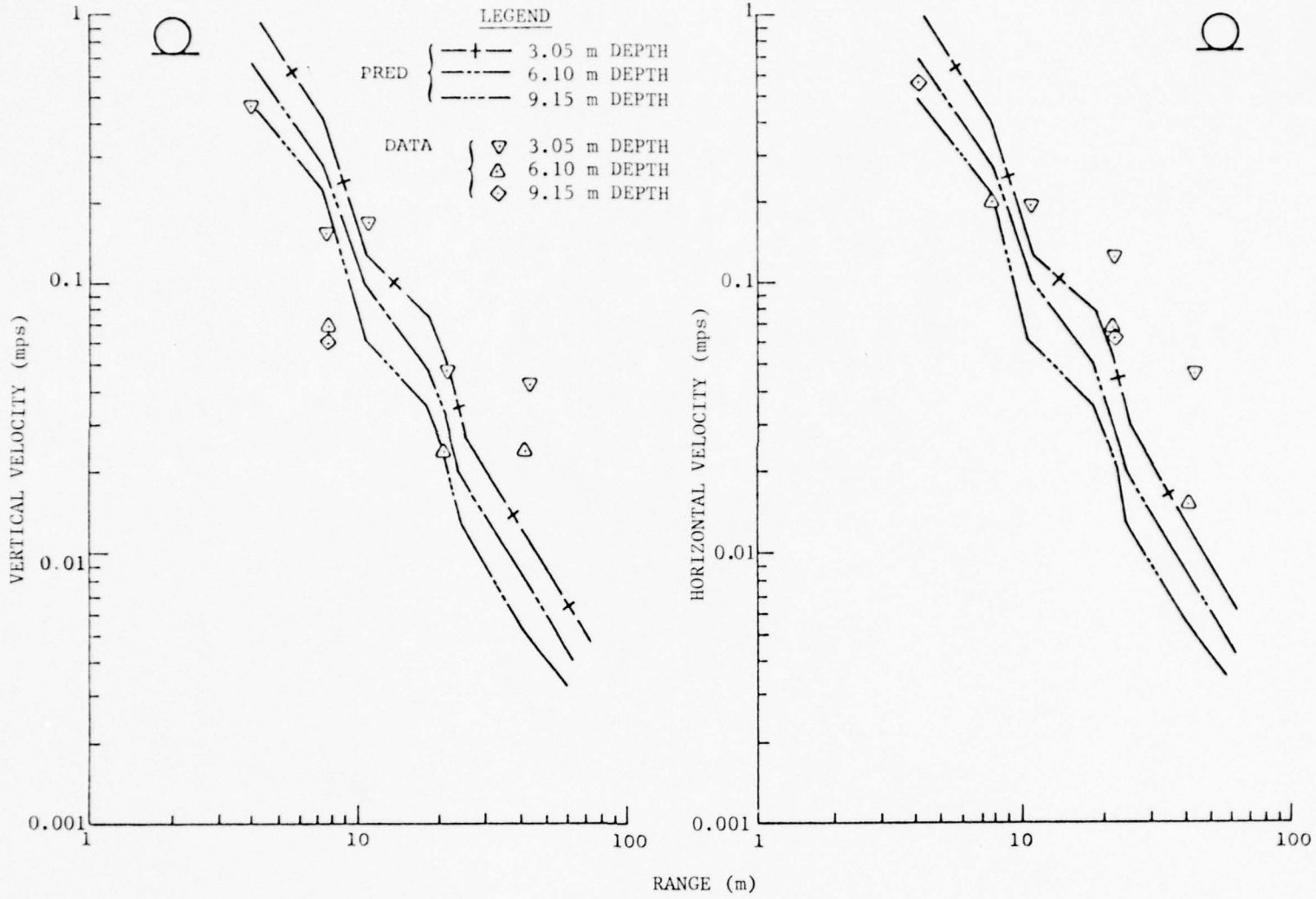

Figure 4.4. Comparison of measured and predicted peak values of airblast induced velocity below the 1.52 meter depth (MBI-2).

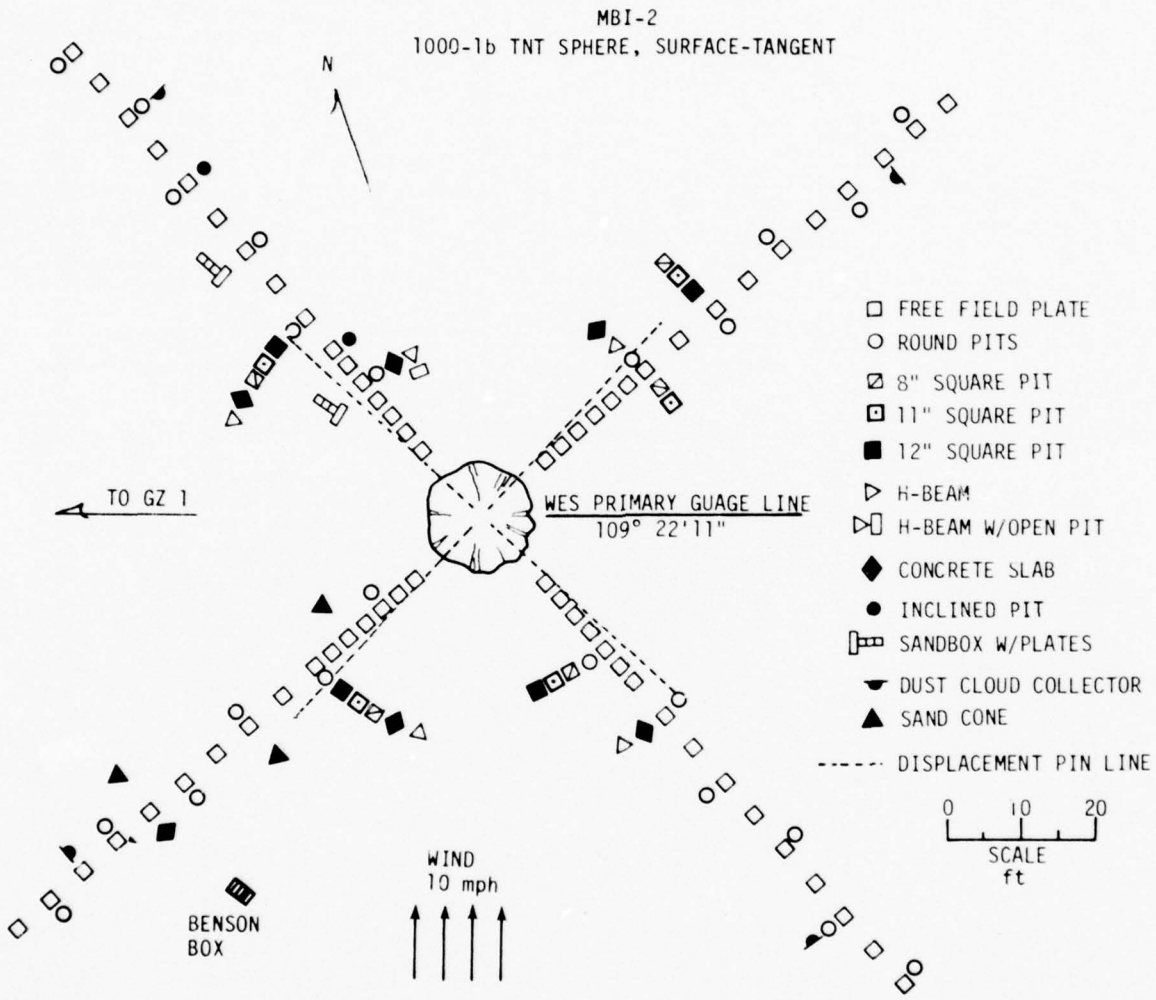

Figure 4.5. Debris collector layout for Event MBI-2.

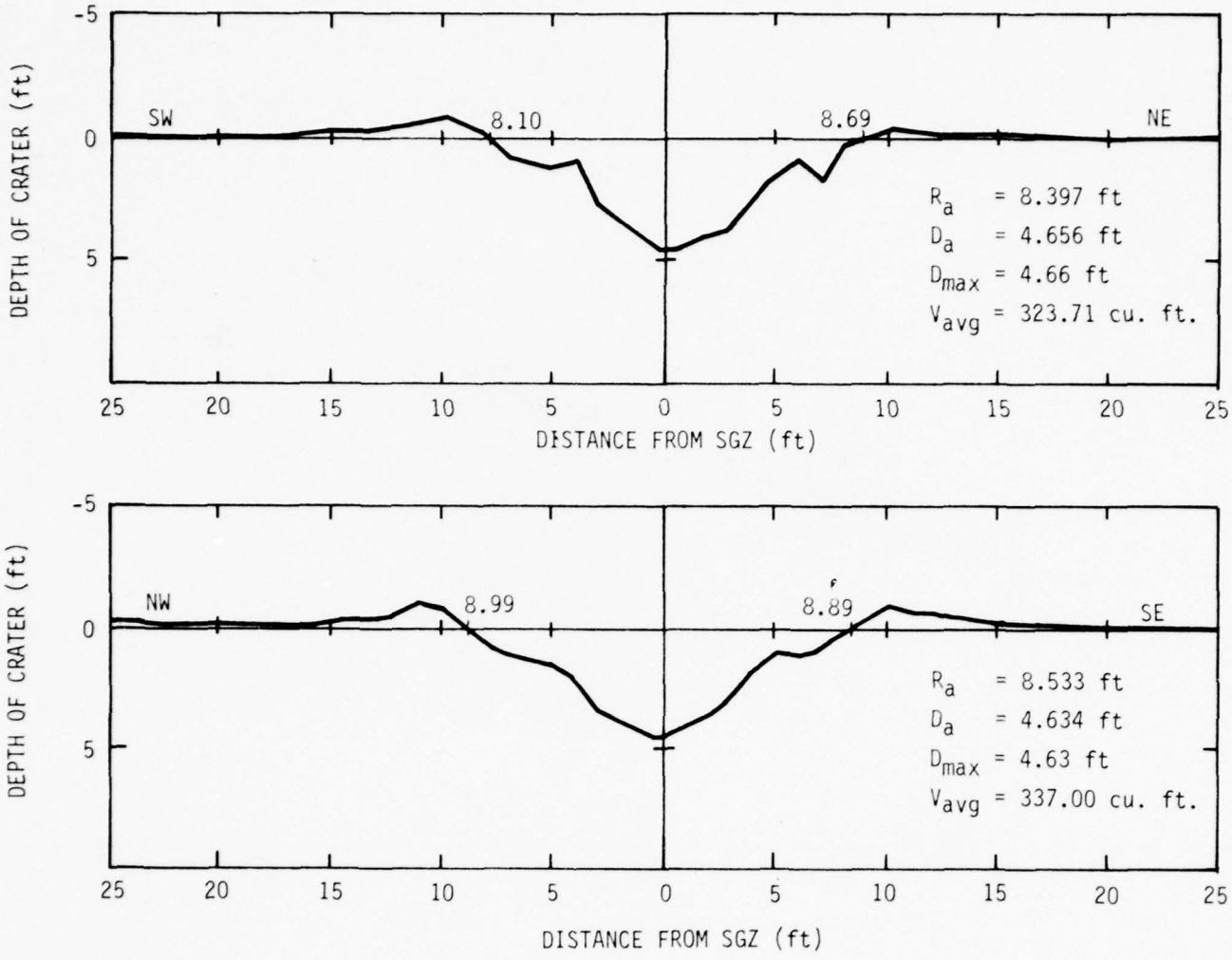

Figure 4.6. Event MBI-2 crater profiles.

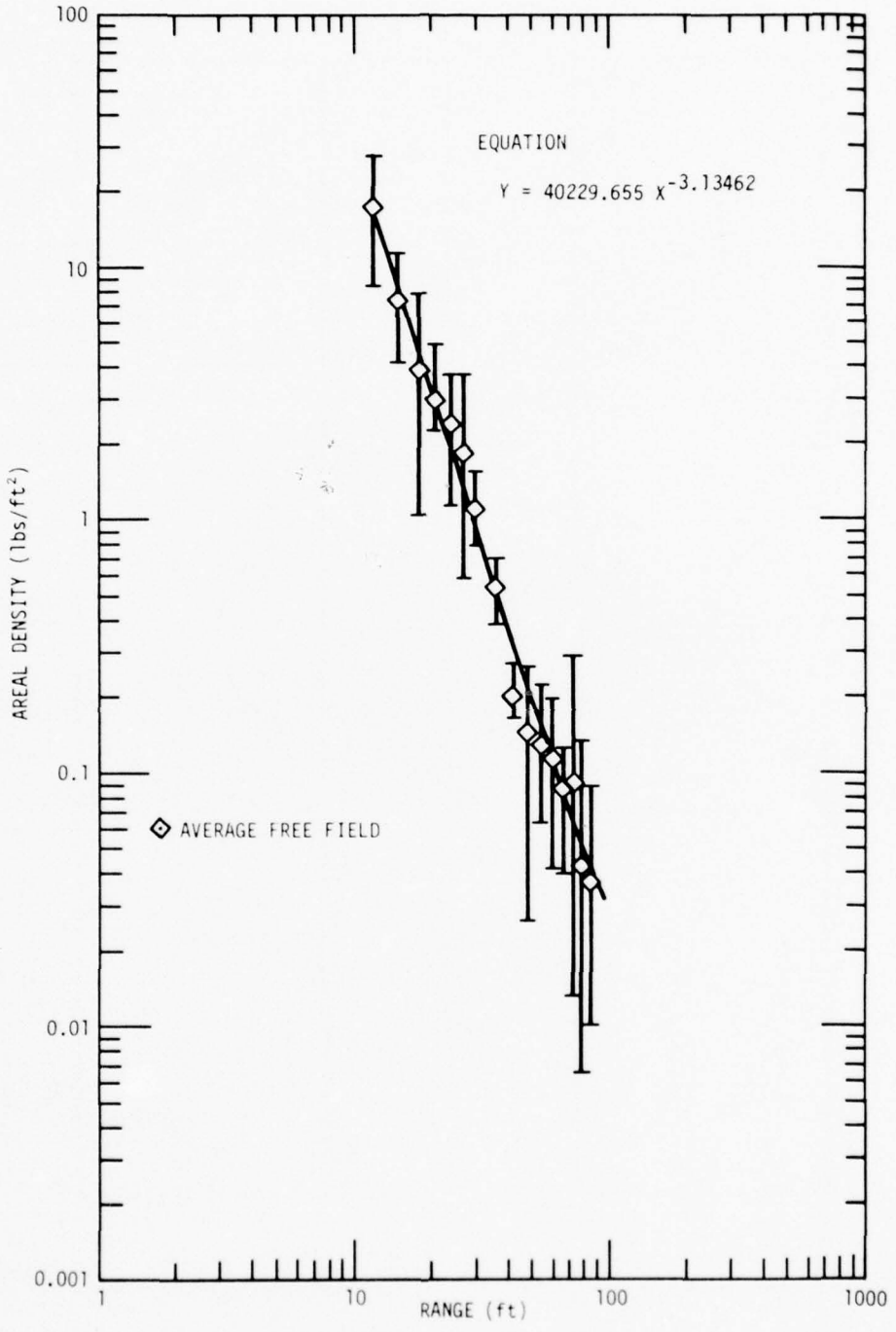

Figure 4.7. Event MBI-2, average free field areal density versus range.

buckets set in the ground (round pits). Various sized square boxes were also used as pits. Vertical steel plates and concrete slabs were used as aboveground structures. The survivability of some of these collectors was poor due to high overpressures.

Figure 4.8 shows the average debris depth of the free field plates and the round pits with scatter for each range; both debris depth and range have been normalized by the cube root of the apparent crater volume. The curves plotted on this graph are the predictions for maximum, median (dashed-line), and minimum debris depth given the actual MBI-2 apparent crater volume.

The four radials of permanent ground displacement were measured. Figure 4.9 is a plot of the average vertical displacement with scatter at each range shown.

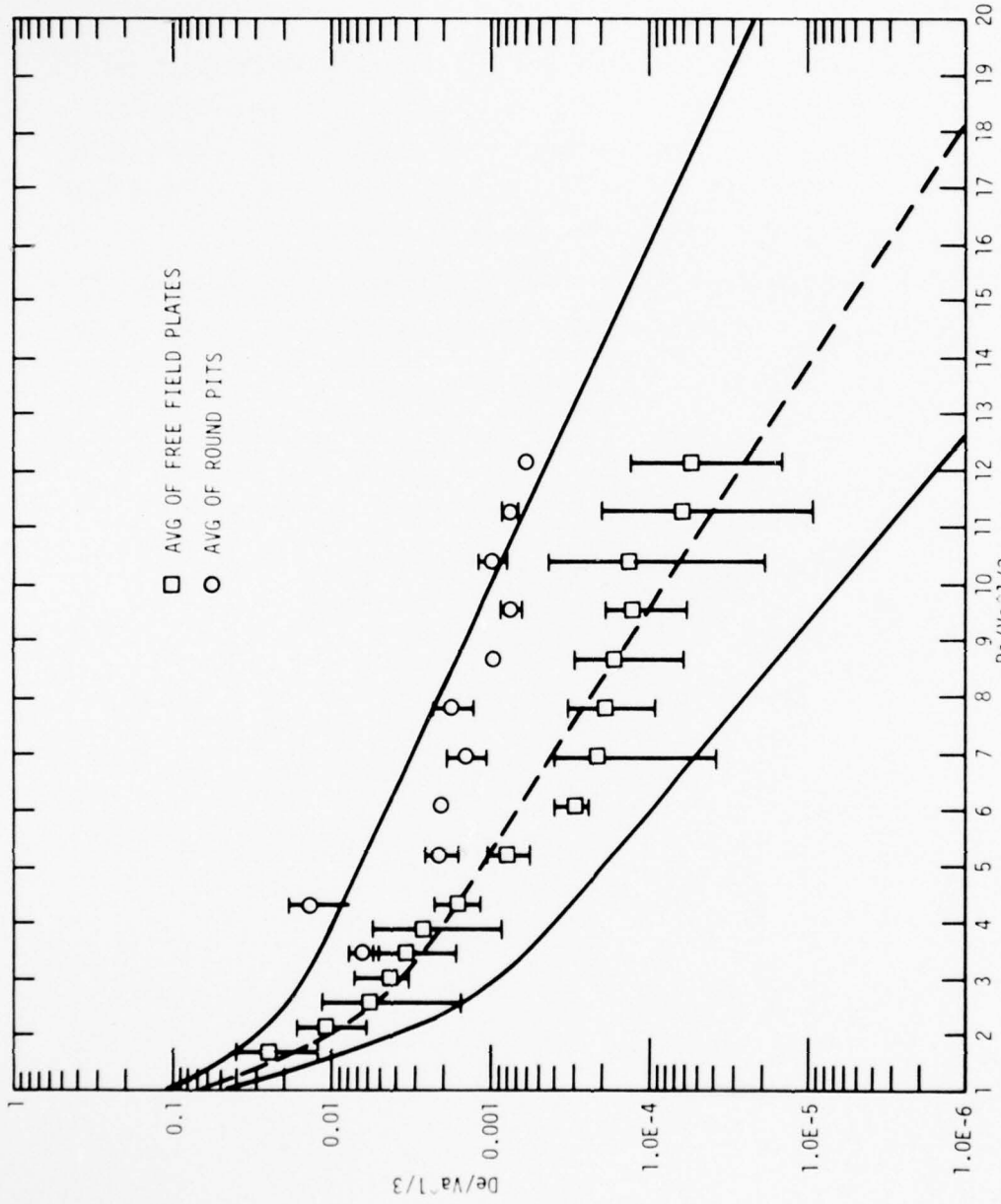

Figure 4.8. Event MBI-2, debris depth versus range, both normalized by $V_a^{1/3}$.

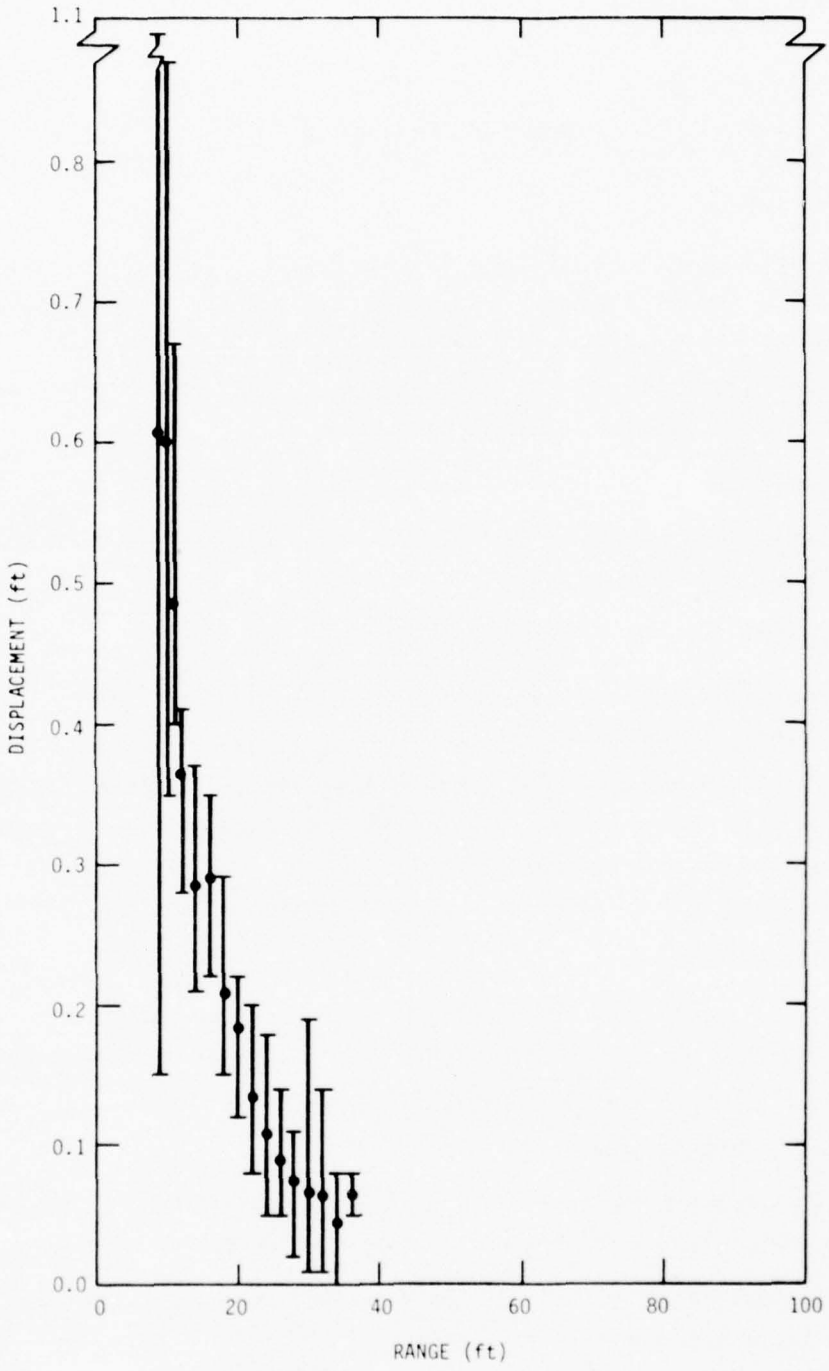

Figure 4.9. Event MBI-2, average permanent vertical displacement versus range.

SECTION 5

MISERS BLUFF EVENT MBI-3

5.1 DESCRIPTION

The third event of MISERS BLUFF Phase I was conducted on 23 August 1977 at the White Sands Missile Range. This event used a 454-kg (1,000-pound) cast TNT, half-buried sphere similar to Event MBI-1, but included a more fully instrumented "Plateau" region, i.e., the intermediate distance region where peak values of ground motion are little attenuated with range.

5.1.1 Water Content

Soil moisture data were obtained for Event MBI-3 and are shown in Table 5.1 and are plotted in Figure 5.1.

5.2 GROUND MOTION AND AIRBLAST EXPERIMENTS

5.2.1 Gage Layout

Ground shock instrumentation covered ranges of 4.57 to 1.097 meters (15 to 360 feet) from SGZ and depths of 0.457 to 6.1 meters (1.5 to 20 feet). Gages were installed principally along a single radial (designated the 0° radial) with supplementary measurements made at 1.57, 3.14 and 4.71 radians (90°, 180° and 270°). Figure 5.2 presents both a plan view and cross section of the gage array.

5.2.2 Instrumentation

Sixty-six gages were installed; 48 accelerometers, 10 velocity gages, 5 soil stress gages, and 3 airblast gages. Table 5.2 is a listing of each gage, denoted by an arbitrarily assigned measurement number.

5.2.3 Typical Data Records

Calibration and recorder start signals from the T&F unit were properly received and translated, and all equipment operated as planned for Event MBI-3.

Data recovery was excellent. Only one accelerometer, measurement No. 3106, failed to produce good quality data.

Table 5.1. Event MBI-3 water content test record.

	Depth m	Depth (ft)	% Moisture
22 Aug 77	0 - 0.152	(0 - 0.5)	9.6
	0.305 - 0.457	(1.0 - 1.5)	14.2
	0.610 - 0.762	(2.0 - 2.5)	14.4
	0.914 - 1.067	(3.0 - 3.5)	18.3
	1.22 - 1.37	(4.0 - 4.5)	22.6
23 Aug 77	0 - 0.152	(0 - 0.5)	7.8
	0.305 - 0.457	(1.0 - 1.5)	13.7
	0.610 - 0.762	(2.0 - 2.5)	14.7
	0.914 - 1.067	(3.0 - 3.5)	19.0
	1.22 - 1.37	(4.0 - 4.5)	20.1

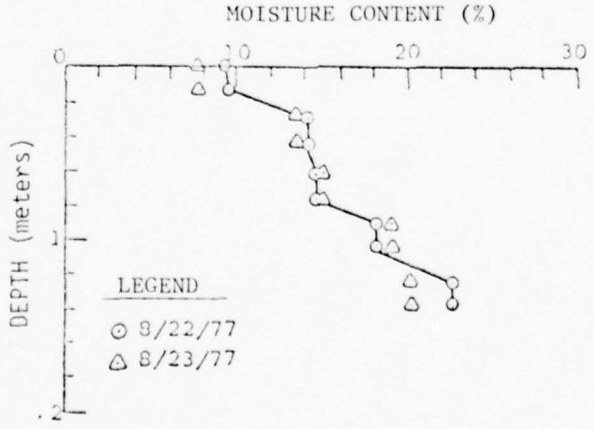

Figure 5.1. Event MBI-3 moisture content data.

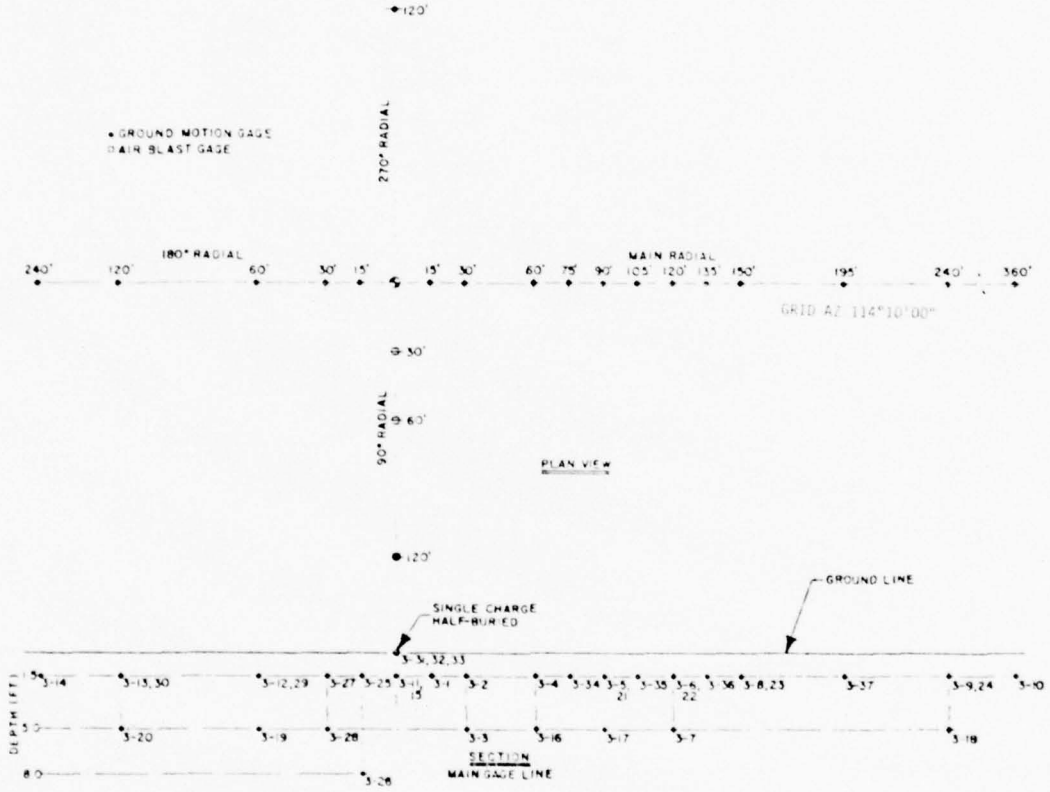

Figure 5.2. Gage layout for MISERS BLUFF Event MBI-3.

Table 5.2. Ground motion and airblast measurement list for Event MBI-3.

Radial		Range		Depth		Measurement Numbers							
Rad	(Deg)	m	(ft)	m	(ft)	AV	AH	AT	UV	UH	SV	SH	AB
0	(0)	4.57	(15)	0.457	(1.5)	3101	3102						
0	(0)	9.14	(30)	0.457	(1.5)	3103	3104						
0	(0)	9.14	(30)	0.457	(1.5)				3701	3702			
0	(0)	9.14	(30)	1.52	(5)	3105	3106						
0	(0)	9.14	(30)	6.10	(20)	3135	3136						
0	(0)	18.3	(60)	0.457	(1.5)	3107	3108						
0	(0)	18.3	(60)	0.457	(1.5)				3711	3713			
0	(0)	18.3	(60)	0.457	(1.5)				3712	3714			
0	(0)	18.3	(60)	1.52	(5)						3201		
0	(0)	22.9	(75)	0.457	(1.5)	3141	3142						
0	(0)	27.4	(90)	0.457	(1.5)	3109	3110						
0	(0)	27.4	(90)	1.52	(5)						3202		
0	(0)	32.0	(105)	0.457	(1.5)	3143	3144						
0	(0)	36.6	(120)	0.457	(1.5)	3111	3112						
0	(0)	36.6	(120)	0.457	(1.5)				3715	3717			
0	(0)	36.6	(120)	0.457	(1.5)				3716	3718			
0	(0)	36.6	(120)	1.52	(5)	3113	3114						
0	(0)	36.6	(120)	6.1	(20)	3137	3138						
0	(0)	41.1	(135)	0.457	(1.5)	3145	3146						
0	(0)	45.7	(150)	0.457	(1.5)	3115	3116						
0	(0)	59.4	(195)	0.457	(1.5)	3147	3148						
0	(0)	73.2	(240)	0.457	(1.5)	3117	3118						
0	(0)	73.2	(240)	1.52	(5)						3203		
0	(0)	73.2	(240)	6.1	(20)	3139	3140						
0	(0)	109.7	(360)	0.457	(1.5)	3119	3120						
1.57	(90)	9.14	(30)	0	(0)								3301
1.57	(90)	18.3	(60)	0	(0)								3302
1.57	(90)	36.6	(120)	0	(0)								3303
1.57	(90)	36.6	(120)	0.457	(1.5)	3121	3122						
3.14	(180)	18.3	(60)	0.457	(1.5)	3123	3124						
3.14	(180)	18.3	(60)	1.52	(5)							3204	
3.14	(180)	27.4	(90)	0.457	(1.5)			3131					

Table 5.2. Ground motion and airblast measurement list for Event MBI-3 (Continued).

Radial		Range		Depth		Measurement Numbers							
Rad	(Deg)	m	(ft)	m	(ft)	AV	AH	AT	UV	UH	SV	SH	AB
3.14	(180)	36.6	(120)	0.457	(1.5)	3125	3126						
3.14	(180)	36.6	(120)	0.457	(1.5)			3132					
3.14	(180)	36.6	(120)	1.52	(5)							3205	
3.14	(180)	45.7	(150)	0.457	(1.5)			3133					
3.14	(180)	73.2	(240)	0.457	(1.5)	3127	3128						
3.14	(180)	73.2	(240)	0.457	(1.5)			3134					
4.71	(270)	36.6	(120)	0.457	(1.5)	3129	3130						

NOTES:

AV Vertical Acceleration
AH Horizontal Acceleration
AT Transverse Acceleration
UV Vertical Velocity
UH Horizontal Velocity
SV Vertical Stress
SH Horizontal Stress
AB Airblast

Typical time histories for the following gages are presented in Figure 5.3.

Type of Measurement	Instrumentation Number	Radial		Range		Depth	
		Rad	(Deg)	m	(ft)	m	(ft)
Vertical Stress (SV)	3202	0	(0)	27.4	(90)	1.52	(5)
Vertical Acceleration (AV)	3111	0	(0)	36.6	(120)	0.457	(1.5)
Vertical Velocity (UV)	3715	0	(0)	36.6	(120)	0.457	(1.5)
Airblast (AB)	3303	1.57	(90)	36.6	(120)	0	(0)

Figure 5.4 shows the comparison of measured and predicted overpressure and impulse data for the half-buried configuration.

5.3 CRATER AND EJECTA EXPERIMENTS

5.3.1 Crater and Collector Layout

Four radial lines were surveyed to determine the parameters for the apparent crater(s). Free field areal density measurements were made along four radials. Several different types of debris collection devices were used as shown in Figure 5.5.

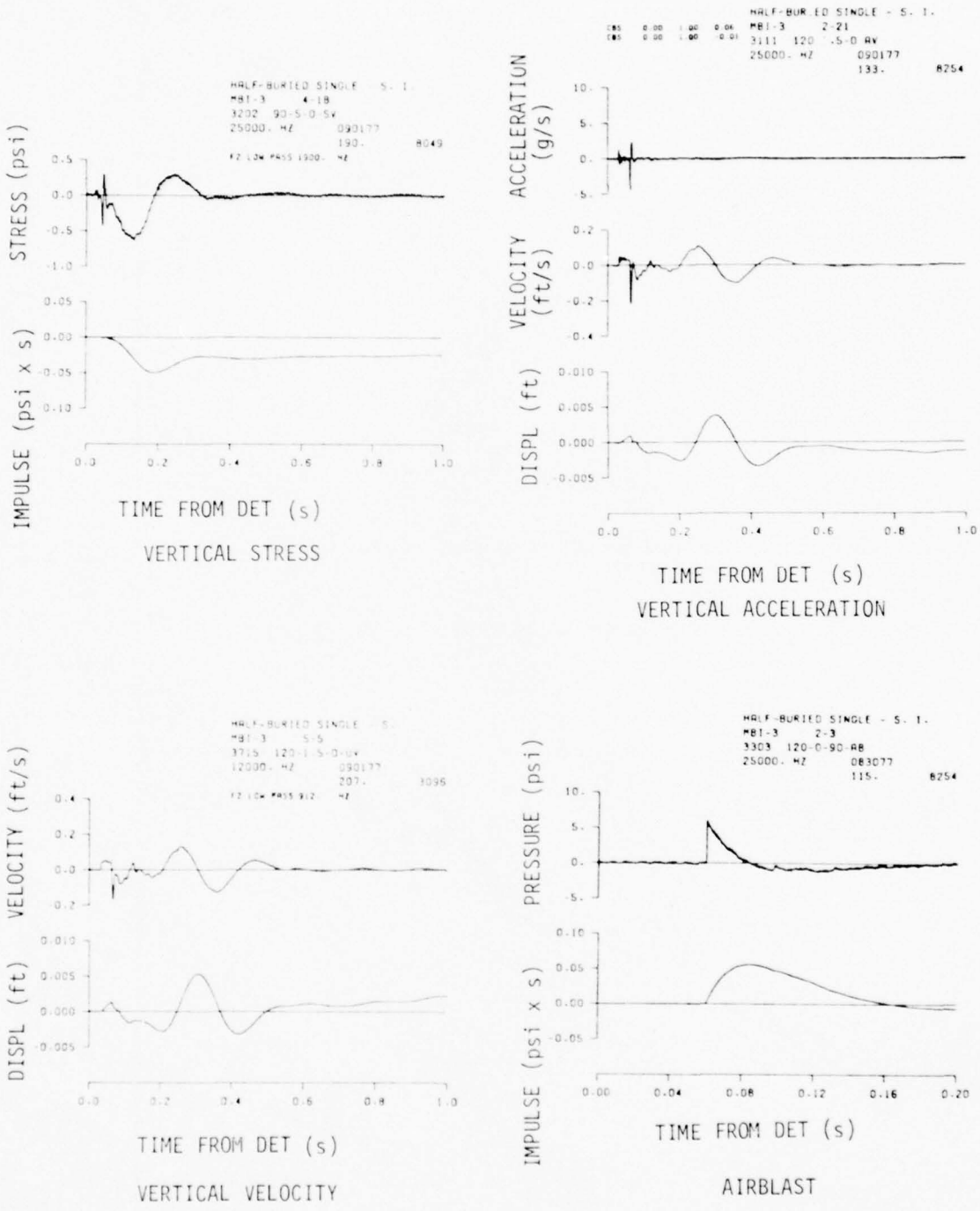

Figure 5.3. Typical time histories for Event MBI-3.

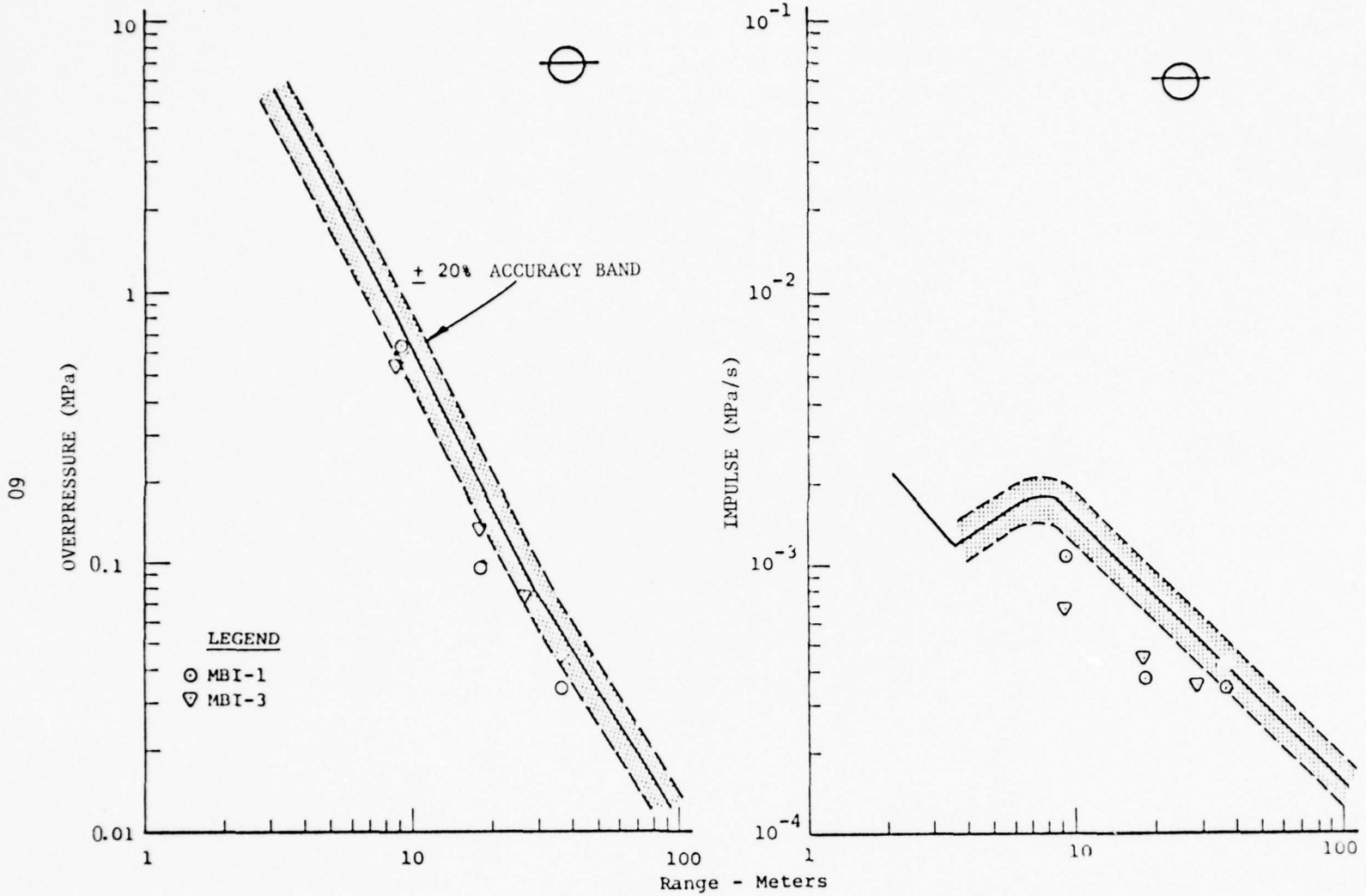

Figure 5.4. Overpressure and impulse data compared with predictions for the half-buried configuration.

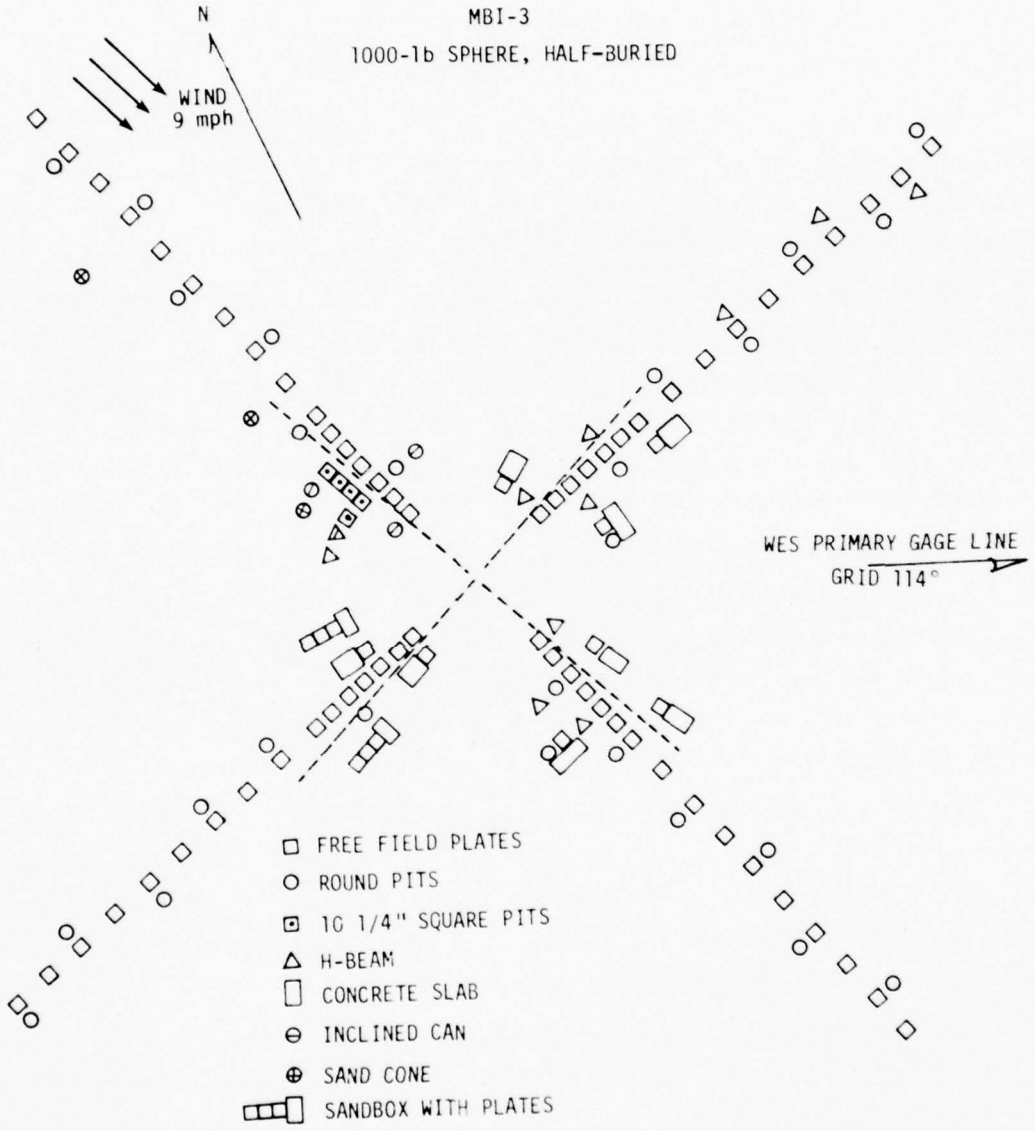

Figure 5.5. Debris collector layout for Event MBI-3.

5.3.2 Results

The average apparent values for the Event MBI-3 crater(s) are:

Volume:	390 m^3 (1378 ft^3)
Radius:	3.47 meters (11.4 feet)
Depth below SGZ:	2.47 meters (8.1 feet)

Maximum depth recorded along the survey lines was 2.47 meters (8.1 feet). Figure 5.6 is a plot of the individual crater profiles. The wind speed at the time of the test was 14.5 km/h (9 mph) from about 4.0 radians (230°) as indicated on Figure 5.5, which is the basic collector layout.

Free field areal density measurements were made along four radials. Average values of the areal density for these radials with the maximum and minimum values for each range are shown in Figure 5.7. The line through the average value points represents the power curve fit to a linear regression model. The relatively wide spread between the minimum-maximum values is attributed to effects of the wind, the lumpy nature of the ejecta field, and the usual rays of non-uniformity in the debris distribution.

Several types of collection devices were used to obtain debris enhancement information. The primary enhancement collector devices were 5-gallon paint buckets set in the ground (round pits). Square boxes were also used as pits. Vertical steel plates and concrete slabs were used as aboveground debris enhancement structures.

Figure 5.8 shows the average debris depth of the free field plates and the round pits with scatter for each range; both debris depth and range have been normalized by the cube root of the apparent crater volume. The curves plotted on this graph are the predictions for maximum, median (dashed-line), and minimum debris depth given the actual MBI-3 apparent volume.

The four radials of permanent ground displacement were measured. Figure 5.9 is a plot of the average horizontal displacement with scatter at each range shown.

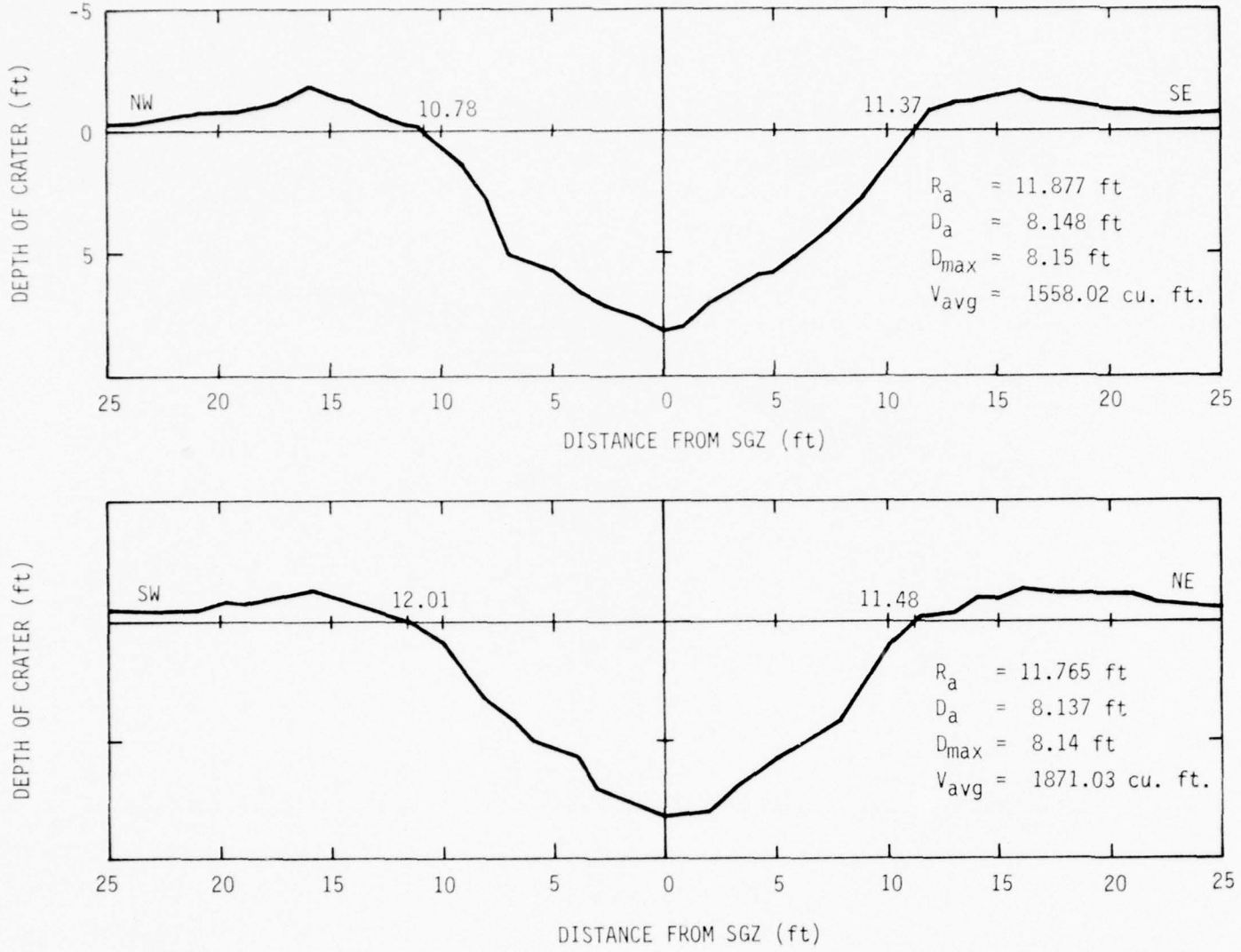

Figure 5.6. Event MBI-3 crater profiles.

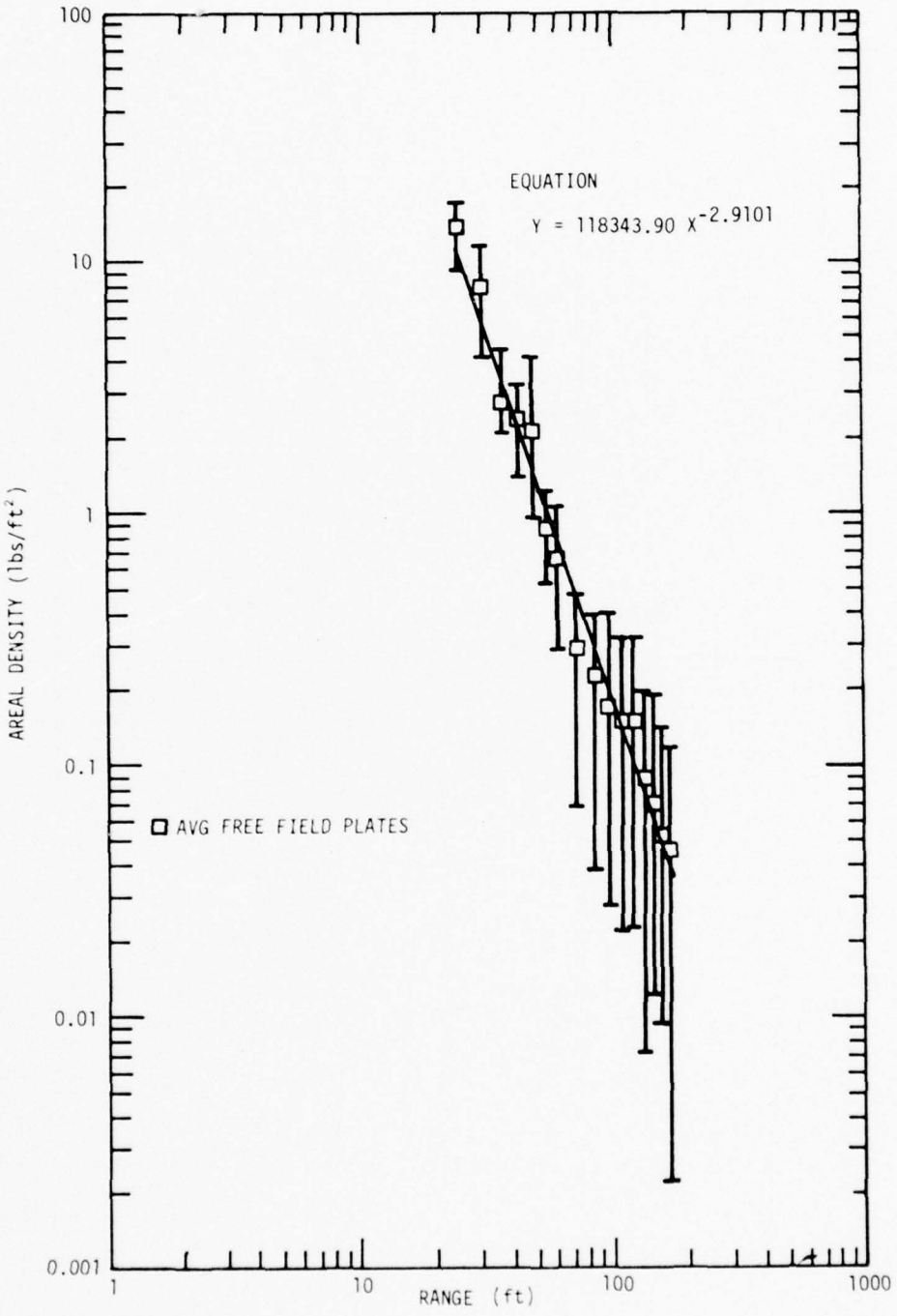

Figure 5.7. Event MBI-3, average free field areal density versus range.

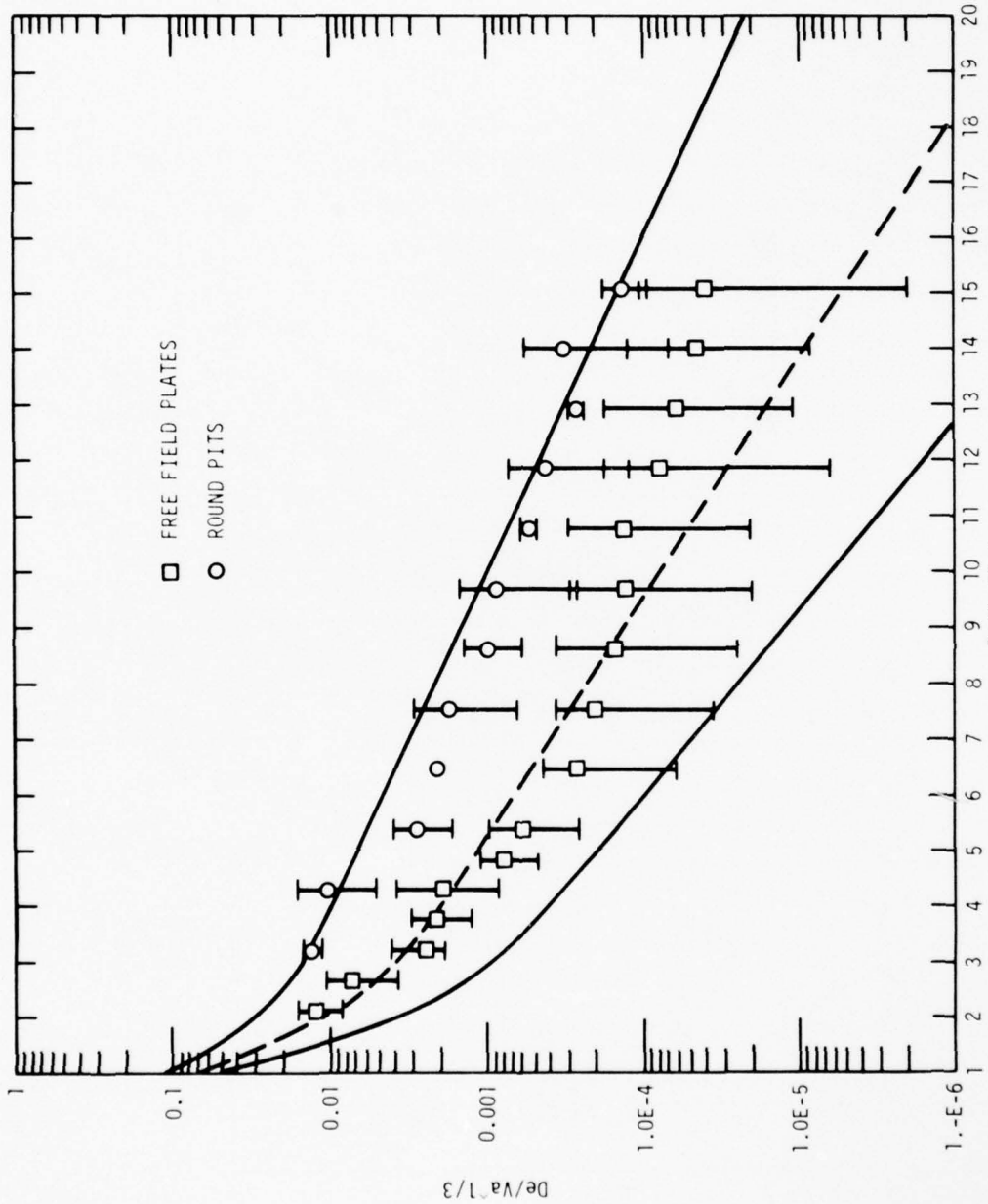

Figure 5.8. Event MBI-3, debris depth versus range, both normalized by $V_a^{1/3}$.

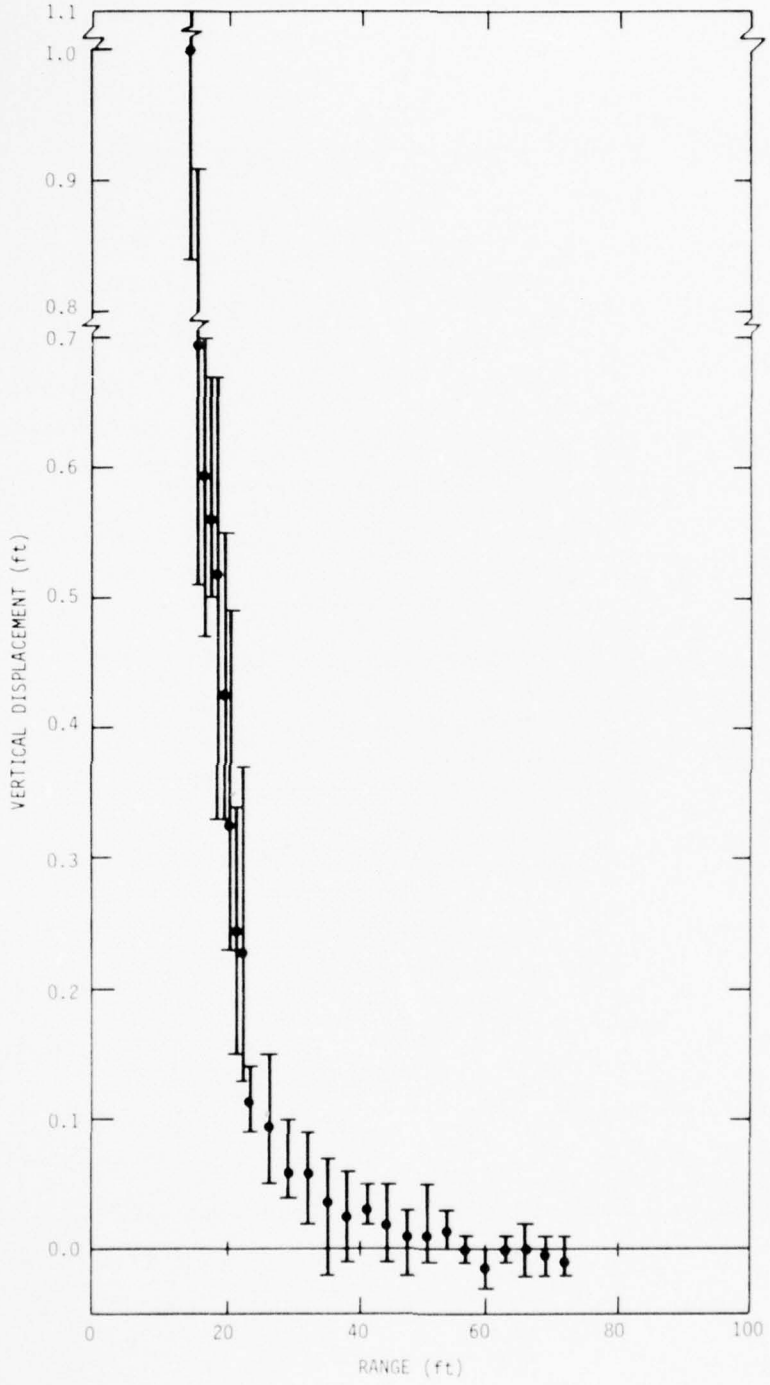

Figure 5.9. Event MBI-3, average permanent vertical displacement versus range.

SECTION 6

EVENT MBI-4

6.1 DESCRIPTION

This event was conducted on 7 September 1978 at the White Sands Missile Range. Event MBI-4 consisted of an array of six 454-kg (1,000-pound) cast TNT surface tangent spheres equally spaced 21.3 meters (70 feet) apart in a hexagonal array, to provide data for multiburst waveform synthesis prediction model, surface tangent charge configuration. Figure 6.1 shows the event detonation sequence.

6.1.1 Water Content

Soil moisture data were obtained for Event MBI-4 and are shown in Table 6.1 and are plotted in Figure 6.2.

6.2 GROUND MOTION AND AIRBLAST EXPERIMENTS

6.2.1 Gage Layout

Ground shock instrumentation was located both on the interior and the exterior of the ring of charges, and between adjacent charges. Gages were placed at depths of 0.457 to 12.2 meters (1.5 to 40 feet). The main (0°) gage line extended from the center of the array through a charge, and contained all the gages placed at depths in excess of 0.457 meters (1.5 feet). Figure 6.3 presents both a plan view and cross section of the gage array.

6.2.2 Instrumentation

A total of 131 gages were installed; 101 accelerometers, 6 velocity gages, 10 soil stress gages, and 14 airblast gages. Table 6.2 is a listing of each gage, denoted by an arbitrarily assigned measurement number.

6.2.3 Typical Data Records

Calibration and recorder start signals from the Timing and Firing (T&F) unit were properly received and translated, and all equipment operated as planned for Event MBI-4.

Data recovery was excellent. Two accelerometers, measurements Nos. 4135 and 4157 failed to produce usable data. One accelerometer and one soil stress gage, measurements Nos. 4103 and 4405, respectively, had noisy signals and are of doubtful usefulness.

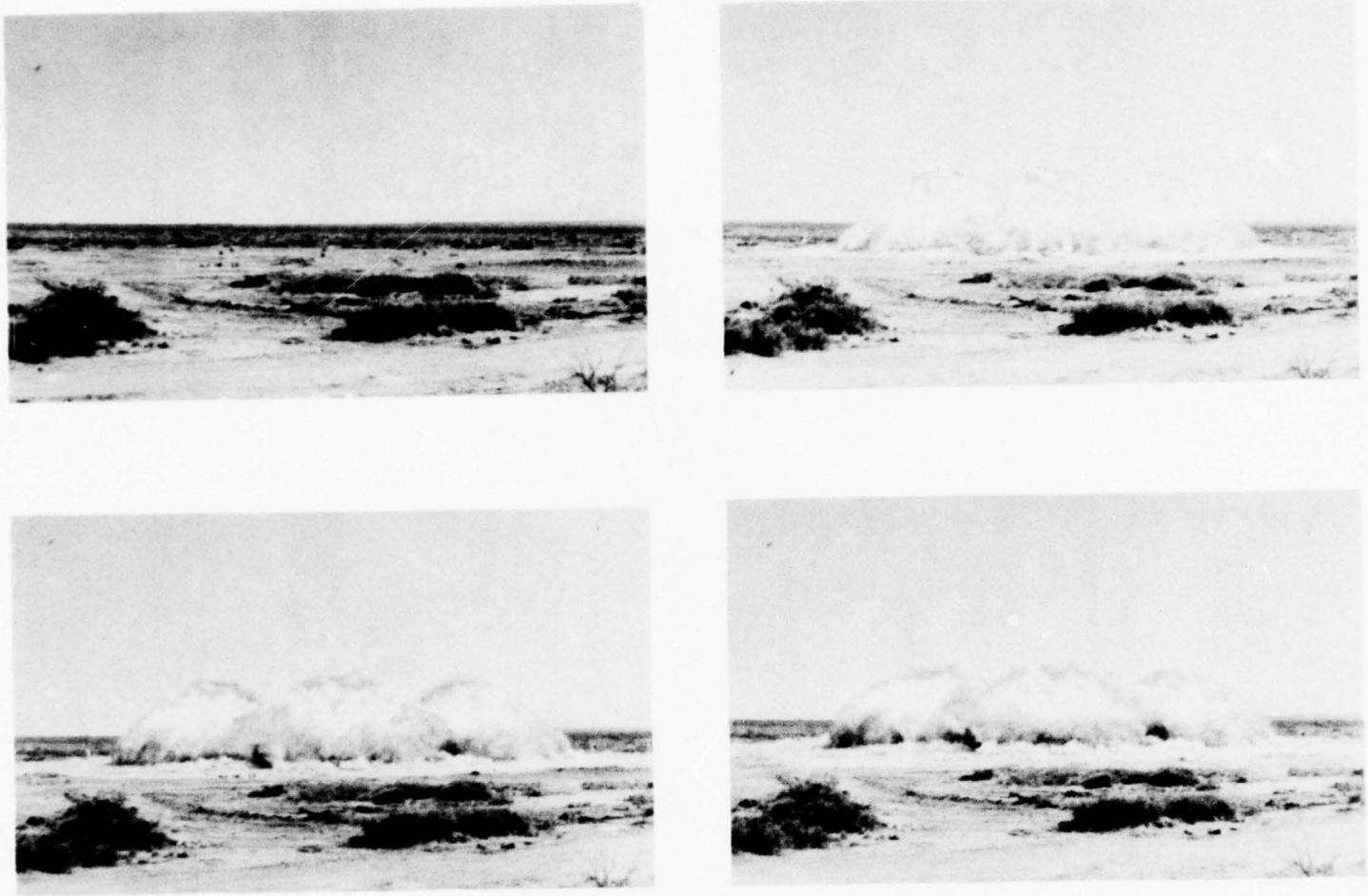

Figure 6.1. MISERS BLUFF MBI-4 detonation sequence.

Table 6.1. Event MBI-4 water content test record.

	Depth		
	m	(ft)	% Moisture
6 Sep 77	0 - 0.0488	(0 - 0.16)	9.6
	0.152	(0.5)	11.1
	0.305 - 0.457	(1 - 1.5)	12.9
	0.610 - 0.762	(2 - 2.5)	13.2
	0.914 - 1.07	(3 - 3.5)	16.2
	1.22 - 1.37	(4 - 4.5)	21.0

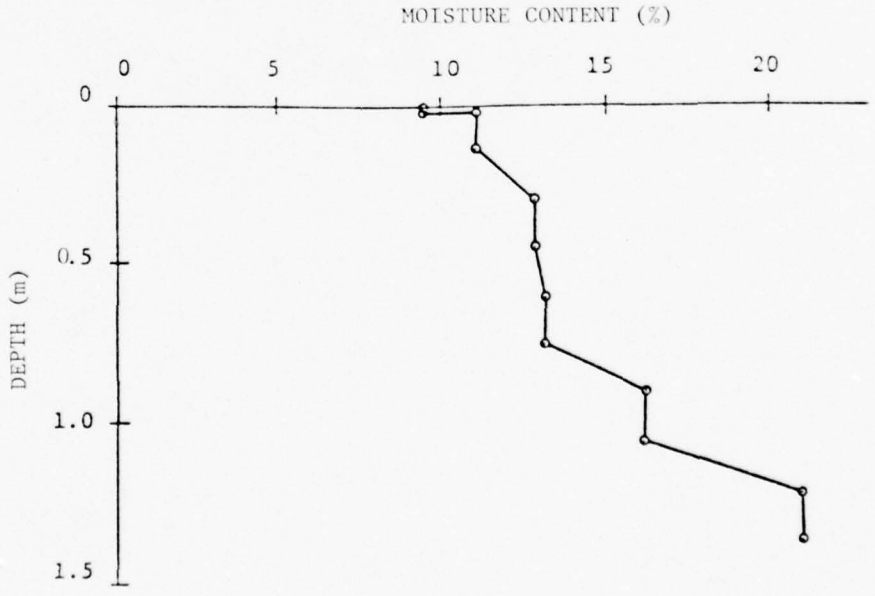

Figure 6.2. Moisture content measurements for Event MBI-4.

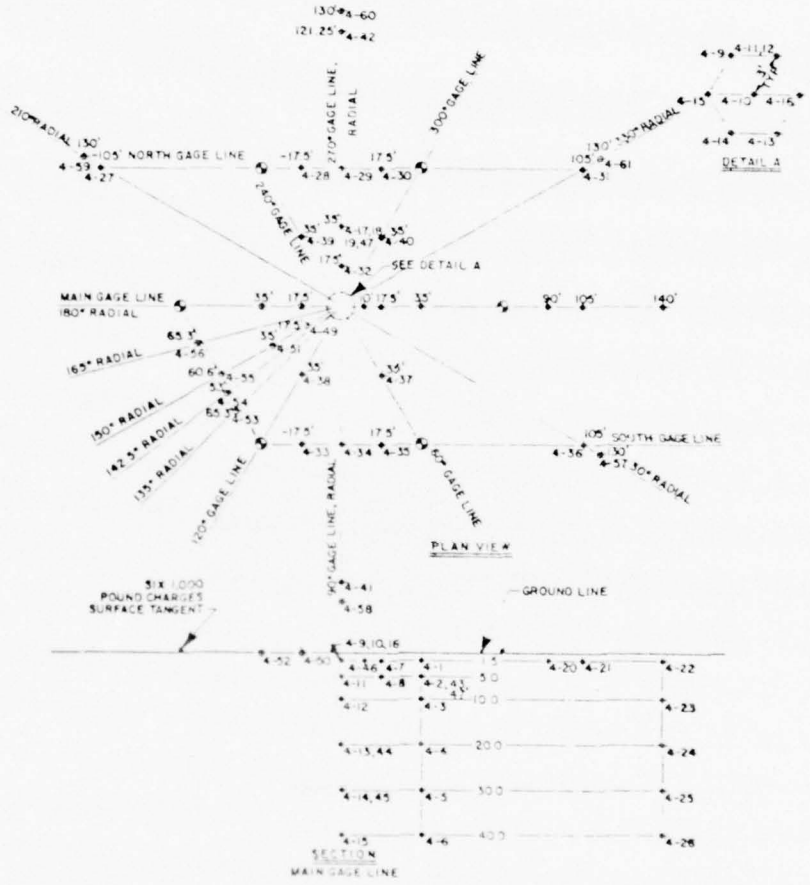

Figure 6.3. Gage layout for MISERS BLUFF Event MBI-4.

Table 6.2. Ground motion and airblast measurement list for Event MBI-4.

Radial		Range		Depth		Measurement Numbers							
Rad	(Deg)	m	(ft)	m	(ft)	AV	AH	AT	UV	UH	SV	SH	AB
0	(0)	0	(0)	0.457	(1.5)	4137	4138	4139					
0	(0)	0	(0)	0.457	(1.5)	4120	4121	4122					
0	(0)	0	(0)	0.457	(1.5)	4123	4124	4125					
0	(0)	0	(0)	1.52	(5)	4126	4127						
0	(0)	0	(0)	3.05	(10)	4128	4129	4130					
0	(0)	0	(0)	6.10	(20)	4131	4132						
0	(0)	0	(0)	6.10	(20)						4403	4404	
0	(0)	0	(0)	9.14	(30)	4133	4134						
0	(0)	0	(0)	9.14	(30)						4405	4406	
0	(0)	0	(0)	17.2	(40)	4135	4136						
0	(0)	5.33	(17.5)	0.457	(1.5)	4115	4116	4117					
0	(0)	5.33	(17.5)	1.52	(5)	4118	4119						
0	(0)	10.7	(35)	0.457	(1.5)	4101	4102	4103					
0	(0)	10.7	(35)	1.52	(5)	4104	4105						
0	(0)	10.7	(35)	1.52	(5)						4401	4402	
0	(0)	10.7	(35)	3.05	(10)	4106	4107	4108					
0	(0)	10.7	(35)	6.10	(20)	4109	4110						
0	(0)	10.7	(35)	9.14	(30)	4111	4112						
0	(0)	10.7	(35)	12.2	(40)	4113	4114						
0	(0)	26.7	(87.5)	0.457	(1.5)	4148	4149						
0	(0)	32.0	(105)	0.457	(1.5)	4150	4151						
0	(0)	42.7	(140)	0.457	(1.5)	4152	4153	4154					
0	(0)	42.7	(140)	3.05	(10)	4155	4156	4157					
0	(0)	42.7	(140)	6.10	(20)	4158	4159						
0	(0)	42.7	(140)	9.14	(30)	4160	4161						
0	(0)	42.7	(140)	12.2	(40)	4162	4163						
0.524	(30)	36.9	(121.2)	0.457	(1.5)	4174	4175	4176					
0.524	(30)	39.9	(131)	0.457	(0)								4311
1.05	(60)	1.83	(6)	0.457	(1.5)						4407	4408	
1.05	(60)	10.7	(35)	0.457	(1.5)	4180	4181	4182					
1.29	(74)	19.2	(63.1)	0.457	(1.5)	4172	4173						
1.57	(90)	18.5	(60.6)	0.457	(1.5)	4170	4171						

Table 6.2. Ground motion and airblast measurement list for Event MBI-4 (Continued).

Radial		Range		Depth		Measurement Numbers							
Rad	(Deg)	m	(ft)	m	(ft)	AV	AH	AT	UV	UH	SV	SH	AB
1.57	(90)	36.9	(121.2)	0.457	(1.5)	4164	4165						
1.57	(90)	39.9	(131)	0.457	(1.5)								4310
1.85	(106)	19.2	(63.1)	0.457	(1.5)	4168	4169						
2.09	(120)	10.7	(35)	0.457	(1.5)	4177	4178	4179					
2.34	(134)	19.2	(63.1)	0	(0)								4309
2.48	(142)	18.7	(61.2)	0	(0)								4308
2.62	(150)	0.914	(3)	0	(0)								4301
2.62	(150)	5.33	(17.5)	0	(0)								4303
2.62	(150)	10.7	(35)	0	(0)								4305
2.62	(150)	18.5	(60.6)	0	(0)								4307
2.90	(166)	19.2	(63.1)	0	(0)								4306
3.14	(180)	5.33	(17.5)	0	(0)								4302
3.14	(180)	10.7	(35)	0	(0)								4304
3.67	(210)	36.9	(121.2)	0.457	(1.5)	4189	4190						
3.67	(210)	39.9	(131)	0	(0)								4314
4.19	(240)	10.7	(35)	0.457	(1.5)	4183	4184	4185					
4.19	(240)	10.7	(35)	0.457	(1.5)				4719	4720			
4.43	(254)	19.2	(63.1)	0.457	(1.5)	4191	4192						
4.71	(270)	5.33	(17.5)	0.457	(1.5)	4166	4167						
4.71	(270)	5.33	(17.5)	0.457	(1.5)				4721	4722			
4.71	(270)	10.7	(35)	0.457	(1.5)	4140	4141	4142					
4.71	(270)	10.7	(35)	1.52	(5)	4143	4144						
4.71	(270)	10.7	(35)	1.52	(5)						4409	4410	
4.71	(270)	10.7	(35)	3.05	(10)	4145	4146	4147					
4.71	(270)	18.5	(60.6)	0.457	(1.5)	4193	4194						
4.71	(270)	36.9	(121.2)	0.457	(1.5)	4200	4201						
4.71	(270)	39.6	(130)	0	(0)								4313
4.99	(286)	19.2	(63.1)	19.2	(63.1)	4195	4196						
5.24	(300)	10.7	(35)	0.457	(1.5)	4186	4187	4188					
5.76	(330)	10.7	(35)	0.457	(1.5)				4701	4702			

Table 6.2. Ground motion and airblast measurement list for Event MBI-4 (Continued).

Radial		Range		Depth		Measurement Numbers							
Rad	(Deg)	m	(ft)	m	(ft)	AV	AH	AT	UV	UH	SV	SH	AB
5.76	(330)	36.9	(121.2)	0.457	(1.5)	4197	4198	4199					
5.76	(330)	39.9	(131)	0.457	(1.5)								4312

NOTES:

AV Vertical Acceleration
AH Horizontal Acceleration
AT Transverse Acceleration
UV Vertical Velocity
UH Horizontal Velocity
SV Vertical Stress
SH Horizontal Stress
AB Airblast

Typical time histories for the following gages are presented in Figure 6.4.

Type of Measurement	Instrumentation Number	Radial		Range		Depth	
		Rad	(Deg)	m	(ft)	m	(ft)
Vertical Stress (SV)	4403	0	(0)	0	(0)	6.10	(20)
Vertical Acceleration (AU)	4131	0	(0)	0	(0)	6.10	(20)
Vertical Velocity (UV)	4721	4.71	(270)	5.33	(17.5)	0.457	(1.5)
Airblast (AB)	4303	2.62	(150)	5.33	(17.5)	0	(0)

Figure 6.5 shows the comparison of measured and empirical predicted waveform of the vertical velocity between charges on the bisector.

6.3 CRATER AND EJECTA EXPERIMENTS

6.3.1 Crater and Collector Layout

Four radial lines were surveyed in each of the craters to determine the parameters for the apparent craters. Free field areal density measurements were made along three primary radials and along a line between charges. Several different types of debris collection devices were used as shown in Figure 6.6.

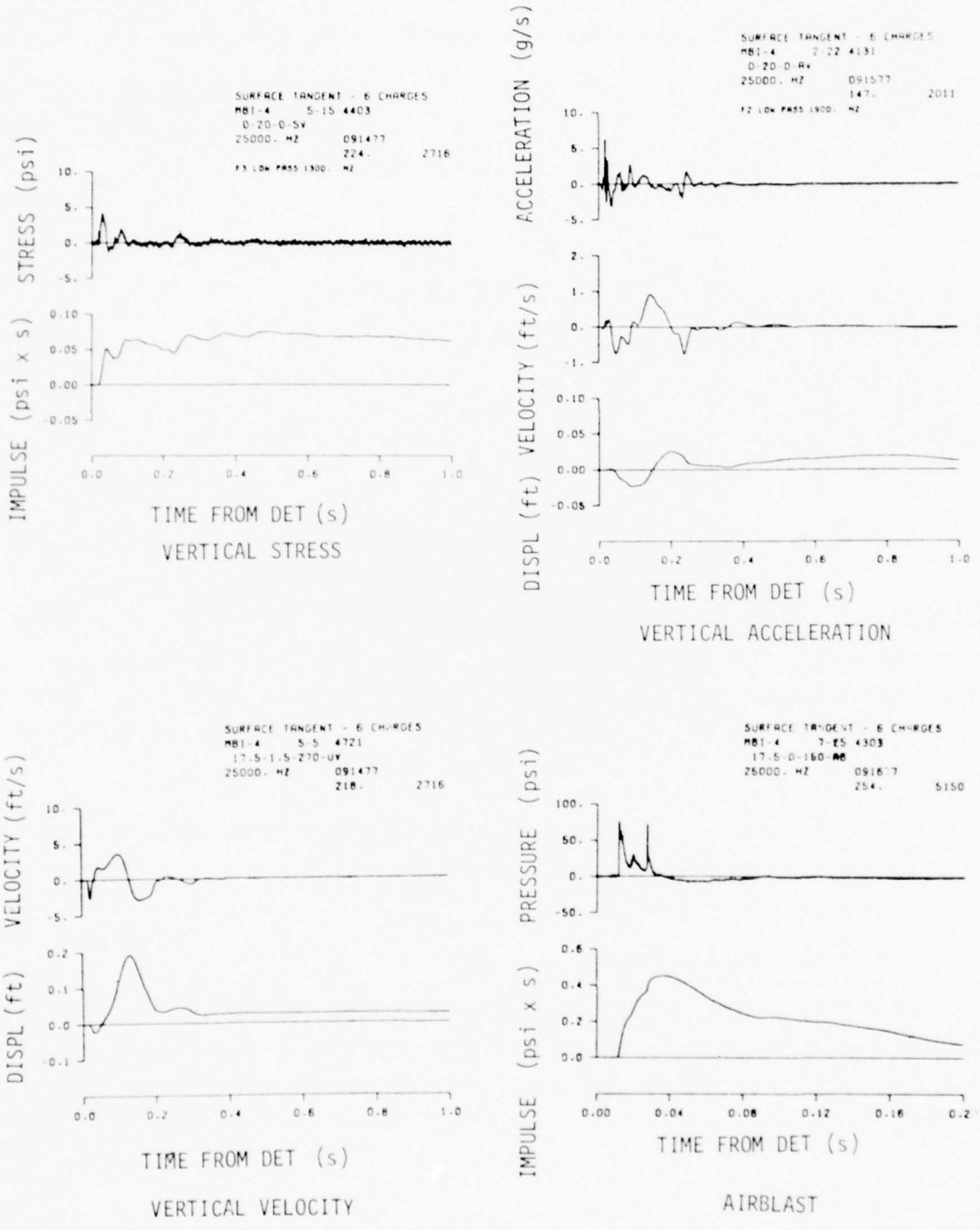

Figure 6.4. Typical time histories for Event MBI-4.

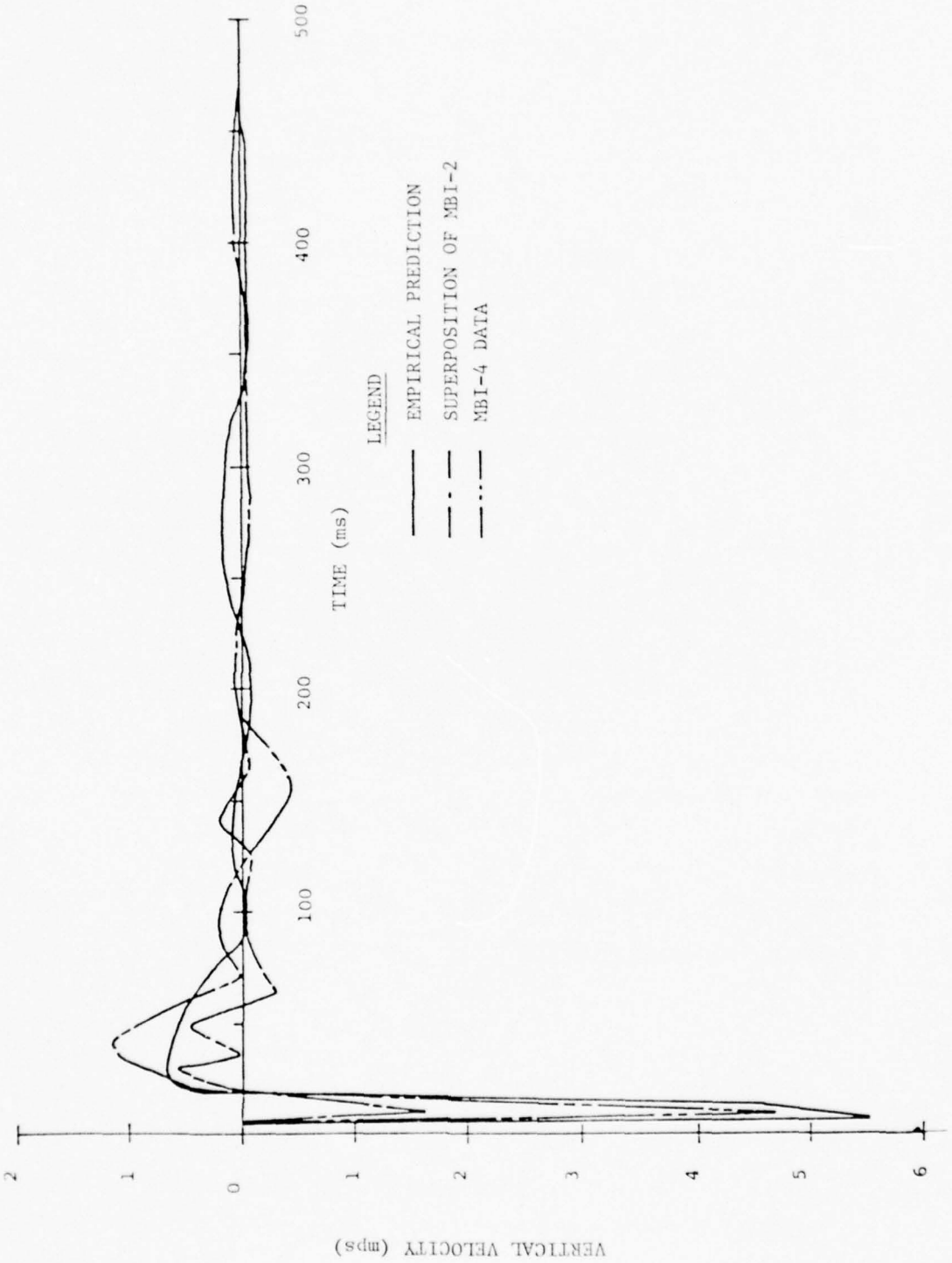

Figure 6.5. Event MBI-4 waveform comparisons of vertical velocity between charges on the bisector.

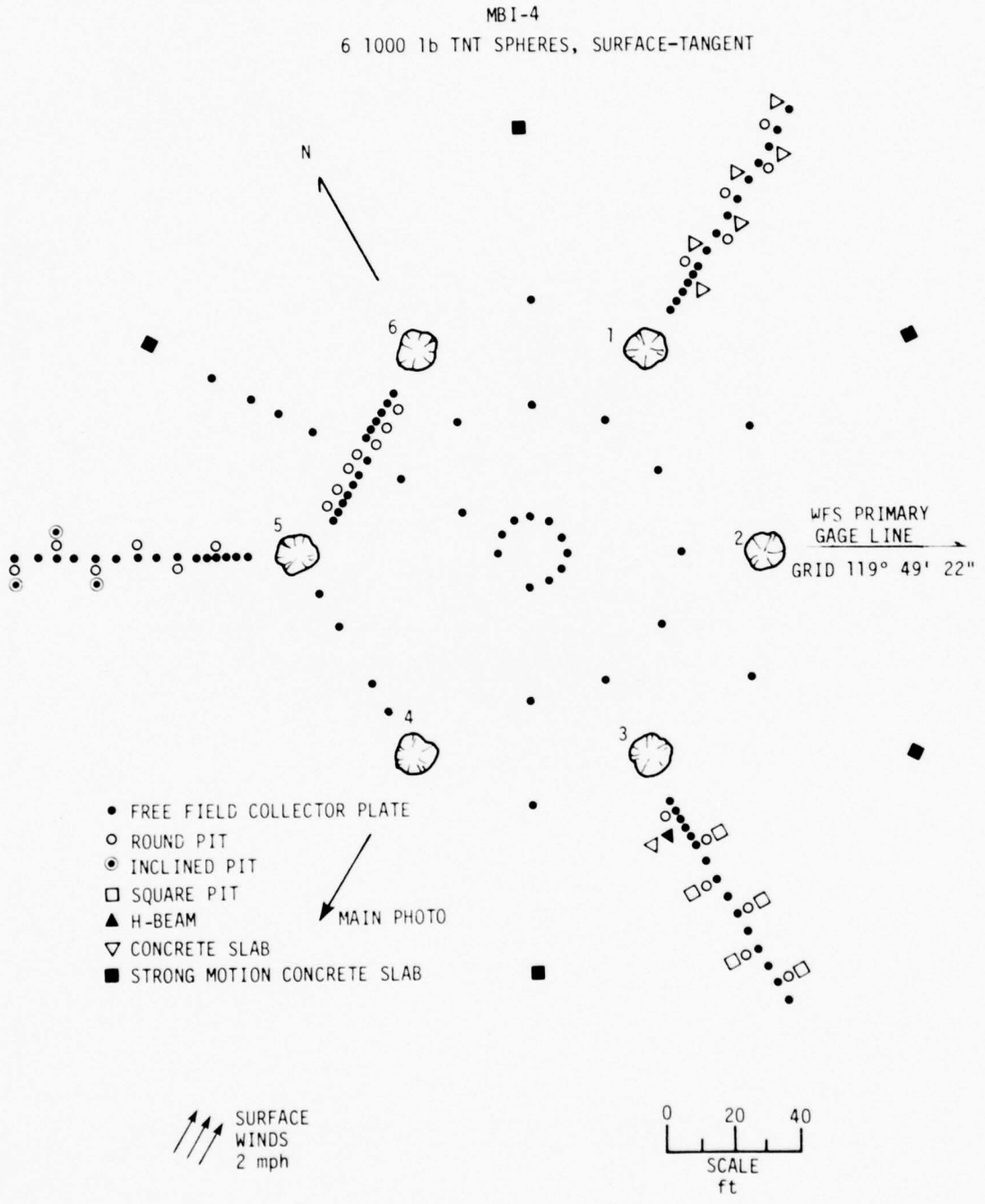

Figure 6.6. Debris collector layout for Event MBI-4.

6.3.2 Results

The average pertinent parameters for each crater are:

	SGZ No. 1		SGZ No. 2		SGZ No. 3	
	m	(ft)	m	(ft)	m	(ft)
Apparent radius	2.29	(7.5)	2.47	(8.1)	2.35	(7.7)
Apparent depth	1.16	(3.8)	1.34	(4.4)	1.28	(4.2)
Maximum depth	1.19	(3.9)	1.40	(4.6)	1.28	(4.2)
Volume	6.51 m^3	(230 ft^3)	8.51 m^3	(304 ft^3)	6.88 m^3	(243 ft^3)

	SGZ No. 4		SGZ No. 5		SGZ No. 6	
	m	(ft)	m	(ft)	m	(ft)
Apparent radius	2.47	(8.1)	2.74	(9.0)	2.19	(7.2)
Apparent depth	1.37	(4.5)	1.52	(5.0)	1.25	(4.1)
Maximum depth	1.40	(4.6)	1.52	(5.0)	1.28	(4.2)
Volume	7.82 m^3	(276 ft^3)	10.4 m^3	(367 ft^3)	6.65 m^3	(235 ft^3)

The differences in crater sizes are attributed to slight variation in the soil geology at each ground zero. Figures 6.7 through 6.12 are plots of the individual crater profiles. The direction of the windspeed at the time of the test with respect to height above the ground was variable. It was recorded as being less than 11.3 km/h (7 mph) at every height. At the ground level it was 3.2 km/h (2 mph) from the direction of SGZ No. 4 towards SGZ No. 1 as indicated on Figure 6.6.

The average free field areal density versus range is shown in Figure 6.13. The debris depth versus range normalized by the cube root of the apparent crater volumes for craters 1, 3 and 5 are shown in Figure 6.14. Figure 6.15 shows the average permanent vertical displacements versus range for the same craters.

Several types of collection devices were used to obtain debris enhancement information. The primary enhancement collector devices were 5-gallon paint buckets set in the ground (round pits). Square boxes were also used as pits. Vertical steel plates and concrete slabs were used as aboveground debris enhancement structures.

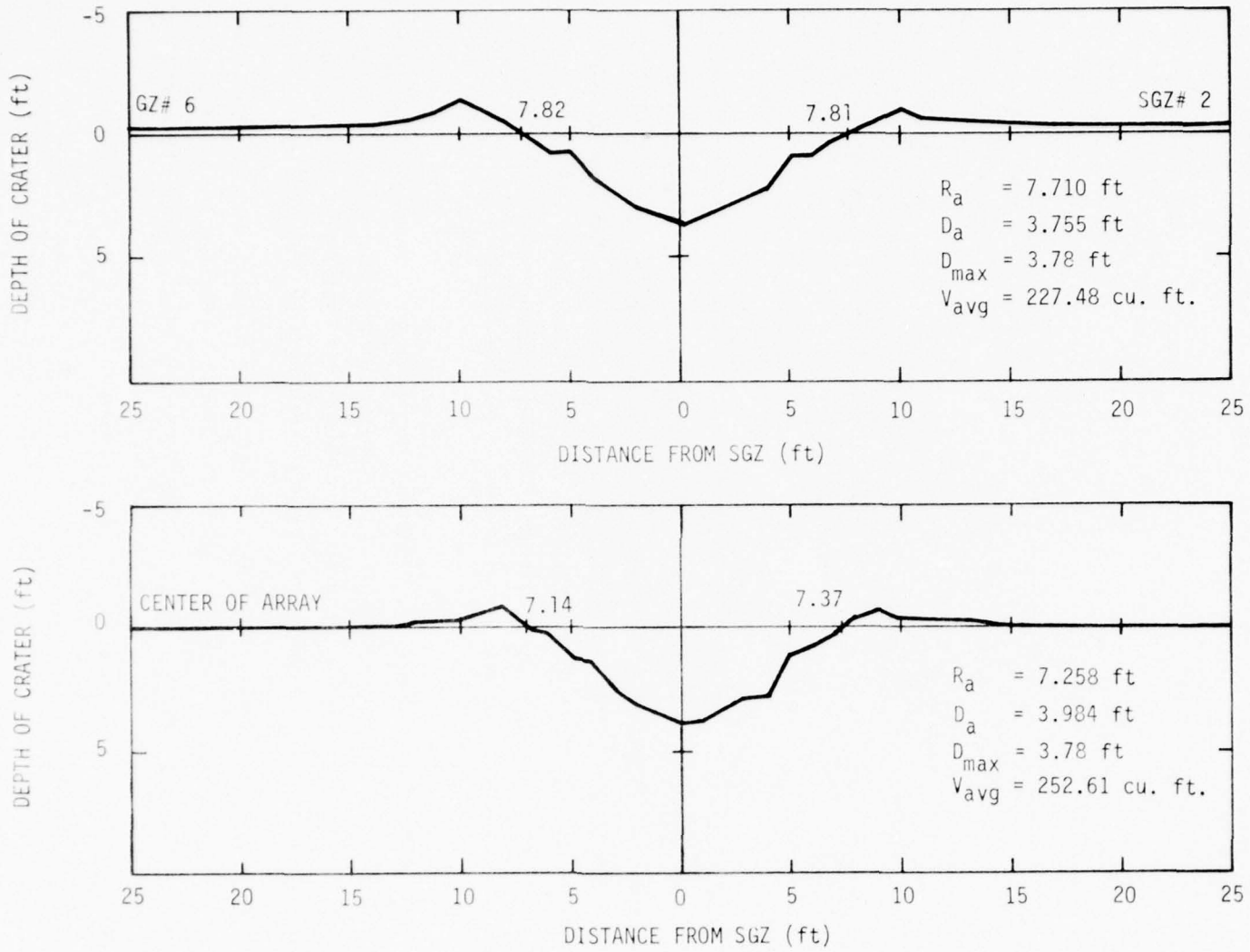

Figure 6.7. Event MBI-4 crater profiles for SGZ No. 1.

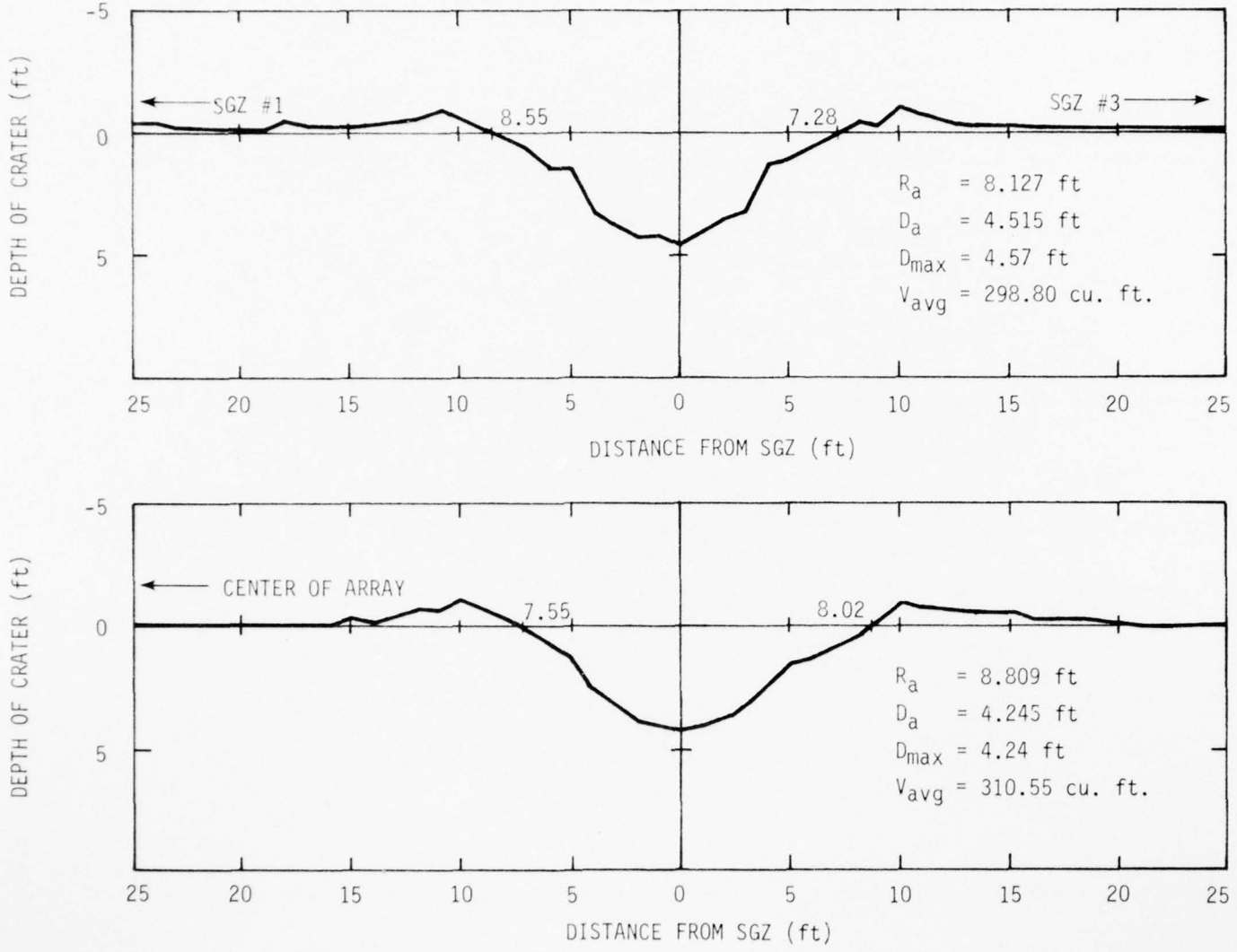

Figure 6.8. Event MBI-4 crater profile for GZ No. 2.

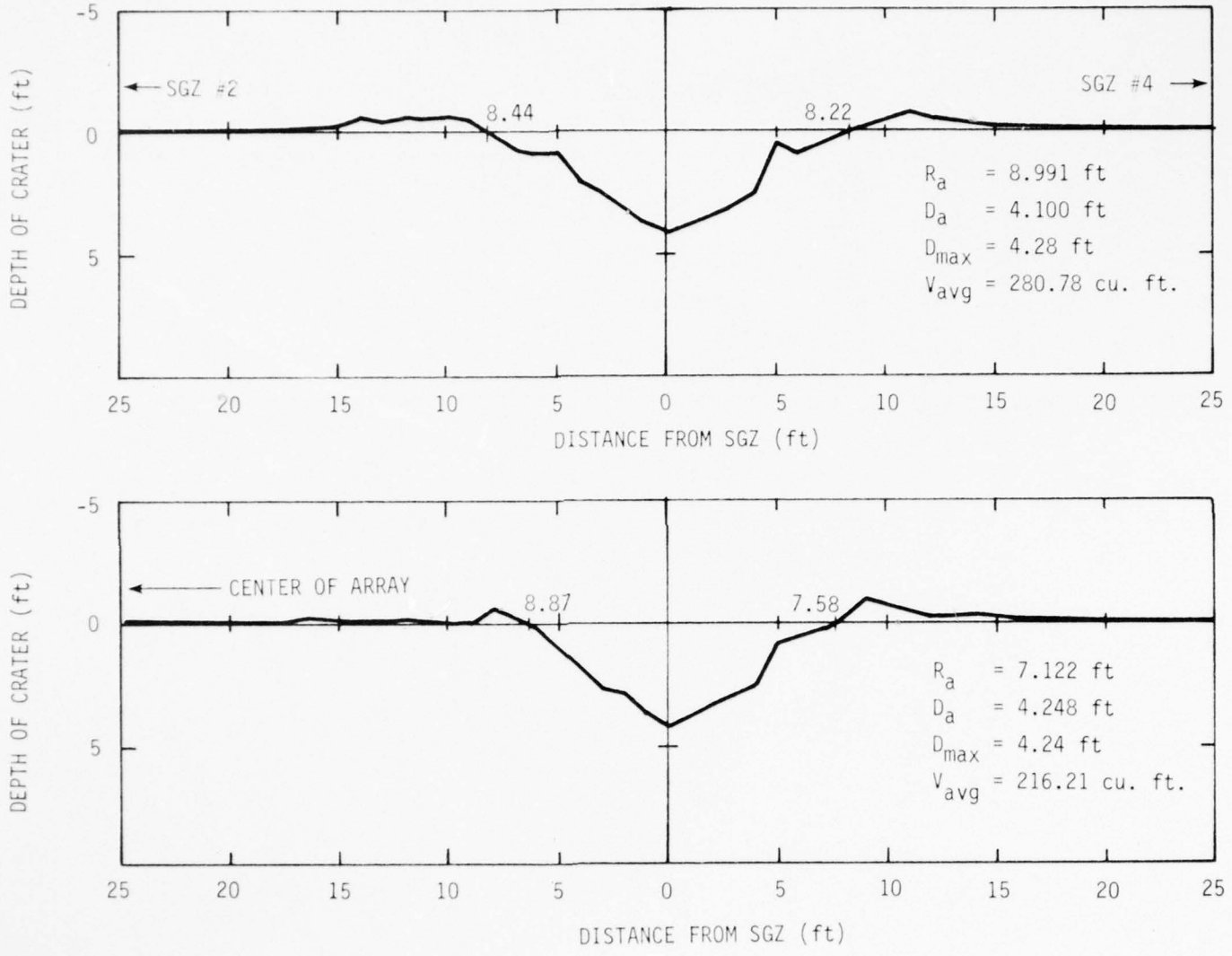

Figure 6.9. Event MBI-4 crater profile for GZ No. 3.

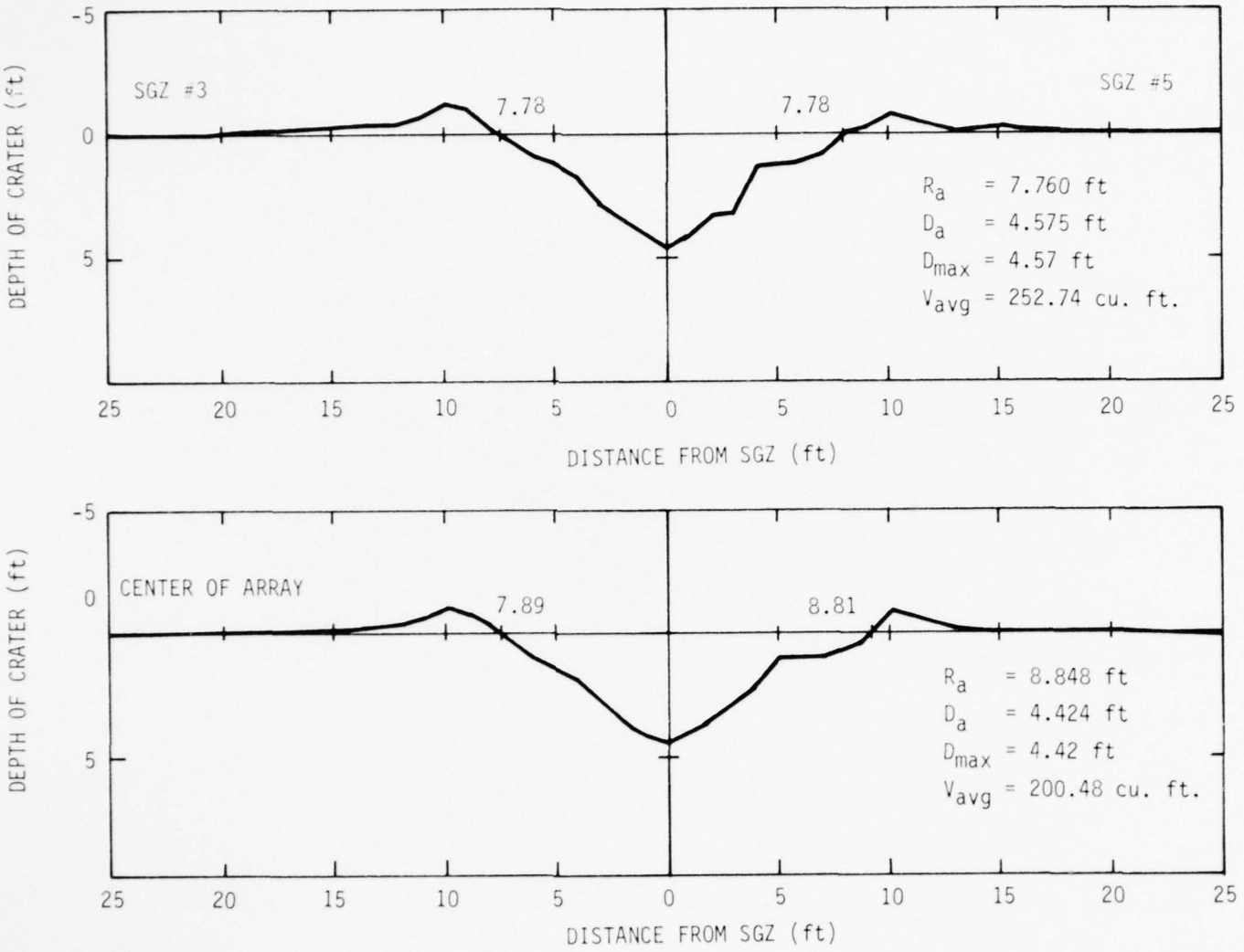

Figure 6.10. Event MBI-4 crater profile for GZ No. 4.

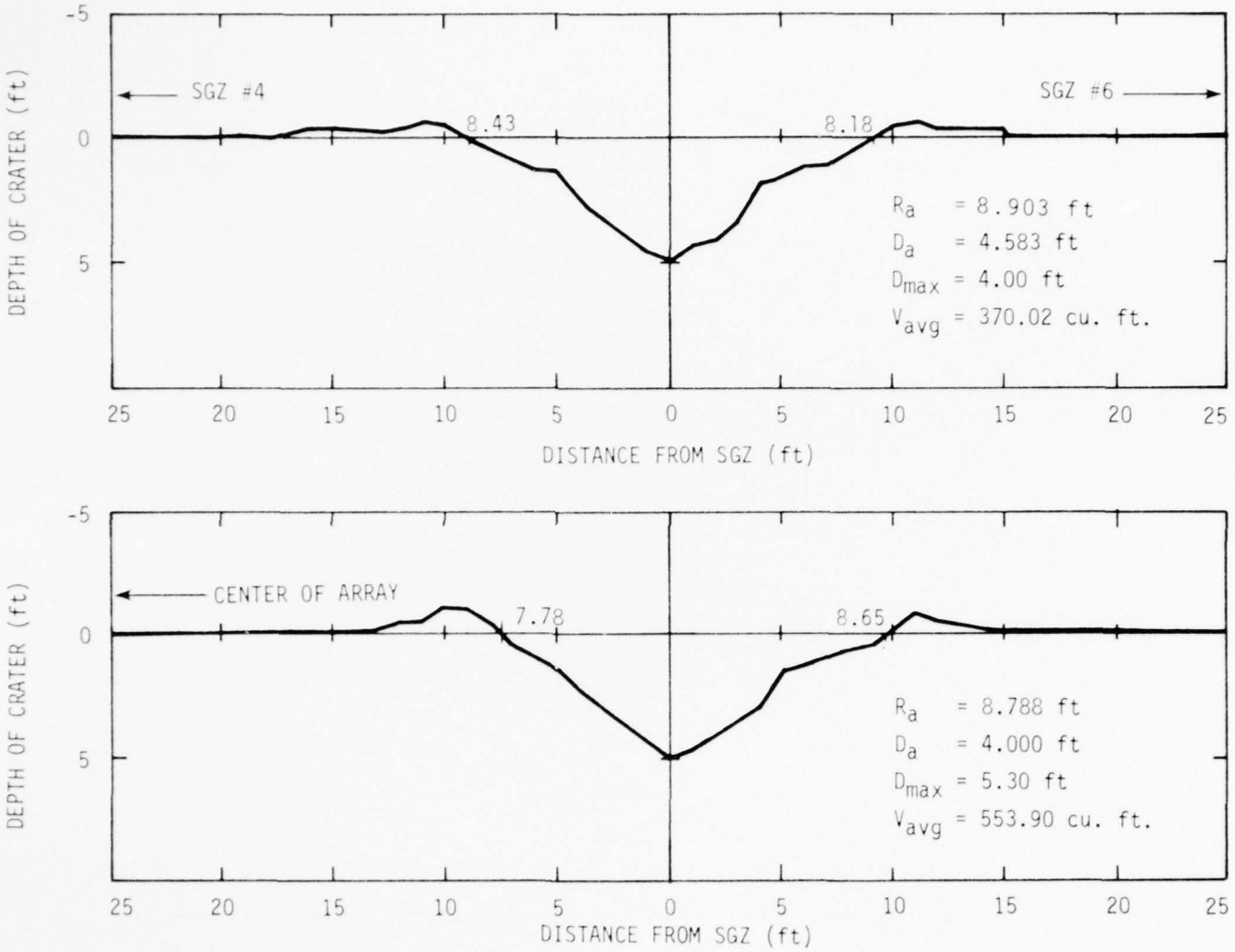

Figure 6.11. Event MBI-4 crater profile for GZ No. 5.

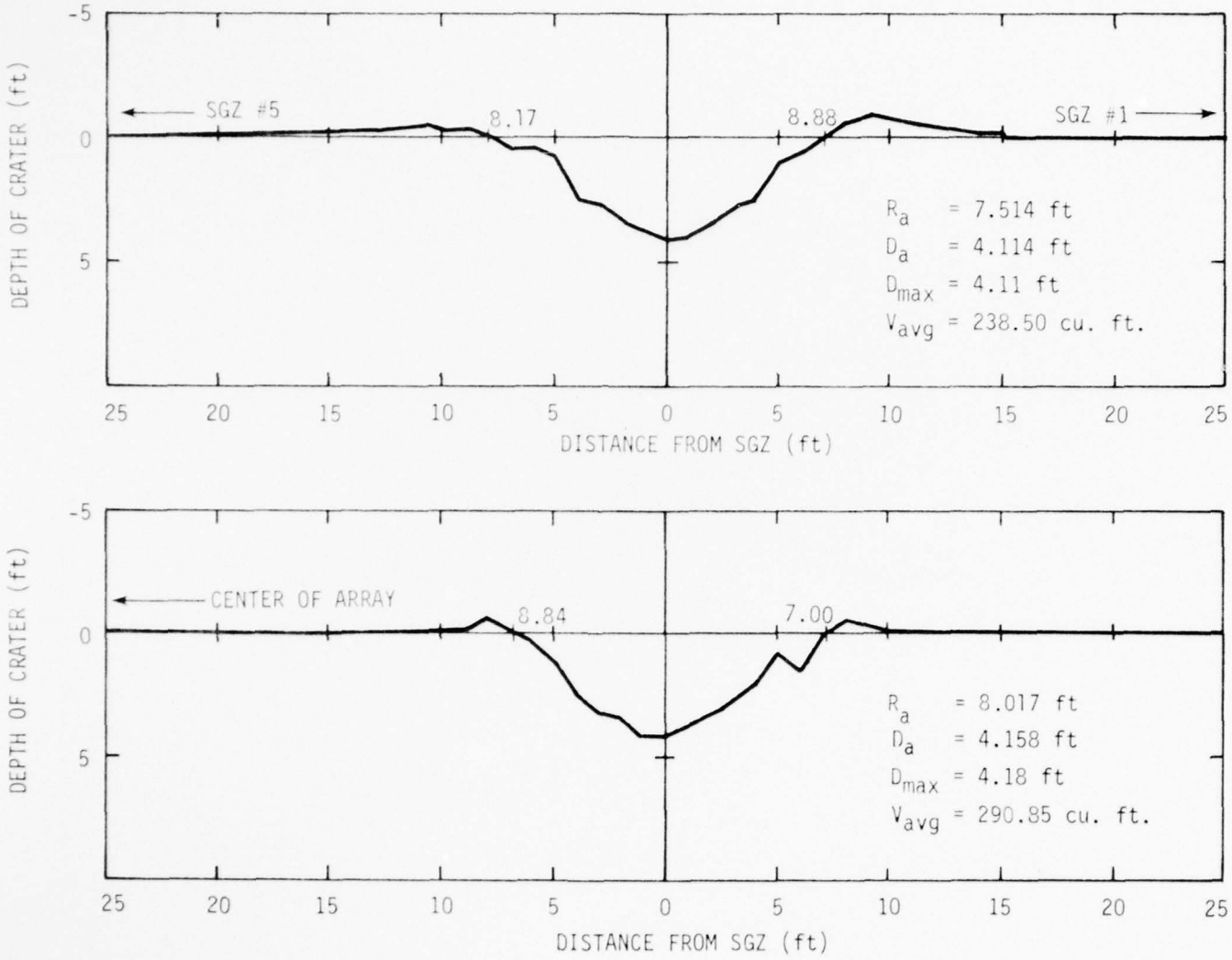

Figure 6.12. Event MBI-4 crater profile for GZ No. 6.

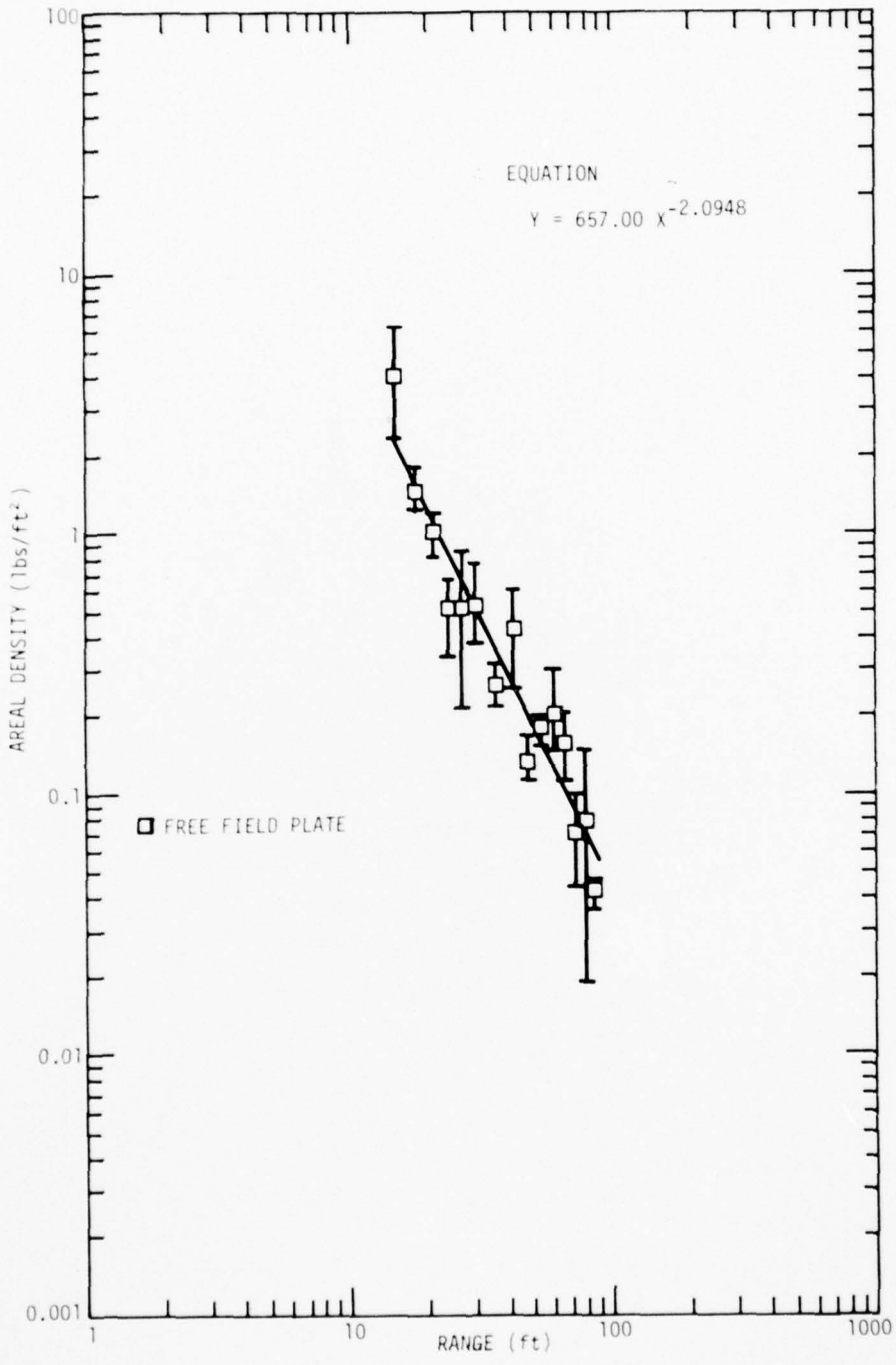

Figure 6.13. Event MBI-4, average free field areal density versus range.

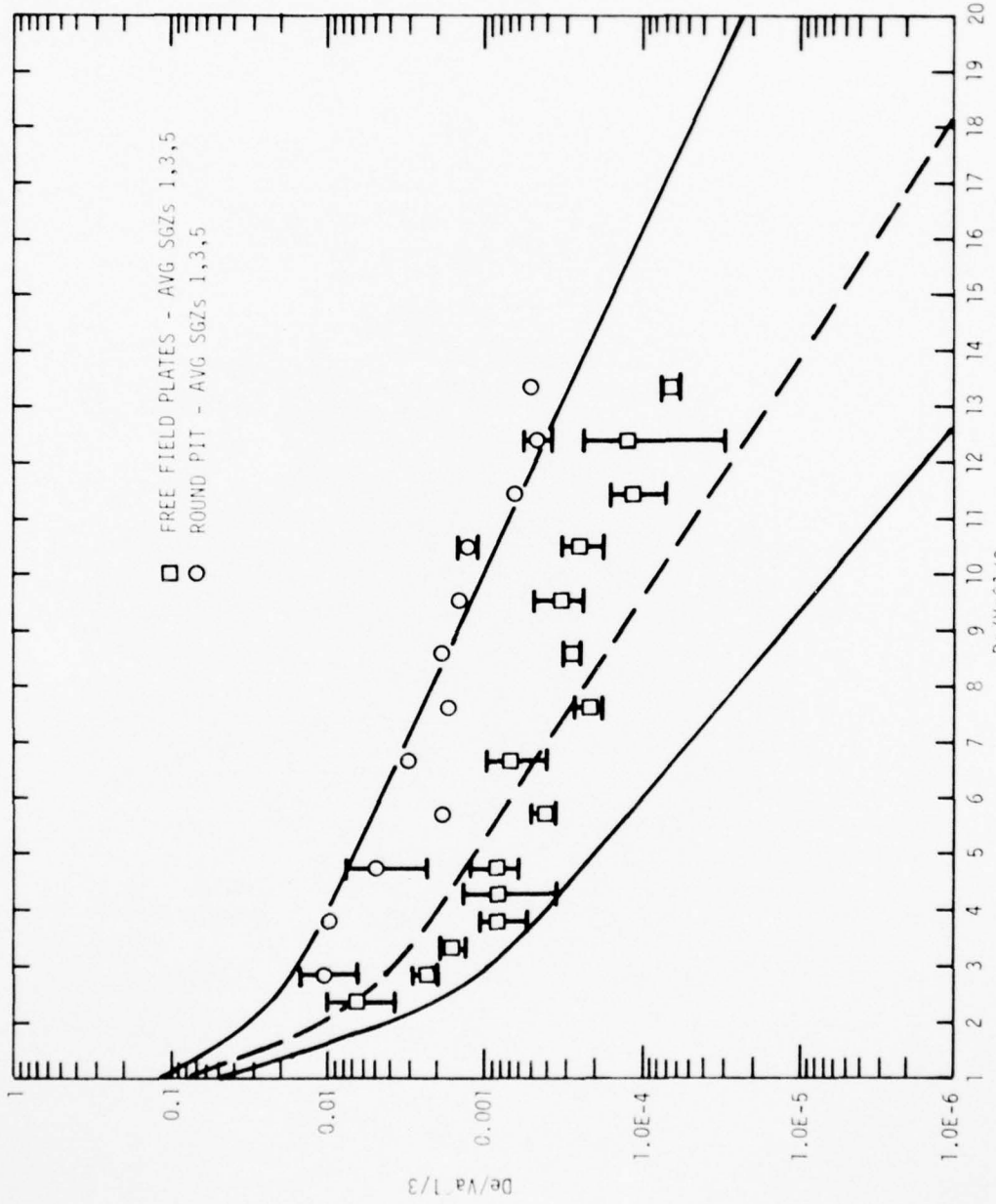

Figure 6.14. Event MBI-4, debris depth versus range, both normalized by $V_a^{1/3}$.

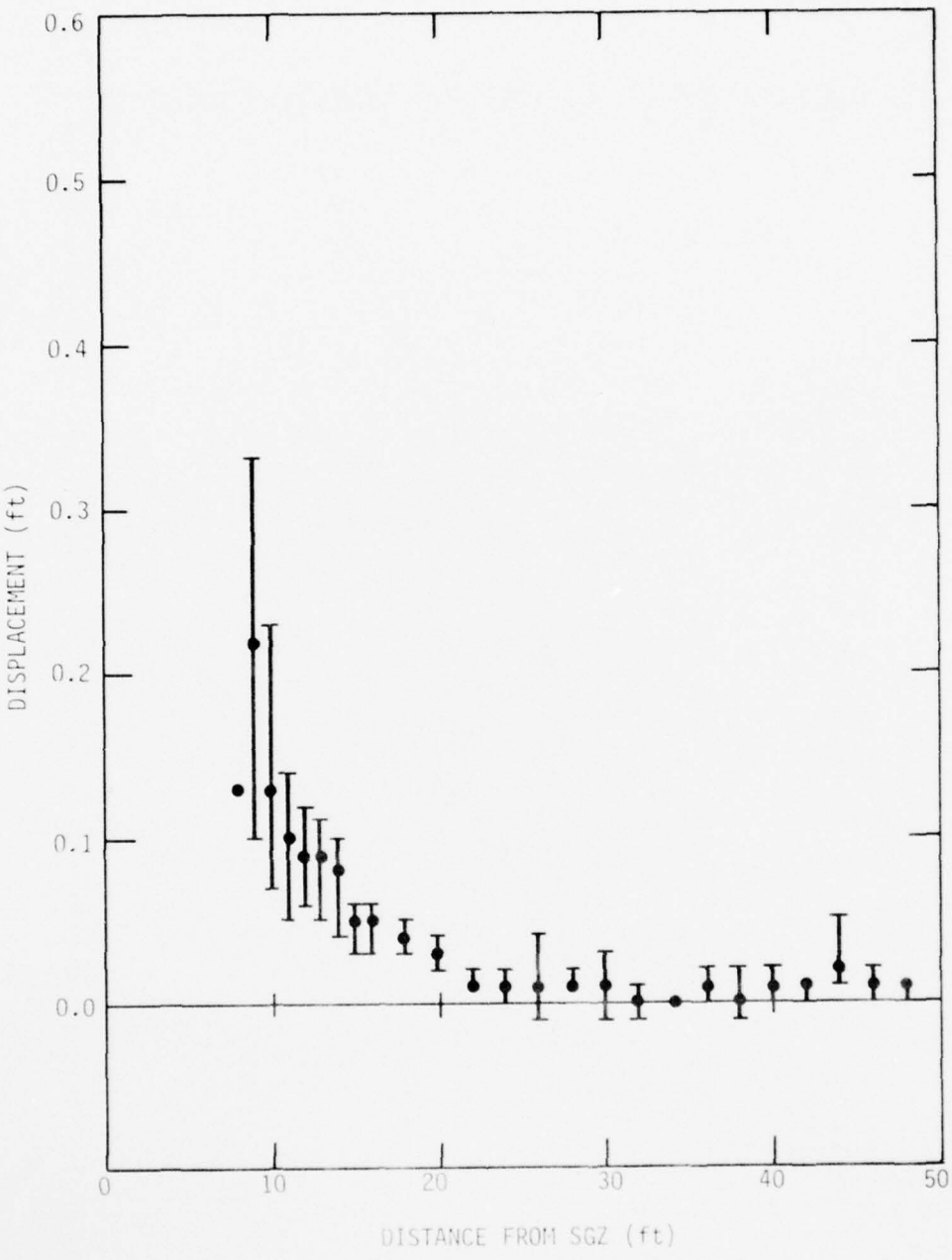

Figure 6.15. Event MBI-4, average of SGZ No. 1, No. 3, and No. 5 permanent vertical displacements versus range.

SECTION 7

EVENT MBI-5

7.1 DESCRIPTION

This event was conducted on 22 September 1978 at the White Sands Missile Range. This event used a 454-kg (1000-pound) cast TNT, fully buried (surface tangent below) sphere to check the effect of depth-of-burial and reduce airblast-induced ground motion.

7.1.1 Water Content

Soil moisture data were obtained for Event MBI-5 and are shown in Table 7.1 and are plotted in Figure 7.1.

7.2 GROUND MOTION AND AIRBLAST EXPERIMENTS

7.2.1 Gage Layout

Ground shock instrumentation covered ranges of 4.57 to 73.2 meters (15 to 240 feet) from SGZ and depths of 0.457 to 12.2 meters (1.5 to 40 feet). Gages were installed principally along a single radial [designated the 0 radian (0°) radial] with supplementary measurements made at 1.57, 3.14 and 4.71 radians (90°, 180°, and 270°.)

Figure 7.2 presents both a plan view and cross section of the gage array.

7.2.2 Instrumentation

Seventy-eight gages were installed; 60 accelerometers, 6 velocity gages, 5 soil stress gages, and 7 airblast gages. Table 7.2 is a listing of each gage, denoted by an arbitrarily assigned measurement number.

7.2.3 Typical Data Records

Calibration and recorder start signals from the Timing and Firing (T&F) unit were properly received and translated, and all equipment operated as planned for Event MBI-5.

Data recovery was good. Four accelerometers, measurement Nos. 5103, 5104, 5113 and 5114, were apparently damaged at shock arrival and yielded no useful data. Airblast measurement No. 5301 was also apparently damaged and showed no useful response.

Table 7.1. Event MBI-5 water content test record.

	Depth		
	m	(ft)	% Moisture
26-27 Sep 77	0 - 0.152	(0 - 0.5)	12.03
	0.305 - 0.457	(1 - 1.5)	13.66
	0.610 - 0.762	(2 - 2.5)	19.56
	0.914 - 1.067	(3 - 3.5)	19.16
	1.22 - 1.37	(4 - 4.5)	24.53

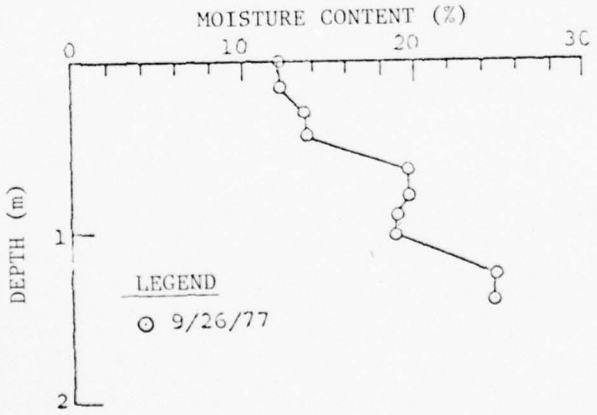

Figure 7.1. Event MBI-5 moisture content data.

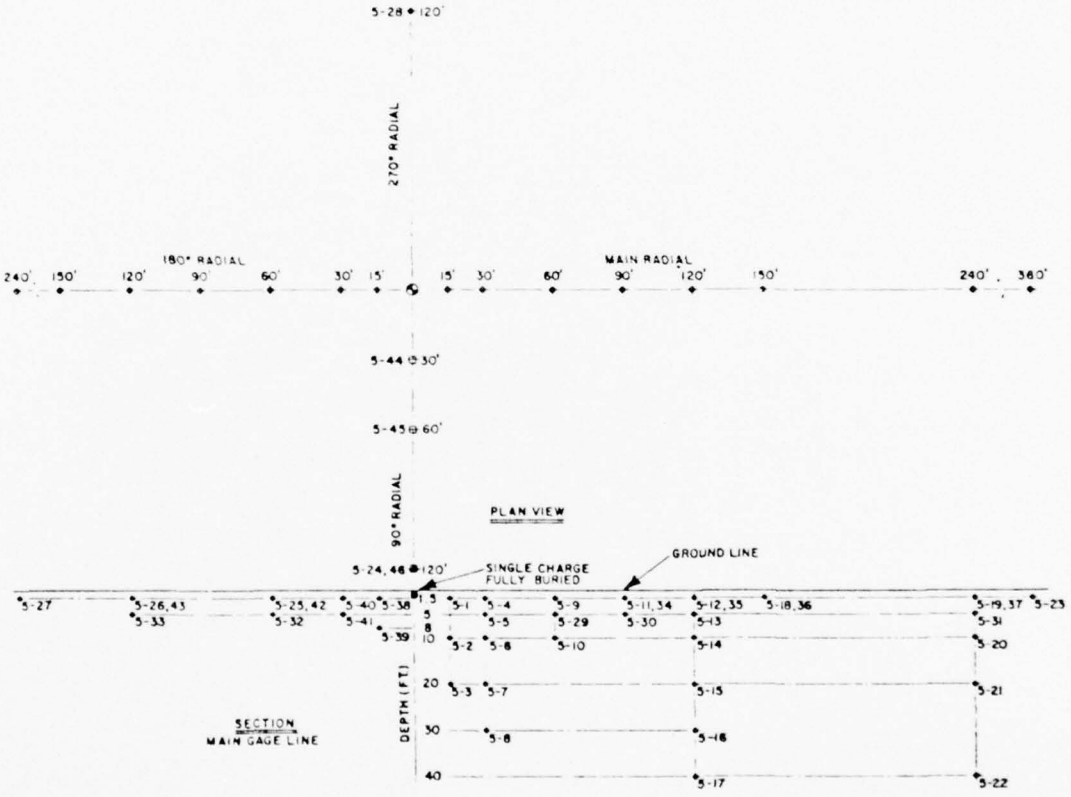

Figure 7.2. Gage layout for MISERS BLUFF Event MBI-5.

Table 7.2. Ground motion and airblast measurement list for Event MBI-5.

Radial		Range		Depth		Measurement Numbers							
Rad	(Deg)	m	(ft)	m	(ft)	AV	AH	AT	UV	UH	SV	SH	AB
0	(0)	4.57	(15)	0.457	(1.5)	5101	5102						
0	(0)	4.57	(15)	3.05	(10)	5103	5104						
0	(0)	4.57	(15)	9.14	(30)	5105	5106						
0	(0)	9.14	(30)	0.457	(1.5)	5107	5108						
0	(0)	9.14	(30)	0.457	(1.5)				5719	5720			
0	(0)	9.14	(30)	1.52	(5)	5109	5110						
0	(0)	9.14	(30)	3.05	(10)	5111	5112						
0	(0)	9.14	(30)	6.10	(20)	5113	5114						
0	(0)	9.14	(30)	9.14	(30)	5115	5116						
0	(0)	18.3	(60)	0.457	(1.5)	5117	5118						
0	(0)	18.3	(60)	0.457	(1.5)				5721	5722			
0	(0)	18.3	(60)	1.52	(5)						5201		
0	(0)	18.3	(60)	3.05	(10)	5119	5120						
0	(0)	27.4	(90)	0.457	(1.5)	5121	5122						
0	(0)	27.4	(90)	0.457	(1.5)			5157					
0	(0)	27.4	(90)	1.52	(5)						5202		
0	(0)	36.6	(120)	0.457	(1.5)	5123	5124						
0	(0)	36.6	(120)	0.457	(1.5)			5158					
0	(0)	36.6	(120)	0.457	(1.5)				5723	5724			
0	(0)	36.6	(120)	1.52	(5)	5125	5126						
0	(0)	36.6	(120)	3.05	(10)	5127	5128						
0	(0)	36.6	(120)	6.10	(20)	5129	5130						
0	(0)	36.6	(120)	9.14	(30)	5131	5132						
0	(0)	36.6	(120)	12.2	(40)	5133	5134						
0	(0)	45.7	(150)	0.457	(1.5)	5135	5136						
0	(0)	45.7	(150)	0.457	(1.5)			5159					
0	(0)	70.7	(232)	0.457	(1.5)	5137	5138						
0	(0)	70.7	(232)	0.457	(1.5)			5160					
0	(0)	70.7	(232)	1.52	(5)						5203		
0	(0)	70.7	(232)	3.05	(10)	5139	5140						
0	(0)	73.2	(240)	6.10	(20)	5141	5142						
0	(0)	73.2	(240)	12.2	(40)	5143	5144						

Table 7.2. Ground motion and airblast measurement list for Event MBI-5 (Continued).

Radial		Range		Depth		Measurement Numbers							
Rad	(Deg)	m	(ft)	m	(ft)	AV	AH	AT	UV	UH	SV	SH	AB
1.57	(90)	36.6	(120)	0.457	(1.5)	5147	5148						
3.14	(180)	18.3	(60)	0.457	(1.5)	5149	5150						
3.14	(180)	18.3	(60)	1.52	(5)							5204	
3.14	(180)	36.6	(120)	0.457	(1.5)	5151	5152						
3.14	(180)	36.6	(120)	1.52	(5)							5205	
3.14	(180)	73.2	(240)	0.457	(1.5)	5153	5154						
3.14	(180)	109.7	(360)	0.457	(1.5)	5145	5146						
4.71	(270)	1.83	(6)	0	(0)								5301
4.71	(270)	3.05	(10)	0	(0)								5302
4.71	(270)	4.57	(15)	0	(0)								5303
4.71	(270)	9.14	(30)	0	(0)								5304
4.71	(270)	18.3	(60)	0	(0)								5305
4.71	(270)	36.6	(120)	0	(0)								5306
4.71	(270)	36.6	(120)	0.457	(1.5)	5155	5156						
4.71	(270)	73.2	(240)	0	(0)								5307

NOTES:

AV Vertical Acceleration
AH Horizontal Acceleration
AT Transverse Acceleration
UV Vertical Velocity
UH Horizontal Velocity
SV Vertical Stress
SH Horizontal Stress
AB Airblast

Typical time histories for the following gages are presented in Figure 7.3.

Type of Measurement	Instrumentation Number	Radial		Range		Depth	
		rad	(deg)	m	(ft)	m	(ft)
Vertical Stress (SV)	5201	0	(0)	18.3	(60)	1.52	(5)
Vertical Acceleration (AV)	5117	0	(0)	18.3	(60)	0.457	(1.5)
Vertical Velocity (UV)	5721	0	(0)	18.3	(60)	0.457	(1.5)
Airblast (AB)	5305	4.71	(270)	18.3	(60)	----	(---)

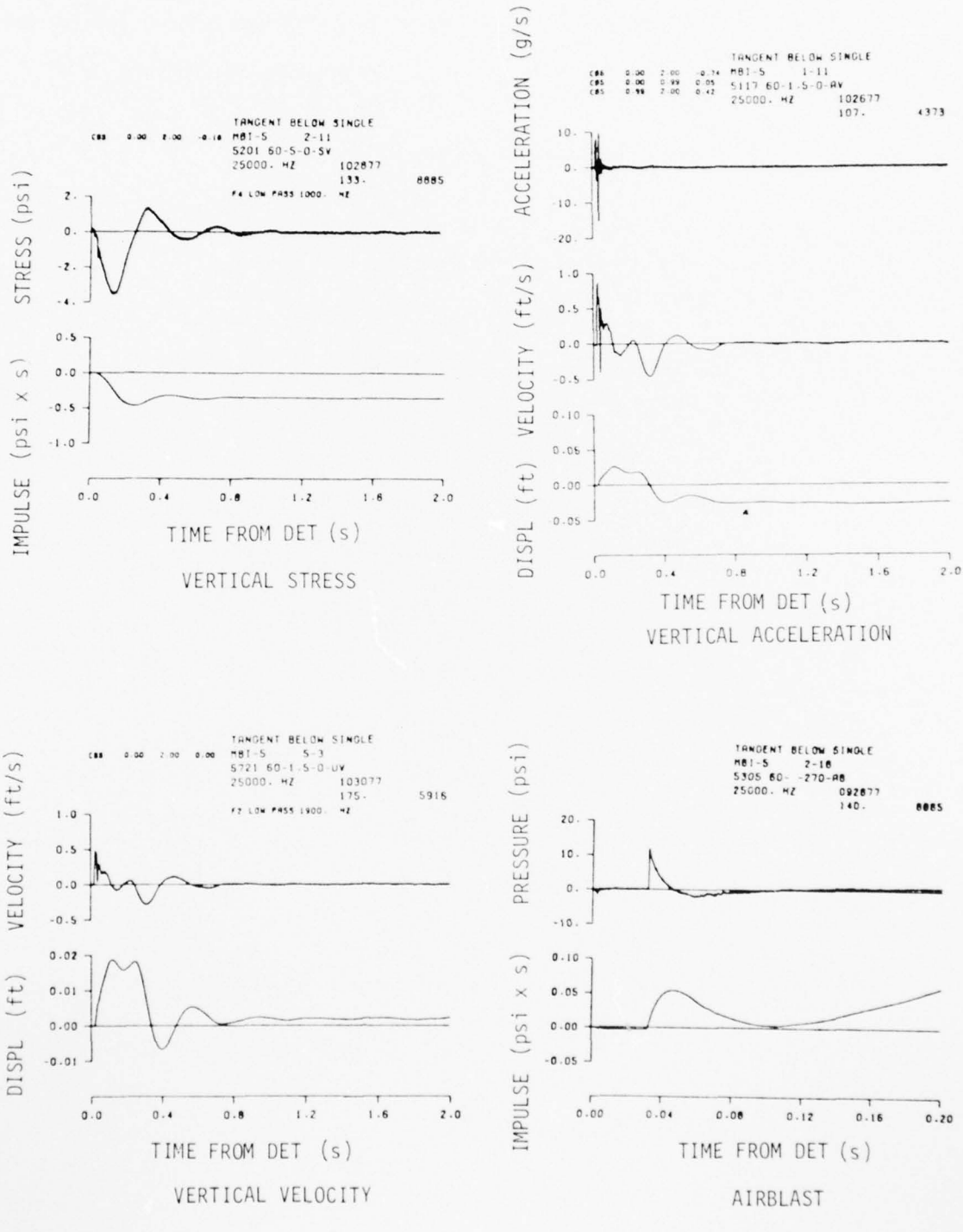

Figure 7.3. Typical time histories for Event MBI-5.

Figure 7.4 shows the comparison of measured and predicted vertical waveforms at the 36.6 meter range and 0.46 meter depth.

7.3 CRATER AND EJECTA EXPERIMENTS

7.3.1 Crater and Ejecta Layout

Four radial lines were surveyed to determine the parameters for the apparent crater. Free field areal density measurements were made along the four radials. Several different types of debris collection devices were used as shown in Figure 7.5.

7.3.2 Results

The average apparent values for the Event MBI-5 crater are:

Volume:	99.2 m^3 (3504 ft^3)
Radius:	4.57 meters (15.0 feet)
Depth below SGZ:	3.28 meters (10.8 feet)

Figure 7.6 is a plot of the crater profile. The average free field areal density versus range plot is given in Figure 7.7.

Figure 7.8 shows the debris depth versus range normalized by the cube root of the apparent crater volume. The average permanent vertical displacement versus range is shown in Figure 7.9.

AD-A070 526 DEFENSE NUCLEAR AGENCY WASHINGTON DC F/G 19/1
MISERS BLUFF. PRELIMINARY RESULTS REPORT. VOLUME I. PHASE I.(U)
JAN 79 R G DERAAD

UNCLASSIFIED DNA-POR-6980-VOL-1 DOE-WT-6980-VOL-1 NL

2 OF 2
AD
A070526

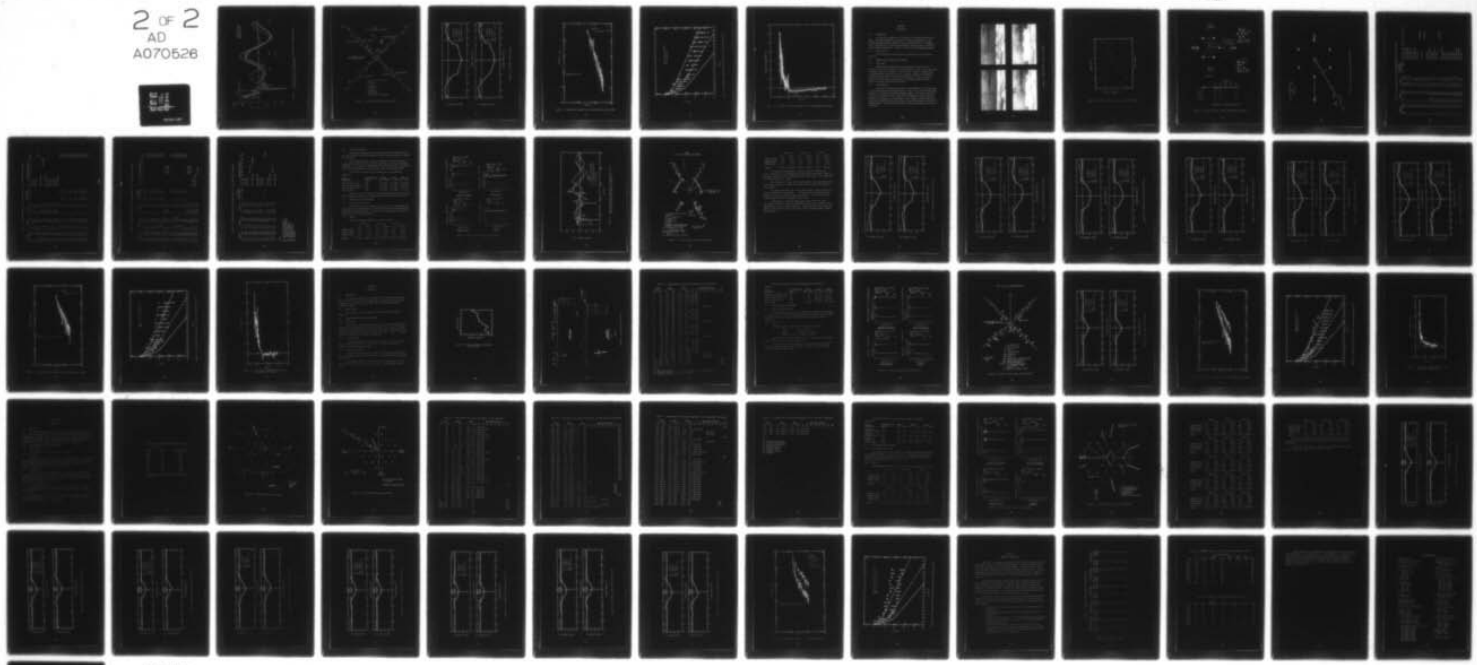

END
DATE
FILMED
8-79
DDC

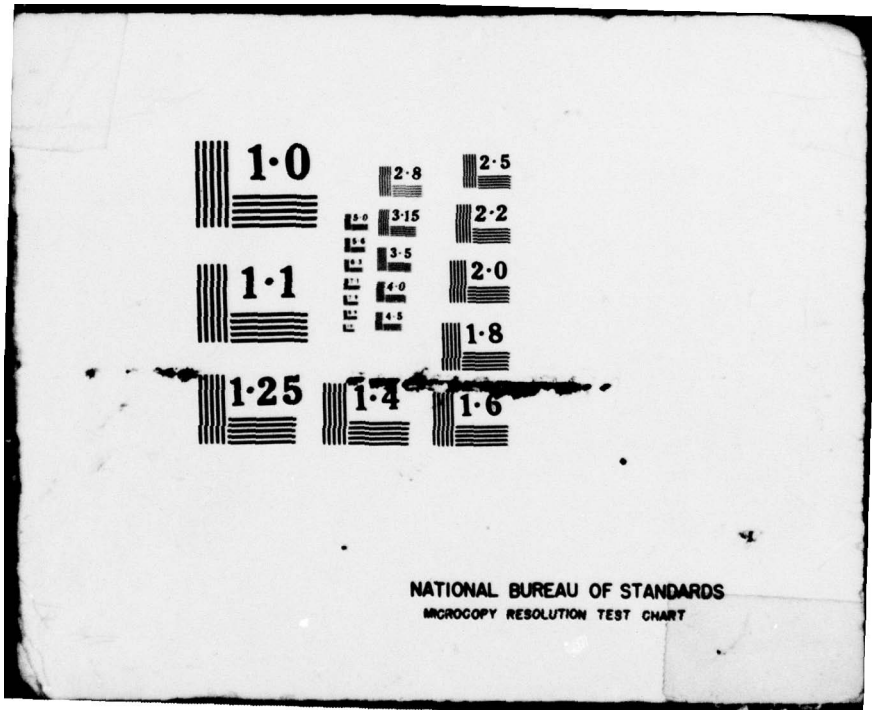
1·0
1·1
1·25
1·4
1·6
1·8
2·0
2·2
2·5
2·8
3·15
3·5
4·0
4·5
NATIONAL BUREAU OF STANDARDS
MICROCOPY RESOLUTION TEST CHART

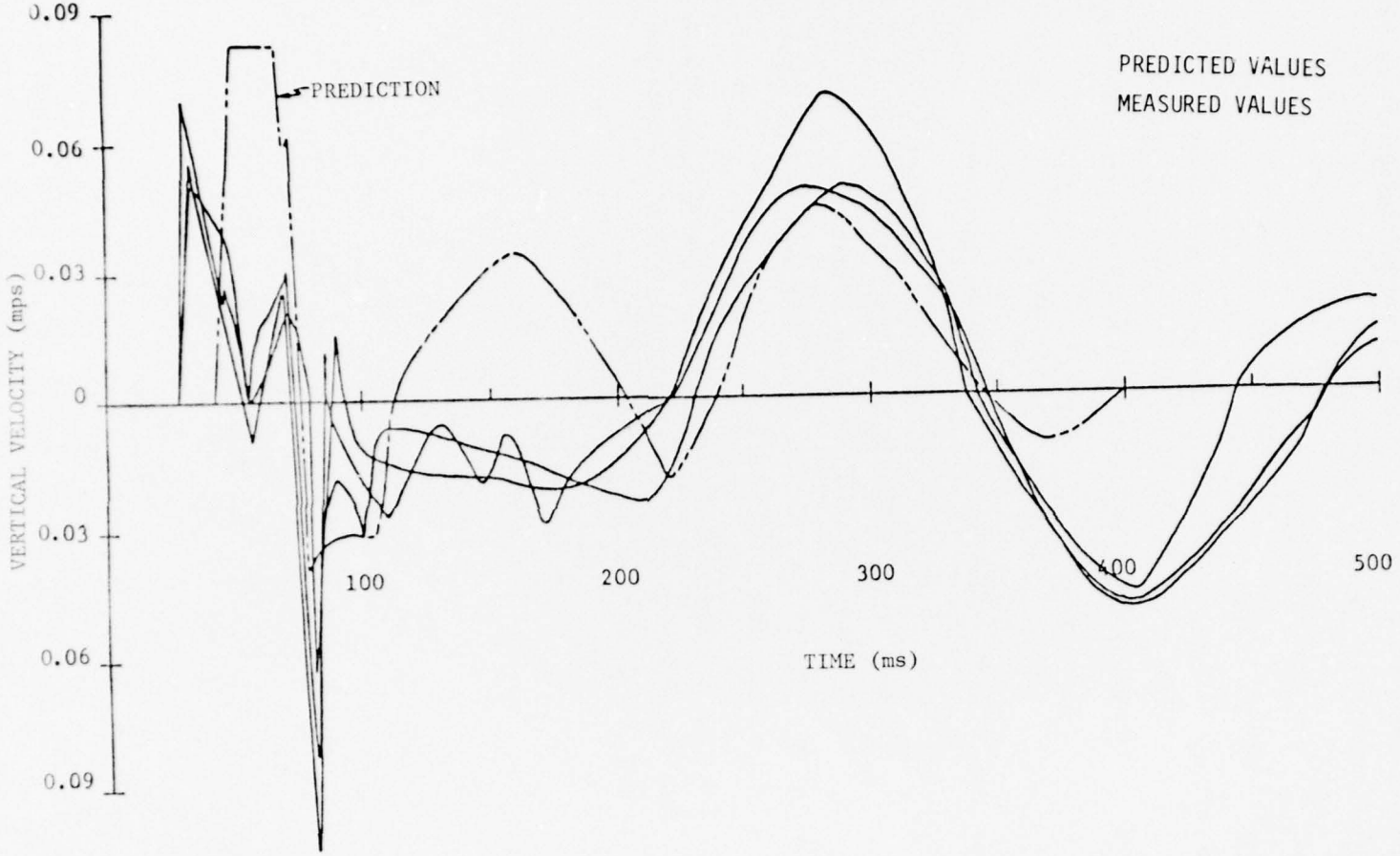

Figure 7.4. Event MBI-5 comparison of measured and predicted vertical waveforms at the 36.6 meter range and 0.46 meter depth.

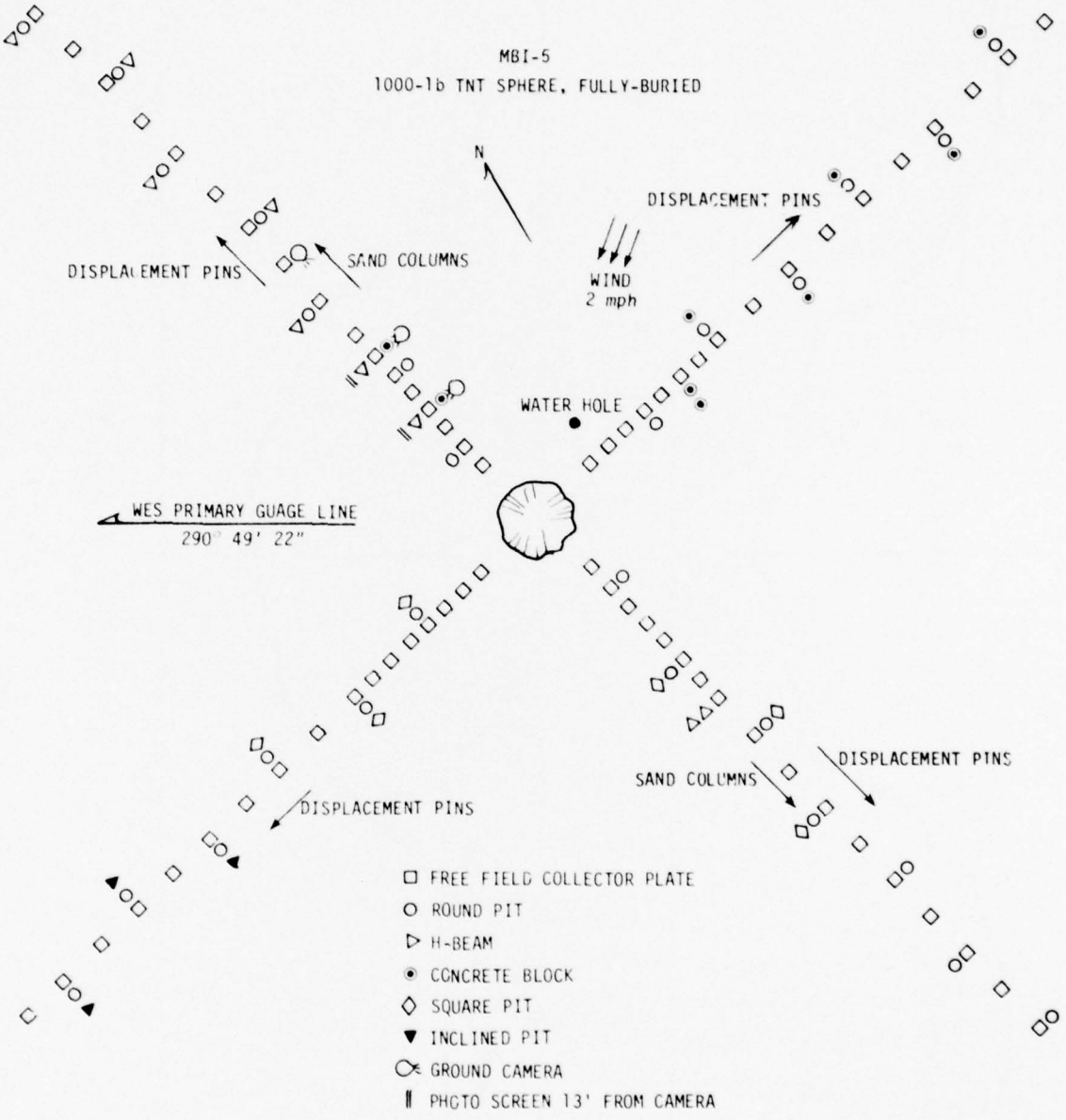

Figure 7.5. Debris collector layout for Event 5.

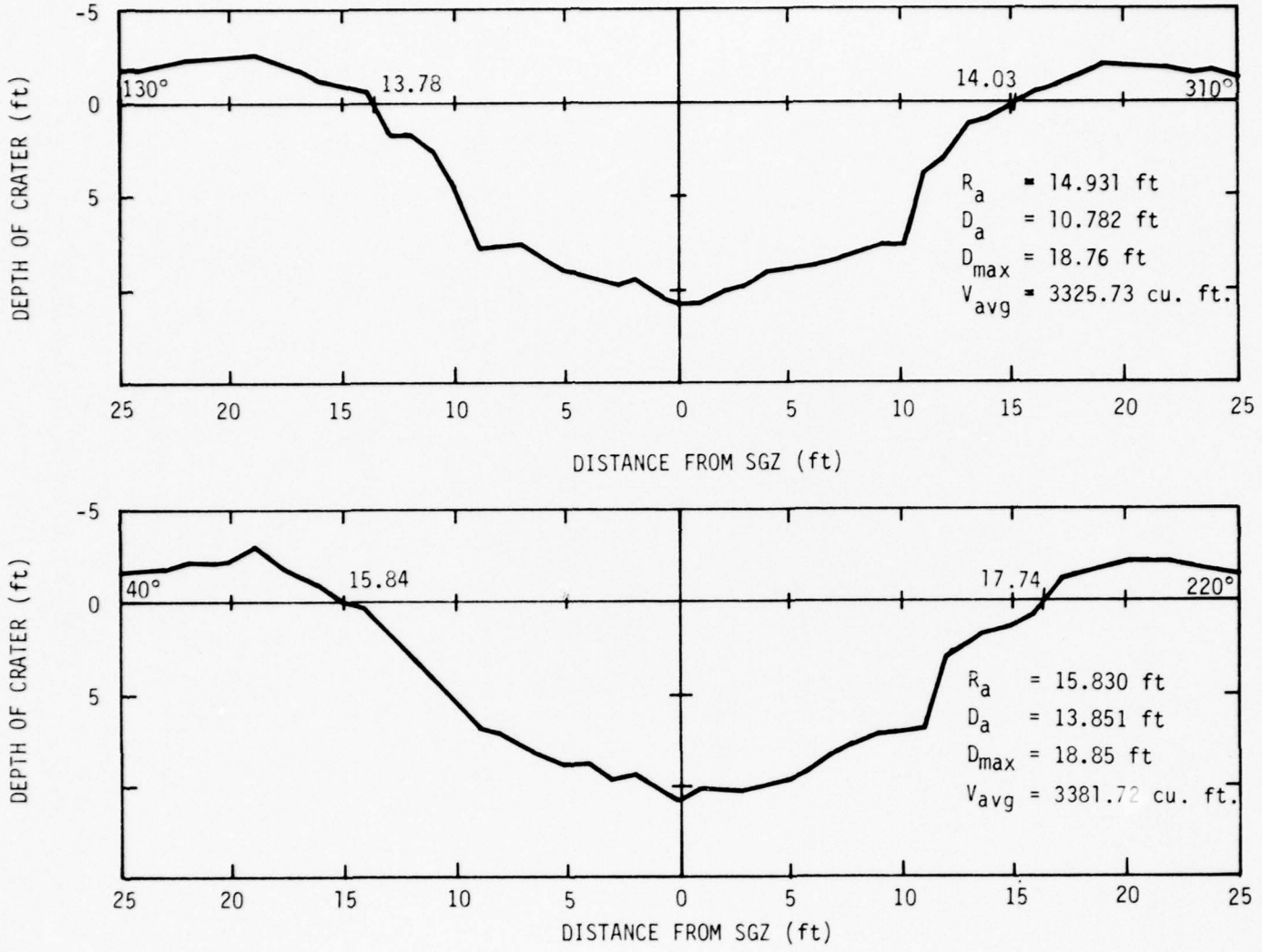

Figure 7.6. Event MBI-5 crater profiles.

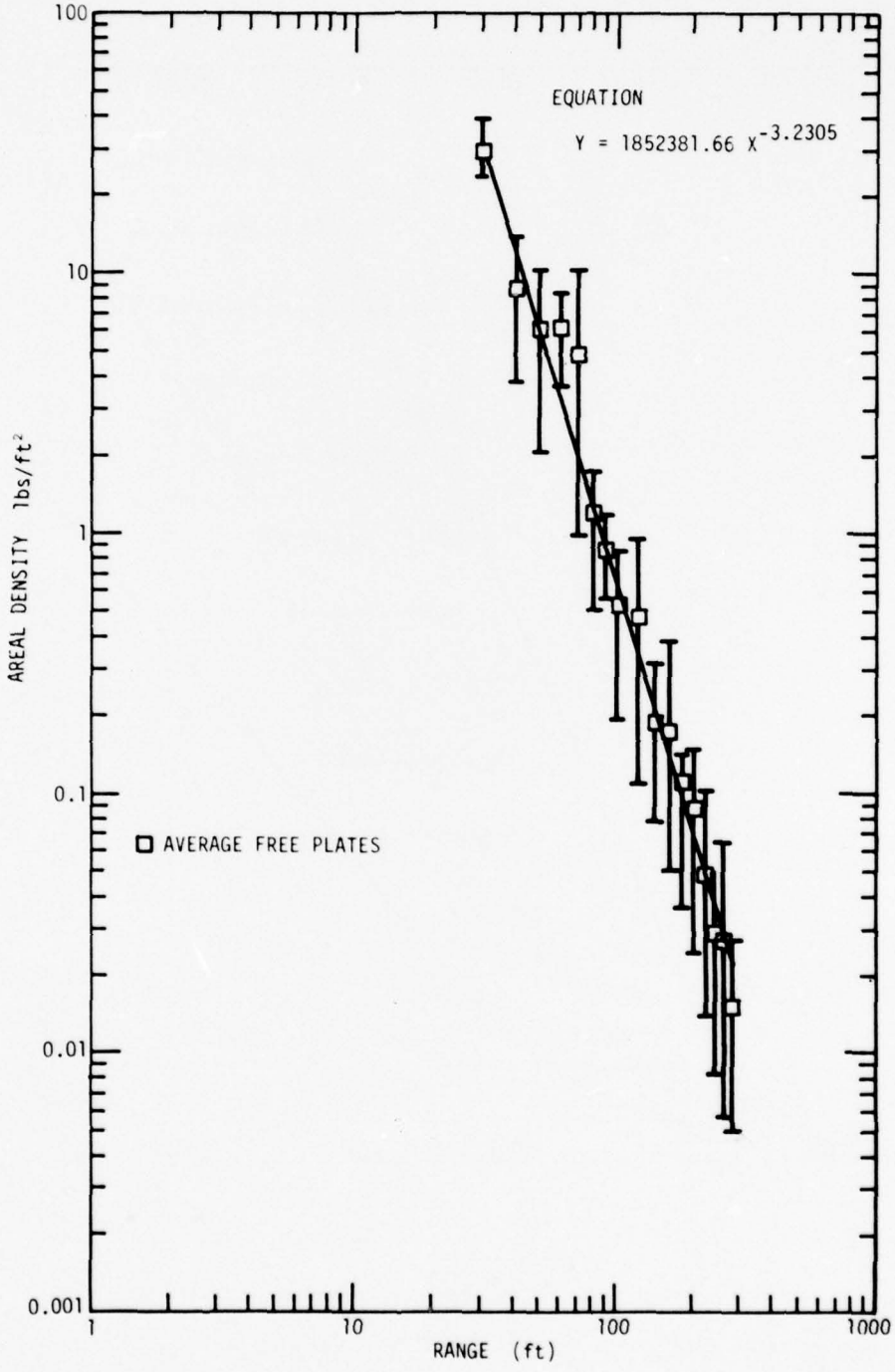

Figure 7.7. Event MBI-5, average free field areal density versus range.

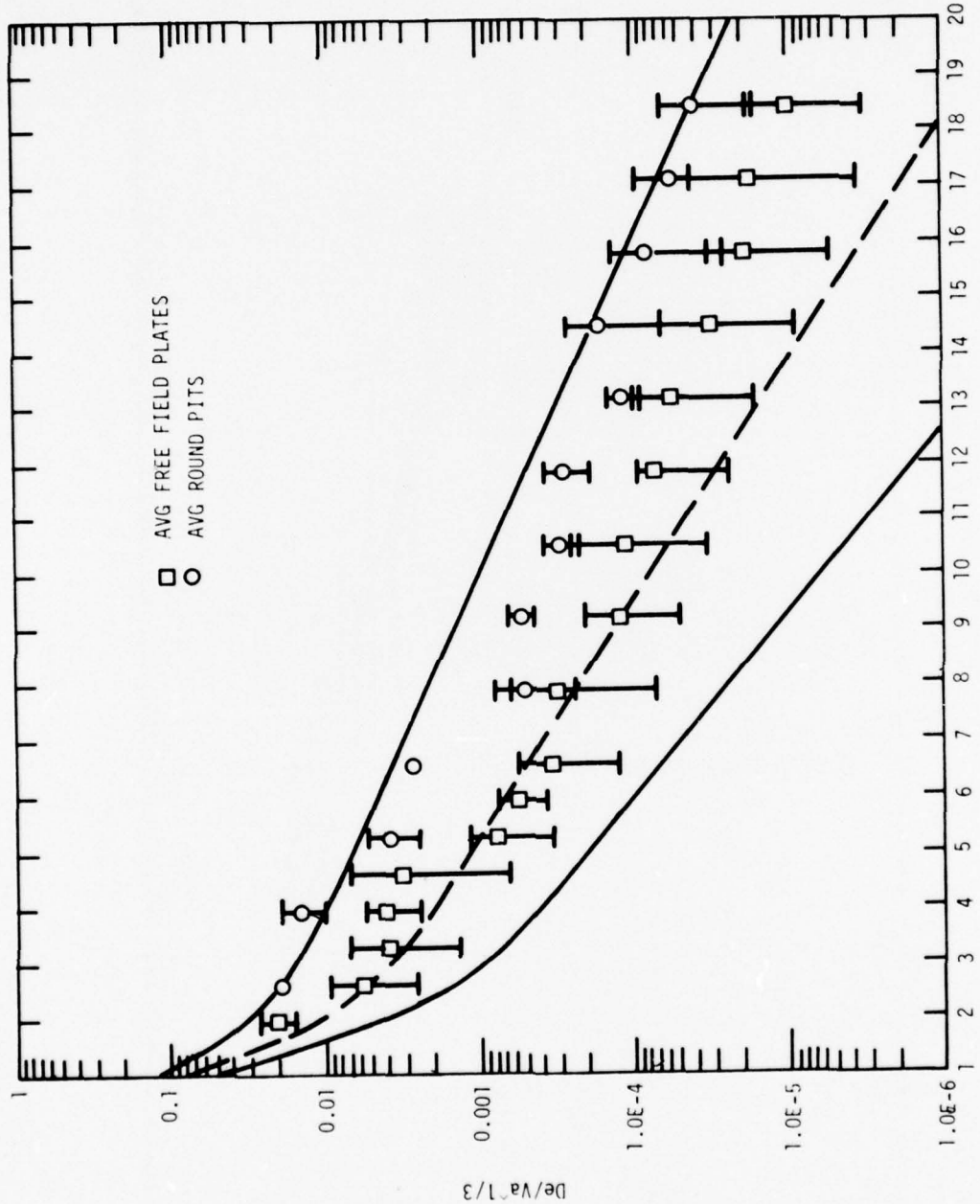

Figure 7.8. Event MBI-5, debris depth versus range, both normalized by $V_a^{1/3}$.

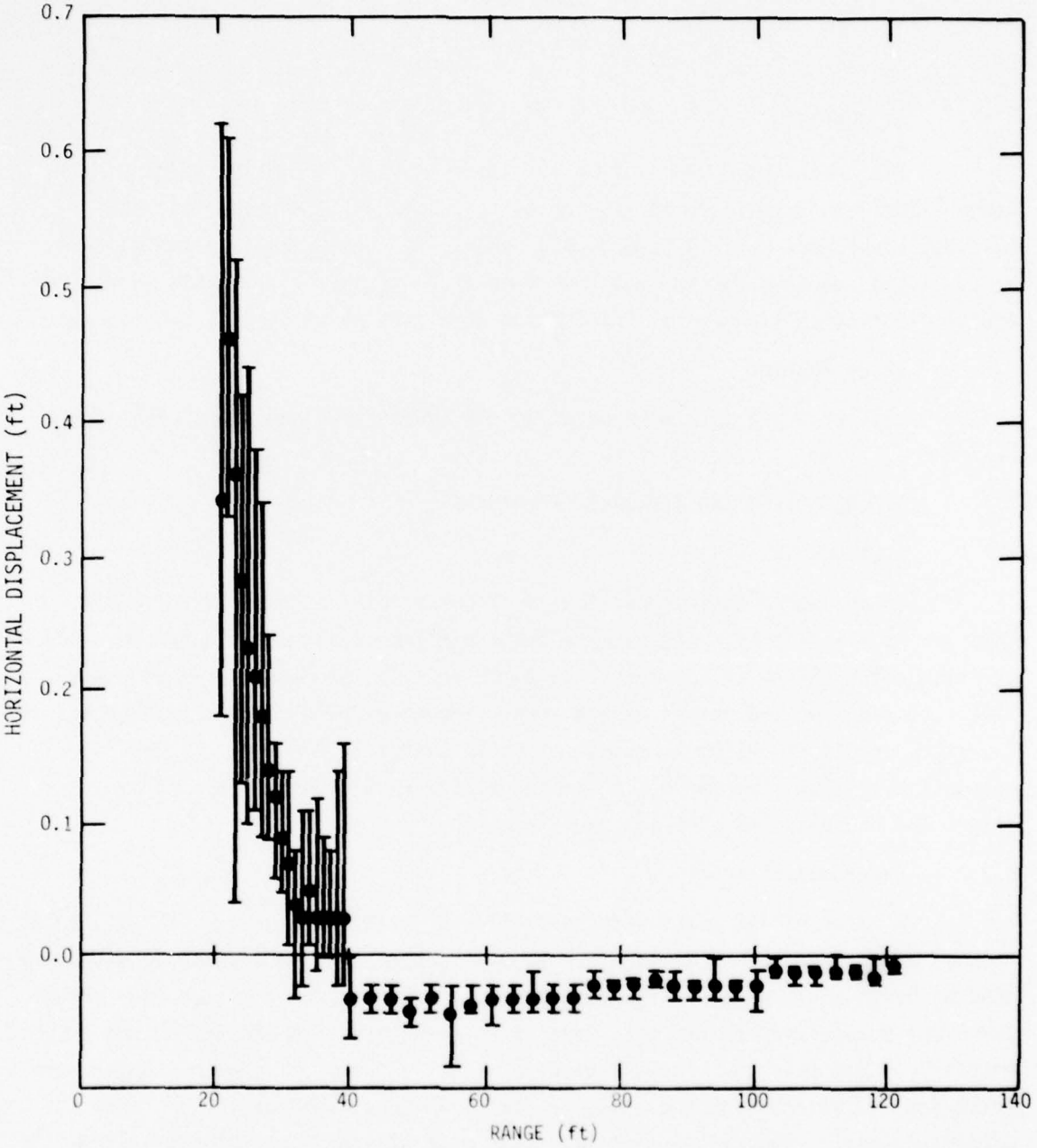

Figure 7.9. Event MBI-5, average permanent vertical displacement versus range.

SECTION 8

EVENT MBI-6

8.1 DESCRIPTION

This event was conducted on 13 October 1977 at the White Sands Missile Range. The event consisted of an array of six 454-kg (1000-pound) cast TNT half-buried spheres equally spaced 36.6 meters (120 feet) apart in a hexagonal array to provide data for the multiburst waveform synthesis prediction model for the half-buried configuration. Figure 8.1 shows the event detonation sequence.

8.1.1 Water Content

Soil moisture data were obtained for Event MBI-6 and are plotted in Figure 8.2.

8.2 GROUND MOTION AND AIRBLAST EXPERIMENTS

8.2.1 Gage Layout

Ground shock instrumentation was located both in the interior and exterior of the ring of charges, also between adjacent charges. Gages were placed at depths of 0.457 to 12.2 meters (1.5 to 40 feet). The main (0 radian) gage line extended from the center of the array through a charge, and contained all the gages placed at depths in excess of 0.457 meters (1.5 feet). Figure 8.3 presents both plan view and cross section of the ground motion gage array. Figure 8.4 presents the airblast gage layout.

8.2.2 Instrumentation

A total of 146 gages were installed; 99 accelerometers, 6 velocity gages, 12 soil stress gages, and 29 airblast gages. Table 8.1 is a listing of each gage, denoted by an arbitrarily assigned measurement number. The airblast gage array for Event 6 consisted of two main gage lines--one through a charge and one on a bisector of two charges. For the bisector line, a number of airblast gages were installed at offsets from the actual radial. These offsets appear in Table 8.1 as negative numbers, indicating that the gages were placed counterclockwise from the true radial.

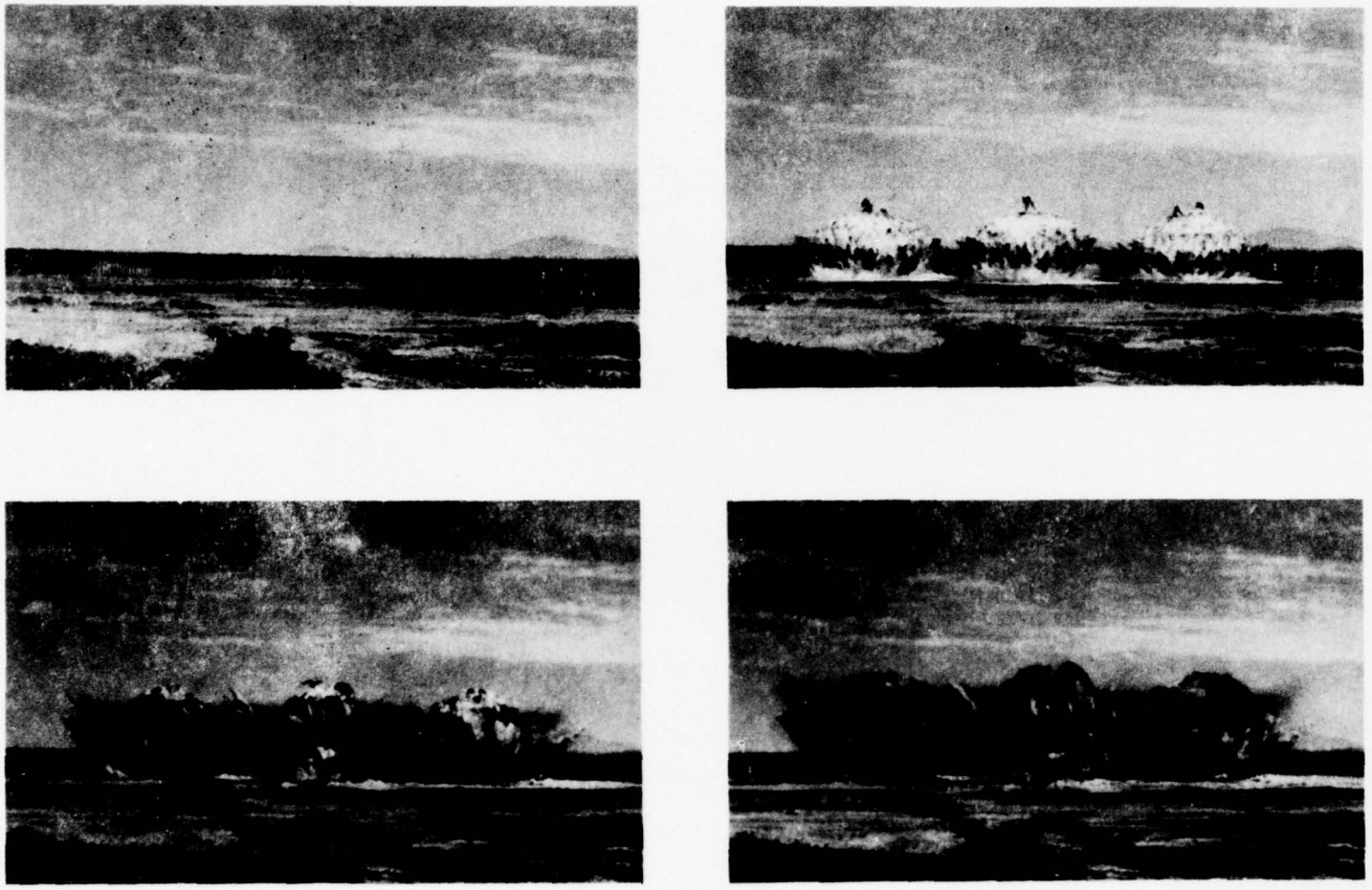

Figure 8.1. MISERS BLUFF MBI-6 detonation sequence.

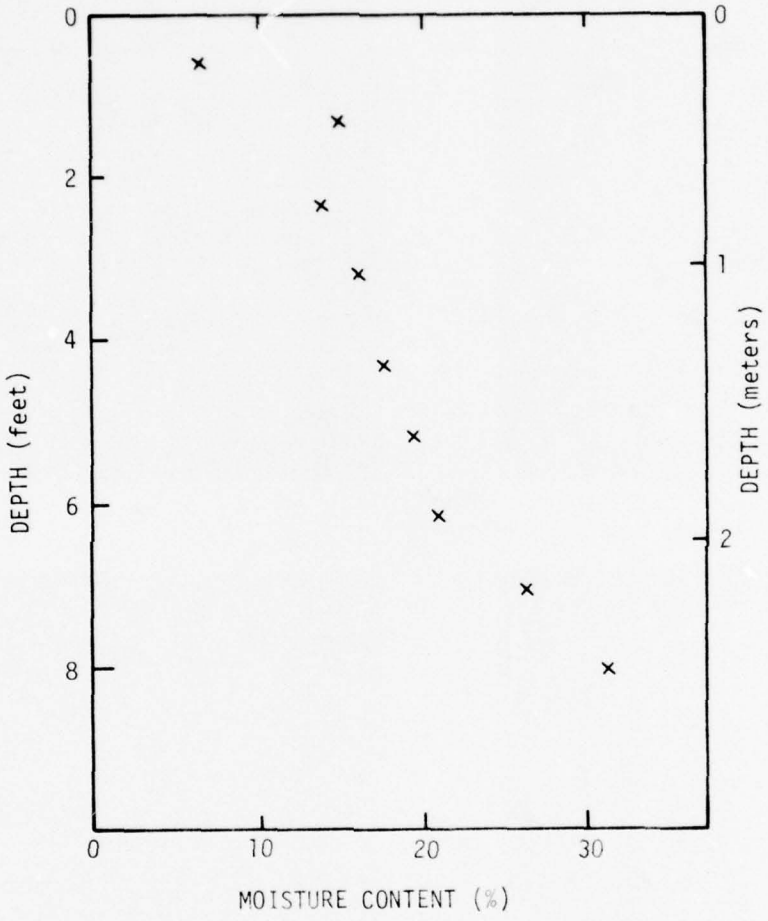

Figure 8.2. Moisture content data measured from Event MBI-6.

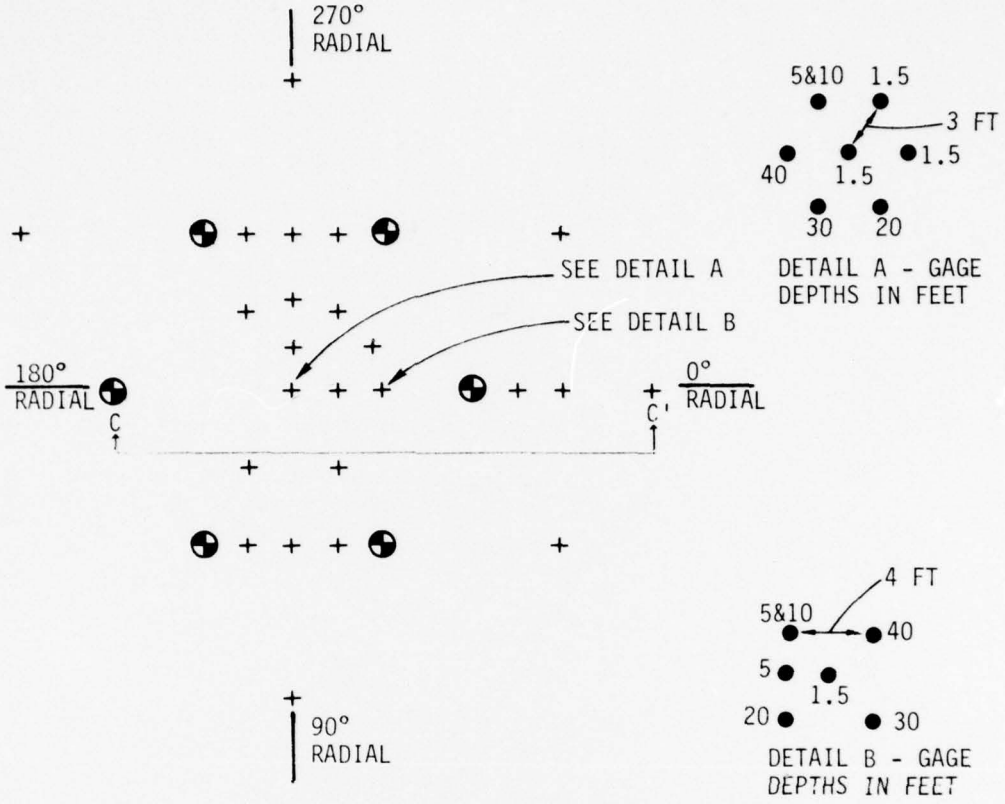

Figure 8.3. Ground motion gage layout, MISERS BLUFF Event MBI-6.

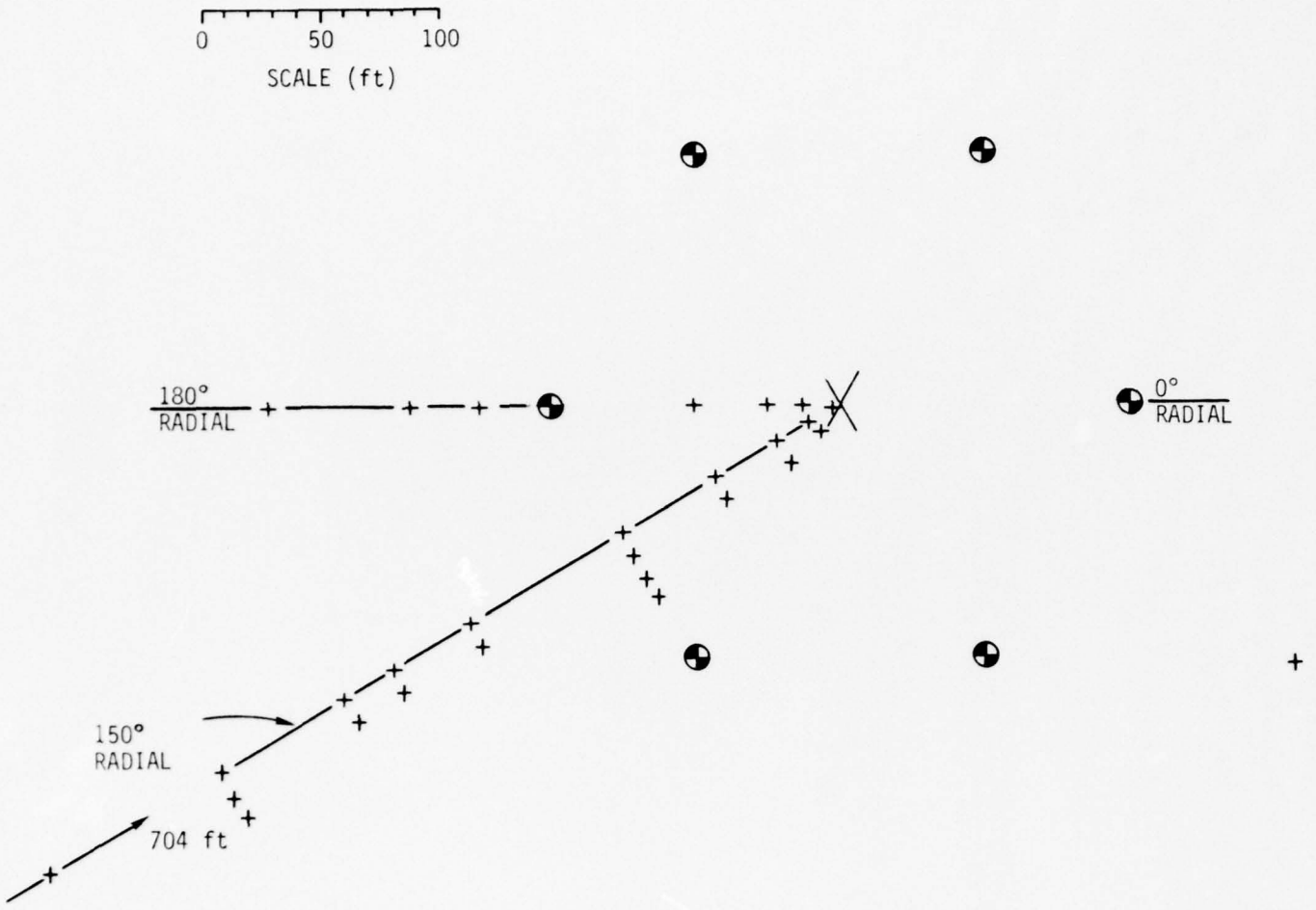

Figure 8.4. Airblast gage layout, MISERS BLUFF MBI-6.

Table 8.1. Ground motion and airblast measurement list for Event MBI-6.

Radial		Range		Depth		AB. Offset from Radial									
Rad	(Deg)	m	(ft)	m	(ft)	m	(ft)	AV	AH	AT	UV	UH	SV	SH	AB
0	(0)	0	(0)	0.457	(1.5)			6117	6118	6188					
0	(0)	0	(0)	0.457	(1.5)			6119	6120	6189					
0	(0)	0	(0)	0.457	(1.5)			6131	6132	6191					
0	(0)	0	(0)	1.52	(5)			6121	6122						
0	(0)	0	(0)	3.05	(10)			6123	6124	6190					
0	(0)	0	(0)	6.10	(20)			6125	6126						
0	(0)	0	(0)	6.10	(20)								6405	6406	
0	(0)	0	(0)	9.14	(30)			6127	6128						
0	(0)	0	(0)	9.14	(30)								6403	6404	
0	(0)	0	(0)	12.2	(40)			6129	6130						
0	(0)	9.14	(30)	0.457	(1.5)			6113	6114	6187					
0	(0)	9.14	(30)	1.52	(5)			6115	6116						
0	(0)	18.3	(60)	0.457	(1.5)			6101	6102	6185					
0	(0)	18.3	(60)	1.52	(5)			6103	6104						
0	(0)	18.3	(60)	1.52	(5)								6401	6402	
0	(0)	18.3	(60)	3.05	(10)			6105	6106	6186					
0	(0)	18.3	(60)	6.10	(20)			6107	6108						
0	(0)	18.3	(60)	9.14	(30)			6109	6110						
0	(0)	18.3	(60)	12.2	(40)			6111	6112						
0	(0)	45.7	(150)	0.457	(1.5)			6139	6140						
0	(0)	54.9	(180)	0.457	(1.5)			6141	6142						
0	(0)	73.2	(240)	0.457	(1.5)			6143	6144	6194					
0	(0)	73.2	(240)	3.05	(10)			6145	6146	6195					
0	(0)	73.2	(240)	6.10	(20)			6147	6148						

Table 8.1. Ground motion and airblast measurement list for Event MBI-6 (Continued).

Radial		Range		Depth		AB. Offset from Radial		Measurement Numbers							
Rad	(Deg)	m	(ft)	m	(ft)	m	(ft)	AV	AH	AT	UV	UH	SV	SH	AB
0	(0)	73.2	(240)	9.14	(30)			6149	6150						
0	(0)	73.2	(240)	12.2	(40)			6151	6152						
0.524	(30)	66.1	(217)	0	(0)										6328
0.524	(30)	73.2	(240)	0.457	(1.5)			6163	6164	6196					
1.057	(60)	1.83	(6)	0.457	(1.5)								6407	6408	
1.057	(60)	18.3	(60)	0.457	(1.5)			6167	6168	6198					
1.29	(74)	32.9	(108)	0.457	(1.5)			6161	6162						
1.57	(90)	31.7	(104)	0.457	(1.5)			6159	6160						
1.57	(90)	63.4	(208)	0.457	(1.5)			6153	6154						
1.85	(106)	32.9	(108)	0.457	(1.5)			6157	6158						
2.09	(120)	18.3	(60)	0.457	(1.5)			6165	6166	6197					
2.62	(150)	0.914	(3)	0	(0)	0	(0)								6301
2.62	(150)	3.05	(10)	0	(0)	-0.823	(-2.7)								6302
2.62	(150)	4.57	(15)	0	(0)	0	(0)								6303
2.62	(150)	9.14	(30)	0	(0)	0	(0)								6304
2.62	(150)	9.14	(30)	0	(0)	-3.05	(-10)								6305
2.62	(150)	18.3	(60)	0	(0)	0	(0)								6306
2.62	(150)	18.3	(60)	0	(0)	-3.05	(-10)								6307
2.62	(150)	31.7	(104)	0	(0)	0	(0)								6308
2.62	(150)	31.7	(104)	0	(0)	-3.05	(-10)								6309
2.62	(150)	31.7	(104)	0	(0)	-7.62	(-20)								6310
2.62	(150)	31.7	(104)	0	(0)	-9.14	(-30)								6311
2.62	(150)	54.3	(178)	0	(0)	0	(0)								6312

Table 8.1. Ground motion and airblast measurement list for Event MBI-6 (Continued).

Radial		Range		Depth		AB. Offset from Radial		Measurement Numbers							
Rad	(Deg)	m	(ft)	m	(ft)	m	(ft)	AV	AH	AT	UV	UH	SV	SH	AB
2.62	(150)	54.3	(178)	0	(0)	-3.05	(-10)								6313
2.62	(150)	66.1	(217)	0	(0)	0	(0)								6314
2.62	(150)	66.1	(217)	0	(0)	-3.05	(-10)								6315
2.62	(150)	73.2	(240)	0	(0)	0	(0)								6316
2.62	(150)	73.2	(240)	0	(0)	-3.05	(-10)								6317
2.62	(150)	5.24	(300)	0	(0)	0	(0)								6318
2.62	(150)	5.24	(300)	0	(0)	-3.05	(-10)								6319
2.62	(150)	5.24	(300)	0	(0)	-6.10	(-20)								6320
2.62	(150)	146	(480)	0.457	(1.5)						6901	6902			
2.62	(150)	213	(700)	0.457	(1.5)						6903	6904			
2.62	(150)	215	(704)	0	(0)	0	(0)								6321
3.14	(180)	1.83	(6)	0	(0)	0	(0)								6327
3.14	(180)	3.11	(10.2)	0	(0)	0	(0)								6323
3.14	(180)	5.87	(19.25)	0	(0)	0	(0)								6322
3.14	(180)	7.62	(25)	0	(0)	0	(0)								6326
3.14	(180)	8.23	(27)	0	(0)	0	(0)								6324
3.14	(180)	29.3	(96)	0	(0)	0	(0)								6325
3.14	(180)	146	(480)	0.457	(1.5)						6905	6906			
3.14	(180)	215	(704)	0.457	(1.5)						6907	6908			
3.67	(210)	63.4	(208)	0.457	(1.5)			6173	6174						
4.19	(240)	18.3	(60)	0.457	(1.5)			6169	6170	6199					
4.19	(240)	18.3	(60)	0.457	(1.5)						6719	6720			

Table 8.1. Ground motion and airblast measurement list for Event MBI-6 (Continued).

Radial		Range		Depth		AB. Offset from Radial		Measurement Numbers							
Rad	(Deg)	m	(ft)	m	(ft)	m	(ft)	AV	AH	AT	UV	UH	SV	SH	AB
4.43	(254)	32.9	(108)	0.457	(1.5)			6175	6176						
4.71	(270)	9.14	(30)	0.457	(1.5)			6155	6156						
4.71	(270)	9.14	(30)	0.457	(1.5)						6711	6713			
4.71	(270)	18.3	(60)	0.457	(1.5)			6133	6134	6192			6409	6410	
4.71	(270)	18.3	(60)	1.52	(5)										
4.71	(270)	18.3	(60)	3.05	(10)			6137	6138	6193					
4.71	(270)	31.7	(104)	0.457	(1.5)			6177	6178						
4.71	(270)	63.4	(208)	0.457	(1.5)			6183	6184						
4.71	(270)	66.1	(217)	0	(0)	0	(0)								6329
4.99	(286)	32.9	(108)	0.457	(1.5)			6179	6180						
5.24	(300)	18.3	(60)	0.457	(1.5)			6171	6172	6200					
5.76	(330)	18.3	(60)	0.457	(1.5)						6701	6702			
5.76	(330)	63.4	(208)	0.457	(1.5)			6181	6182	6201					

NOTES:

AV Vertical Acceleration
AH Horizontal Acceleration
AT Transverse Acceleration
UV Vertical Velocity
UH Horizontal Velocity
SV Vertical Stress
SH Horizontal Stress
AB Airblast

8.2.3 Typical Data Records

Calibration and recorder start signals from the Timing and Firing (T&F) unit were properly received and translated, and all equipment operated as planned for Event MBI-6.

Data recovery was good. Three accelerometers and one velocity gage, measurement Nos. 6104, 6186, 6149 and 6901, respectively, yielded no useful data. In addition, stress gages Nos. 6403 and 6404, accelerometer No. 6152, and airblast gage No. 6320 produced data sufficiently noisy to be of questionable value.

Typical time histories for the following gages are presented in Figure 8.5.

Type of Measurement	Instrumentation Number	Radial rad (deg)	Range m (ft)	Depth m (ft)
Vertical Stress (SV)	6409	4.71 (270)	18.3 (60)	1.52 (5.0)
Vertical Acceleration (AV)	6133	4.71 (270)	18.3 (60)	0.46 (1.5)
Vertical Velocity (UV)	6719	4.19 (240)	18.3 (60)	0.46 (1.5)
Airblast (AB)	6306	2.62 (150)	18.3 (60)	0 (0)

Figure 8.6 shows the comparison of measured and empirical predicted waveform of the vertical velocity one charge spacing (120 feet) outside the array.

8.3 CRATER AND EJECTA EXPERIMENTS

8.3.1 Crater and Ejecta Layout

Four radial lines were surveyed in each of the craters to determine the parameters for the apparent craters. Free field areal density measurements were made along three primary radials. Several different types of debris collection devices were used as shown in Figure 8.7.

8.3.2 Results

The average pertinent parameters for each crater are:

	SGZ No. 1		SGZ No. 2		SGZ No. 3	
	m	(ft)	m	(ft)	m	(ft)
Apparent radius	3.26	(10.7)	3.20	(10.5)	3.35	(11.0)
Apparent depth	2.26	(7.4)	2.23	(7.3)	2.10	(6.9)
Maximum depth	2.29	(7.5)	2.23	(7.3)	2.13	(7.0)
Volume	30.4 m^3	1075 ft^3	28.0 m^3	990 ft^3	29.7 m^3	1050 ft^3

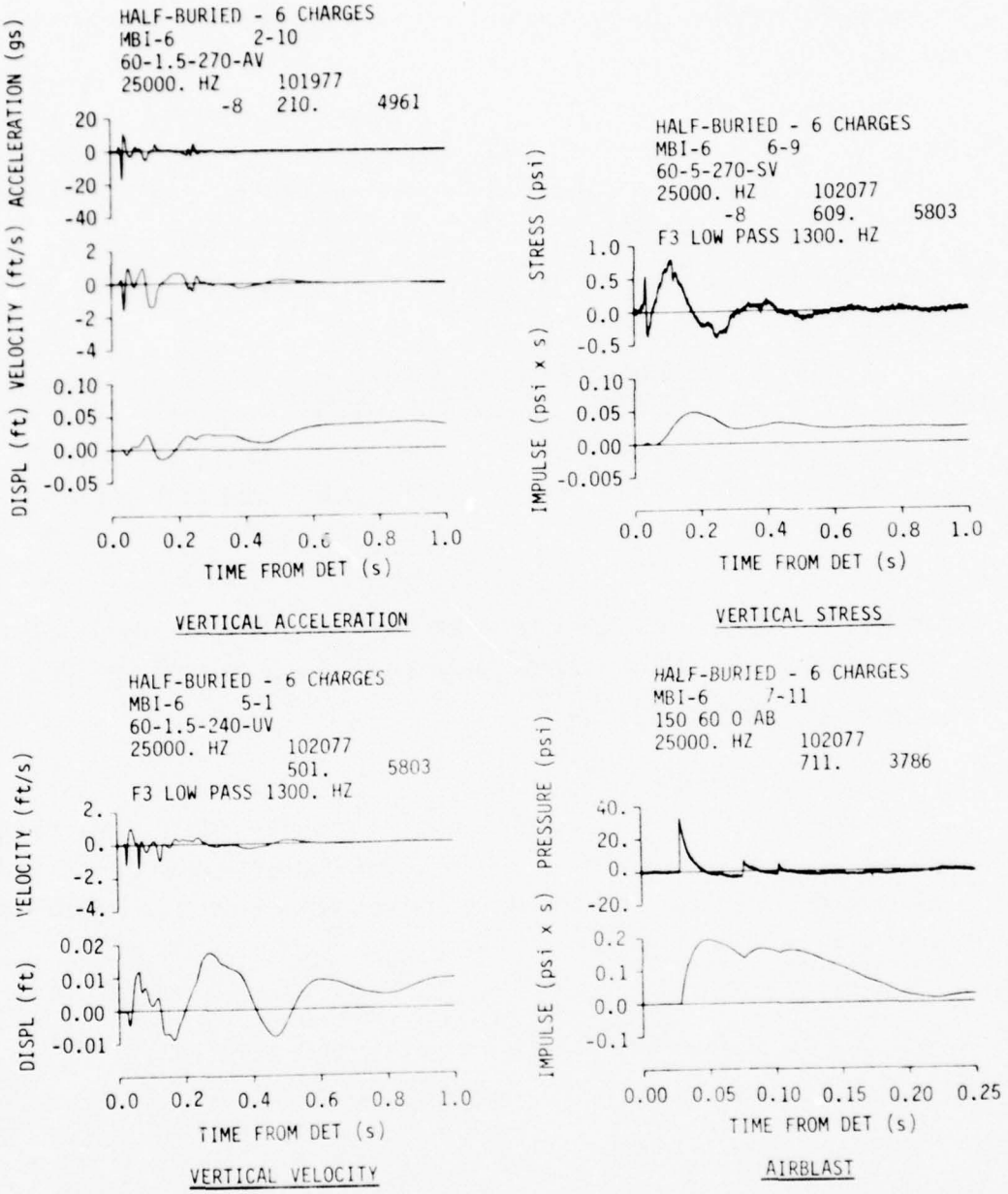

Figure 8.5. Typical time histories for Event MBI-6.

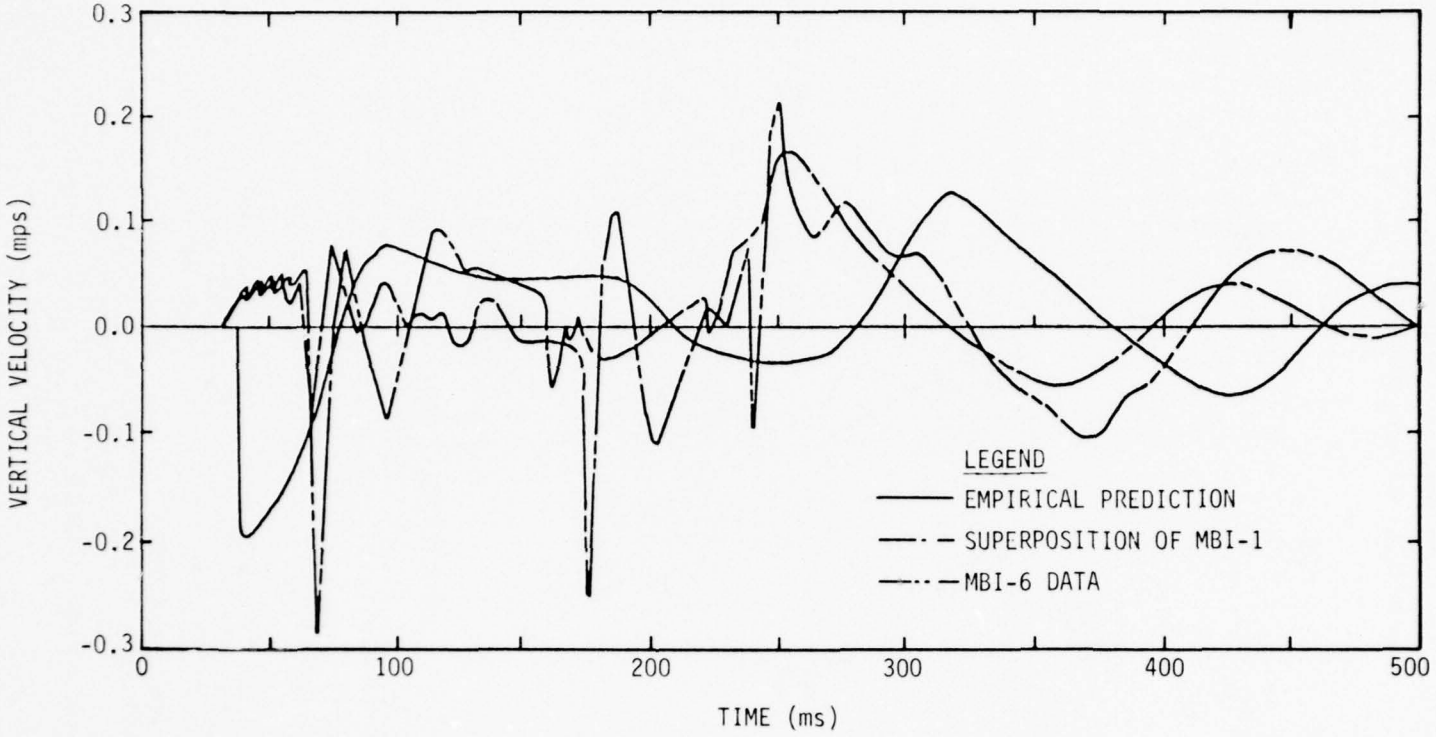

Figure 8.6. Event MBI-6 waveform comparisons of vertical velocity one charge spacing outside the array on a bisector.

MBI-6
6 1000 lb TNT SPHERES, HALF-BURIED

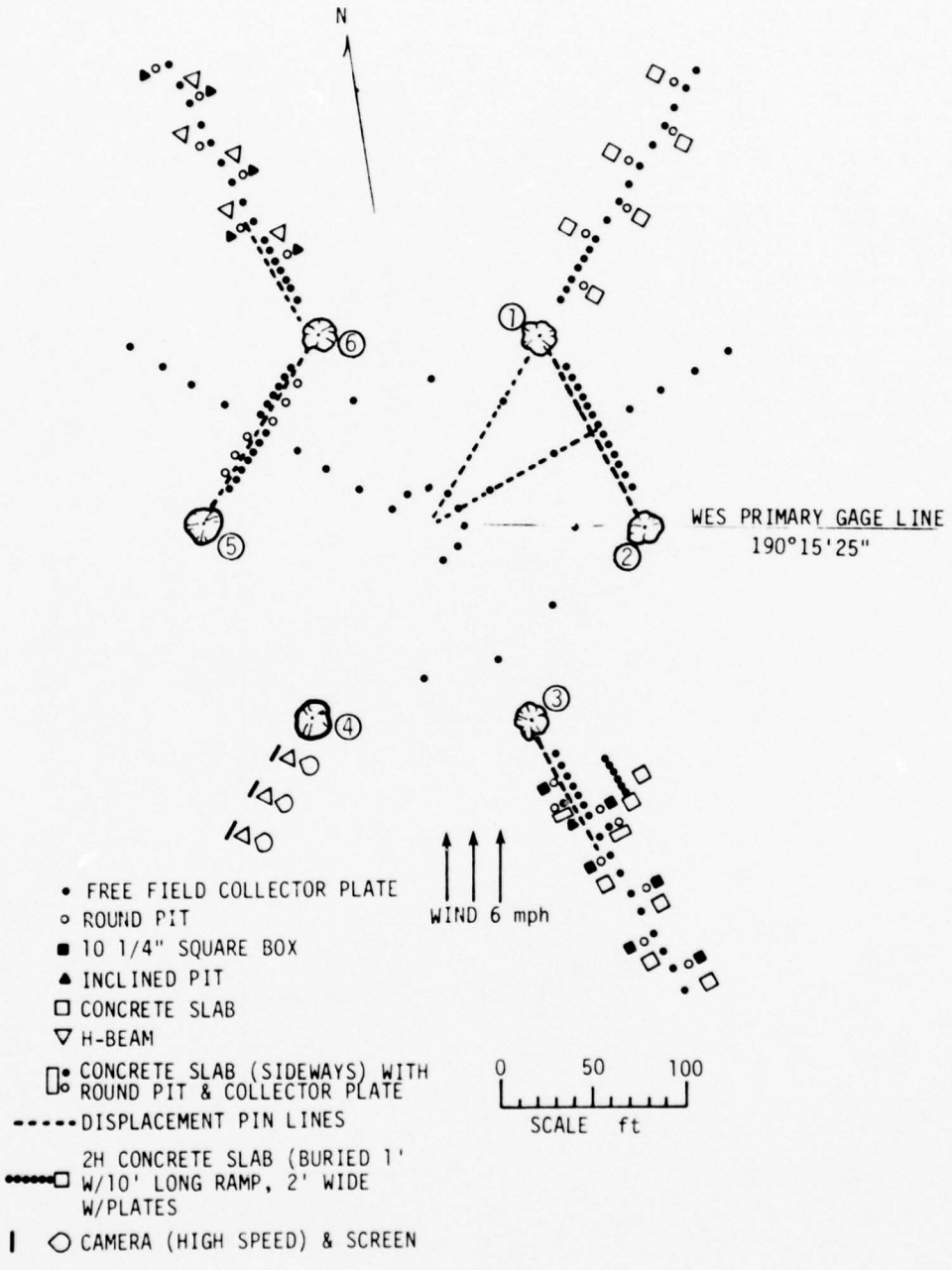

Figure 8.7. Debris collector layout for Event MBI-6.

	SGZ No. 4		SGZ No. 5		SGZ No. 6	
	m	(ft)	m	(ft)	m	(ft)
Apparent radius	3.51	(11.5)	3.38	(11.1)	3.41	(11.2)
Apparent depth	2.19	(7.2)	2.16	(7.1)	2.35	(7.7)
Maximum depth	2.26	(7.4)	2.16	(7.1)	2.38	(7.8)
Volume	29.4 m^3	1040 ft^3	33.0 m^3	1165 ft^3	34.5 m^3	1220 ft^3

The higher than normal depth of the debris from the collectors for SGZ No. 1 and SGZ No. 6 is attributed to the steady wind as indicated in Figure 8.7. The wind is also cause for the enhancement factors from SGZ No. 3 to be higher than the radials from SGZ Nos. 1 and 6.

The differences in crater sizes are attributed to slight variation in the soil geology at each site. Figures 8.8 through 8.13 are plots of the individual crater profiles.

The average free field areal density versus range is shown in Figure 8.14. The debris depth versus range normali by the cube root of the apparent crater volumes for craters 1, 3 and 6 are shown in Figure 8.15. Figure 8.16 shows the average permanent vertical displacements versus range.

Several types of collection devices were used to obtain the debris enhancement information. The primary enhancement collector devices were 5-gallon paint buckets set in the ground (round pits). Square boxes were also used as pits. Vertical steel plates and concrete slabs were used as aboveground debris enhancement structures.

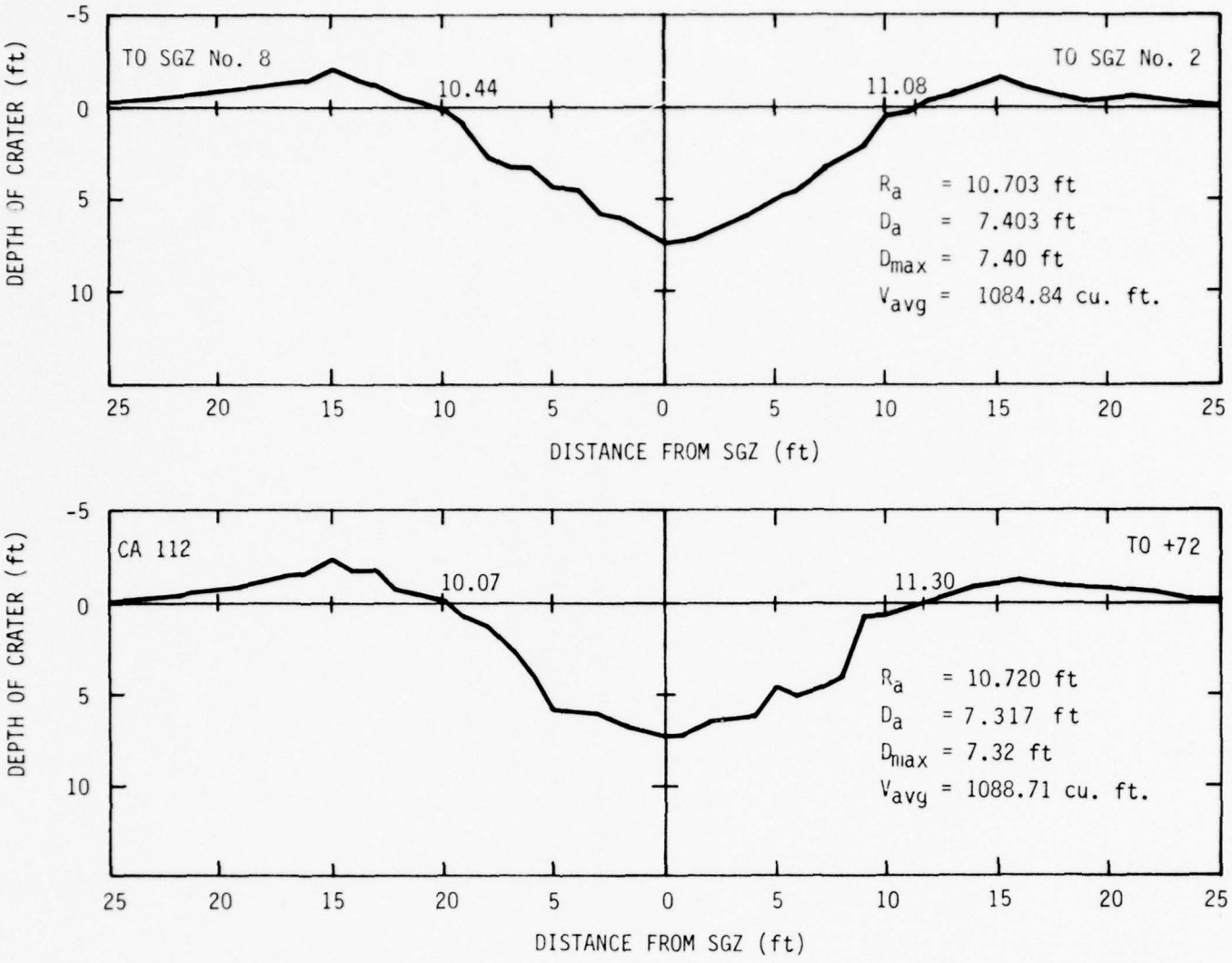

Figure 8.8. Event MBI-6 crater profiles for GZ No. 1.

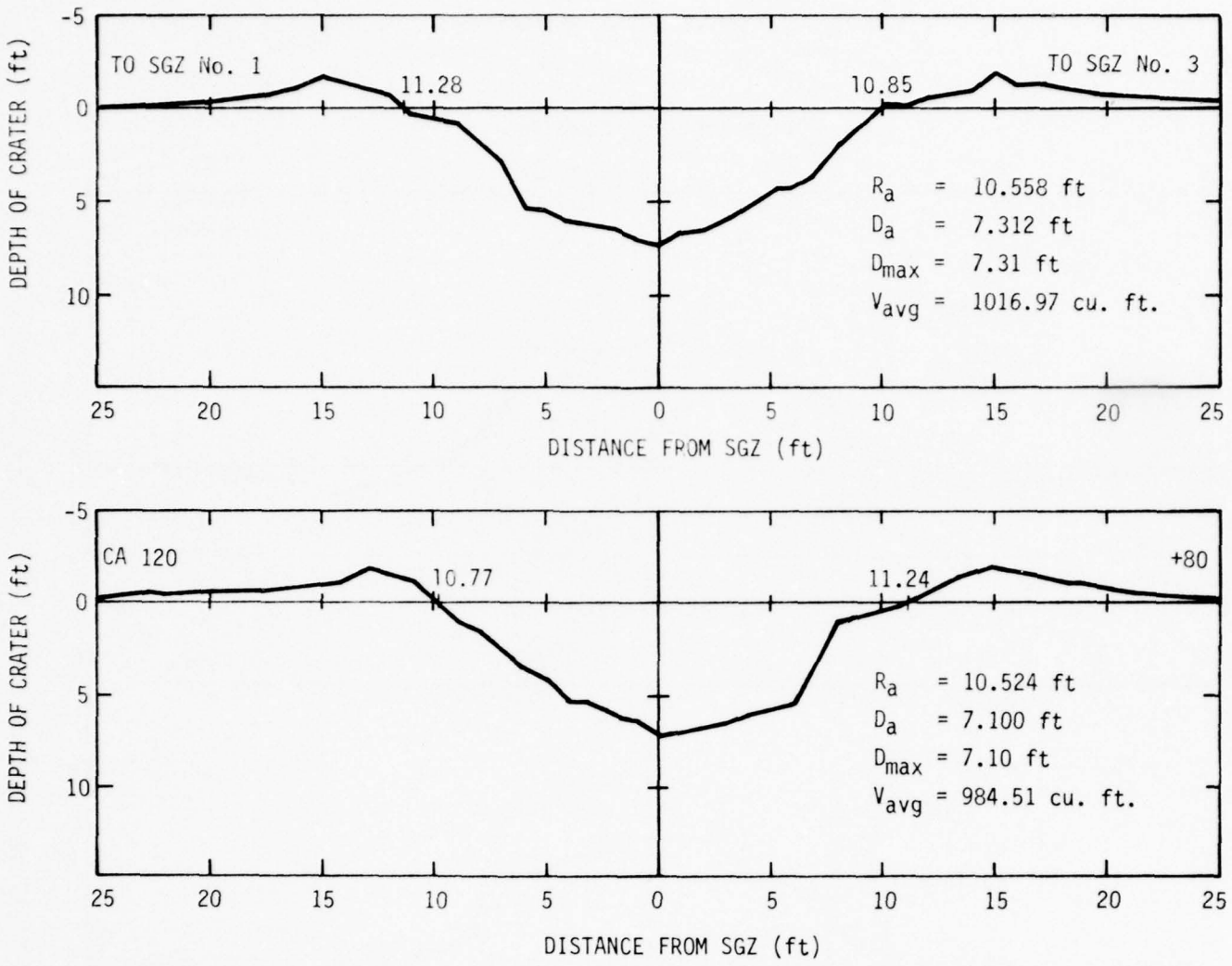

Figure 8.9. Event MBI-6 crater profiles for GZ No. 2.

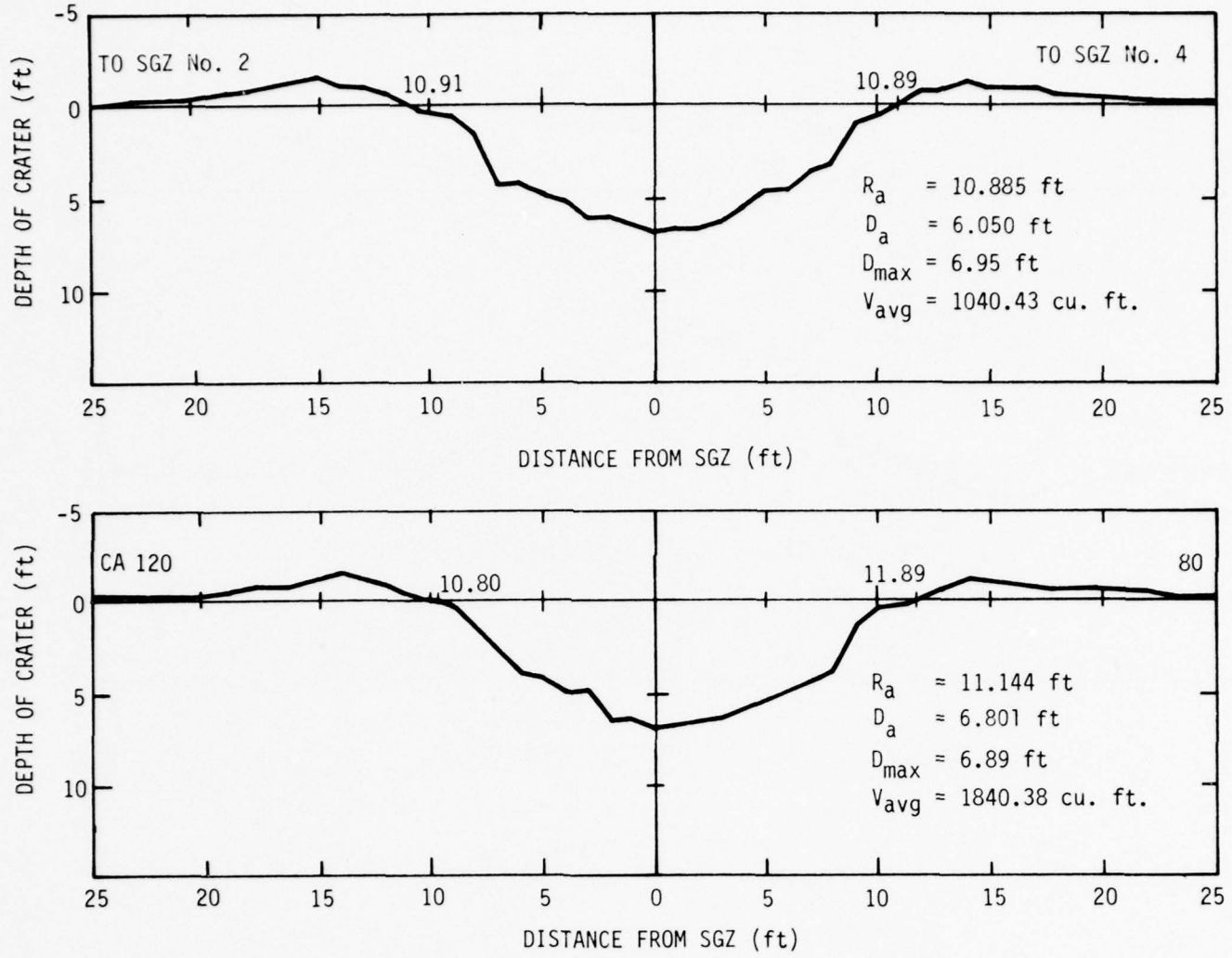

Figure 8.10. Event MBI-6 crater profile for GZ No. 3.

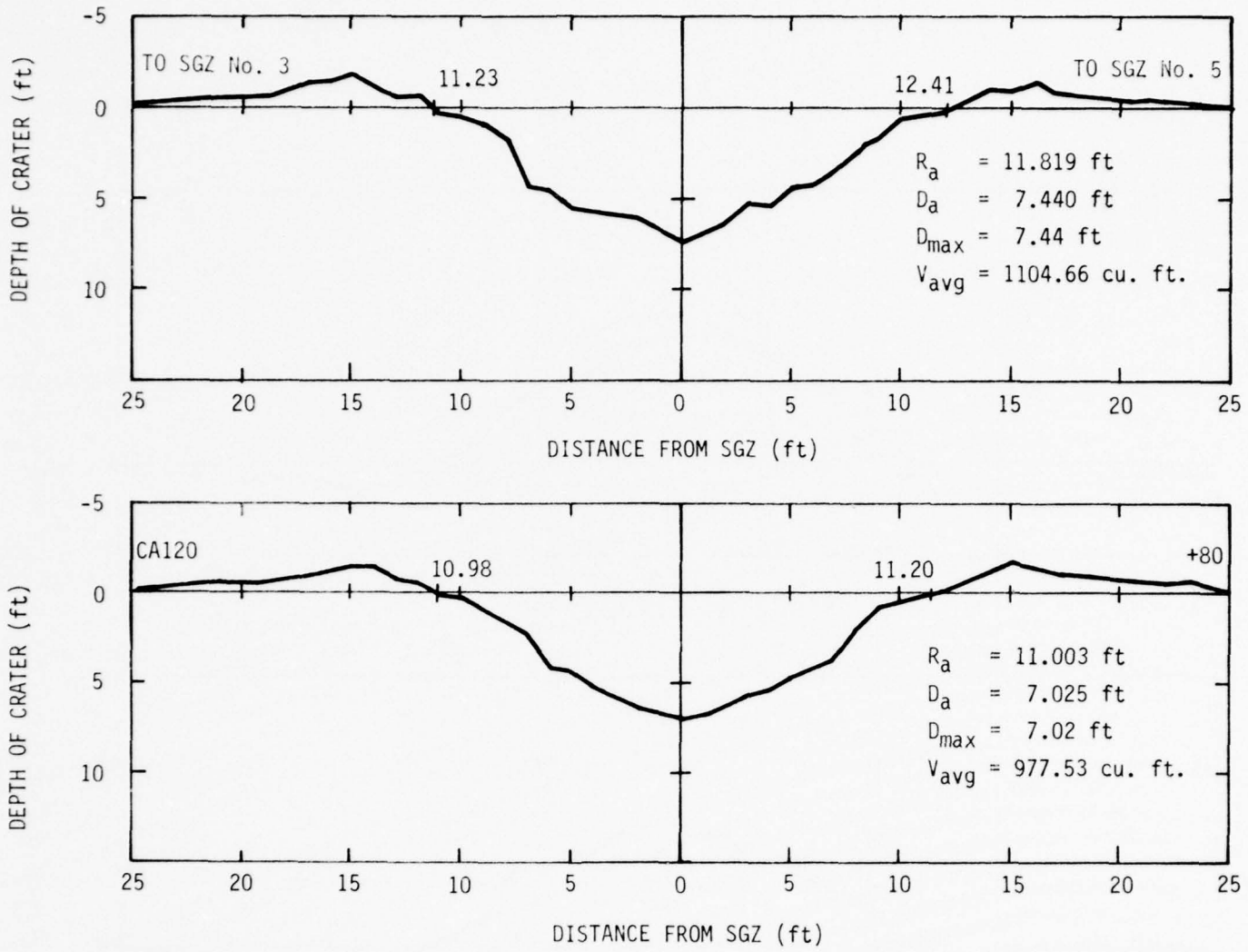

Figure 8.11. Event MBI-6 crater profile for GZ No. 4.

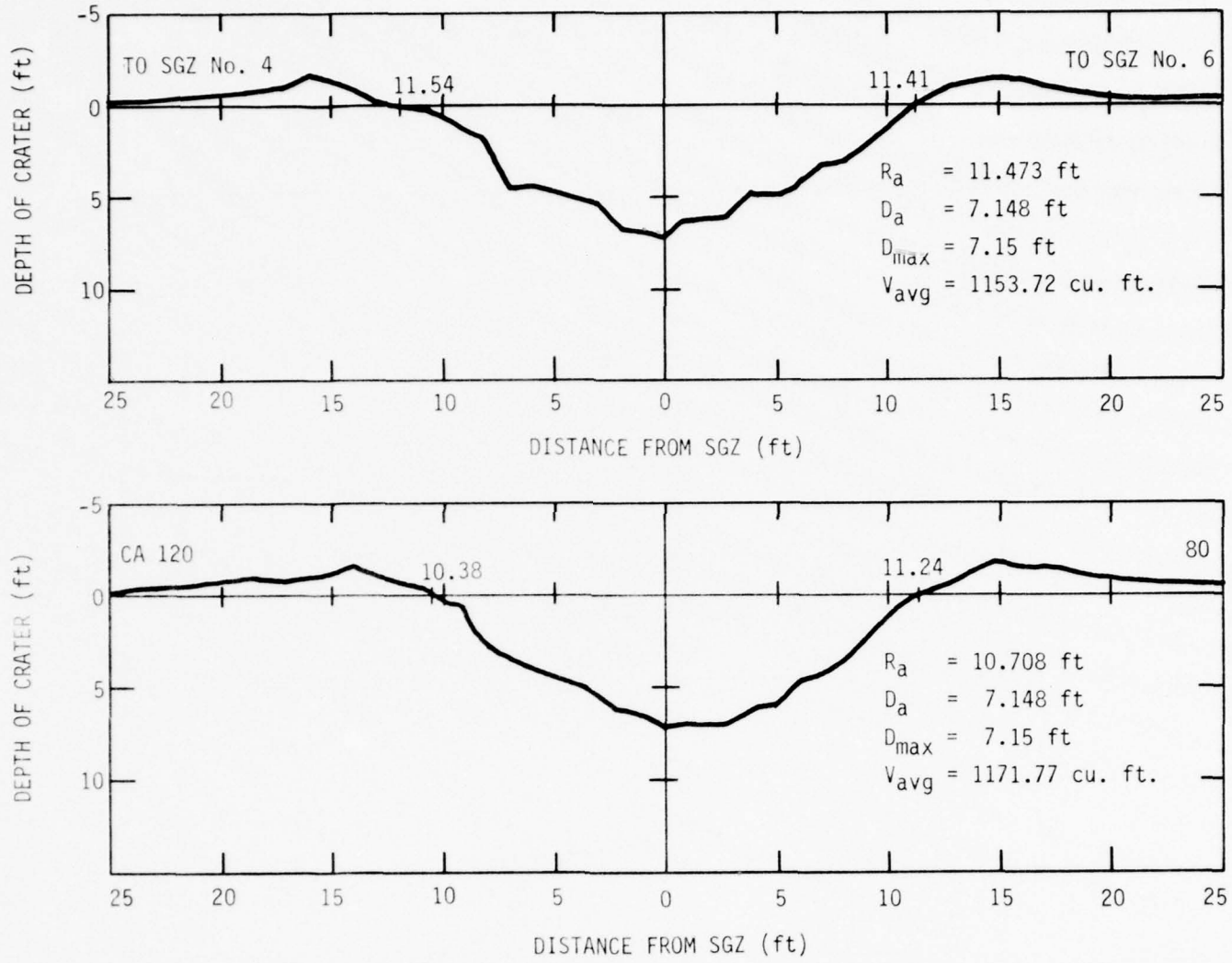

Figure 8.12. Event MBI-6 crater profile for GZ No. 5.

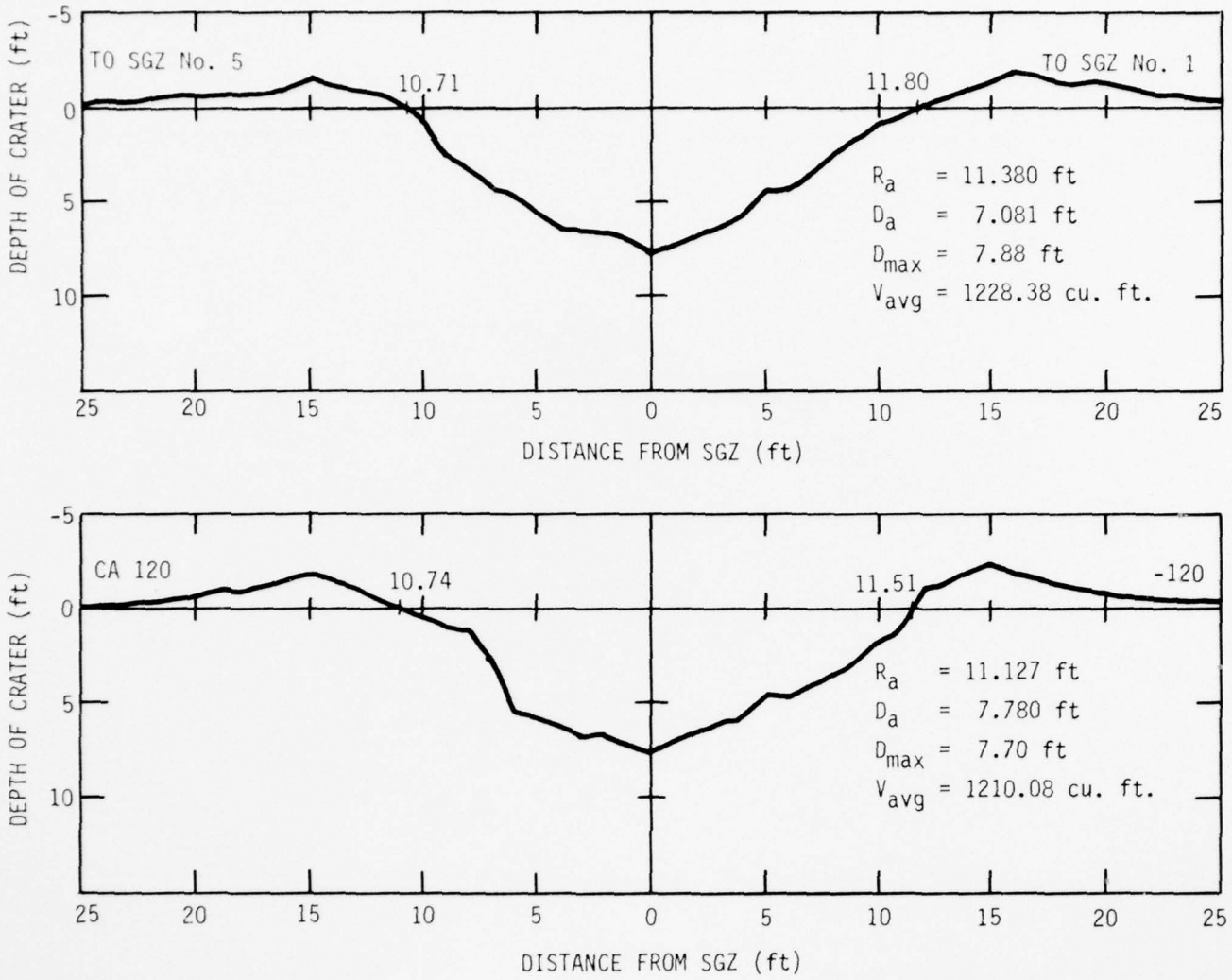

Figure 8.13. Event MBI-6 crater profile for GZ No. 6.

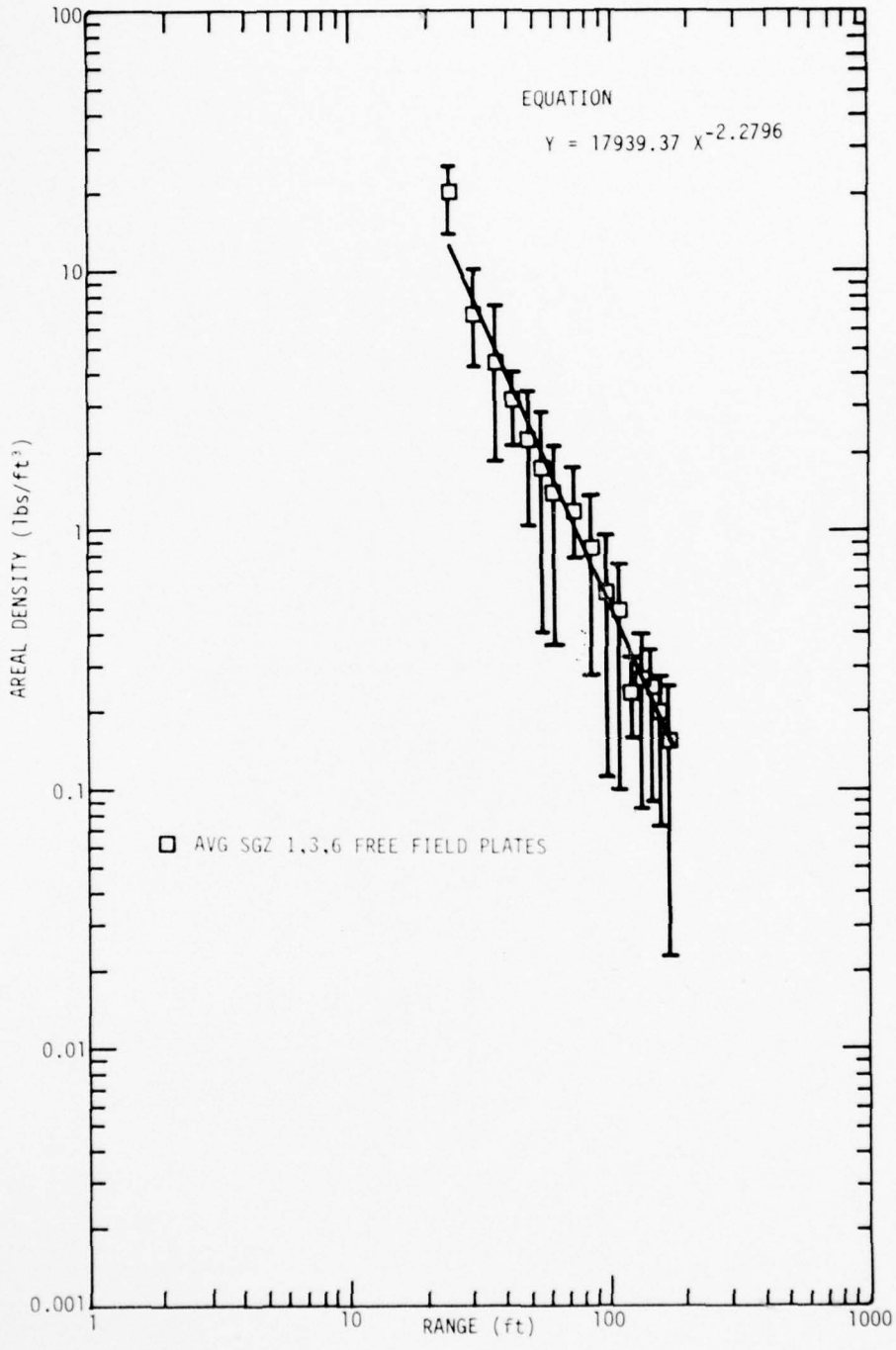

Figure 8.14. Event MBI-6, average free-field areal density versus range.

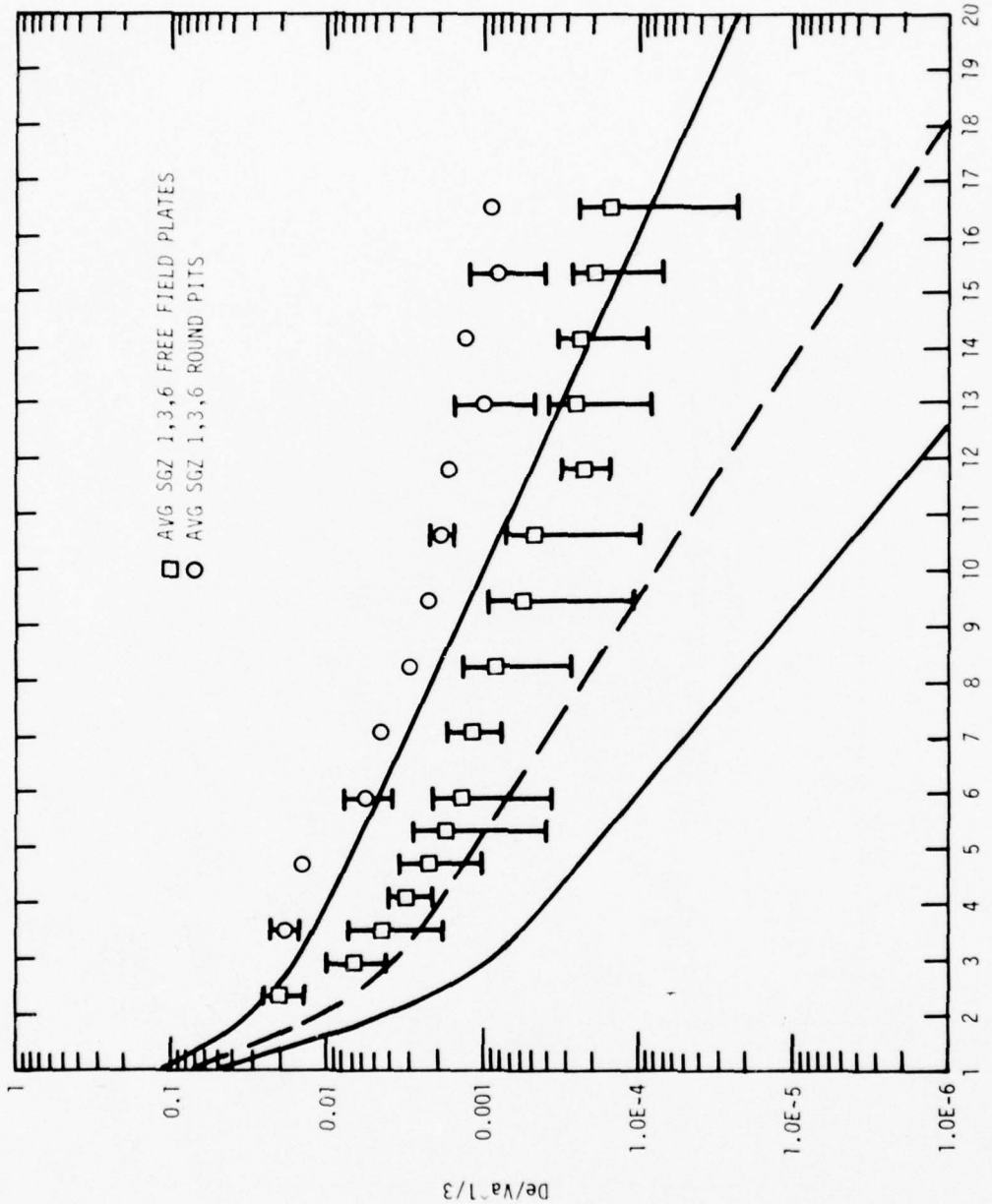

Figure 8.15. Event MBI-6, debris depth versus range, both normalized by $V_a^{1/3}$.

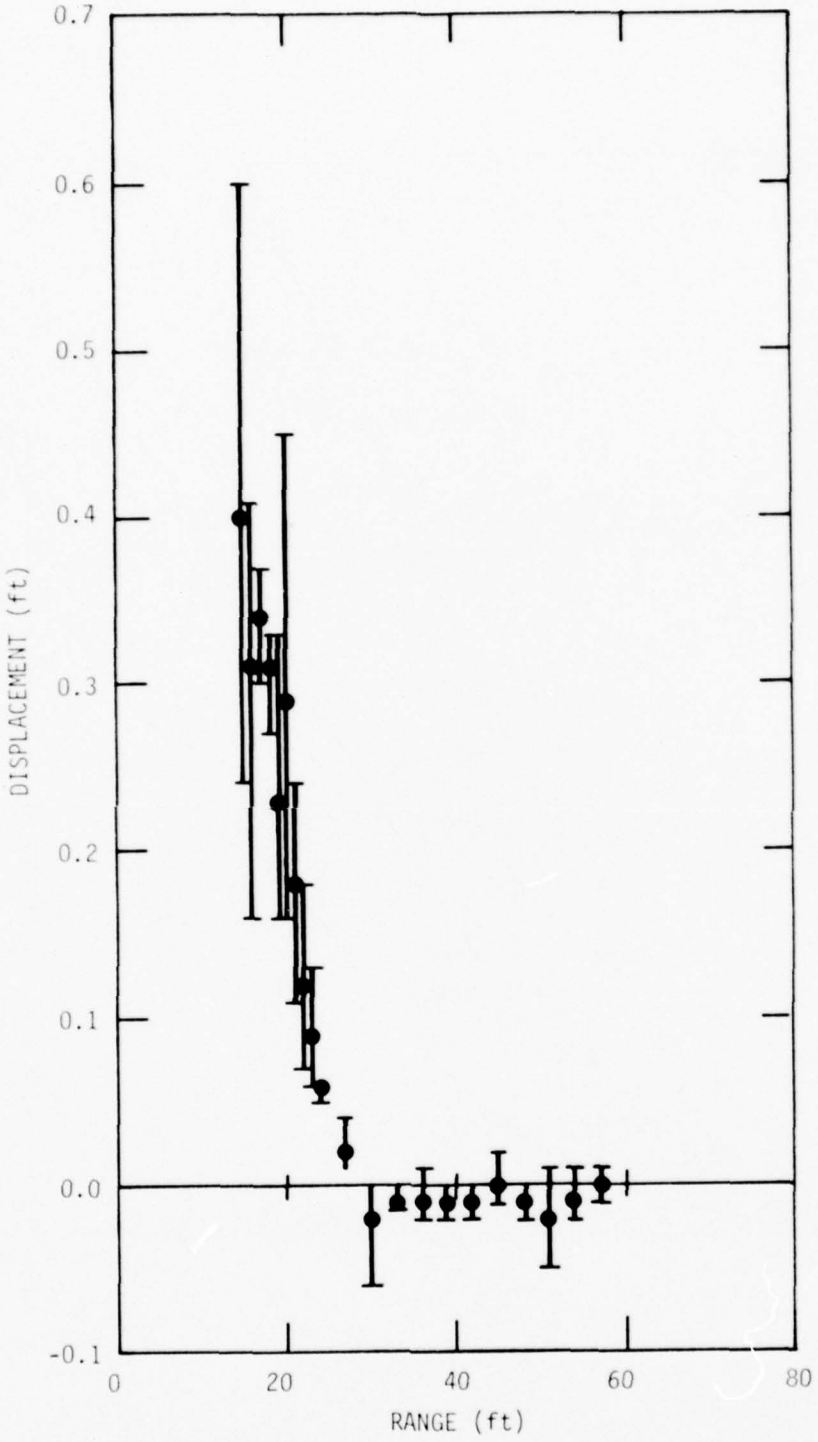

Figure 8.16. Event MBI-6, average permanent vertical displacement versus range.

SECTION 9

EVENT MBI-7

9.1 DESCRIPTION

This event was conducted on 26 October 1978 at the White Sands Missile Range. The event used a 116-kg (256-pound) cast TNT, half-buried sphere to provide data on crater-induced scaling between 454-kg (1000-pound) and 116-kg (256-pound) charges.

9.1.1 Water Content

Soil moisture data were obtained for Event MBI-7 and are plotted in Figure 9.1.

9.2 GROUND MOTION AND AIRBLAST EXPERIMENTS

9.2.1 Gage Layout

Ground shock instrumentation covered ranges of 2.90 to 146 meters (9.5 to 480 feet) from SGZ and depths of 0.457 to 3.05 meters (1.5 to 10 feet). Motion gages were installed along a single radial (designated the 0 radian radial), with airblast measurements made on the 4.71 radian (270°) radial. Figure 9.2 presents both a plan view and cross section of the gage array.

9.2.2 Instrumentation

Fifty-five gages were installed; 42 accelerometers, 10 velocity gages, and 3 airblast gages. Table 9.1 is a listing of each gage, denoted by an arbitrarily assigned measurement number.

9.2.3 Typical Data Records

Calibration and recorder start signals from the Timing and Firing (T&F) unit were properly received and translated, and all equipment operated as planned for Event MBI-7.

Data recovery was good. Three accelerometers, measurement Nos. 7110, 7135 and 7136, and one velocity gage, measurement No. 7902, yielded no useful data.

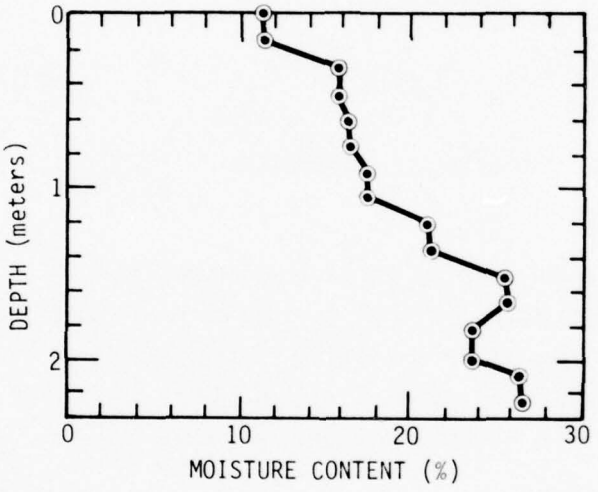

Figure 9.1. Moisture content data measured from Event MBI-7.

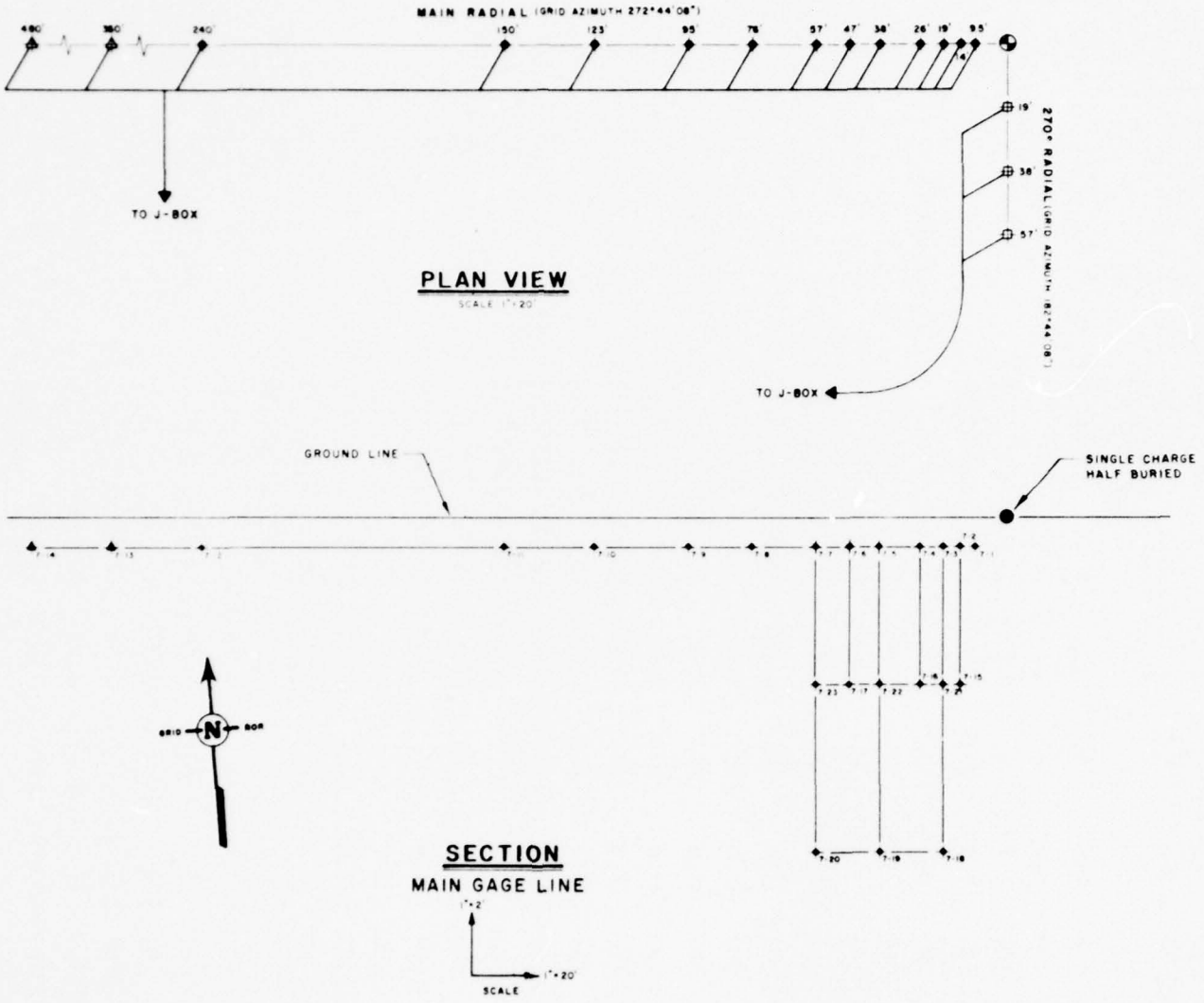

Figure 9.2. Gage layout for Event MBI-7.

Table 9.1. Ground motion and airblast measurement list for Event MBI-7.

Radial		Range		Depth		Measurement Numbers							
Rad	(Deg)	m	(ft)	m	(ft)	AV	AH	AT	UV	UH	SV	SH	AB
0	(0)	2.90	(9.5)	0.280	(0.92)	7101	7102						
0	(0)	4.27	(14)	0.280	(0.92)	7103	7104						
0	(0)	4.27	(14)	1.52	(5)	7105	7106						
0	(0)	5.79	(19)	0.280	(0.92)	7107	7108						
0	(0)	5.79	(19)	1.52	(5)	7137	1738						
0	(0)	5.79	(19)	1.52	(5)				7701	7702			
0	(0)	5.79	(19)	3.05	(10)	7109	7110						
0	(0)	7.92	(26)	0.280	(0.92)	7111	7112						
0	(0)	7.92	(26)	1.52	(5)	7113	7114						
0	(0)	11.6	(38)	0.280	(0.92)	7115	7116						
0	(0)	11.6	(38)	1.52	(5)	7139	7140						
0	(0)	11.6	(38)	1.52	(5)				7711	7713			
0	(0)	11.6	(38)	3.05	(10)	7117	7118						
0	(0)	14.3	(47)	0.280	(0.92)	7119	7120						
0	(0)	14.3	(47)	1.52	(5)	7121	7122						
0	(0)	17.4	(57)	0.280	(0.92)	7123	7124						
0	(0)	17.4	(57)	1.52	(5)	7141	7142						
0	(0)	17.4	(57)	1.52	(5)				7703	7705			
0	(0)	17.4	(57)	0.280	(0.92)	7125	7126						
0	(0)	23.2	(76)	1.52	(5)	7127	7128						
0	(0)	29.0	(95)	1.52	(5)	7129	7130						
0	(0)	37.5	(123)	3.05	(10)	7131	7132						
0	(0)	45.7	(150)	0.280	(0.92)	7133	7134						
0	(0)	73.2	(240)	0.280	(0.92)	7135	7136						
0	(0)	110	(360)	0.280	(0.92)				7901	7902			
0	(0)	146	(480)	0.280	(0.92)				7903	7904			
4.71	(270)	5.79	(19)	0.280	(0.92)								7301
4.71	(270)	11.6	(38)	0.280	(0.92)								7302
4.71	(270)	17.4	(57)	0.280	(0.92)								7303

NOTES:

AV Vertical Acceleration
AH Horizontal Acceleration
AT Transverse Acceleration
UV Vertical Velocity
UH Horizontal Velocity
SV Vertical Stress
SH Horizontal Stress
AB Airblast

Typical time histories for the following gages are presented in Figure 9.3.

Type of Measurement	Instrumentation Number	Radial rad	(deg)	Range m	(ft)	Depth m	(ft)
Horizontal Acceleration (AH)	7138	0	(0)	5.79	(19)	1.52	(5)
Vertical Acceleration (AV)	7137	0	(0)	5.79	(19)	1.52	(5)
Vertical Velocity (UV)	7701	0	(0)	5.79	(19)	1.52	(5)
Airblast (AB)	7301	4.71	(270)	5.79	(19)	0.28	(0.92)

9.3 CRATER AND EJECTA EXPERIMENTS

9.3.1 Crater and Ejecta Layout

Four radial lines were surveyed to determine the parameters for the apparent crater. Free field areal density measurements were made along the four radials. Several different types of debris collection devices were used as shown in Figure 9.4.

9.3.2 Results

The average apparent values for the Event MBI-7 crater are:

Volume: 6.97 m^3 (246 ft^3)
Radius: 2.13 meters (7.0 feet)
Depth below SGZ: 1.37 meters (4.5 feet)

Figure 9.5 is a plot of the crater profile. The average free field areal density versus range plot is given in Figure 9.6.

Figure 9.7 shows the debris depth versus range normalized by the cube root of the apparent crater volume and Figure 9.8 shows the average permanent vertical displacement versus range.

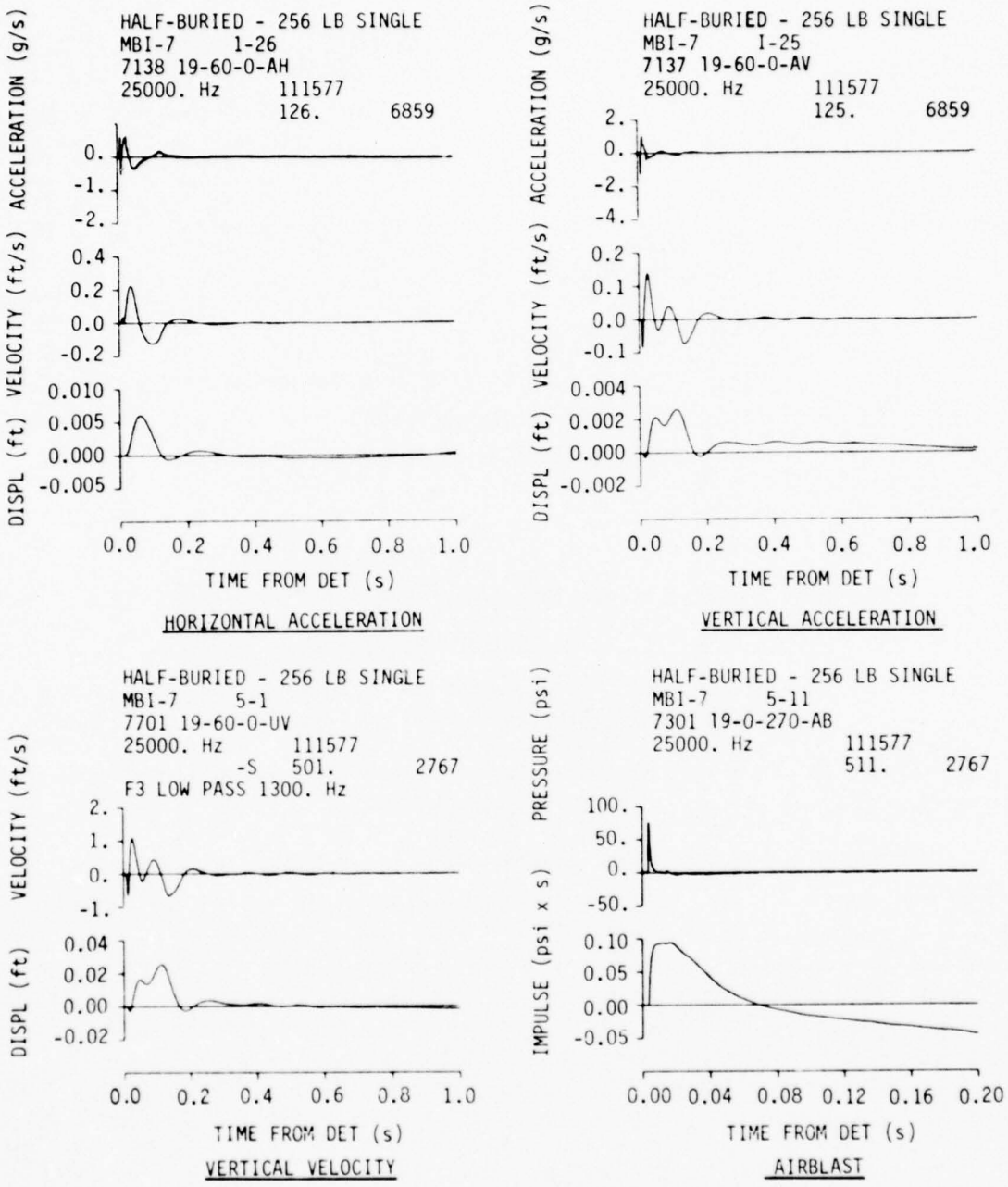

Figure 9.3. Typical time histories for Event MBI-7.

MBI-7 256 lbs TNT SPHERE, HALF-BURIED

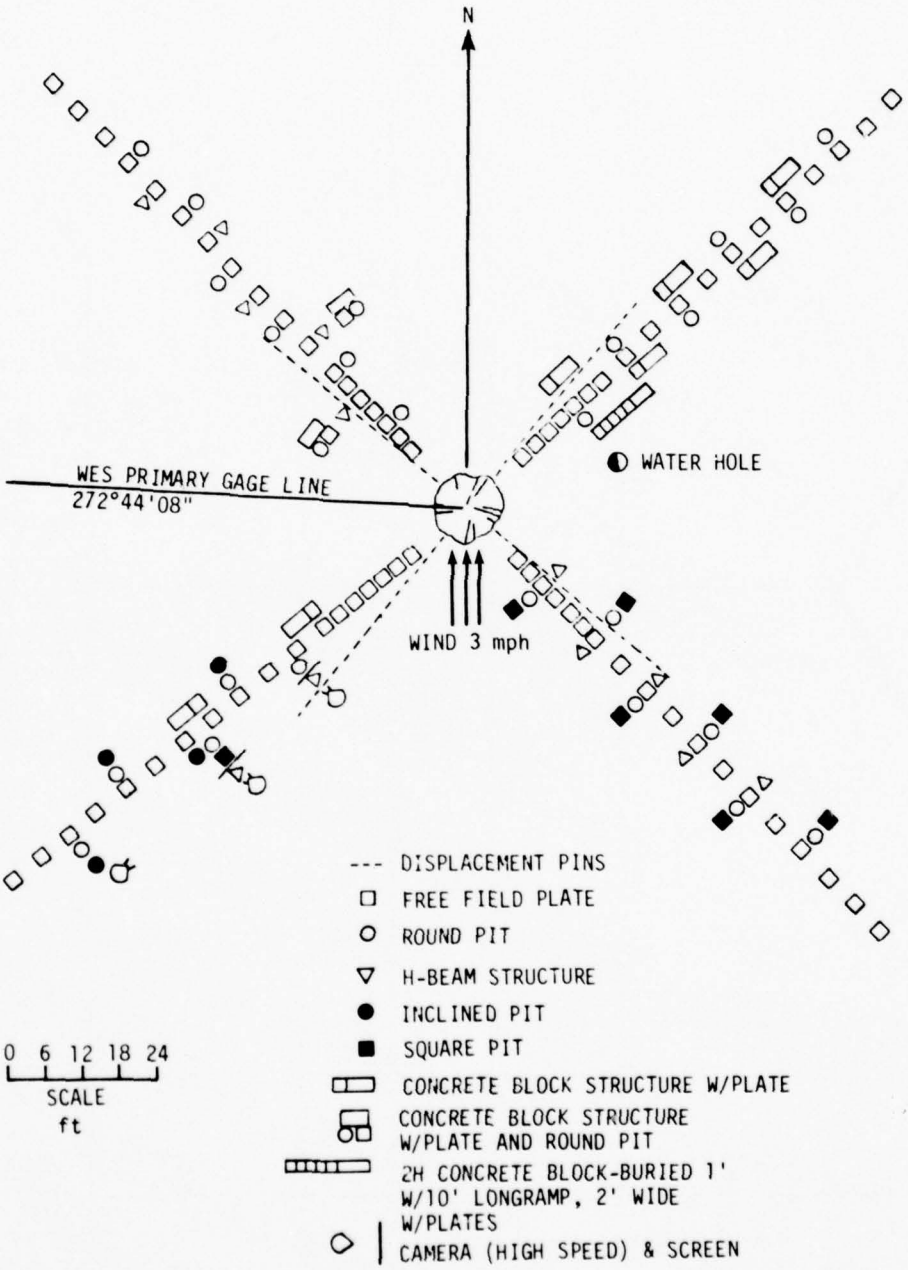

Figure 9.4. Debris collector layout for Event MBI-7.

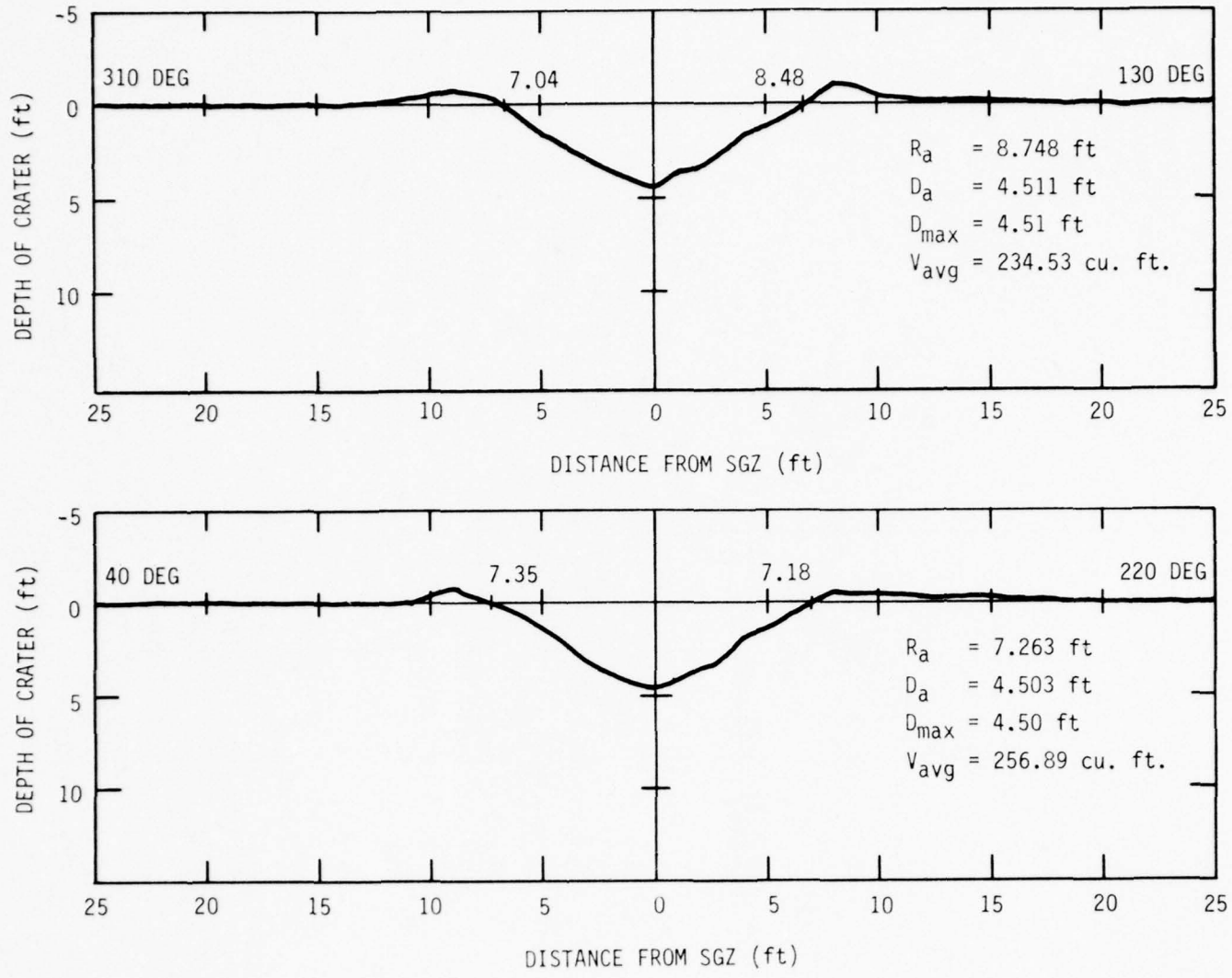

Figure 9.5. Event MBI-7 crater profiles.

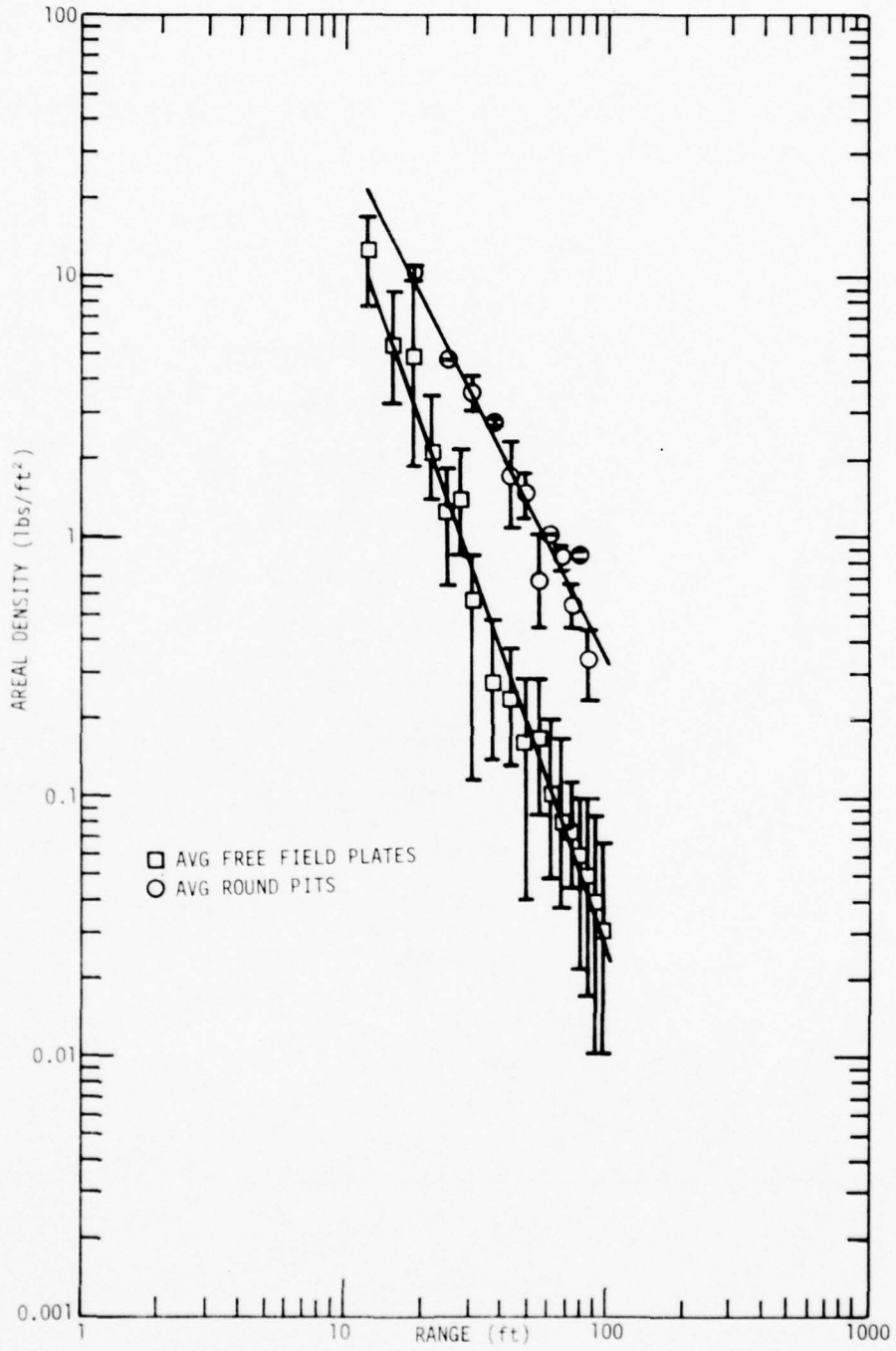

Figure 9.6. Event MBI-7, average free field areal density versus range.

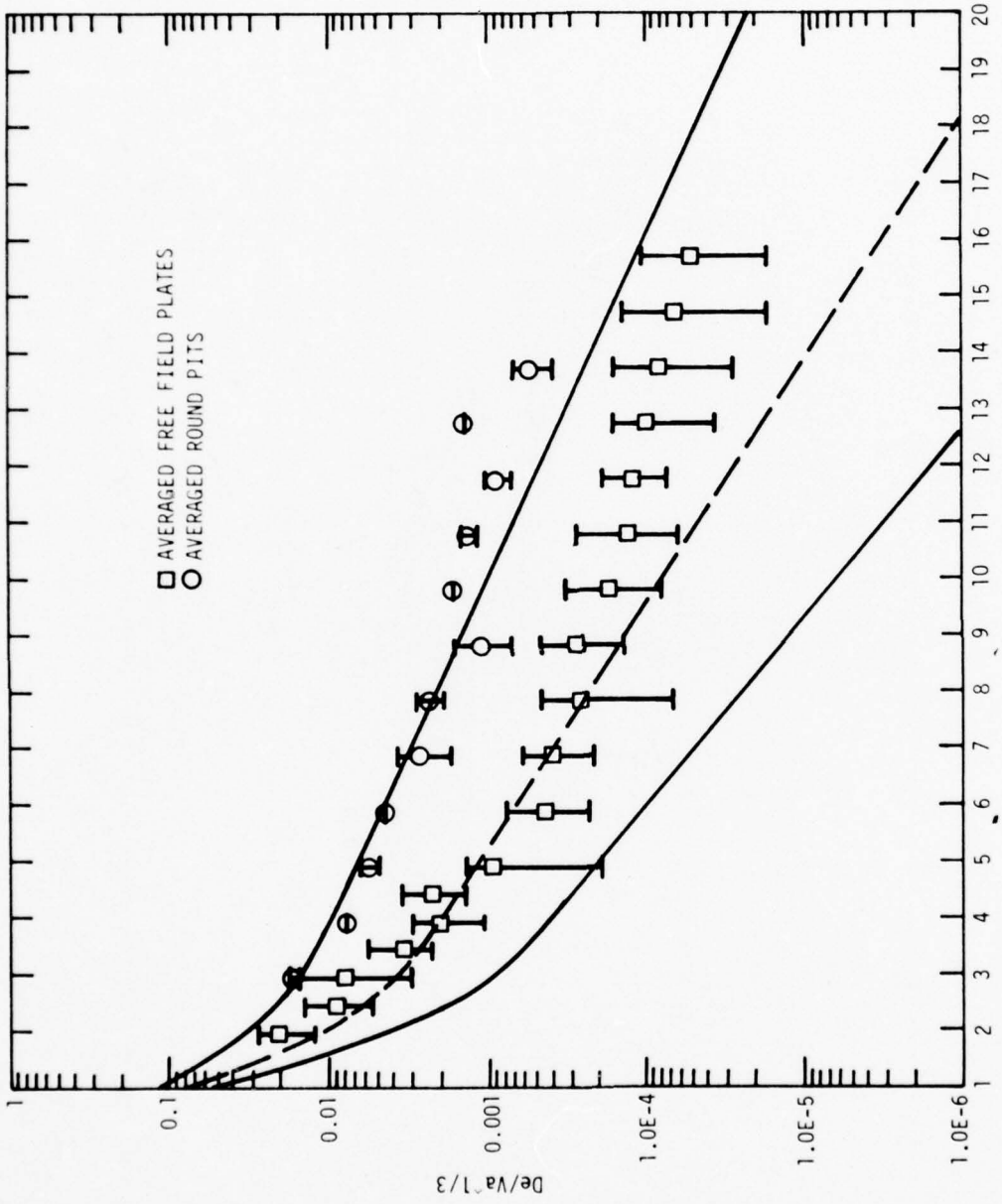

Figure 9.7. Event MBI-7, debris depth versus range both normalized by $V_a^{1/3}$.

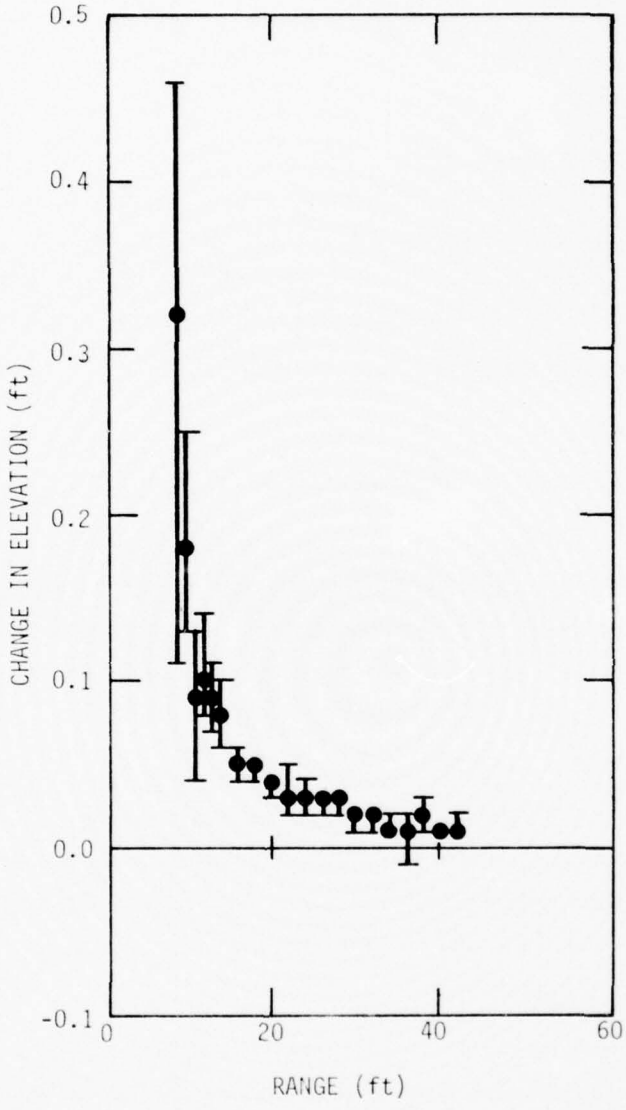

Figure 9.8. Event MBI-7, average permanent vertical displacement versus range.

SECTION 10

EVENT MBI-8

10.1 DESCRIPTION

This event was conducted on 7 December 1977 at the White Sands Missile Range. The event consisted of an array of 24, 454-kg (1000-pound) cast TNT surface tangent spheres configured to be 21.3 meters (70 feet) apart and to contain seven identical 6-charge arrays to address the reproducibility of multiburst data and to investigate the effects of charges surrounding the primary hexagonal array.

10.2 GROUND MOTION AND AIRBLAST EXPERIMENTS

10.2.1 Water Content

Soil moisture data for MBI-8 are shown in Table 10.1.

10.2.2 Gage Layout

Figure 10.1 is a plan view of the Event 8 ground motion gage array. Motion gages were distributed generally throughout the interior and exterior of the charge array, although the deeper gages were concentrated within the innermost ring of charges. The airblast gage array is shown in Figure 10.2.

10.2.3 Instrumentation

Table 10.2 is a listing of each gage by measurement number, azimuth relative to the 0 radian radial, depth and distance from the charge array center. One-hundred seventy-one gages were installed for Event 8; 127 accelerometers, 6 velocity gages, 8 soil stress gages and 30 airblast gages.

10.2.4 Typical Data Records

Calibration and recorder start signals from the Timing and Firing (T&F) unit were properly received and translated, and all equipment operated as planned for Event MBI-8.

Data recovery was good. Ten accelerometers failed to produce usable data; these were measurement Nos. 8118, 8119, 8121, 8123, 8141, 8142, 8160, 8161, 8207 and 8227. The remaining gages all yielded good data.

Table 10.1. Event MBI-8 water content test record.

Depth*		
meters	feet	Percent Moisture
0.152	0.5	11.6
0.457	1.5	17.9
0.762	2.5	16.1
1.07	3.5	18.0
1.37	4.5	19.8
1.68	5.5	22.0
1.98	6.5	23.6
2.29	7.5	26.9

*Measured from a drill hole located in the center of the array.

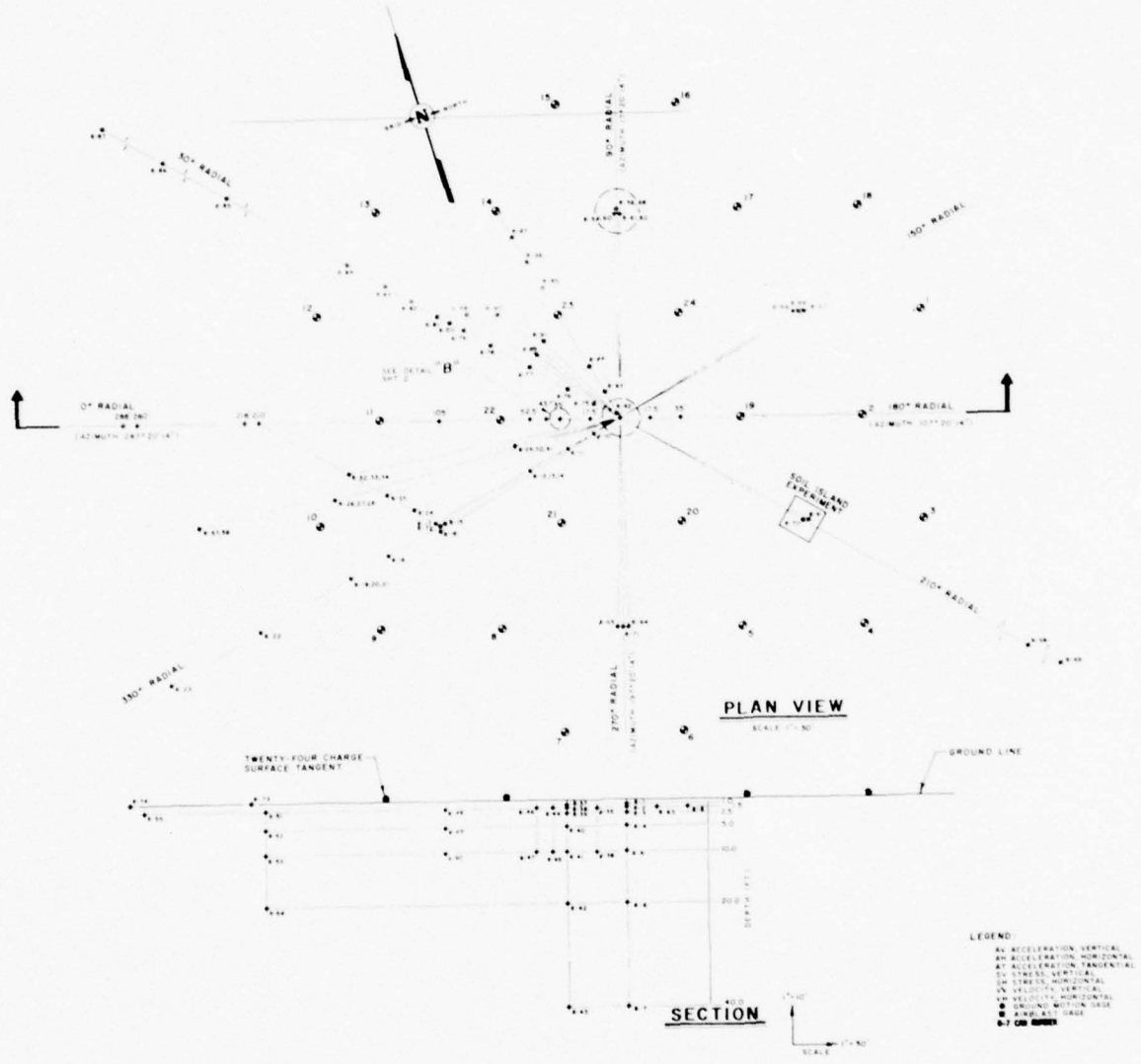

Figure 10.1. Event MBI-8 motion gage layout.

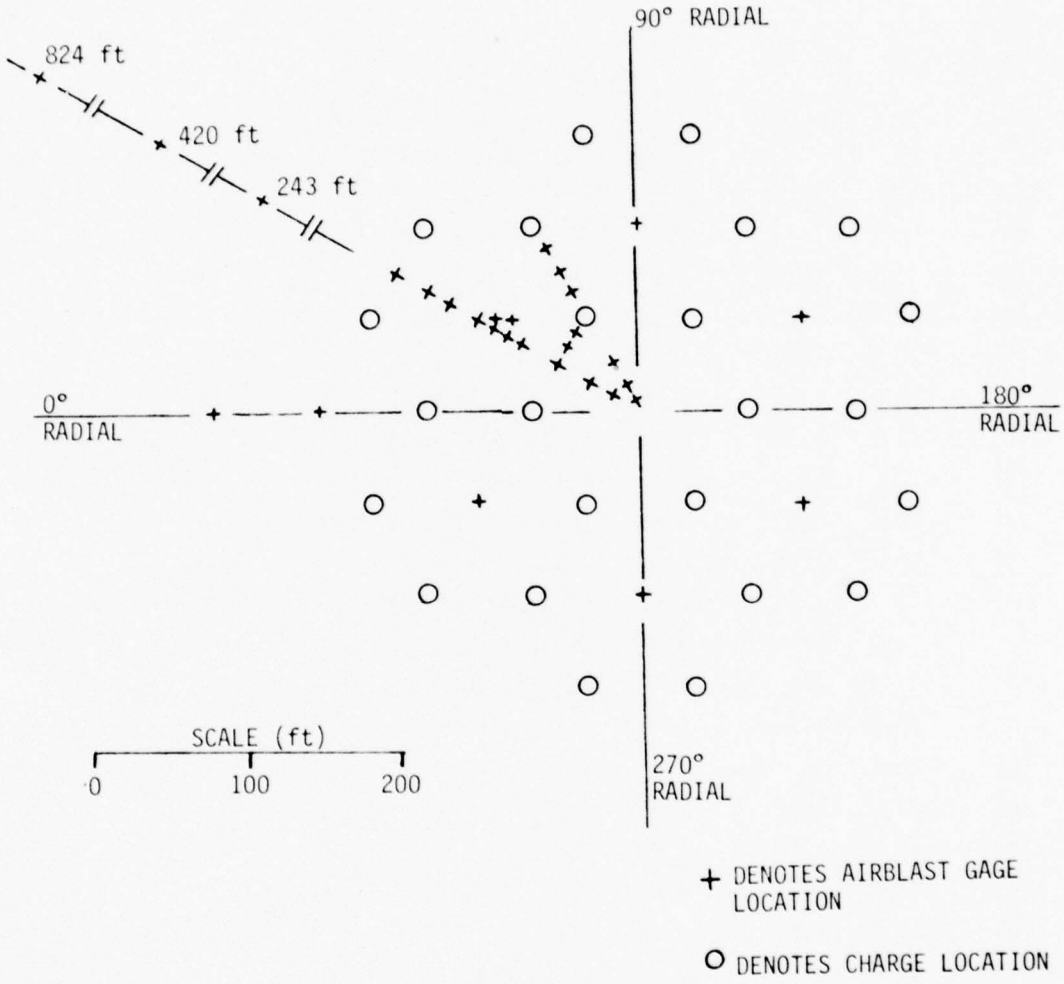

Figure 10.2. Event MBI-8 airblast gage locations.

Table 10.2. Ground motion and airblast measurement list for Event MBI-8.

Radial		Range		Depth		Measurement Numbers							
Rad	(Deg)	m	(ft)	m	(ft)	AV	AH	AT	UV	UH	SV	SH	AB
0	(0)	0	(0)	0.305	(1)	8204	8205						
0	(0)	0	(0)	0.457	(1.5)	8206	8207	8208					
0	(0)	0	(0)	0.762	(2.5)	8209	8210						
0	(0)	0	(0)	1.52	(5)	8211	8212	8213					
0	(0)	0	(0)	3.05	(10)	8214	8215	8216					
0	(0)	0	(0)	6.10	(20)	8217	8218						
0	(0)	0	(0)	12.2	(40)	8219	8220						
0	(0)	5.33	(17.5)	0.457	(1.5)	8200	8201						
0	(0)	5.33	(17.5)	3.05	(10)	8202	8203						
0	(0)	10.7	(35)	0.305	(1)	8184	8185						
0	(0)	10.7	(35)	0.457	(1.5)	8186	8187	8188					
0	(0)	10.7	(35)	0.762	(2.5)	8189	8190						
0	(0)	10.7	(35)	1.52	(5)	8191	8192						
0	(0)	10.7	(35)	3.05	(10)	8193	8194	8195					
0	(0)	10.7	(35)	6.10	(20)	8196	8197						
0	(0)	10.7	(35)	12.2	(40)	8198	8199						
0	(0)	13.3	(43.75)	0.457	(1.5)	8180	8181						
0	(0)	13.3	(43.75)	3.05	(10)	8182	8183						
0	(0)	16.0	(52.5)	0.457	(1.5)	8176	8177						
0	(0)	16.0	(52.5)	3.05	(10)	8178	8179						
0	(0)	32.0	(105)	0.457	(1.5)	8168	8169	8170					
0	(0)	32.0	(105)	1.52	(5)	8171	8172						
0	(0)	32.0	(105)	3.05	(10)	8173	8174	8175					
0	(0)	64.0	(210)	0	(0)								8322
0	(0)	64.0	(210)	0.457	(1.5)	8160	8161						
0	(0)	64.0	(210)	1.52	(5)	8162	8163						
0	(0)	64.0	(210)	3.05	(10)	8164	8165						
0	(0)	64.0	(210)	6.10	(20)	8166	8167						
0	(0)	85.3	(280)	0.457	(1.5)	8158	8159						
0	(0)	86.1	(282.4)	0	(0)								8321
0.524	(30)	5.33	(17.5)	0	(0)								8302
0.524	(30)	10.7	(35)	0	(0)								8305
0.524	(30)	18.5	(60.6)	0	(0)								8306

Table 10.2. Ground motion and airblast measurement list for Event MBI-8 (Continued).

Radial		Range		Depth		Measurement Numbers							
Rad	(Deg)	m	(ft)	m	(ft)	AV	AH	AT	UV	UH	SV	SH	AB
0.524	(30)	26.3	(86.2)	0	(0)								8309
0.524	(30)	31.6	(103.7)	0	(0)								8311
0.524	(30)	34.5	(113.2)	0	(0)								8313
0.524	(30)	36.9	(121.2)	0	(0)								8314
0.524	(30)	42.3	(138.7)	0	(0)								8315
0.524	(30)	47.6	(156.2)	0	(0)								8316
0.524	(30)	55.4	(181.8)	0	(0)								8317
0.524	(30)	74.1	(243)	0	(0)								8318
0.524	(30)	128	(420)	0	(0)								8319
0.524	(30)	251	(824)	0	(0)								8320
0.611	(35)	35.4	(116.2)	0	(0)								8312
0.663	(38)	18.8	(61.6)	0	(0)								8307
0.681	(39)	28.1	(92.2)	0	(0)								8310
0.803	(46)	19.2	(63.1)	0	(0)								8308
1.05	(60)	2.44	(8)	0	(0)								8301
1.05	(60)	5.33	(17.5)	0	(0)								8303
1.05	(60)	10.7	(35)	0	(0)								8304
1.05	(60)	26.7	(87.5)	0	(0)								8328
1.05	(60)	32.0	(105)	0	(0)								8329
1.05	(60)	37.3	(122.5)	0	(0)								8330
1.57	(90)	36.9	(121.2)	0	(0)								8327
1.57	(90)	36.9	(121.2)	0.305	(1)	8228							
1.57	(90)	36.9	(121.2)	1.52	(5)							8403	
1.57	(90)	36.9	(121.2)	1.52	(5)							8405	
1.57	(90)	36.9	(121.2)	6.10	(20)							8404	
1.57	(90)	36.9	(121.2)	6.10	(20)							8406	
2.62	(150)	36.9	(121.2)	0	(0)								8326
2.62	(150)	36.9	(121.2)	0.457	(1.5)	8226	8227						
2.62	(150)	36.9	(121.2)	0.457	(1.5)				8719	8720			
3.14	(180)	5.33	(17.5)	0.457	(1.5)	8221	8222						
3.14	(180)	5.33	(17.5)	0.457	(1.5)				8701	8702			
3.14	(180)	10.7	(35)	0.457	(1.5)	8223	8224	8225					

Table 10.2. Ground motion and airblast measurement list for Event MBI-8 (Continued).

Radial		Range		Depth		Measurement Numbers							
Rad	(Deg)	m	(ft)	m	(ft)	AV	AH	AT	UV	UH	SV	SH	AB
3.67	(210)	36.9	(121.2)	0	(0)								8325
3.67	(210)	36.9	(121.2)	0.457	(1.5)	8123	8124						
3.67	(210)	183	(601.2)	0.457	(1.5)				8901	8902			
3.67	(210)	250	(821.2)	0.457	(1.5)				8903	8904			
4.71	(270)	36.9	(121.2)	0	(0)								8324
4.71	(270)	36.9	(121.2)	0.457	(1.5)	8105	8106						
4.71	(270)	36.9	(121.2)	0.457	(1.5)				8707	8709			
5.76	(330)	5.33	(17.5)	0.457	(1.5)	8156	8157						
5.76	(330)	10.7	(35)	0.457	(1.5)	8154	8155						
5.76	(330)	18.5	(60.6)	0.305	(1)	8141	8142						
5.76	(330)	18.5	(60.6)	0.457	(1.5)	8145	8146	8147					
5.76	(330)	18.5	(60.6)	0.762	(2.5)	8143	8144						
5.76	(330)	36.9	(121.2)	0	(0)								8323
5.76	(330)	36.9	(121.2)	0.305	(1)	8116	8117						
5.76	(330)	36.9	(121.2)	0.457	(1.5)	8118	8119	8120					
5.76	(330)	36.9	(121.2)	0.762	(2.5)	8121	8122						
5.76	(330)	47.6	(156.2)	0.457	(1.5)	8114	8115						
5.76	(330)	55.4	(181.8)	0.305	(1)	8107	8108						
5.76	(330)	55.4	(181.8)	0.457	(1.5)	8111	8112	8113					
5.76	(330)	55.4	(181.8)	0.762	(2.5)	8109	8110						
5.76	(330)	73.9	(242.4)	0.457	(1.5)	8103	8104						
5.76	(330)	92.4	(303)	0.457	(1.5)	8101	8102						
5.88	(336.8)	39.8	(130.5)	0.457	(1.5)	8125	8126						
5.98	(342.4)	43.2	(141.8)	0.457	(1.5)	8127	8128						
6.02	(344.7)	52.5	(172.2)	0.305	(1)	8129	8130						
6.02	(344.7)	52.5	(172.2)	0.457	(1.5)	8131	8132						
6.02	(344.7)	52.5	(172.2)	0.762	(2.5)	8133	8134						
6.04	(346)	19.2	(63)	0.305	(1)	8148	8149						
6.04	(346)	19.2	(63)	0.457	(1.5)	8150	8151						
6.04	(346)	19.2	(63)	0.762	(2.5)	8152	8153						
6.04	(346)	76.5	(251)	6.10	(20)							8401	
6.04	(346)	76.5	(251)	6.10	(20)							8402	

Table 10.2. Ground motion and airblast measurement list for Event MBI-8 (Continued).

Radial		Range		Depth		Measurement Numbers							
Rad	(Deg)	m	(ft)	m	(ft)	AV	AH	AT	UV	UH	SV	SH	AB
6.09	(349)	48.8	(160.2)	0.305	(1)	8135	8136						
6.09	(349)	48.8	(160.2)	0.457	(1.5)	8137	8138						
6.09	(349)	48.8	(160.2)	0.762	(2.5)	8139	8140						

NOTES:

AV Vertical Acceleration
AH Horizontal Acceleration
AT Transverse Acceleration
UV Vertical Velocity
UH Horizontal Velocity
SV Vertical Stress
SH Horizontal Stress
AB Airblast

Typical time histories for the following gages are presented in Figure 10.3.

Type of Measurement	Instrumentation Number	Radial rad	Radial (deg)	Range m	Range (ft)	Depth m	Depth (ft)
Horizontal Acceleration (AH)	8222	3.14	(180)	5.33	(17.5)	0.457	(1.5)
Vertical Acceleration (AV)	8226	2.62	(150)	36.9	(121.1)	0.457	(1.5)
Vertical Velocity (UV)	8719	2.62	(150)	36.9	(121.1)	0.457	(1.5)
Airblast (AB)	8326	2.62	(150)	36.9	(121.2)	0	(0)

10.3 CRATER AND EJECTA EXPERIMENTS

10.3.1 Crater and Ejecta Layout

Four radial lines in each crater were surveyed to determine the parameters for the apparent craters. Free field areal density measurements were made along several primary radials and between charges. Several different types of debris collection devices were used as shown in Figure 10.4.

10.3.2 Results

The average apparent values for the 24 craters of Event MBI-8 craters are:

	SGZ No. 1 m	SGZ No. 1 (ft)	SGZ No. 2 m	SGZ No. 2 (ft)	SGZ No. 3 m	SGZ No. 3 (ft)
Apparent radius	1.92	(6.3)	2.23	(7.3)	2.22	(7.27)
Apparent depth	1.40	(4.6)	1.40	(4.6)	1.25	(4.1)
Maximum depth	1.40	(4.6)	1.43	(4.7)	1.25	(4.1)
Volume	6.31 m^3	223 ft^3	7.65 m^3	270 ft^3	6.85 m^3	242 ft^3

	SGZ No. 4 m	SGZ No. 4 (ft)	SGZ No. 5 m	SGZ No. 5 (ft)	SGZ No. 6 m	SGZ No. 6 (ft)
Apparent radius	2.23	(7.3)	1.95	(6.4)	1.98	(6.5)
Apparent depth	1.31	(4.3)	1.16	(3.8)	1.16	(3.8)
Maximum depth	1.31	(4.3)	1.19	(3.9)	1.25	(4.1)
Volume	8.38 m^3	296 ft^3	5.78 m^3	204 ft^3	5.66 m^3	200 ft^3

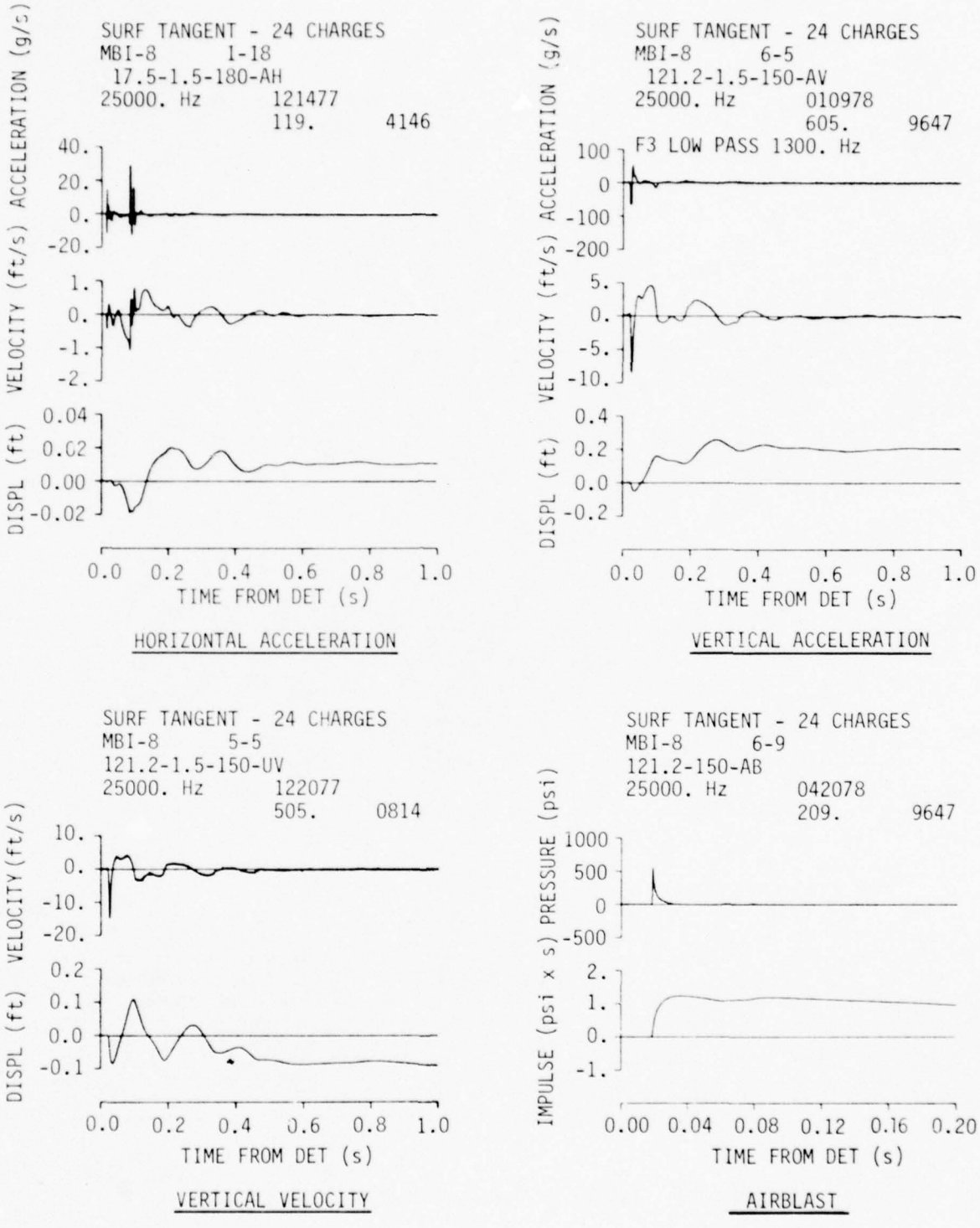

Figure 10.3. Typical time histories for Event MBI-8.

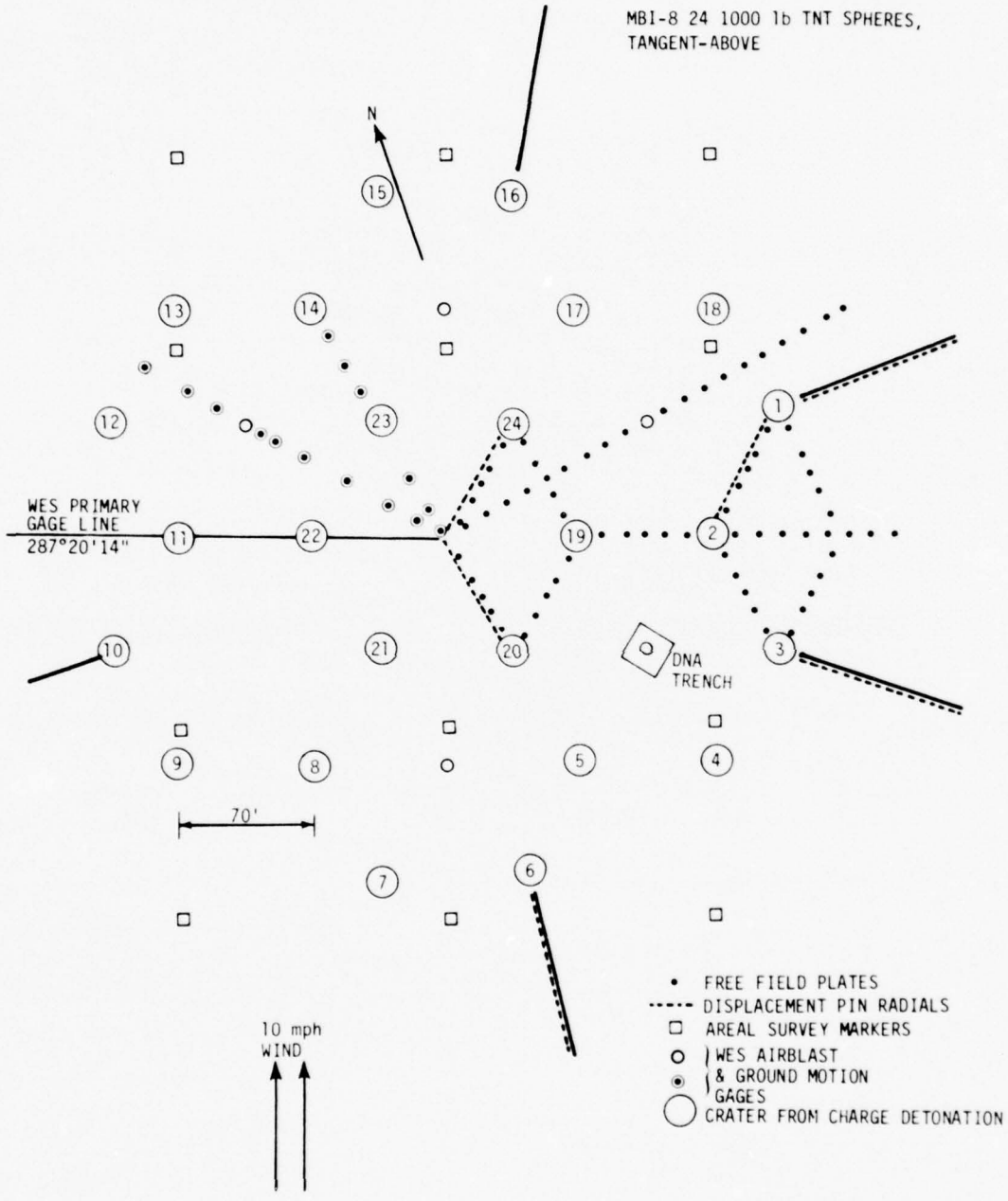

Figure 10.4. Debris collector layout for Event MBI-8.

	SGZ No. 7		SGZ No. 8		SGZ No. 9	
	m	(ft)	m	(ft)	m	(ft)
Apparent radius	2.07	(6.8)	2.01	(6.6)	2.04	(6.7)
Apparent depth	1.25	(4.1)	1.22	(4.0)	1.10	(3.6)
Maximum depth	1.28	(4.2)	1.22	(4.0)	1.10	(3.6)
Volume	5.78 m^3	204 ft^3	6.00 m^3	212 ft^3	5.83 m^3	206 ft^3

	SGZ No. 10		SGZ No. 11		SGZ No. 12	
	m	(ft)	m	(ft)	m	(ft)
Apparent radius	1.74	(5.7)	1.83	(6.0)	1.89	(6.2)
Apparent depth	1.22	(4.0)	1.13	(3.7)	1.13	(3.7)
Maximum depth	1.13	(3.7)	1.16	(3.8)	1.13	(3.7)
Volume	4.87 m^3	172 ft^3	4.87 m^3	172 ft^3	4.84 m^3	171 ft^3

	SGZ No. 13		SGZ No. 14		SGZ No. 15	
	m	(ft)	m	(ft)	m	(ft)
Apparent radius	1.83	(6.0)	1.77	(5.8)	2.41	(7.9)
Apparent depth	1.16	(3.8)	0.85	(2.8)	1.58	(5.2)
Maximum depth	1.16	(3.8)	0.88	(2.9)	1.58	(5.2)
Volume	4.47 m^3	158 ft^3	3.51 m^3	124 ft^3	9.00 m^3	318 ft^3

	SGZ No. 16		SGZ No. 17		SGZ No. 18	
	m	(ft)	m	(ft)	m	(ft)
Apparent radius	2.50	(8.2)	2.41	(7.9)	2.38	(7.8)
Apparent depth	1.40	(4.6)	1.43	(4.7)	1.40	(4.6)
Maximum depth	1.40	(4.6)	1.46	(4.8)	1.49	(4.9)
Volume	9.71 m^3	343 ft^3	8.92 m^3	315 ft^3	8.92 m^3	315 ft^3

	SGZ No. 19		SGZ No. 20		SGZ No. 21	
	m	(ft)	m	(ft)	m	(ft)
Apparent radius	2.01	(6.6)	1.83	(6.0)	1.85	(6.07)
Apparent depth	1.16	(3.8)	0.823	(2.7)	1.04	(3.4)
Maximum depth	1.19	(3.9)	0.853	(2.8)	1.07	(3.5)
Volume	5.61 m^3	198 ft^3	4.28 m^3	151 ft^3	4.70 m^3	166 ft^3

	SGZ No. 22		SGZ No. 23		SGZ No. 24	
	m	(ft)	m	(ft)	m	(ft)
Apparent radius	2.13	(7.0)	1.92	(6.3)	2.13	(7.0)
Apparent depth	1.31	(4.3)	1.10	(3.6)	1.31	(4.3)
Maximum depth	1.31	(4.3)	1.31	(4.3)	1.31	(4.3)
Volume	6.48 m^3	229 ft^3	5.38 m^3	190 ft^3	7.22 m^3	255 ft^3

Figures 10.5 through 10.12 are plots of the selected crater profiles. The average areal density versus range plot for SGZ 1, 3, 6, and 16 is given in Figure 10.13.

Figure 10.14 shows the debris depth versus range normalized by the cube root of the apparent crater volume for SGZ 1, 3, 8, and 18.

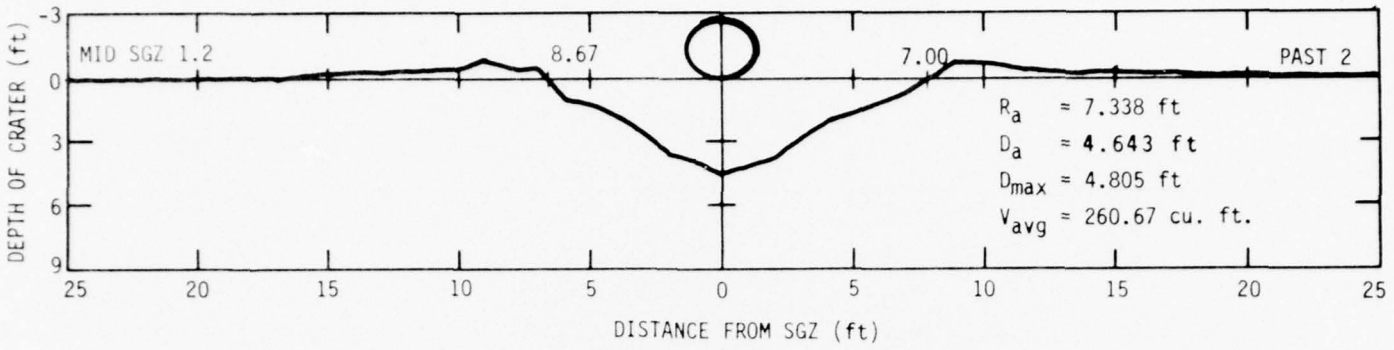

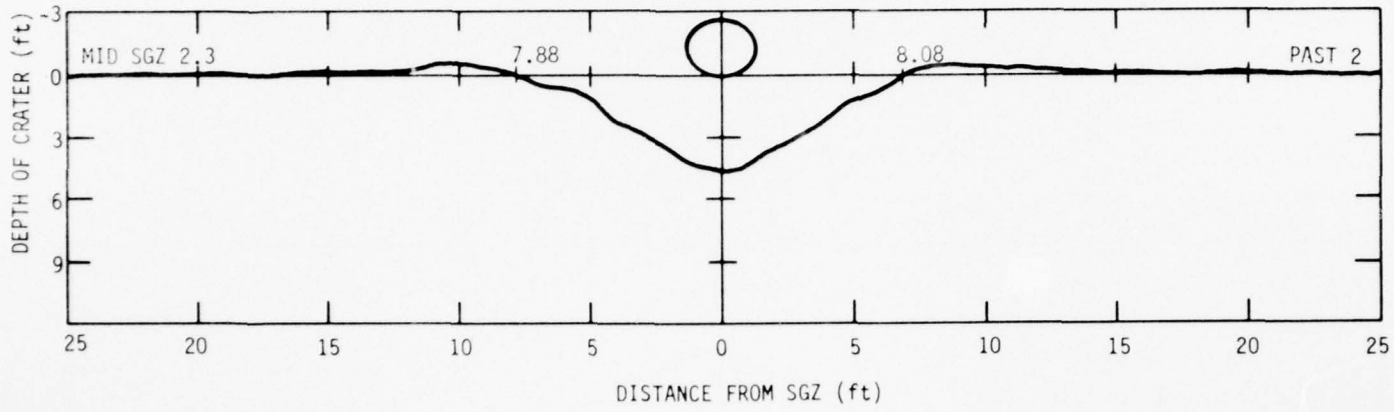

Figure 10.5. Event MBI-8 crater profile for GZ No. 2.

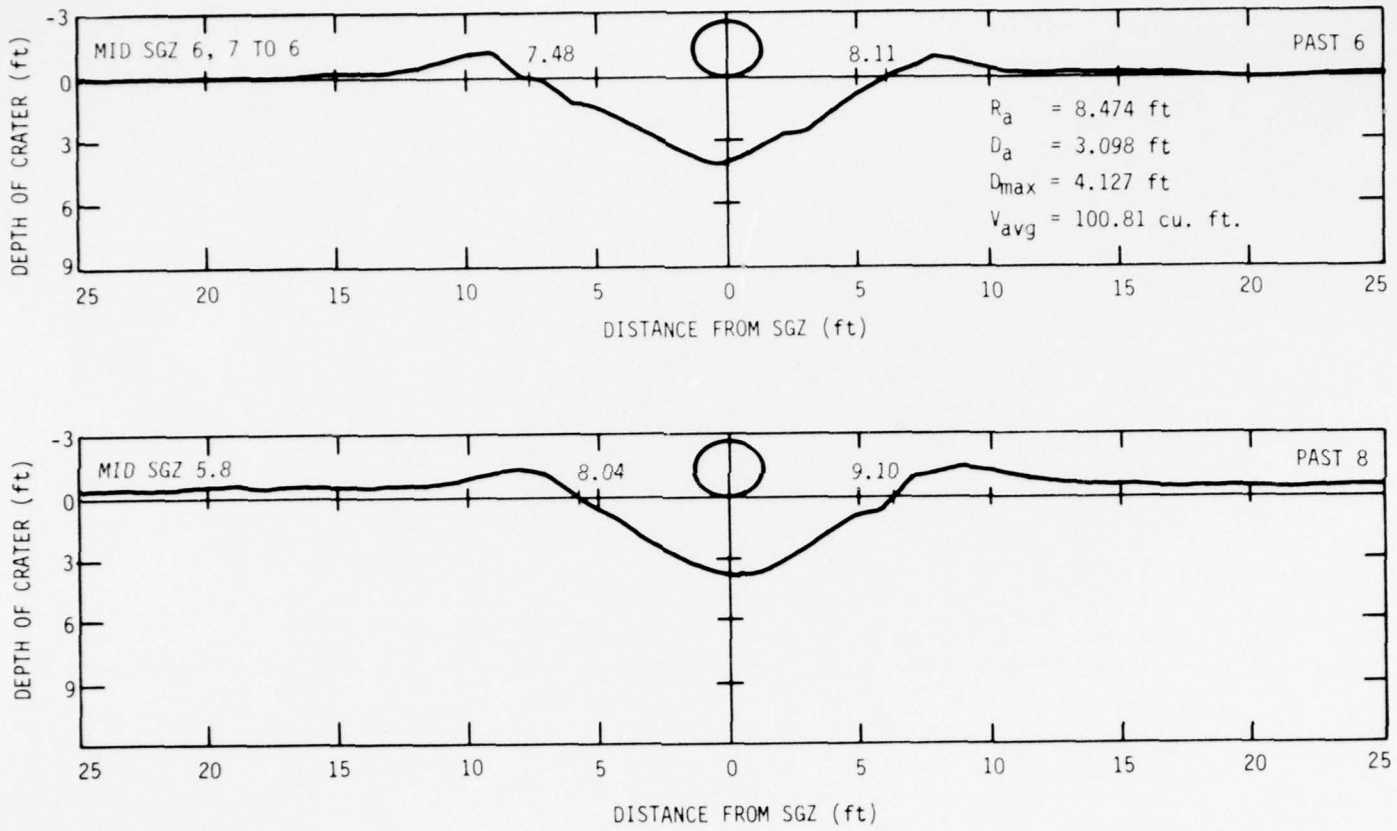

Figure 10.6. Event MBI-8 crater profile for GZ No. 6.

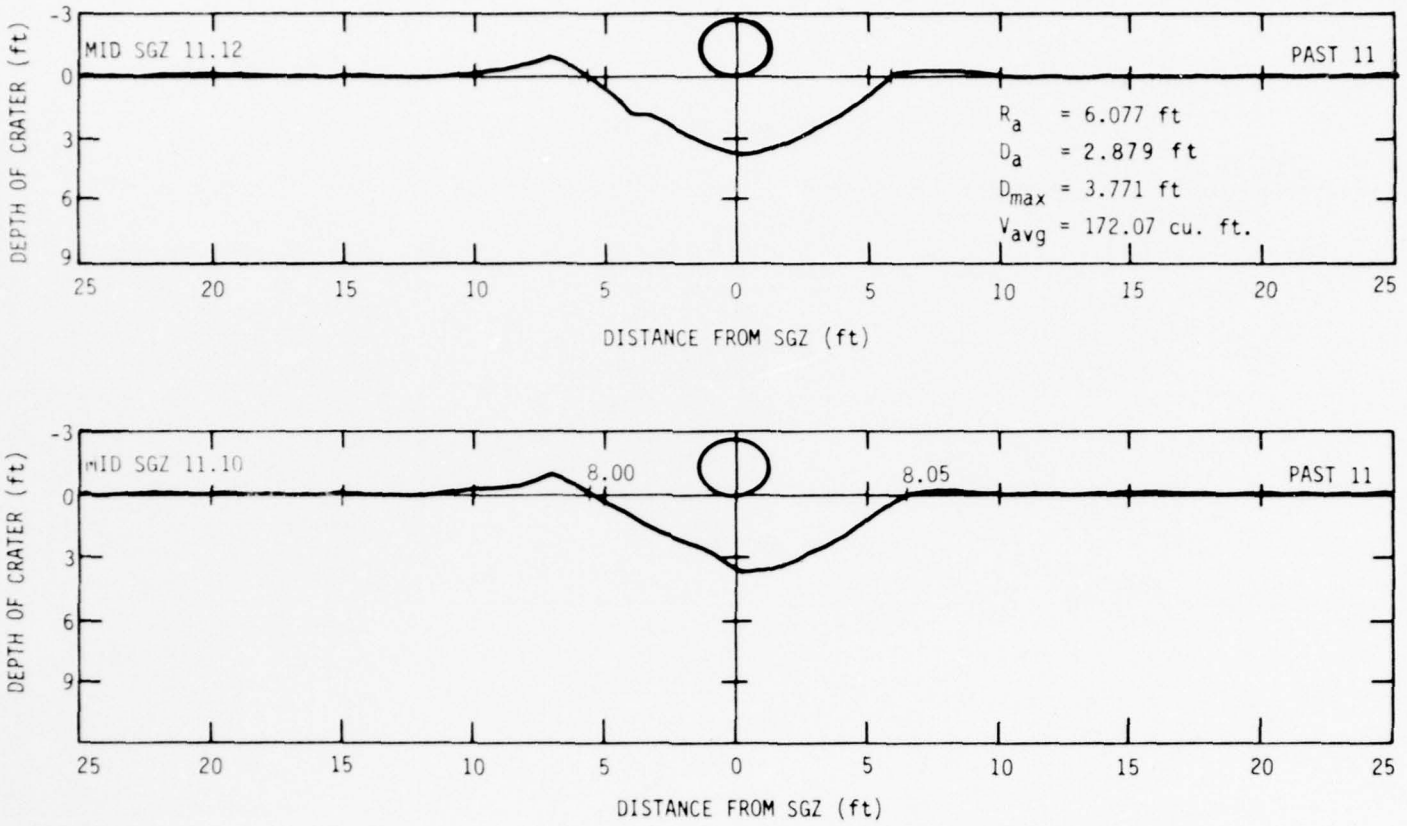

Figure 10.7. Event MBI-8 crater profile for GZ No. 11.

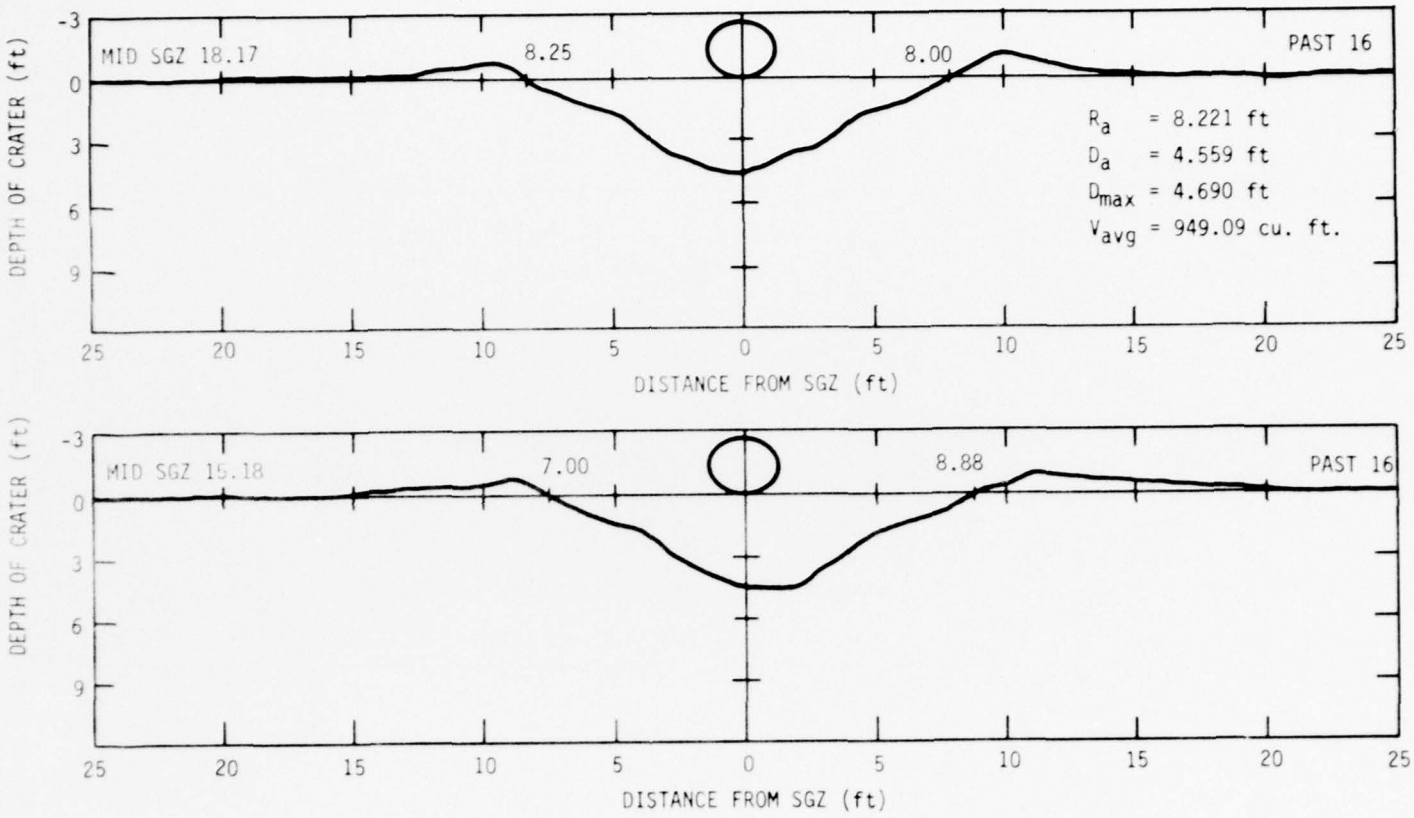

Figure 10.8. Event MBI-8 crater profile for GZ No. 16.

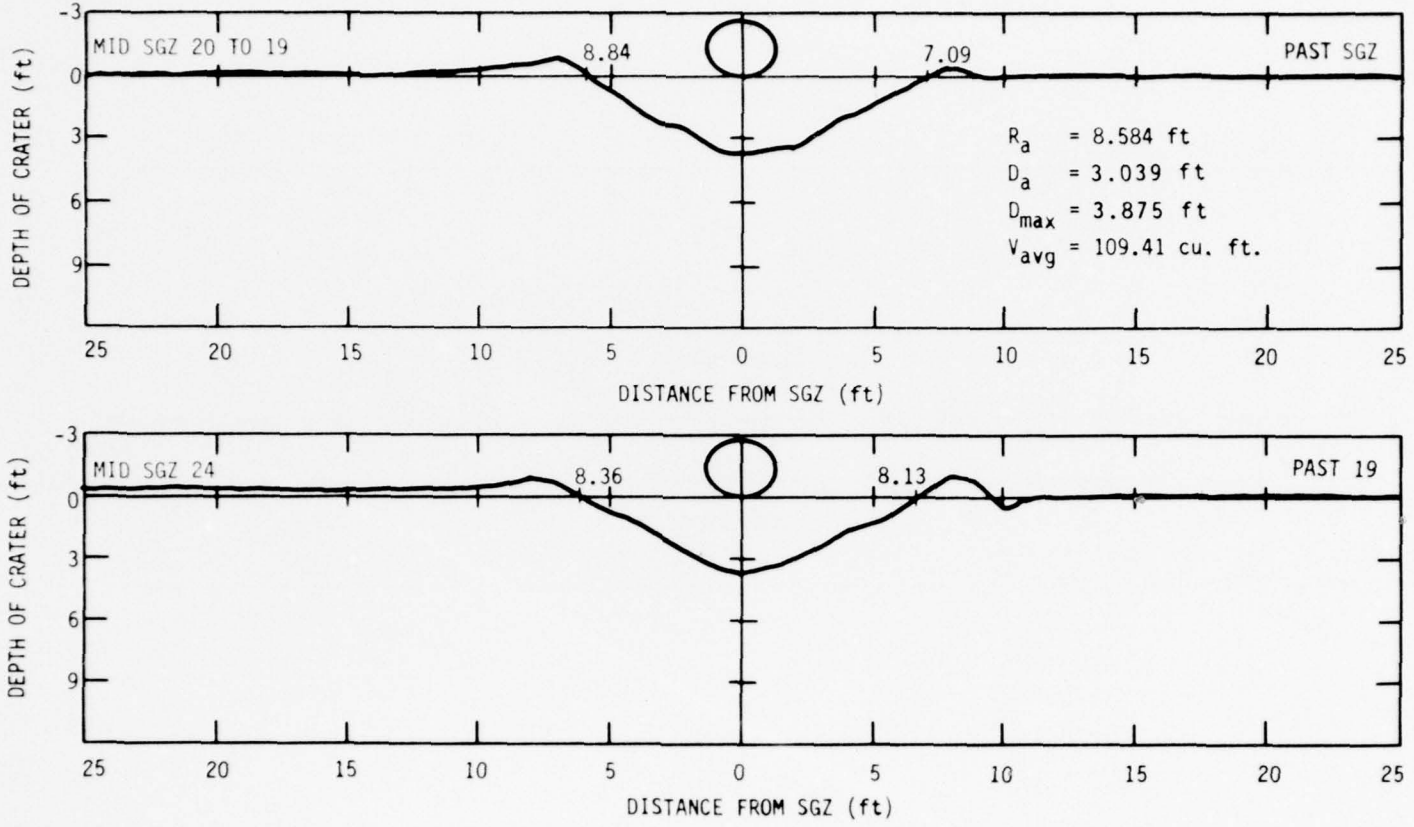

Figure 10.9. Event MBI-8 crater profile for GZ No. 19.

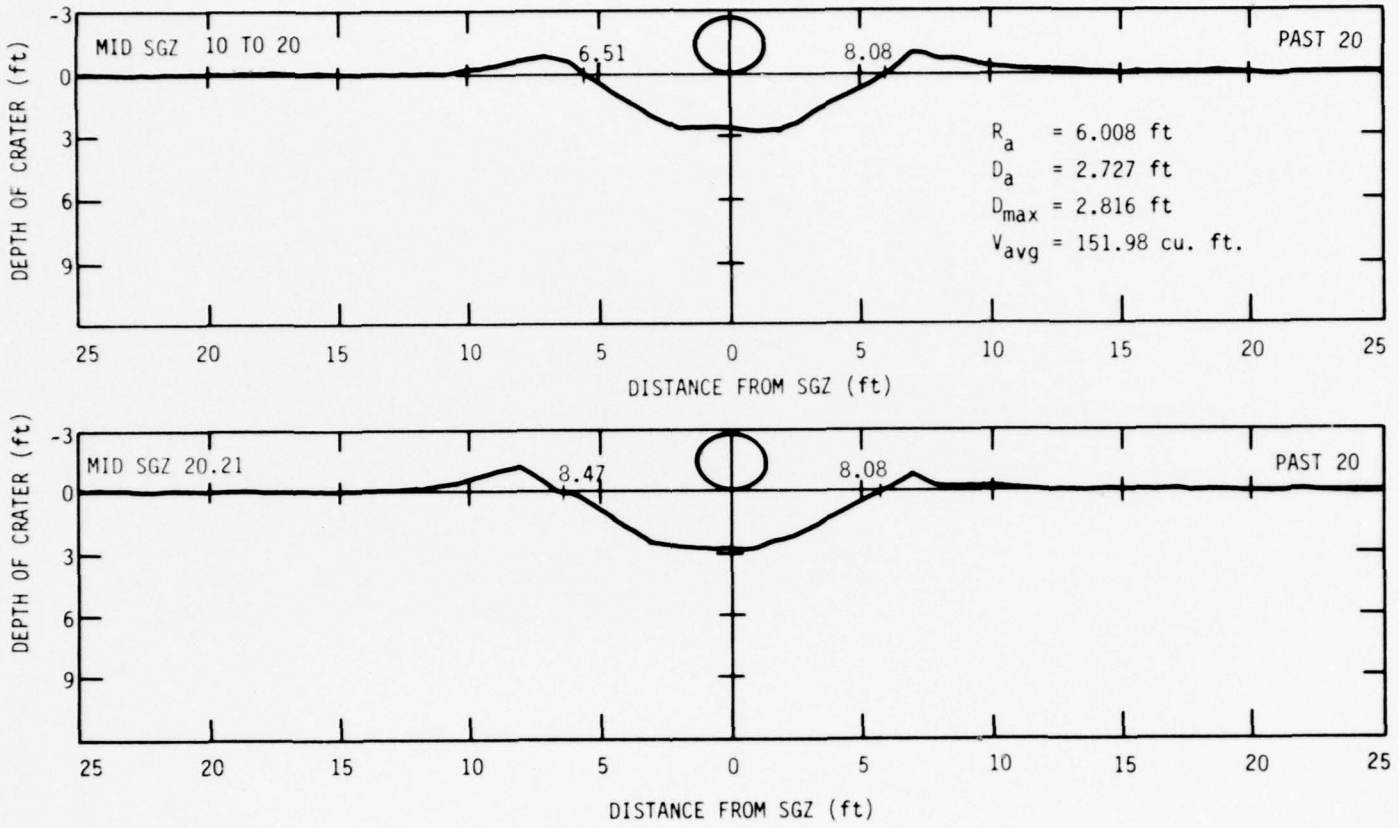

Figure 10.10. Event MBI-8 crater profile for GZ No. 20.

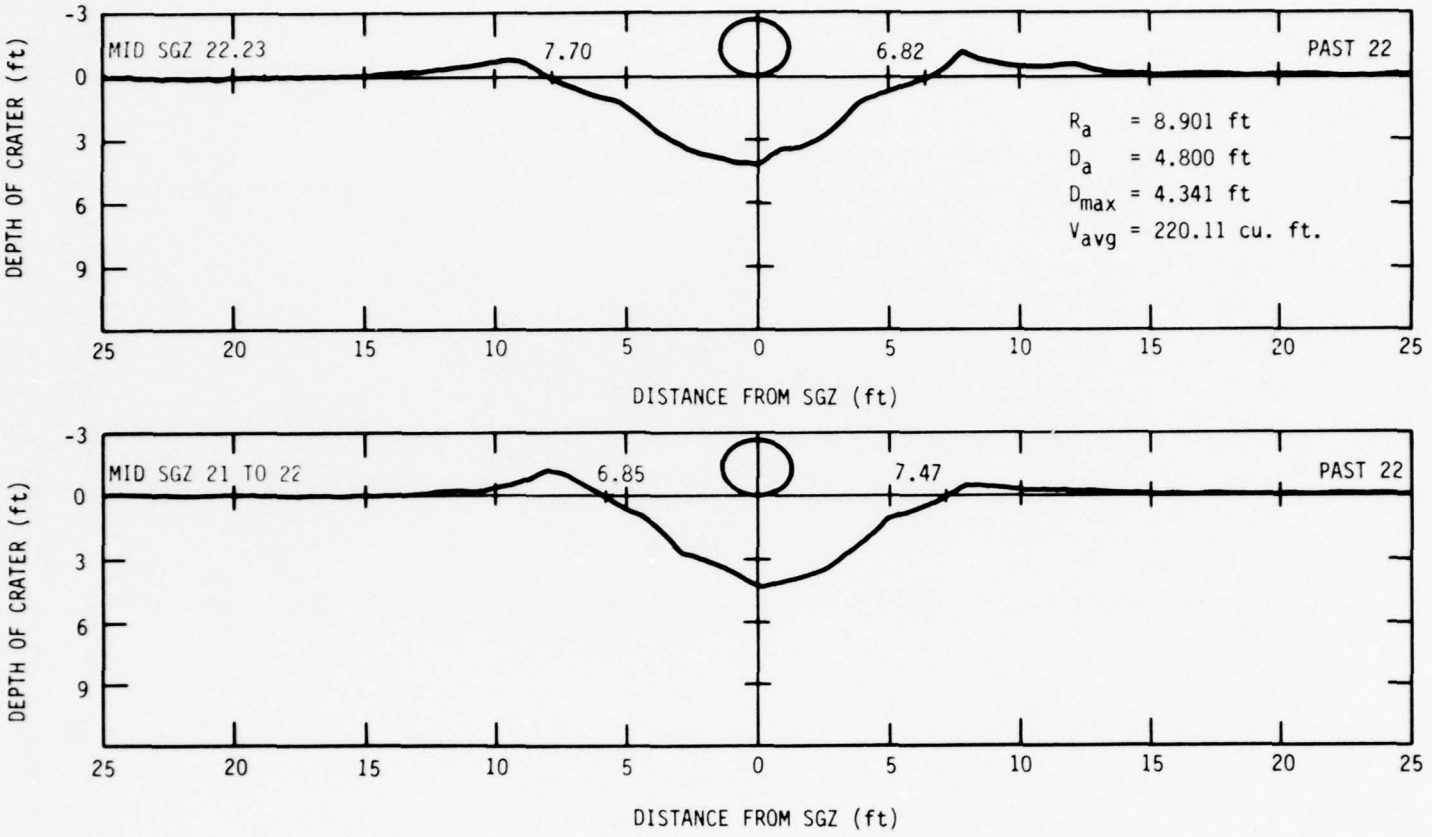

Figure 10.11. Event MBI-8 crater profile for GZ No. 22.

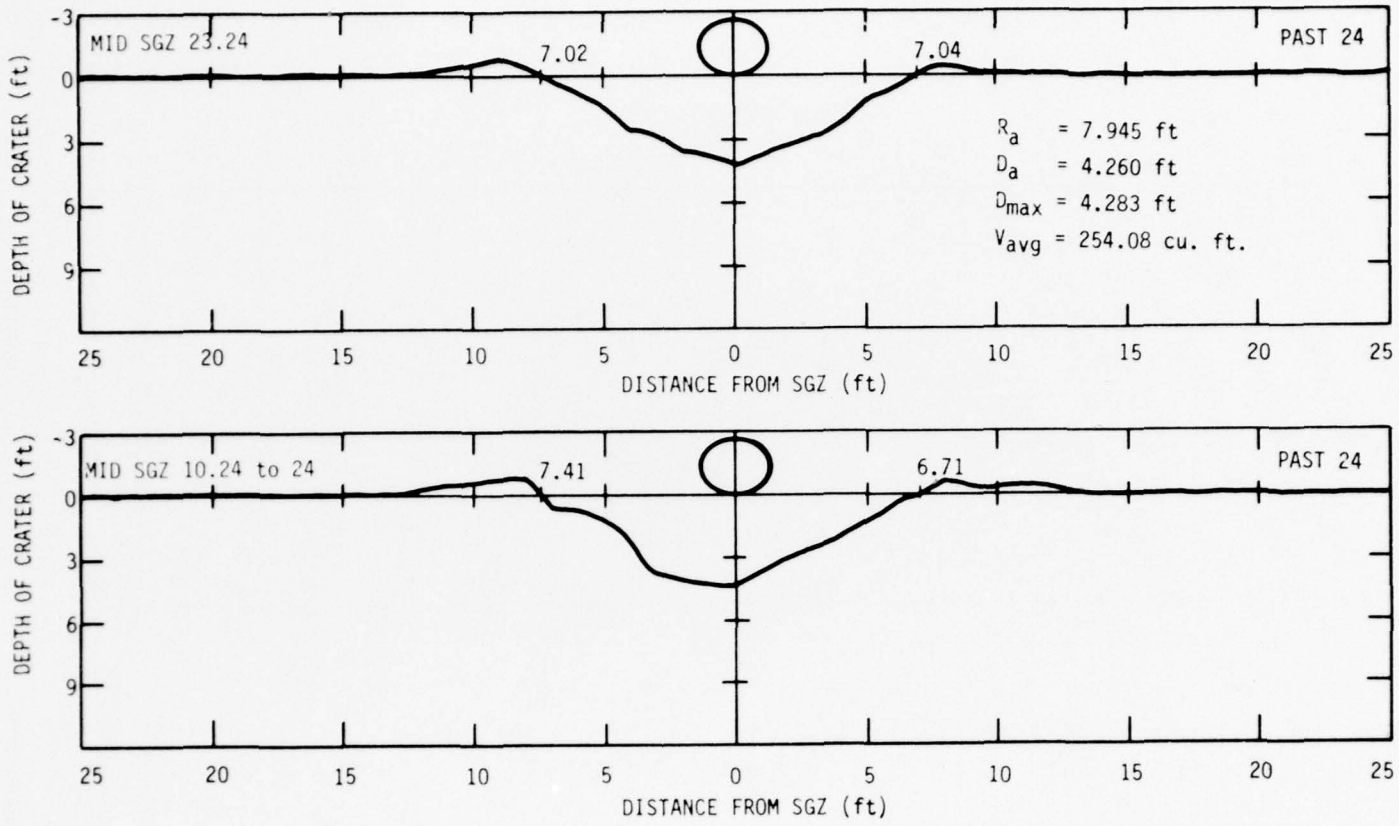

Figure 10.12. Event MBI-8 crater profile for GZ No. 24.

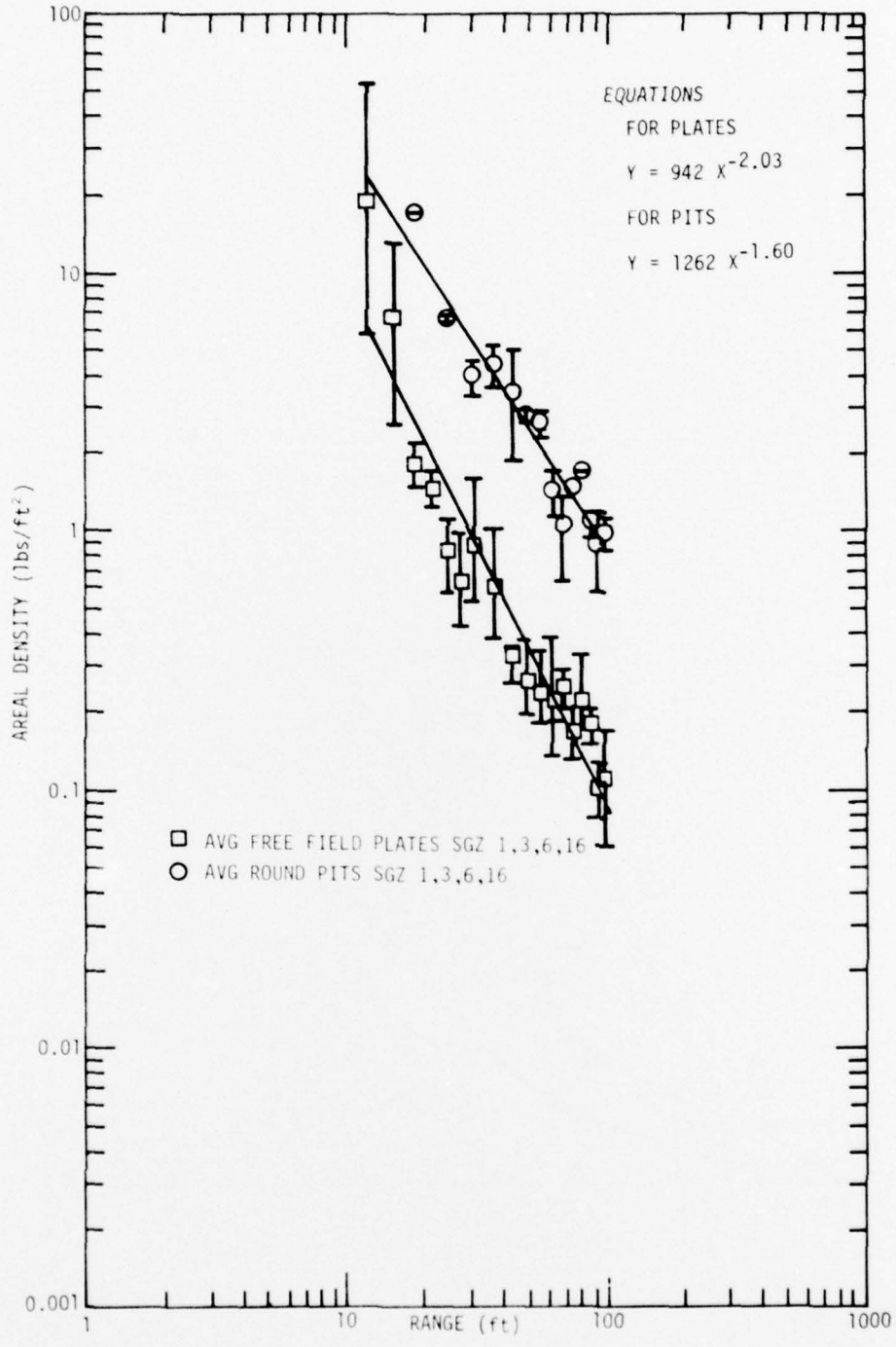

Figure 10.13. Event MBI-8, average areal density versus range.

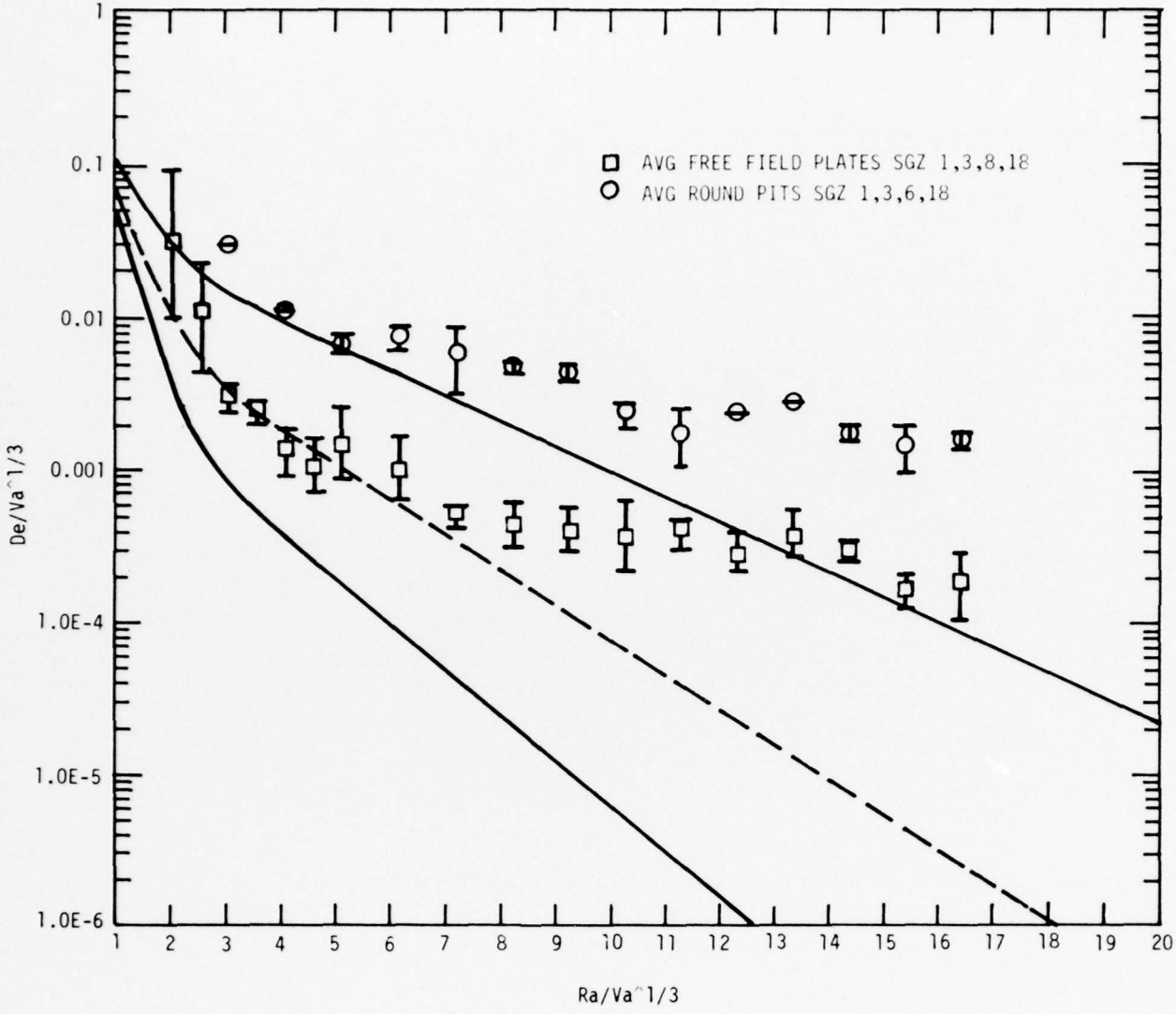

Figure 10.14. Event MBI-8, debris depth versus range both normalized by $V_a^{1/3}$.

SECTION 11

SUMMARY AND CONCLUSIONS

Table 11.1 is a summary of the ground motion and airblast gages used on the eight events of Phase I of the MISERS BLUFF Program. As shown, there was a 95 percent overall data recovery from the 840 measurements. There were a total of 923 debris collectors used on the various events as summarized in Table 11.2. Technical photography was accomplished by the Denver Research Institute using 11 cameras for the single burst events and 20 cameras for the multiple burst events as shown in Table 11.3.

The single burst events of MISERS BLUFF Phase I provided the basic data for use in evaluation of the superposition principle in predicting the ground shock effects of multiburst experiments. In addition, they provided an opportunity for evaluating the current empirical procedures for predicting the ground shock effects of high explosive experiments. A set of good quality multiple burst ground motion data for two burst heights has been generated in Phase I testing.

One of the main objectives of the Phase I multiple burst experiments was to determine the regions in which the superposition assumption is valid and invalid. From the study of the data the following conclusions about the superposition assumption were drawn:

a. Superposition is satisfactory at all locations and depths outside the charge array;
b. All depths below the phreatic surface are adequately described by superposition;
c. Failure of superposition occurs at all gage locations above the phreatic surface within a circle having a radius of 1/2 the charge spacing centered at the array center;
d. At the near surface gage locations inside the array and at ranges greater than 1/2 the charge spacing (as measured for the array center) superposition is not as accurate as at the previous locations, but is showing a definite trend of improvement.

Table 11.1. Summary of ground motion and airblast gages.

Event	Acceleration Gages		Velocity Gages		Stress Gages		Airblast Gages		Total Gages	
	No. of Measure-ments	Percent Data Recovery	No. of Measure-ments	Percent Data Recovery	No. of Measure-ments	Percent Data Recovery	No. of Measure-ments	Percent Data Recovery	No. of Measure-ments	Percent Data Recovery
MBI-1	74	97	18	100	3	100	3	100	98	98
MBI-2	72	94	18	100	3	100	3	100	96	97
MBI-3	48	98	10	100	5	100	3	100	66	98
MBI-4	101	97	6	100	10	90	15	100	132	97
MBI-5	39	90	6	100	5	100	7	86	57	91
MBI-6	99	96	14	93	10	80	29	97	152	95
MBI-7	42	93	10	90	-	-	3	100	55	93
MBI-8	138	93	10	100	6	100	30	100	184	95
TOTALS	613	95	92	98	42	93	93	98	840	95

Table 11.2. Types and number of debris collectors in MISERS BLUFF, Phase I.

	Type of Collectors							
Event	Pits	H Beam	Concrete Slabs	Plates	Benson Box	Sand Mounds	Dust Cloud	Total
MBI-1	41	5	8	4	1	1	3	63
MBI-2	36	6	6	65	1	2	4	120
MBI-3	33	8	8	73		3		125
MBI-4	32	1	12	90				135
MBI-5	34	7	9	68				118
MBI-6	38	7	12	110				167
MBI-7	34	11	8	72				125
MBI-8	—	—	—	70	—	—	—	70
TOTAL	248	45	63	545	2	6	7	923

Table 11.3. Photographic coverage for MISERS BLUFF, Phase I.

Event	HYCAM	NOVAS	Hulcher Photosonic	Milliken	Photosonic	DYNA FAX	Total
MBI-1	1	2	3	1	4		11
MBI-2	1	2	3	1	4		11
MBI-3	1	2	3	1	4		11
MBI-4	1	6	3	2	4	4	20
MBI-5	1	2	3	1	4		11
MBI-6	1	6	3	2	4	4	20
MBI-7	1	2	3	1	4		11
MBI-8	1	6	3	2	4	4	20

Another objective was the development of a procedure to predict the multiple burst environment in a more general sense. In analyzing Phase I, it was obvious that the empirical prediction procedures and superposition methods were inadequate in specific regions. An empirical "fix" to produce results consistent with Phase I MISERS BLUFF experiments would yield a model with little confidence in extension to another test configurations.

DISTRIBUTION LIST

DEPARTMENT OF DEFENSE

Assistant to the Secretary of Defense
Atomic Energy
ATTN: Executive Assistant

Defense Documentation Center
12 cy ATTN: DD

Defense Nuclear Agency
ATTN: STSP
ATTN: DDST
ATTN: PAO, W. McGee
4 cy ATTN: TITL
3 cy ATTN: SPSS
3 cy ATTN: SPTD
3 cy ATTN: SPAS
2 cy ATTN: RAAE

Field Command
Defense Nuclear Agency
ATTN: FCTMOF
ATTN: FCPR
ATTN: FCP
3 cy ATTN: FCTMOT
3 cy ATTN: FCTMD
4 cy ATTN: FCTME
2 cy ATTN: FCTMA

Field Command
Defense Nuclear Agency
ATTN: FCPRL

Field Command Test Directorate
Test Construction Division
Defense Nuclear Agency
ATTN: FCTC, J. LaComb

Under Secy. of Def. for Rsch. & Engrg.
ATTN: Strategic & Space Systems (OS)

DEPARTMENT OF THE ARMY

Harry Diamond Laboratories
Department of the Army
ATTN: DELHD-N-P
ATTN: DELHD-N-P, J. Gwaltney
ATTN: DELHD-N-P, J. Meszardos

U.S. Army Ballistic Research Labs
ATTN: DRDAR-BLE, J. Keefer
ATTN: DRDAR-BLE, G. Teel
ATTN: DRDAR-BLT, N. Ethridge

U.S. Army Engineer Waterways Experiment Station
ATTN: WESSA, W. Flathau
ATTN: WESSE, L. Ingram
ATTN: WESSE, D. Day
ATTN: WESSE, D. Murrell
ATTN: WESSE, A. Rooke
ATTN: WESSE, J. Drake
ATTN: WESGH, P. Hadala
ATTN: WESGH, S. Cooper
ATTN: WESGR, J. Gatz
ATTN: WESSD, G. Jackson
ATTN: WESSD, A. Jackson
ATTN: WESSS, R. Ballard

DEPARTMENT OF THE ARMY (Continued)

White Sands Missile Range
Department of the Army
ATTN: STEWS-TE-MG, R. Dysart
ATTN: STEWS-FE, D. Green

DEPARTMENT OF THE NAVY

Naval Surface Weapons Center
ATTN: Code F31

DEPARTMENT OF THE AIR FORCE

Air Force Systems Command
ATTN: DLX-IG, J. Neal

Air Force Weapons Laboratory, AFSC
ATTN: SUL
ATTN: NT, B. Wheeler
ATTN: DES, G. Ganong
ATTN: DES, C. Needham
ATTN: DES, R. Reinke
ATTN: DES, J. Thomas
ATTN: DES, R. Jolley
ATTN: DES, R. Henny
ATTN: DES, K. Filippelli

Space & Missile Systems Organization
Air Force Systems Command
ATTN: MNNH, D. Gage
ATTN: MNNH, T. Edwards

OTHER GOVERNMENT AGENCY

Department of the Interior
U.S. Geological Survey
ATTN: D. Roddy

DEPARTMENT OF ENERGY CONTRACTORS

Sandia Laboratories
ATTN: J. Reed
ATTN: J. Johnson
ATTN: P. Cooper

DEPARTMENT OF DEFENSE CONTRACTORS

California Research & Technology, Inc.
ATTN: D. Orphal

Civil Systems, Inc.
ATTN: J. Bratton
ATTN: E. Bultmann
ATTN: S. Melzer
ATTN: J. Phillips

University of Denver
Colorado Seminary
Denver Research Institute
ATTN: J. Wisotski

EG&G, Inc.
Special Projects Division
ATTN: R. Ward

DEPARTMENT OF DEFENSE CONTRACTORS (Continued)

Eric H. Wang
Civil Engineering Rsch. Fac.
ATTN: D. Calhoun
ATTN: K. Benson
ATTN: J. Rinehart
ATTN: E. Tremba

Electro-Mechanical Systems of New Mexico, Inc.
ATTN: R. Shunk

General Electric Company-TEMPO
ATTN: G. Perry

General Electric Company-TEMPO
ATTN: DASIAC
ATTN: W. Chan

Jaycor
ATTN: H. Linnerud

Ken O'Brien and Associates, Inc.
ATTN: D. Collins

Physics International Co.
ATTN: F. Sauer

DEPARTMENT OF DEFENSE CONTRACTORS (Continued)

R & D Associates
ATTN: C. McDonald
ATTN: R. Port
ATTN: A. Kuhl

Systems, Science, & Software, Inc.
ATTN: K. Pyatt
ATTN: D. Grine
ATTN: D. Lambert

Systems, Science, & Software, Inc.
ATTN: D. Guarino
ATTN: C. Hastings
ATTN: E. DeMaris

Tech Reps, Inc.
ATTN: B. Collins

Williamson Aircraft Co.
ATTN: R. Williamson

R & D Associates
ATTN: H. Cooper